IMPERIAL COLLEGE OF SCIENCE AND TECHNOLOGY

UNIVERSITY OF LONDON

Department of Electrical Engineering

COMPUTER PROTECTION OF HIGH VOLTAGE TRANSMISSION LINES

by

ALI-MOHAMMAD RANJBAR

M.Sc.

Thesis submitted for the degree of Doctor of Philosophy in the Faculty of Engineering

London, October 1975

ABSTRACT

Increasing interest is being shown in the use of digital computers for the protection, switching and data acquisition required in modern high voltage substations. One of the most difficult functions to fulfil by digital methods is that of transmission line protection employing samples of the voltage and current waveforms taken from high voltage transducer equipment at the usual relaying point. Given adequate speed of sampling and conversion to digital form for processing, problems remain of calculating the fault conditions within a defined protection zone of the transmission line, particularly when exponential dc offset, harmonics, nonharmonics and noise are present.

This work explores the accuracy of the digital methods for protection of high voltage transmission lines under transient fault conditions. By using Z transform the spectrums of all methods are calculated and from these the optimum rate of sampling which is one of the decisive factors in the implementation of digital algorithms is determined.

Spectrums and transient time responses of analog and digital filters are studied and the most suitable filter from protection point of view is determined.

Different algorithms are tested off-line and on-line and the best algorithm is chosen based on simplicity and accuracy of performance. By careful determination of the type, order and cut-off frequency the analog filter, the fault generated high frequency components and noise are filtered out.

Close-up faults and problems involved in the protection of parallel lines with mutual coupling are also considered.

ACKNOWLEDGEMENTS

The work in this thesis was carried out under the supervision of Dr. B.J. Cory, B.Sc.(Eng.), D.Sc., A.C.G.I., C.Eng., F.I.E.E., Reader in Electrical Engineering, Imperial College of Science and Technology, London. I wish to thank Dr. Cory for his helpful guidance, constant encouragement and keen interest during the preparation and completion of this project.

I am grateful to the Arya-Mehr University of Technology Tehran, Iran and British Council for the financial support which made this work possible.

Finally I would like to thank all my colleagues, particularly Messrs. E. Horne, G. Gonzalez, A. Traca and P. Ong who contributed directly or indirectly to this work.

To my late mother

TABLE OF CONTENTS

LIST OF SYMBOLS AND ABBREVIATIONS

SYMBOLS

Capitals

A_v, A_i, B_v, B_i	Real and imaginary parts of voltage and current.
API	Automatic priority interrupt.
D	Denominator of resistance and inductance formulas in McInnes method.
FIA	Fault inception angle
I_a, I_b and I_c	Phase currents
I_L	Input current of phase comparison relay
I_o	Zero sequence current of single circuit line
I_{01}, I_{02}	Zero sequence currents of circuits 1 and 2 of a double circuit line
I_A, I_B, I_C	Currents in neighbouring parallel line.
I_P	Current peak.
L_{aa}, ..., L_{ab},...	Self and mutual inductances of transmission line.
L_0, L_1	Zero and positive sequence inductances.

M_R, M_L Numerators of resistance and inductance formulas in McInnes method.

N Number of samples per cycle.

R_{aa}, ...,R_{ab},.. Self and mutual resistances of transmission line.

R_L Resistive part of Z_L

Rg Fault resistance

R_1, R_0 Positive and zero sequence resistances.

T Time between two consecutive samples.

V_P Voltage Peak

V_L Input voltage of phase comparison relay.

V_1, V_2 Voltage outputs of mixing and measuring circuits of phase comparison relay.

V_a, V_b, V_c Sending end phase voltages.

V_a, V_b, V_c Fault point voltages

X_L Reactive part of Z_L

Z_{R1}, Z_{R2} Transfer impedances

Z_{aa}, Z_{bb}, Z_{cc} Self impedances of transmission line

Z_{ab}, Z_{ac}, ...	Mutual impedances of transmission line
Z_1, Z_2, Z_0	Positive, negative and zero sequence impedances
Z_{m0}, Z_{m1}, Z_{m2}	Zero, positive and negative sequence mutual impedances in parallel line.
Z_L	V_L/I_L

Small letters

f	Frequency
i_d, i_b, i_c	Instantaneous Phase currents.
i_k	The kth current sample
i'	First derivative of current
j	$\sqrt{-1}$
s	Laplace transform variable
s/c	Samples per cycle
t	Time
u_k	The kth output of digital filter
v' and v"	First and second derivatives of voltage
v_k	The kth voltage sample
v_a, v_b, v_c	Instantaneous phase voltages
z	z - transform variable

Greek letters

ω	Angular frequency
γ	Starting angle for Fourier Coefficients
α	Phase angle between V_1 and V_2
α_1, α_2	Phase angles of V_1 and V_2
θ_1, θ_2	Phase angles of Z_{R1} and Z_{R2}
ϕ_L	Phase angle of I_L

Abbreviations

( )	Bracket
[ ]	Bracket
| |	Matrix, Modulus, absolute value
$\int$	Integral sign
$\oint$	Closed integral

CHAPTER 1

INTRODUCTION

Continuing rapid advances in digital computer technology have prompted a re-evaluation of protective devices and techniques. It is desirable that the protective relays should operate with minimum possible delay compatible with proper selection of faulty primary system sections. The electromechanical and static relays have performed this function adequately until now but it does not necessarily follow that these are the only or the best devices for system protection. The use of digital computers for system protection should be compared with the existing techniques and adopted if found more economical, flexible and have advantages in application.

A very attractive digital computer characteristic is its ability to readily alter its decision making criteria. For example protection zones can be modified by monitoring the system configuration and the protection scheme can be easily expanded or modified and new priorities can be assigned by revising or changing the software package as the power system grows.

To investigate the relative advantages and disadvantages of power system protection with on-line digital computers one corner of a mesh type high voltage substation used typically on the 400 KV system of the C.E.G.B. was chosen and it was decided to develop algorithm and program for the following purposes:

i) Data collection and recording

ii) Sequence switching and interlocking

iii) Mesh corner bus-bar protection

iv) Transmission line fault measurement and detection

v) Transformer protection able to discriminate between internal fault and inrush conditions.

This research reported here has attempted to find a practical algorithm and to develop the necessary programs for transmission line protection (part iv) and to investigate the implementation problem such as sampling rate, filtering etc.

Chapter 2 contains a brief discription of static distance relays and their associated problems.

Different algorithms are discussed in chapter 3. By using the Z-transform their immunity to d.c. and high frequency components for different rates of sampling are investigated. The overall spectrums of the algorithms with different analogue filters are presented and for every algorithm a practical sampling rate and an analogue filter with a suitable cut-off frequency is recommended.

In chapter 4, the algorithms for different rates of sampling are tested against fault generated exponential d.c. off-set and high frequency components, and the most accurate have been determined.

In chapter 5 analogue and digital filtering methods are studied and compared for spectrum and transient time response and a recommendation made for digital protection.

In chapter 6 the problems of close-up faults and relaying on parallel lines are investigated.

Chapter 7 contains a brief description of the laboratory interface and the results of on-line implementation by different algorithms. In this chapter also the flow chart of the main program is presented and described. The final conclusions are presented in chapter 8.

The original contributions presented in this thesis are as follows:

1) The noise and fault generated components have a continuous spectrum which contains all kind of harmonics and non-harmonics. To investigate how the digital algorithms cope with these components the Z-transform method is introduced in protection for the first time.

2) The frequency responses of different algorithms in the most general form, for varying rates of sampling are obtained and its role with respect to exponential dc off-set and fault generated components is clearly shown.

3) One of the decisive factors in the implementation of digital algorithms is the type,order and cut-off frequency of the analogue filter used for filtering the unwanted components. In all papers on digital distance relaying, usually a frequency corresponding to half the sampling rate has been suggested for the cut-off of the required analogue filter, without mention of the order of the filter. It is shown that the cut-off frequency depends on sampling rate, the order of the filter and the type of the algorithm which is used for impedance calculation. Then for every method, the order and the cut-off frequency of the necessary analogue filter, for a practical sampling rate is determined.

4) In the Fourier method a new technique[32] for calculating R and X is presented which does not involve square root and arctangent calculation.

5) It is shown that in order to have all high frequency components attenuated with respect to the fundamental, the integration terms in the McInnes method must be performed on half a cycle of sampling.

6) A new method[26] for calculation of R and X is described in which during the calculation any harmonic can be filtered out.

CHAPTER 2

ANALOGUE DISTANCE RELAYS

In 1923 Crichton[1] introduced the distance relay as an element in a selective form of transmission line protection. The relay made use of the fact that in a faulted line the impedance between the relaying point and fault was proportional to the distance of the fault. Since then the distance relaying in electromechanical form and recently in static form has become firmly established as a means of transmission line protection. In this chapter the static distance relays will be reviewed for comparison with digital methods.

2.1 DEVELOPMENT OF STATIC DISTANCE RELAY ELEMENT

To overcome some of the difficulties associated with the electromechanical relays (slow operation, large consumption of energy, large dimensions and moving parts problems) and with the increasing availability of electronic components, static relays for distance protection have been developed. The earliest reference to application of electronic circuit principles to power system protection was by Fitzgerald[2] in 1928, who attempted to improve the performance of pilot wire systems. In 1934 Rolfwideroe[3] described how a Thyratron tube can be applied to a number of the more common classes of distance relays. Although the relays described by Wideroe were crude and subject to many practical and theoretical limitations, the principle laid down was the basis for subsequent development work in the field. In 1948 Macpherson, Warrington and McConnel[4] described a distance relay using thermionic valves. The relay consisted of three units, a pulse circuit, a measuring circuit and a tube circuit.

The pulse circuit derived a pulse from the energising voltage at a particular point (usually peak) in its cycle and the measuring circuit derived a complex voltage from the energising voltage and current. The tube circuit noted the polarity of the measuring signal during the time of the derived pulse and if this was negative, it produced a tripping pulse for energising a slave relay. Later on this scheme was abandoned because of the difficulty experienced in the pulsing circuit, due to the effect of random pulses at fault inception giving rise to false operation. In 1954 Kennedy[5] described the principle of phase angle comparison in electronic carrier relaying scheme and in 1956 Adamson and Wedepohl[6] generalised the works of Kennedy[5] and Macpherson[4] and introduced the application of junction-transistor circuits to protective gear. The two systems used by Adamson and Wedepohl are shown in figures (2.1) and (2.2). In Fig.(2.1) the so called pulse relay, the two mixing and measuring circuits produce two voltages V_1 and V_2 from the input current and voltage I_L and V_L. V_2 is applied to a pulsing circuit which produces a positive pulse once every cycle, when V_2 is at its positive maximu. V_1 and the pulse derived from V_2 are then applied to the terminals of a coincidence circuit which requires both input terminals to become positive before producing any potential change at its output terminals. If α is the phase angle between V_1 and V_2, it follows that α must be between $\frac{-\pi}{2}$ and $\frac{+\pi}{2}$ for the coincidence circuit to have a change in its output potential. Random pulses caused spurious[6] operation of this relay during normal operating conditions and fault occurance and so it was abandoned.

In Fig. (2.2) the direct phase comparator is shown. In this relay the two measuring circuits are as before producing

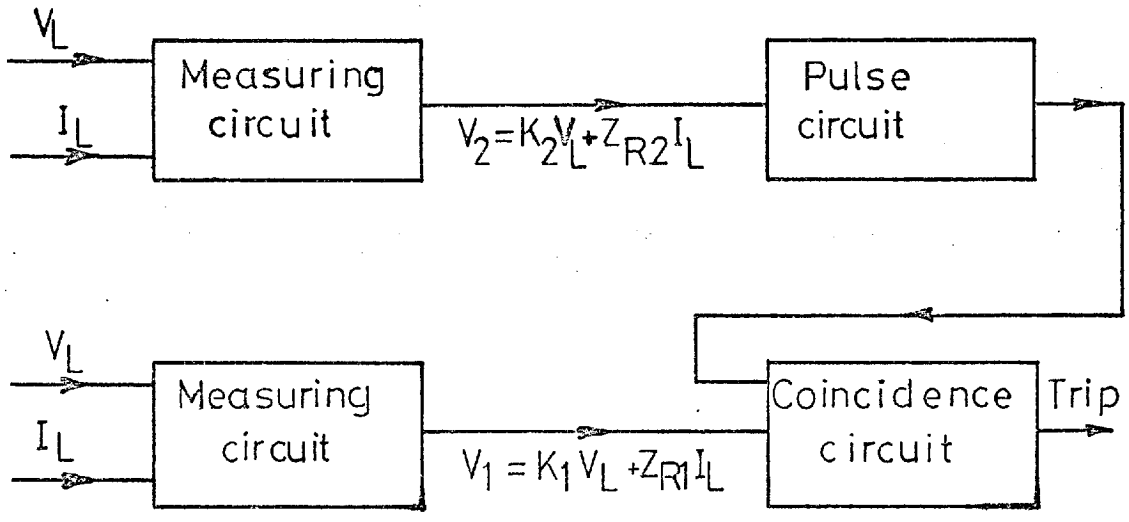

Fig.(2.1) Pulse relay

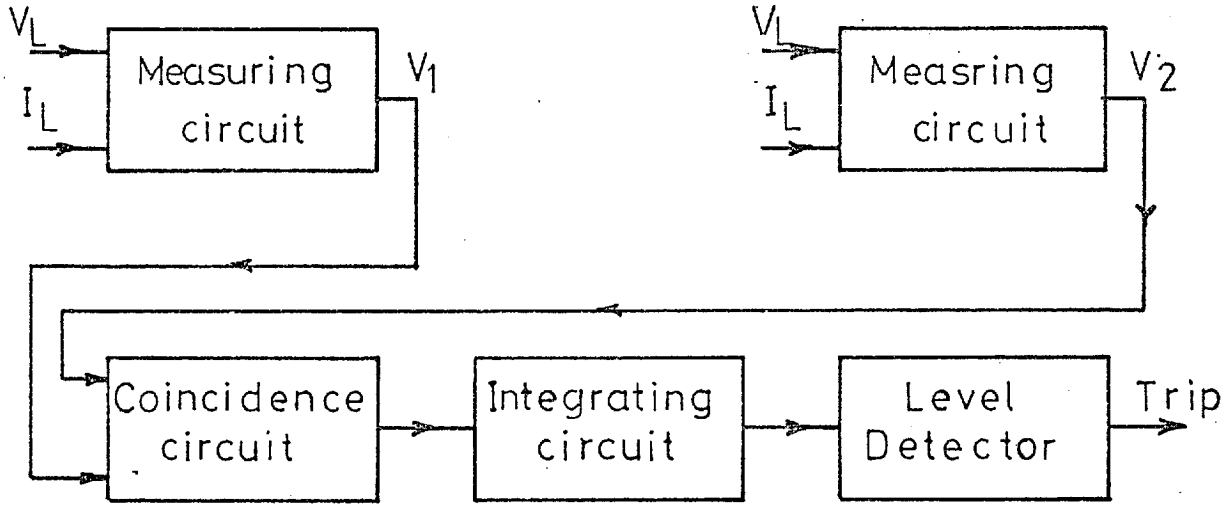

Fig. (2.2) Direct-phase-comparison relay

the same two output voltages V_1 and V_2, but here both voltages are applied directly to the coincidence circuit, so that the output is a square pulse lasting for the duration of coincidence (Fig. 2.3). These pulses are then applied to an integrating circuit whose output is connected to a level detector, which determines whether the pulse is greater than $\pi/2$ radians in duration, and if so it produces a change in output voltage. The criterion for operation is therefore that the duration of coincidence should be greater than $\pi/2$ radians. This means that the phase angle between the two voltages V_1 and V_2, should be less than $\pi/2$ radians, which is the same condition as for the pulse relay. The major difficulty encountered by this relay was faulty operation due to transient components of fault voltage and current. To overcome this deficiency Adamson and Wedepohl[7] proposed a dual phase comparator (Fig. 2.4) wherein two identical comparators were arranged to compare signals on alternate half-cycles, and their outputs were gated so that transient overreach in one element was blocked by the other. In this scheme the operation would not occur until the transient components had decayed sufficiently to have negligible effect and hence this attempt to preserve dynamic measuring accuracy sacrifices speed of operation and leads to long operating times.

In 1968 Jackson[8] introduced the block average comparator in which the duration of polarity coincidence was measured on both half cycles of the input signals, and the average value was determined in a linear integrating circuit, a trip signal being produced if a specified average value was maintained for more than a prescribed duration. Relays using the block-average-comparison principle have been used successfully in field trials and this principle now forms the basis for various production

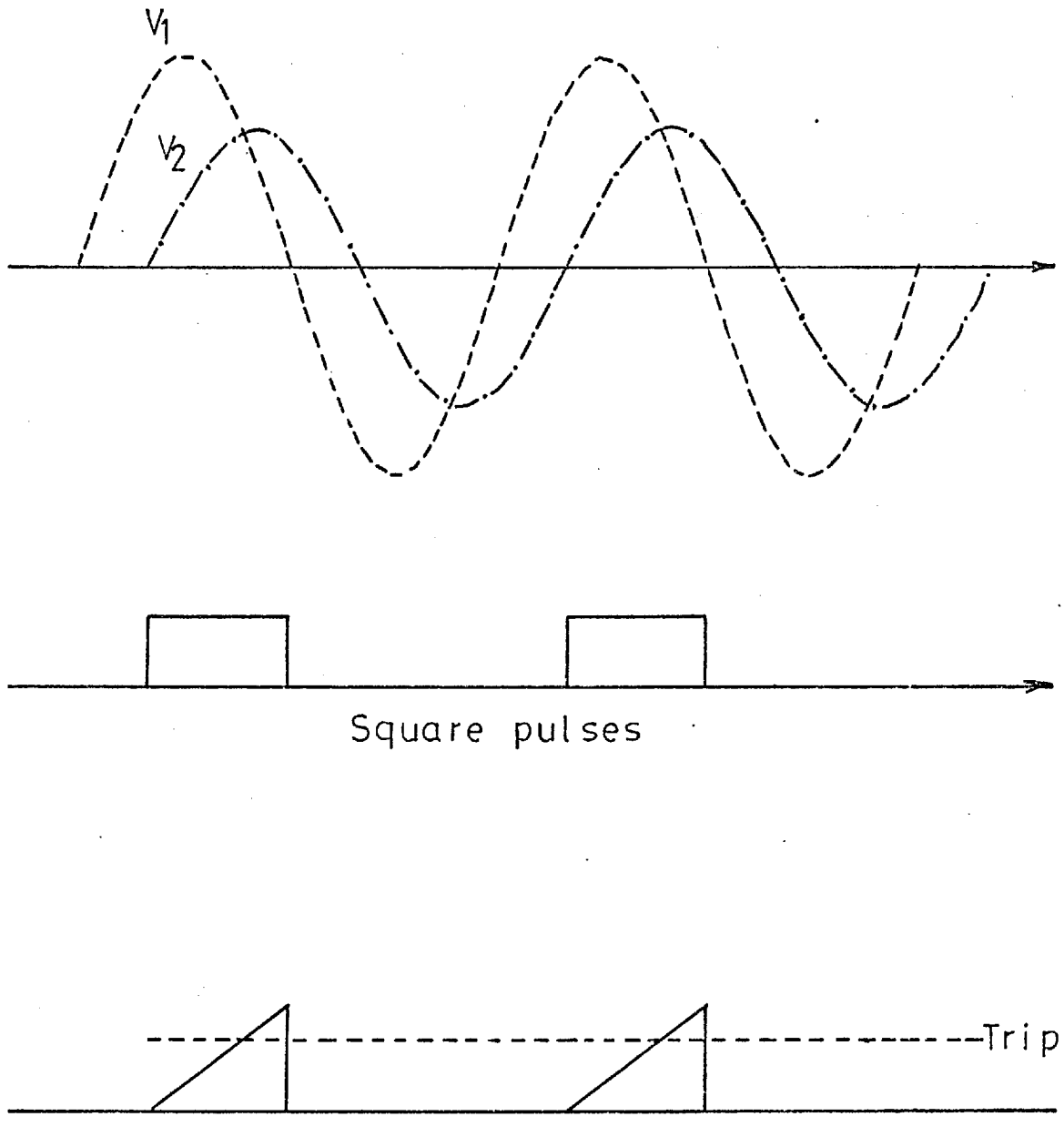

Fig.(2.3) Direct phase comparison waveforms

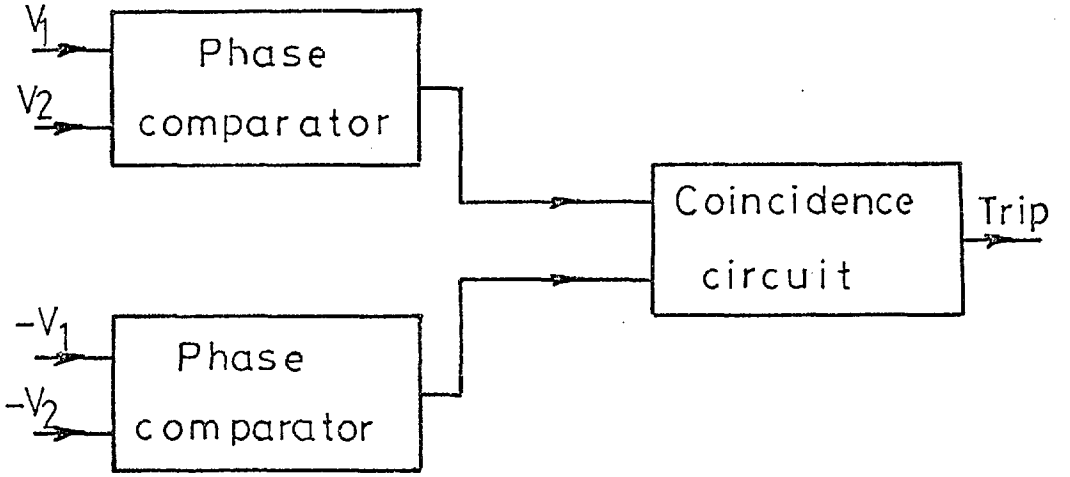

Fig.(2-4) Block diagram of dual phase comparator

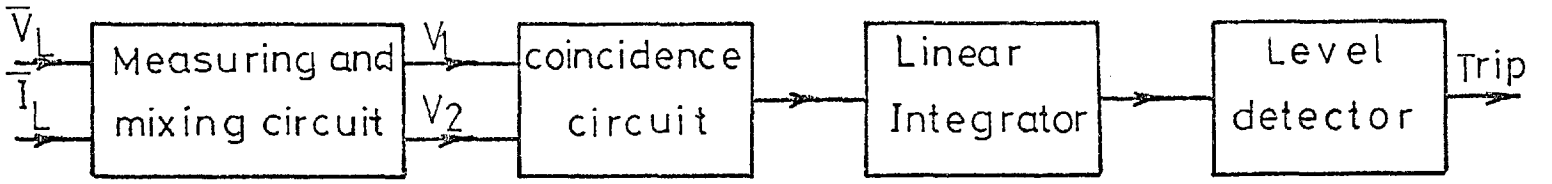

Fig.(2-5) Basic block average comparison relay

designs. Figure (2.5) shows the schematic diagram of a basic relay using the block-average-comparison principle. The voltage and current V_L and I_L are applied to a measuring and mixing circuit, which produces two output voltages V_1 and V_2. These two voltages are compared in a coincidence circuit producing square pulses. These pulses are applied to a linear integrating circuit whose output increases linearly during the time when V_1 and V_2 are of the same polarity and decreases when V_1 and V_2 are of opposite polarity. Figures (2.6) and (2.7) show the relevant waveforms in the steady state for phase displacements between V_1 and V_2 greater than $\pi/2$ and less than $\pi/2$ respectively. The relay operates when this phase displacement is between $\pi/2$ and $-\pi/2$. The time of operation of this relay for steady state operation can be estimated and it can be arranged to be 1/2 cycle for zero phase displacement, but increasing phase displacement increases the operating time which becomes infinite when the phase displacement is $\pi/2$ radians.

In recent years there has been an increasing demand for relay characteristics other than the conventional circle type, designed specifically to provide greater immunity from power swing and heavy system loading. Many papers have been published suggesting how to deal with this problem by using multirelay principles or multi-input comparators, but all of them have failed to have any practical significance. Jackson[9] introduced a modified block average relay in which the phase angle criterion of the comparator is a function of the primary system quantities and is therefore continuously variable between well defined limits around the characteristic boundary. The new relay provides a characteristic with optimum fault coverage and immunity from extreme balanced system condition such as heavy loads and power swing.

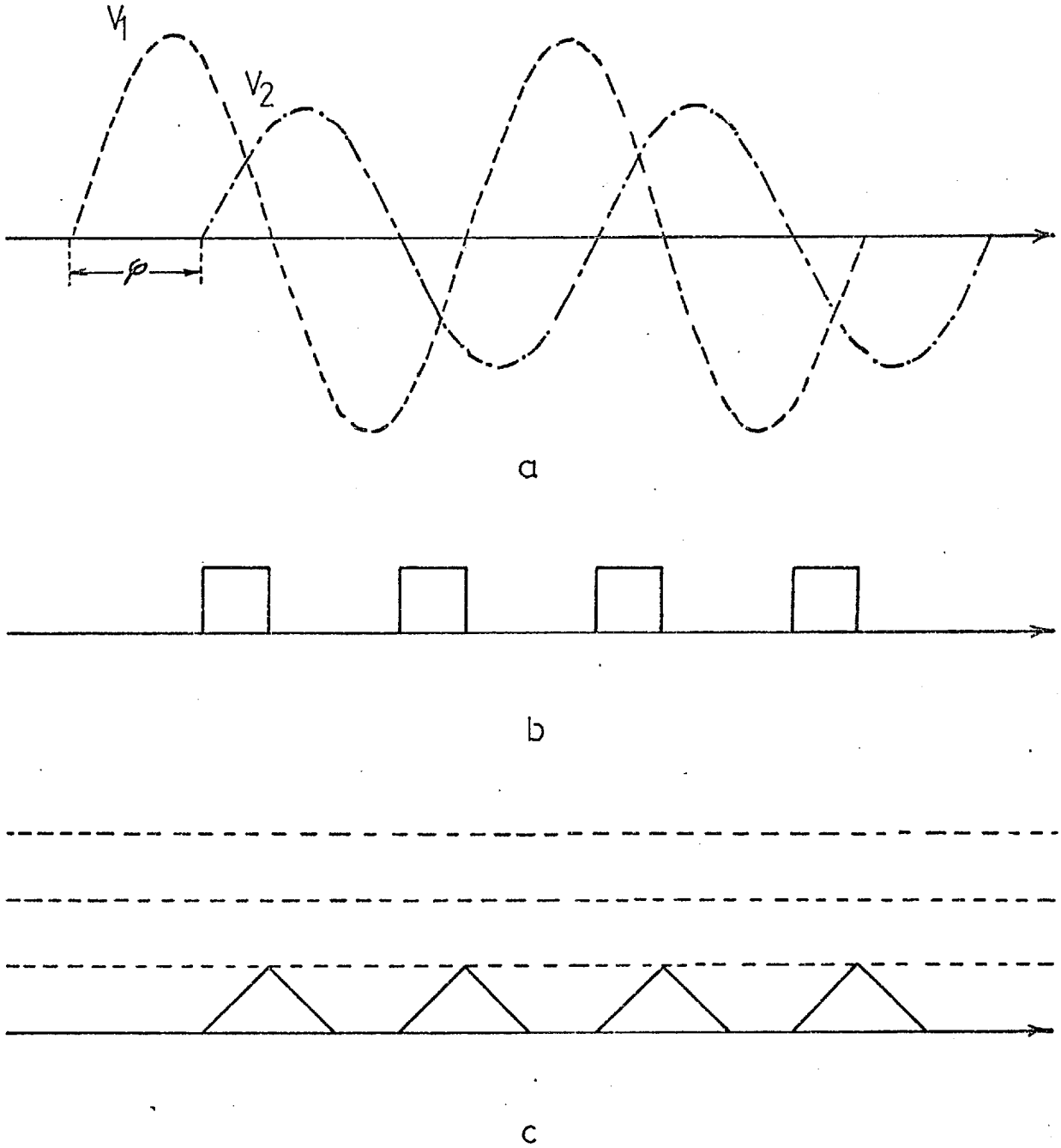

Fig.(2.6) Block average relay waveforms for $\varphi > \pi/2$

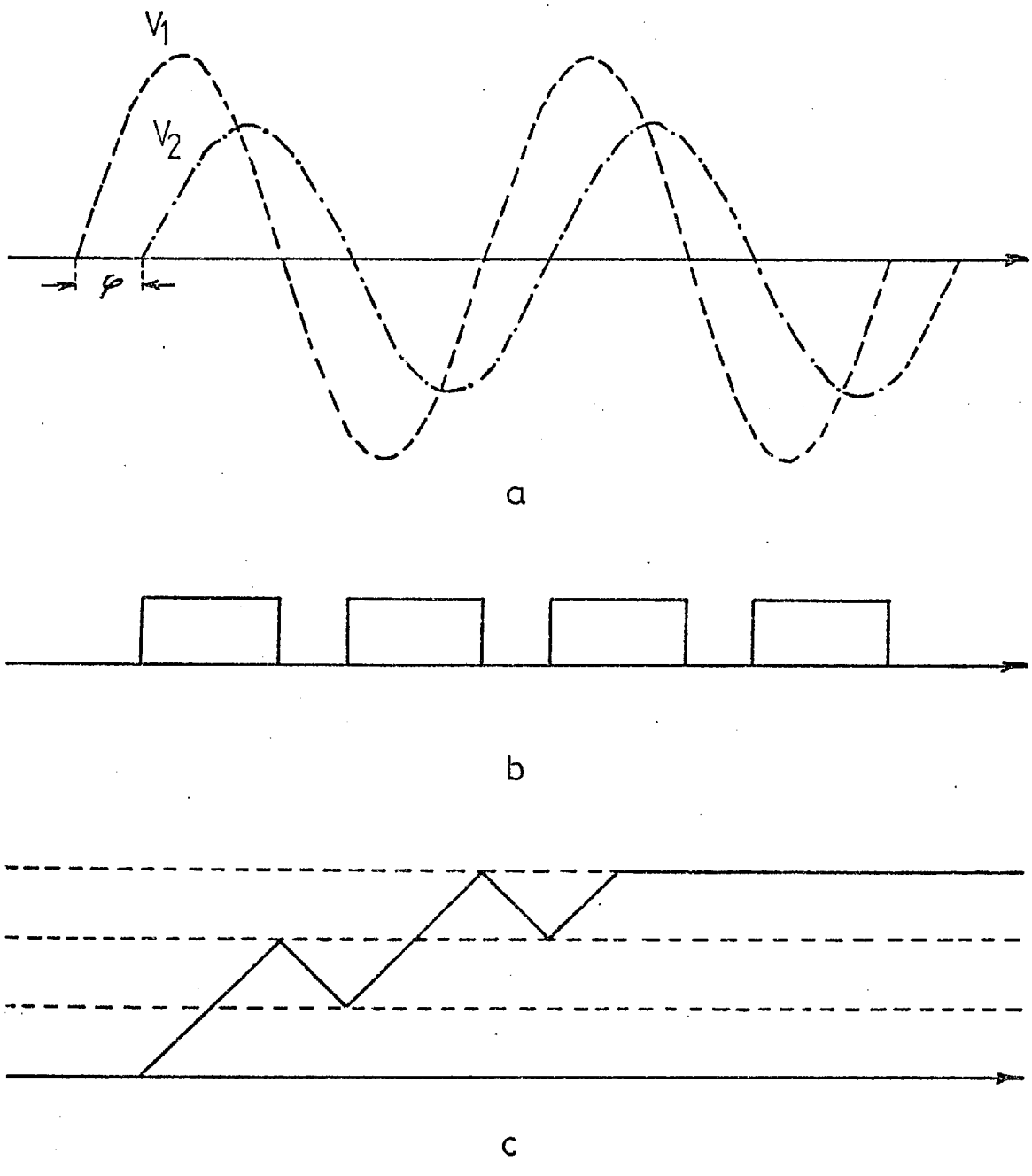

Fig.(2.7) Block average relay waveforms for $\varphi < \pi/2$

2.2 PHASE COMPARATOR CHARACTERISTICS

There are two types of comparators[10], amplitude and phase. Amplitude comparators compare the scalar magnitude of the two inputs; they operate when the modulus of one input is larger than the other. One example of an amplitude comparator is the rectifier-bridge comparator. Phase comparators depend for their operation on the phase difference between the inputs, operating over a range of phase-angle differences and restraining over the remaining portion of the full 2π radians circular arc. The induction cup relay or the block-average principle are two examples of phase comparators. It has been[10] shown that there is no fundamental difference between these two principles and hence only phase comparators will be considered here.

From Fig. (2.2) the outputs of the measuring circuits can be written as follows:

$$V_1 = a+jb = |V_1| \angle\alpha 1 = K_1 V_L + Z_{R1} I_L \qquad (2.1)$$

$$V_2 = c+jd = |V_2| \angle\alpha 2 = K_2 V_L + Z_{R2} I_L$$

Then $$\frac{V_1}{V_2} = \frac{a+jb}{c+jd} = \frac{ac+bd+j(bc-ad)}{c^2 + d^2} = \frac{V_1}{V_2} \angle\alpha 1-\alpha 2 = \left|\frac{V_1}{V_2}\right| \angle\alpha$$

and

$$\cos\alpha = \frac{ac + bd}{\sqrt{(ac+bd)^2+(bc-ad)^2}}$$

The criterion for the operation of the relay is that

$$-\pi/2 < \alpha < +\pi/2 \quad \text{i.e.} \quad \cos\alpha > o$$

and therefore

$$ac + bd > o \ldots\ldots \qquad (2.2)$$

Putting $V_L = |V_L| \angle o$

$I_L = |I_L| \angle -\phi L$

$Z_{R1} = |Z_{R1}| \angle\theta 1$

$Z_{R2} = |Z_{R2}| \angle\theta 2$

into equations (2.1) and calculating a,c,b, and d, the inequality (2.2) becomes:

$$K_1K_2|V_L|^2+|V_L||I_L|[K_1|Z_{R2}|\cos(\theta_2-\phi_L)$$

$$+ K_2|Z_{R1}|\cos(\theta_1-\phi_L)] + |Z_{R1}||Z_{R2}||I_L|^2\cos(\theta_1-\theta_2) > o.$$

Now let

$$\frac{V_L}{I_L} = \frac{|V_L|}{|I_L|} \angle\phi_L = |Z_L| \angle\phi_L$$

then

$$K_1K_2|Z_L|^2+|Z_L|[K_1|Z_{R2}|\cos(\theta_2-\phi_L)+K_2|Z_{R1}|\cos(\theta_1-\phi_L)]$$

$$+ |Z_{R1}||Z_{R2}|\cos(\theta_1-\theta_2) > o \ldots\ldots \quad (2.3)$$

from which all specific types of relay characteristic can be derived.

2.2.1 Directional relay characteristic

If $|Z_{R1}| = K_2 = o$ from (2.3)

we obtain

$$|Z_L|K_1|Z_{R2}| \cos(\theta_2-\phi_L) > o$$

or

$$\cos(\theta_2-\phi_L) \quad \ldots\ldots \quad > o \quad (2.4)$$

i.e.

$$-\pi/2 + \theta_2 < \phi_L < \pi/2 + \theta_2 \quad \text{and}$$

operation occurs to the right of straight line shown in figure (2.8).

2.2.2 Ohm relay characteristic

If $K_1 = -K$, $K_2 = o$, $|Z_{R1}|=|Z_{R2}|=|Z_R|$ and $\theta_1 = \theta_2 = \theta$

the inequality (2.3) reduces to:

$$|Z_L|\cos(\theta-\phi_L) < |Z_R|/K \ldots\ldots \quad (2.5)$$

Operation occurs to the left of straight line shown in fig. (2.9). Inequality (2.5) for $\theta = o$ and $\theta = \pi/2$ reduces to resistance and reactance relay characteristics respectively:

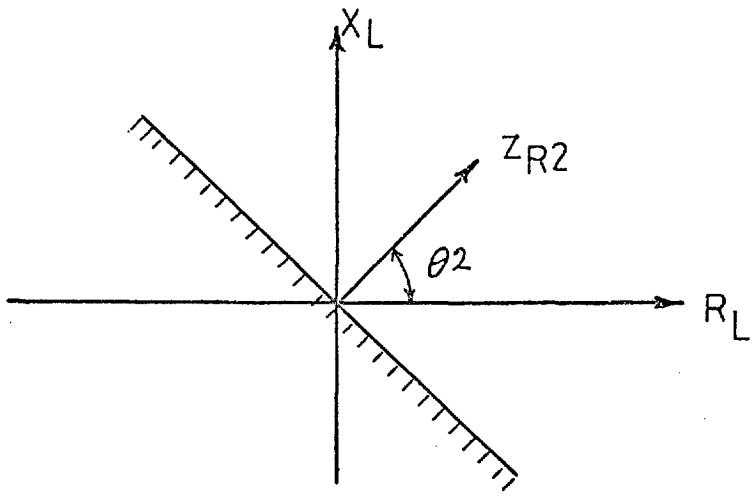

Fig. (2.8) Directional relay characteristic

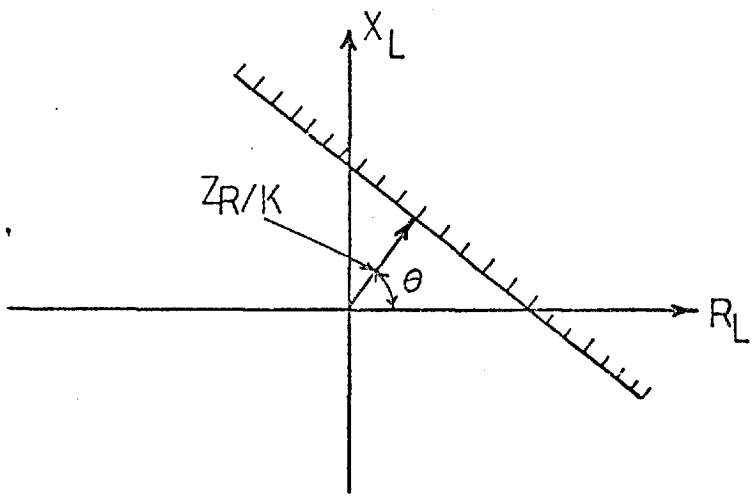

Fig. (2.9) Ohm relay characteristic

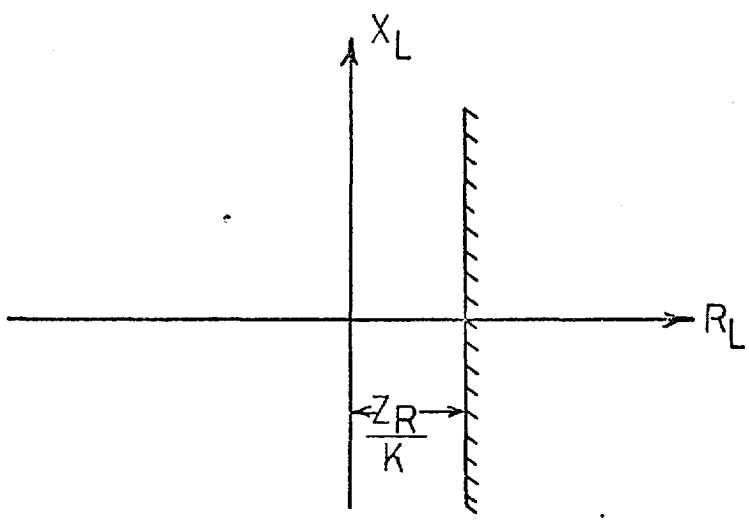

Fig. (2.10) Resistance relay characteristic

i.e. for $\theta = o \quad R_L < |Z_R|/K$ (2.6)

and for $\theta = \pi/2 \quad X_L < |R_R|/K$ (2.7)

These characteristics are shown in fig. (2.10) and (2.11).

2.2.3 Offset impedance relay characteristic

If $K_1=K$, $K_2 = -K$ and $\theta_1 = \theta_2 = \theta$ the inequality (2.3) reduces to:

$$-K^2|Z_L|^2 + KR|Z_L||Z_{R2}|\cos(\theta-\phi_L) - K|Z_L||Z_{R1}|\cos(\theta-\phi_L)$$

$$+ |Z_{R1}||Z_{R2}| > o$$

or

$$[R_L - \frac{1}{2K}(|Z_{R2}|-|Z_{R1}|)\cos\theta]^2$$

$$+ [X_L - \frac{1}{2K}(|Z_{R2}|-|Z_{R1}|)\sin\theta]^2 < (|Z_{R2}|+|Z_{R1}|)^2/4K^2 \quad (2.8)$$

This is the equation of a circle of radius $(|Z_{R1}|+|Z_{R2}|)/2K$ and with centre $(|Z_{R2}|-|Z_{R1}|)/2K$ $\underline{/\theta}$ and is shown in fig.(2.12).

2.2.4 Impedance relay characteristic

For $|Z_{R1}| = |Z_{R2}| = |Z_R|$ the inequality (2.8) reduces to:

$$R_L^2 + X_L^2 < |Z_R|^2/K \quad (2.9)$$

which represents an impedance relay shown in fig. (2.13).

2.2.5 Mho relay characteristic

For $|Z_{R1}| = o$ and $|Z_{R2}| = |Z_R|$ the inequality (2.8) reduces to:

$$(R_L - |\frac{Z_R}{2K}|\cos\theta)^2 + (X_L - |\frac{Z_R}{2K}|\sin\theta)^2 = |\frac{Z_R}{4K^2}|^2 \ldots. \quad (2.10)$$

which represents a mho relay shown in (2.14).

2.3 PROBLEMS OF ANALOGUE RELAYS

The small but finite inertia of induction cup relay serve to filter out high frequency harmonic and non-harmonic components in the relay inputs. Also the induced eddy current

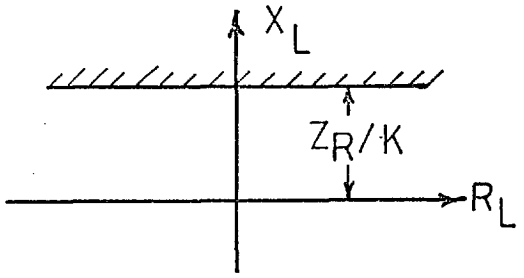

Fig. (2.11) Reactance relay characteristic

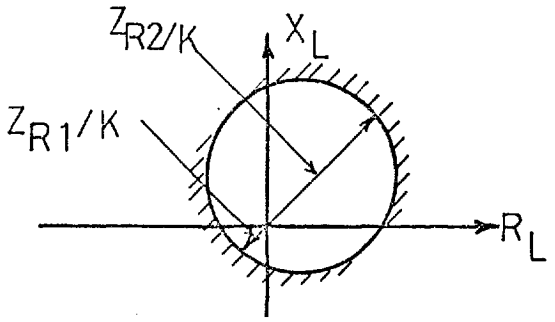

Fig. (2.12) Offset impedance relay

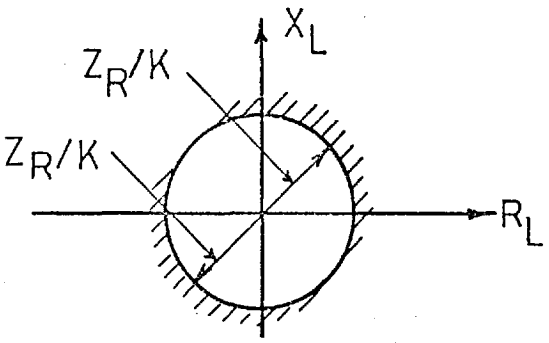

Fig. (2.13) Impedance relay

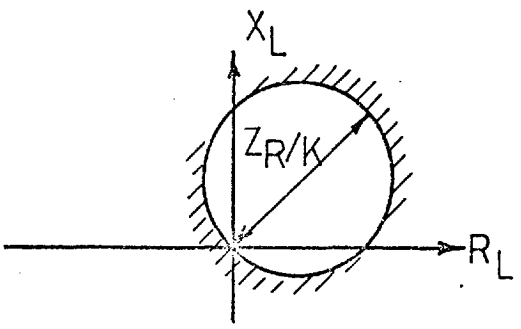

Fig. (2.14) Mho relay

in the cup due to the exponential dc offset and its resulting torque is negligible and so this relay tends to have immunity to dc offset and other transient components. But this immunity is achieved at the expense of operating speed. At low voltage levels this slow operation can be tolerated but for a high voltage integrated system, is not desirable. Although the static distance relay has the advantage of being free from inertia and other mechanical problems, it is still sensitive to noise, transient dc offset and fault generated harmonics. These relays must be equipped with a very sharp analog filter to remove dc and other unwanted components of the voltage and current waveforms which delays the relay operation. The reason why the block-average relay has been successful in practice is that at present there is no need for a distance relay to operate in less than two cycles thus making it possible to tolerate filter time delays and to equip the relay with a very sharp cut-off filter.

In the future from the stability point of view there is a need to detect the fault in one cycle or less, the block-average relay can not be relied upon. Another major drawback is that it is difficult and expensive, though not impossible, to provide an efficient and reliable supervisory system that checks the relay all the time and estimates its behaviour during possible faults and prints or displays the necessary information. One solution to these problems is the use of a digital relay or computer relaying. Digital relays could be made inherently faster than block-average and other static relays. They can calculate the resistance and reactance of the line continuously and it would be possible for them to show the result on a small display, if required a central computer can effectively supervise the behaviour of many digital relays and give an alarm whenever it

finds a defective part or element. Digital relaying by choice of an appropriate algorithm, can effectively cope with dc offset and other unwanted components of current and voltage waveforms. It can also provide an optimum characteristic with an effective fault coverage and immunity to extreme balanced system conditions such as heavy loads and power swing. In the next chapter these aspects of digital algorithms will be studied.

CHAPTER 3

ALGORITHMS FOR DISTANCE PROTECTION

3.1 INTRODUCTION

Increasing interest is being shown in the use of digital processors for the protection switching and data acquisition required in modern high-voltage substations. One of the most difficult functions to fulfill by digital methods is that of transmission line protection employing samples of the voltage and current waveforms taken from high voltage transducer equipment at the usual relaying point. Given an adequate speed of sampling and conversion to digital form for processing, problems remain of calculating the fault conditions within a defined protection zone of the transmission line. For this purpose the most onerous condition is when a fault occurs at a voltage maximum on one phase, because the consequent discharge of capacitive energy through the line inductance causes harmonics and non-harmonics to be generated in the current and voltage. In addition, noise and non-linearity of the transducers result in further unwanted components against which any algorithm used to calculate fault impedance should be immune. The smoothness of the current and in particular the voltage waveforms depend upon generator source reactance and transmission line length. With a high reactance source and a long line considerable distortion occurs as is born out by a field oscillogram reproduced in fig. (3.1) for a three phase fault. It can be seen that during the first fault cycle the voltages exhibit considerable noise and distortion although in this case such noise could be attributed to the use of a capacitor-divider voltage transducer. In fig. (4.8) simulated current and voltage waveforms are depicted in which again the

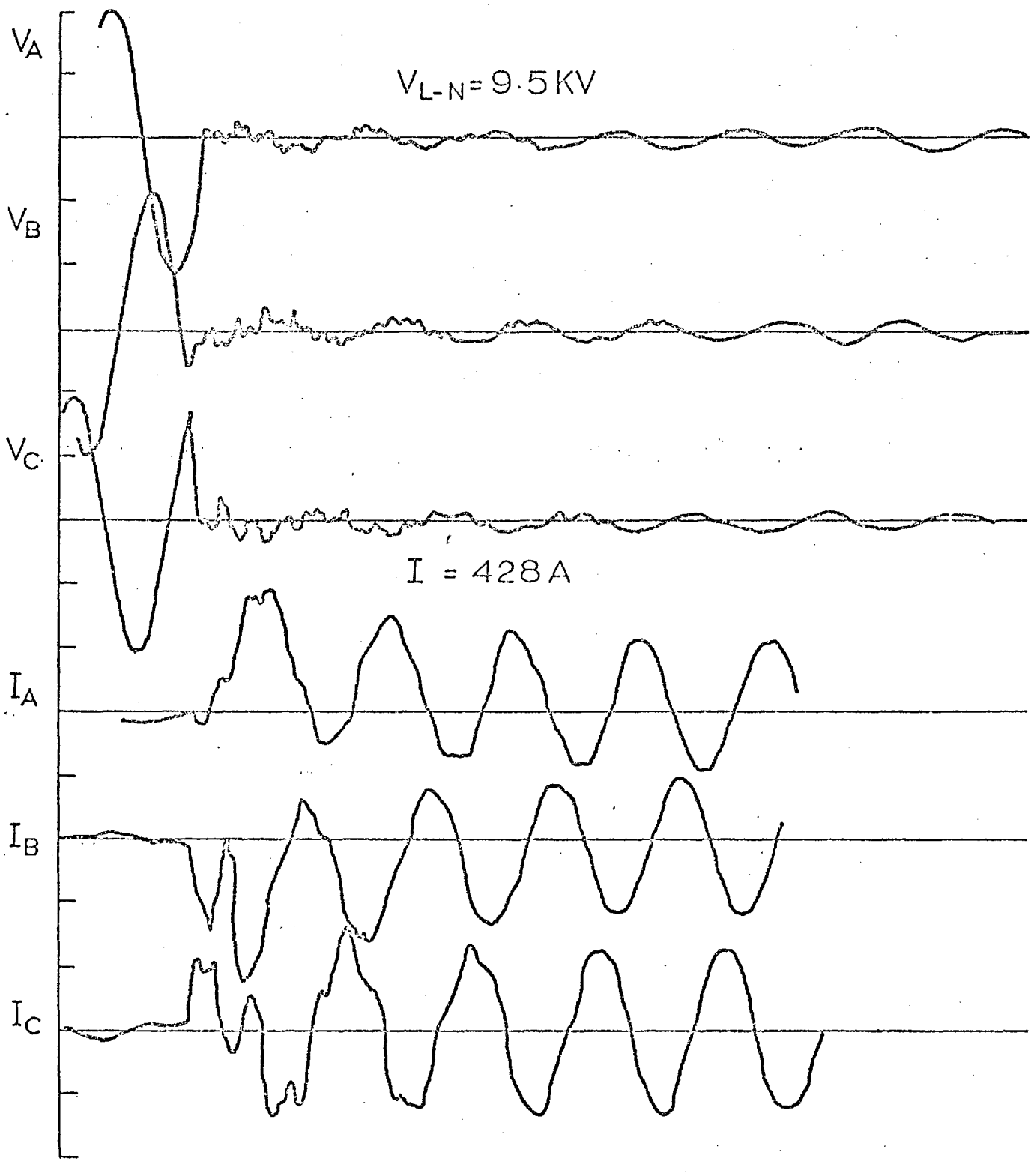

NOTE : Voltage obtained from a capacitive divider.

*FIG.*3·1 Field oscillogram for 3 phase fault on long line.

importance of fault generated harmonics and non-harmonics in both current and voltage waveforms are clearly seen. Some field oscillograms may not show such a distortion, because of the frequency response of the recorder and transducer which filter high frequency components. In applying digital methods to fault calculation, the following points should be given careful consideration:

(i) Type of algorithm: Some algorithms are capable of removing a portion of the unwanted components or to directly account for them, but others are true and reliable only in steady state, i.e. with sinusoidal currents and voltages.

(ii) Sampling rate: This is one of the most decisive factors in the implementation of digital algorithms for on-line protection. Previously, many papers have suggested various samplin rates from 4^{29} to 40^{21} samples per cycle without justifying the choice. High rate of sampling requires complicated and expensive hardware for digital implementation, whilst too low a sampling rate may impair the accuracy from a numerical computation and filtering point of view. It will be shown that an acceptable accuracy can be obtained by an optimum sampling rate.

(iii) Cut off frequency of the analogue filter: This is another decisive factor in the implementation of digital algorithms. In most papers on digital distance relaying, this factor, like sampling rate, has received little attention. Usually a frequency corresponding to half the sampling rate has been suggested for the cut-off of the required analogue filter, without mention of the order or the filter type. Fig. (3.2) shows the overall spectrum of the Fourier method (section 3.32) with 8 samples per cycle(400Hz) and a single pole Butterworth

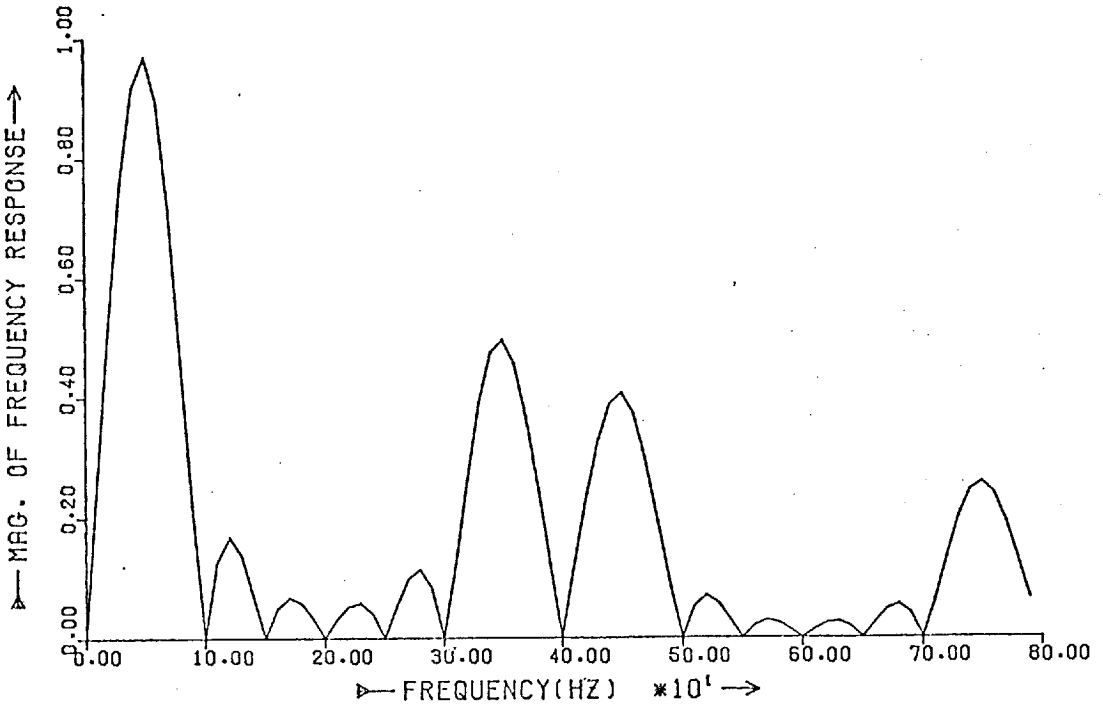

Fig. (3.2) Spectrum of the Fourier method with 8 samples per cycle and a single pole Butterworth filter with 200 Hz cut-off frequency.

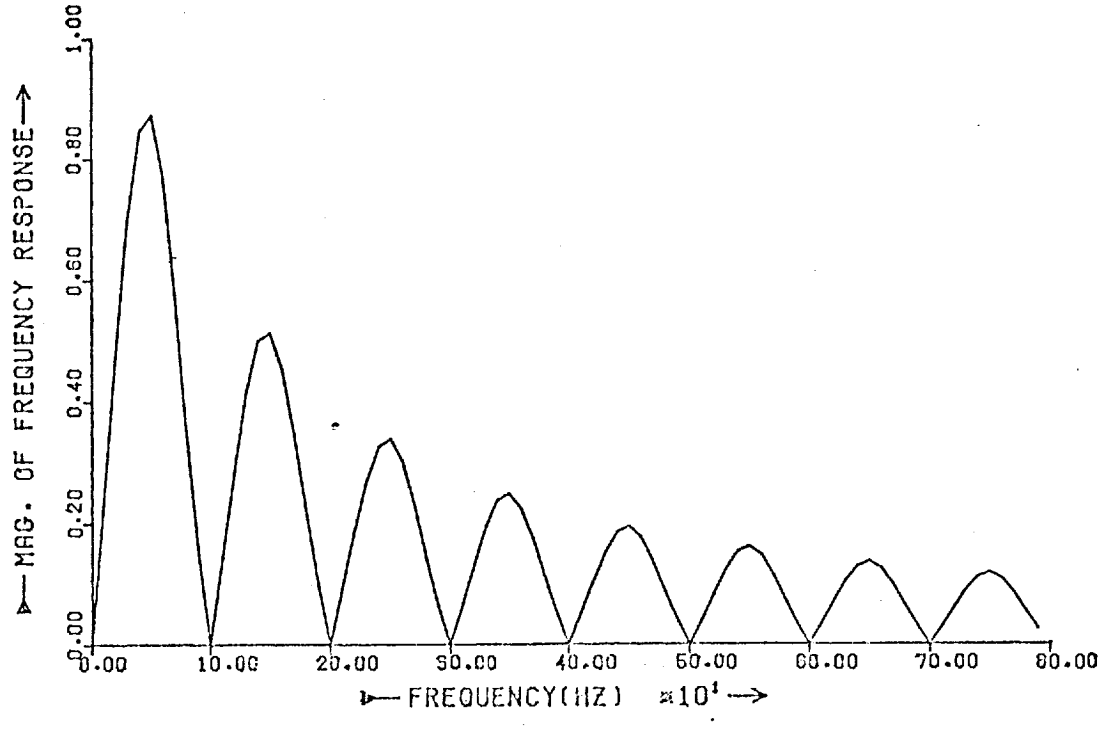

Fig. (3.3) Spectrum of the Fourier method with 4 samples per cycle and a single pole Butterworth filter with 100 Hz cut-off frequency.

filter with a 200 Hz cut-off frequency. Similarly fig.(3.3) shows the spectrum of this method for 4 samples per cycle (200 Hz) and a single pole filter with 100 Hz cut-off frequency. It is quite clear that in the former case the components around 7th and 9th harmonic and in the latter one the components around 3rd, 5th, ... have not been removed effectively, and so in both cases either the cut-off frequencies of the analogue filter must be lowered or filters with more poles should be used. In another case using McInnes's method[25], with any sampling rate the analogue filter at least should be a second order with 60 Hz cut-off frequency. Comparing 60Hz with frequencies of 400 or 500Hz which are usually quoted with 16 or 20 samples per cycle, it can be realized why this very interesting method has been reported to incur large errors during system transients. Considering the foregoing points different distance protection algorithms will be studied, their immunity to noise will be discussed and from these the sampling rate and order of the analogue filter and its cut-off frequency will be determined.

3.2 THEORY OF THREE-PHASE RELAYING

An overhead line with one or more earth wires bonded to ground at each transmission line tower will be considered. These earth wires and earth can be represented by a single equivalent conductor. Disregarding the shunt capacitance, the transmission line can thus be represented by a four conductor arrangement as shown in fig. (3.4).

The voltage drops from the relaying point to the fault point for all types of faults are given by the following expressions:

$$V_a - V_a' = (Z_{aa}I_a + Z_{ab}I_b + Z_{ac}I_c + Z_{ad}I_d) \times \ldots \quad (3.1a)$$

$$V_b - V_b' = (Z_{ba}I_a + Z_{bb}I_b + Z_{bc}I_c + Z_{bd}I_d) \times \ldots \quad (3.1b)$$

$$V_c - V_c' = (Z_{ca}I_a + Z_{cb}I_b + Z_{cc}I_c + Z_{cd}I_d) \times \ldots \quad (3.1c)$$

But $I_a + I_b + I_c + I_d = 0$ and therefore:

$$V_a - V_d' = [(Z_{aa}-Z_{ad})I_a + (Z_{ab}-Z_{ad})I_b + (Z_{ac}-Z_{ad})I_c] \times \ldots (3.2a)$$

$$V_b - V_b' = [(Z_{ba}-Z_{bd})I_a + (Z_{bb}-Z_{bd})I_b + (Z_{bc}-Z_{bd})I_c] \times \ldots (3.2b)$$

$$V_c - V_c = [(Z_{ca}-Z_{cd})I_a + (Z_{cb}-Z_{cd})I_b + (Z_{cc}-Z_{cd})I_c] \times \ldots (3.2c)$$

These equations can be rewritten as:

$$V_a - V_a' = [Z_{sa}I_a + Z_{mab}I_b + Z_{mac}I_c] \times \quad (3.3a)$$

$$V_b - V_b' = [Z_{mba}I_a + Z_{sb}I_b + Z_{mbc}I_c] \times \quad (3.3b)$$

$$V_c - V_c' = [Z_{mca}I_a + Z_{mcb}I_b + Z_{sc}I_c] \times \quad (3.3c)$$

where

$$Z_{sa} = Z_{aa}-Z_{ad},\ Z_{mab} = Z_{ab}-Z_{ad},\ Z_{mac} = Z_{ac}-Z_{ad}$$

$$Z_{sb} = Z_{bb}-Z_{bd},\ Z_{mbd} = Z_{bd}-Z_{bd},\ Z_{mbc} = Z_{bc}-Z_{bd}$$

$$Z_{sc} = Z_{cc}-Z_{cd},\ Z_{mcd} = Z_{cd}-Z_{cd},\ Z_{mcb} = Z_{cb}-Z_{cd}.$$

Assuming that the transmission line is perfectly transposed, equations (3.3) become:

$$V_a - V_a' = [Z_s I_a + Z_m (I_b+I_c)] \times \ldots\ldots \quad (3.4a)$$

$$V_b - V_b' = [Z_s I_b + Z_m (I_a+I_c)] \times \ldots\ldots \quad (3.4b)$$

$$V_c - V_c' = [Z_s I_c + Z_m (I_a+I_b)] \times \ldots\ldots \quad (3.4c)$$

where

$$Z_s = Z_{sa} = Z_{sb} = Z_{sc}$$

$$Z_m = Z_{mab} = Z_{mba} = Z_{mca} = Z_{mac} = Z_{mbc} = Z_{mcb}$$

The positive and negative sequence impedances of the transmission line are equal and are given by:

$$Z_1 = Z_2 = Z_s - Z_m \qquad (3.5a)$$

and the zero sequence impedance is given by:

$$Z_o = Z_s + 2\,Z_m \quad \ldots\ldots\ldots \qquad (3.5b)$$

From these equations it can be seen that

$$Z_s = \frac{1}{3}\,(2Z_1 + Z_o) \quad \ldots\ldots\ldots \qquad (3.6a)$$

and

$$Z_m = \frac{1}{3}\,(Z_o - Z_1) \quad \ldots\ldots\ldots \qquad (3.6b)$$

Substituting Z_s and Z_m from equations (3.6) in equations (3.4) gives:

$$V_a - V_a' = [Z_1 I_a + (Z_o - Z_1)\,I_o] \quad x \ldots\ldots\ldots \qquad (3.7a)$$

$$V_b - V_b' = [Z_1 I_b + (Z_o - Z_1) I_o\,] \quad x \ldots\ldots\ldots \qquad (3.7b)$$

$$V_c - V_c' = [Z_1 I_c + (Z_o - Z_1) I_o\,] \quad x \ldots\ldots\ldots \qquad (3.7c)$$

The voltages at the fault point (V_a', V_b', V_c') will depend on the type of fault, the fault resistance and the fault current which may contain infeed from the remote end. At this stage, for simplicity, the infeed is zero.

Equations (3.3), (3.4) and (3.7) will now be applied to various types of fault.

3.2.1 Single phase to earth fault

Consider a phase a to earth fault through a fault resistance Rg, so that:

$$V_a' = Rg \,.\, I_a \qquad (3.8)$$

and equation (3.3a) becomes

$$V_a = x\, Z_{sa}\left(I_a + \frac{Z_{mab}}{Z_{sa}}\, I_b + \frac{Z_{mac}}{Z_{sa}}\, I_c\right) + Rg.I_a \qquad (3.9)$$

equation (3.9) can be written as:

$$V_a = x\, Z_{sa}\, I_R + Rg\, I_a \quad \ldots\ldots \tag{3.10}$$

where

$$I_R = I_a + \frac{Z_{mab}}{Z_{sa}}\, I_b + \frac{Z_{mac}}{Z_{sa}}\, I_c \tag{3.11}$$

The fault resistance Rg has two components[20], the resistance of the arc and of the ground return. The latter, because of the earth characteristic is somewhat nonlinear. Fault arc resistance can be accounted by the Van Warrington formula:

$$Rarc = \frac{8750\ell}{I^{1.4}} \quad \ldots\ldots \tag{3.12}$$

where ℓ is the length of the arc in feet in still air and I is the fault current. ℓ will initially be equal to the conductor spacing but it will increase in the presence of cross winds according to the following formula

$$Rarc = \frac{8750(s+3ut)}{I^{1.4}} \quad \ldots\ldots \tag{3.13}$$

where s is the conductor spacing and u is the wind velocity in miles per hour and t the duration in seconds. The arc voltage is

$$Varc = \frac{8750(s+3ut)}{I^{0.4}} \quad \ldots\ldots\ldots \tag{3.14}$$

this non-linear relation means that, if an arcing fault occurs near the relay bus, the fault current may be sinusoidal but the voltage waveform will have a rectangular tendency. Thus it can be seen that the fault resistance cannot be fully predicted and for this reason and for the sake of simplicity, the fault resistance will be neglected and equation (3.10) reduces to:

$$V_a = x\, Z_{sa}\, I_R \quad \ldots\ldots \tag{3.11}$$

By shaping the relay characteristic, the underreaching of the distance measurement due to the fault resistance can be avoided.

For a transposed line from equations (3.4) the phase to earth voltage V_a may be written as:

$$V_a = Z_s \, I_{oa} \tag{3.12}$$

where

$$I_{oa} = I_a + \frac{Z_m}{Z_s} \, (I_b + I_c) \tag{3.13}$$

The operating current I_{oa} is made up of the correct proportion of three phase currents and is called the "sound phase compensated current.

In analogue relaying it is obtained by a circuit as in fig. (3.5). In this circuit I_{oa}, I_{ob} and I_{oc} (operating signals for different phase to earth faults) are

$$I_{oa} = \frac{n_1}{n_3} \, [(I_a + \frac{n_2}{n_1} \, (I_b + I_c)] \tag{3.14a}$$

$$I_{ob} = \frac{n_1}{n_3} \, [(I_b + \frac{n_2}{n_1} \, (I_a + I_c)] \tag{3.14b}$$

$$I_{oc} = \frac{n_1}{n_3} \, [(I_c + \frac{n_2}{n_1} \, (I_a + I_b)] \tag{3.14c}$$

where

$$\frac{n_2}{n_1} = |\frac{Z_m}{Z_s}| \tag{3.15}$$

Instead of equations (3.4) we can use equations (3.7) which gives:

$$V_a = Z_1 \, I_{OA} \tag{3.16}$$

where

$$I_{OA} = I_a + \frac{Z_o - Z_1}{Z_1} \, I_o \tag{3.17}$$

I_{OA} is called the residual compensated current and in analogue relaying it is obtained by a circuit as in fig. (3.6).

In this circuit I_{OA}, I_{OB}, I_{OC} (operating signal for different phase-to-earth faults) are

$$I_{OA} = \frac{n_1}{n_3} \, (I_a + \frac{3n_2}{n_1} \, I_o) \tag{3.18a}$$

$$I_{OB} = \frac{n_1}{n_3} \, (I_b + \frac{3n_2}{n_1} \, I_o) \tag{3.18b}$$

$$I_{OC} = \frac{n_1}{n_3} \, (I_c + \frac{3n_2}{n_1} \, I_o) \tag{3.18c}$$

where

$$\frac{n_2}{n_1} = |\frac{Z_o - Z_1}{3Z_1}| \tag{3.19}$$

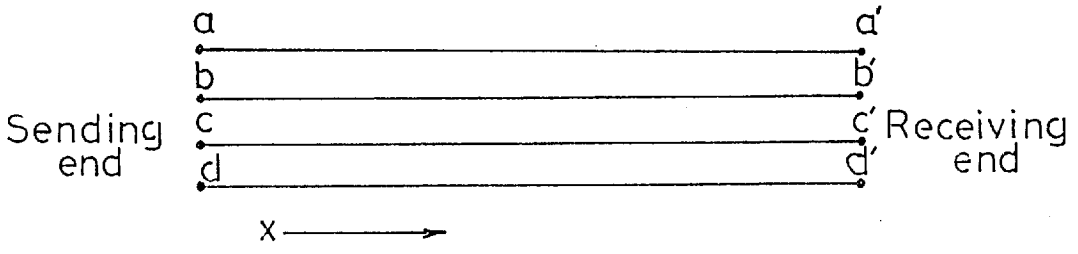

Fig. (3.4) 3-phase and ground line

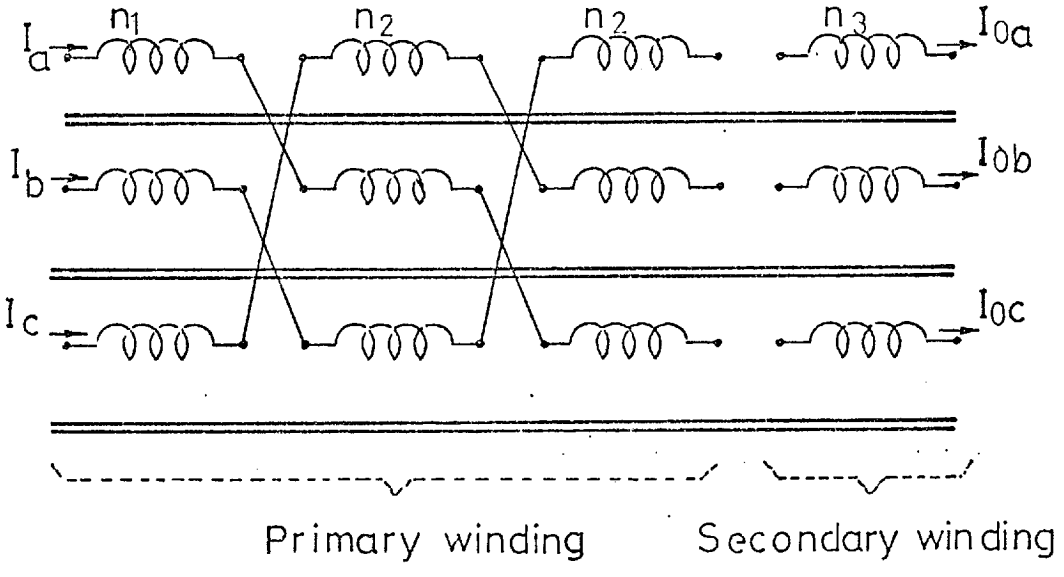

Fig. (3.5) Sound phase compensation

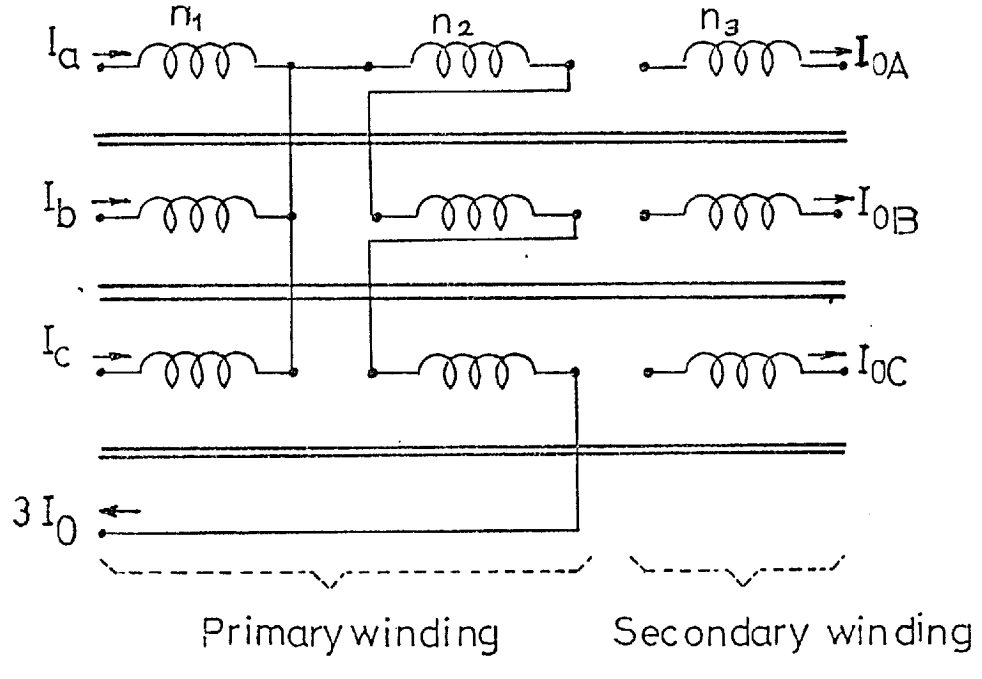

Fig. (3.6) Residual compensation

As can be seen from equations (3.15) and (3.19) in analogue relaying the phase angles of $\frac{Z_m}{Z_s}$ and $\frac{Z_o - Z_1}{3Z_1}$ are neglected, but in computer relaying it is possible to use these coefficients without any approximation. Inevitably this will add to computation time and so wherever there is a need for simplicity, the scalar value could be used.

Using instantaneous values of voltage and current, equation (3.3a) can be written:

$$v_a = xR_{sa}\left(i_a + \frac{R_{mab}}{R_{sa}} i_b + \frac{R_{mac}}{R_{sa}} i_c\right) + xL_{sa} \frac{d}{dt}\left(i_a + \frac{L_{mab}}{L_{sa}} i_b + \frac{L_{mac}}{L_{sa}} i_c\right) \quad (3.20)$$

where

$$R_{sa} = R_{aa} - R_{ad}\,, \quad L_{sa} = L_{aa} - L_{ad}$$

$$R_{mab} = R_{ab} - R_{ad}, \quad L_{mab} = L_{ab} - L_{ad}$$

R

$$R_{mac} = R_{ac} - R_{ad}\,, \quad L_{mac} = L_{ac} - L_{ad}$$

Putting $\left(i_a + \frac{R_{mab}}{R_{sa}} i_b + \frac{R_{mac}}{R_{sa}} i_c\right) = i_x$

and $\left(i_a + \frac{L_{mab}}{L_{sa}} i_b + \frac{L_{mac}}{L_{sa}} i_c\right) = i_y$

equation (3.20) becomes:

$$v_a = x\, R_{sa}\, i_x + x\, L_{sa} \frac{di_y}{dt} \quad (3.21)$$

We can see that the coefficients $\frac{R_{mab}}{R_{sa}}$, ... and $\frac{L_{mab}}{L_{sa}}$, ... are constant and independent of the fault point, so by taking samples of i_a, i_b and i_c the new samples i_x and i_y can be computed. Similarly equations (3.4a) and (3.7a), become:

$$v_a = x\, R_s\left[i_a + \frac{R_m}{R_s}(i_b + i_c)\right] + xLs\frac{d}{dt}\left[i_a + \frac{L_m}{L_s}(i_b + i_c)\right] \quad (3.22)$$

and

$$v_a = x\, R_1\left(i_a + \frac{R_o - R_1}{R_1} i_o\right) + xL_1 \frac{d}{dt}\left(i_a + \frac{L_o - L_1}{L_1} i_o\right) \quad (3.23)$$

and these can also be written in the form of equation (3.21).

3.2.2 Double-phase fault

For a double phase fault, the fault impedance may be represented as in fig.(3.7a) when the fault involves ground and as in fig. (3.7b) when isolated from ground. Under these conditions the voltage to ground of the a and b phases at the sending end become:

$$V_a = x[Z_{sa}I_a+Z_{mab}I_b+Z_{mac}I_c] + \frac{R}{2} I_a+(I_a+I_b)\ Rg$$

and $$V_b = x[Z_{mba}I_a+Z_{sb}I_b+Z_{mbc}I_c] + \frac{R}{2} I_b+(I_a+I_b)\ Rg$$

Subtracting V_b from V_a gives:

$$V_a-V_b=x\ (Z_{sa}-Z_{mba})\left[I_a+ \frac{Z_{mab}-Z_{sb}}{Z_{sa}-Z_{mba}} I_b+ \frac{Z_{mac}-Z_{mbc}}{Z_{sa}-Z_{mba}} I_c\right]+ \frac{R(I_a-I_b)}{2(Z_{sa}-Z_{mba})} \quad (3.24)$$

Since equation (3.24) does not involve Rg, it can be applied to both fig. (3.7a) and fig.(3.7b). In order to put equation (3.24) in realizable form its last term, which is the error caused by arc resistance, must be neglected and hence it reduces to:

$$V_a-V_b = x(Z_{sa}- Z_{mba})\ I_R \quad (3.25)$$

where $$I_R = I_a + \frac{Z_{mab}-Z_{sb}}{Z_{sa}-Z_{mba}} I_b + \frac{Z_{mac}-Z_{mbc}}{Z_{sa}- Z_{mba}} I_c \quad (3.26)$$

For a transposed line the voltage between faulty phases is:

$$V_a-V_b = x\ Z_1\ (I_a-I_b) \quad (3.27)$$

Hence, in this case no extra term is required and the conventional delta relaying current (I_a-I_b) and voltage V_a-V_b may be used to find the positive sequence impedance xZ_1 of the line.

Using instantaneous values of voltage and current for an untransposed line equation (3.24) becomes:

$$\upsilon_a-\upsilon_b = x(R_{sa}-R_{mba})\left[i_a+ \frac{R_{mab}-R_{sb}}{R_{sa}-R_{mba}} i_b+ \frac{R_{mac}-R_{mbc}}{R_{sa}-R_{mba}} i_c\right]$$

$$+ x(L_{sa}-L_{mba})\ \frac{d}{dt}\left[i_a + \frac{L_{mab}-L_{sb}}{L_{sa}-L_{mba}} i_b+ \frac{L_{mac}-L_{mbc}}{L_{sa}-L_{mba}} i_c\right] \quad (3.28)$$

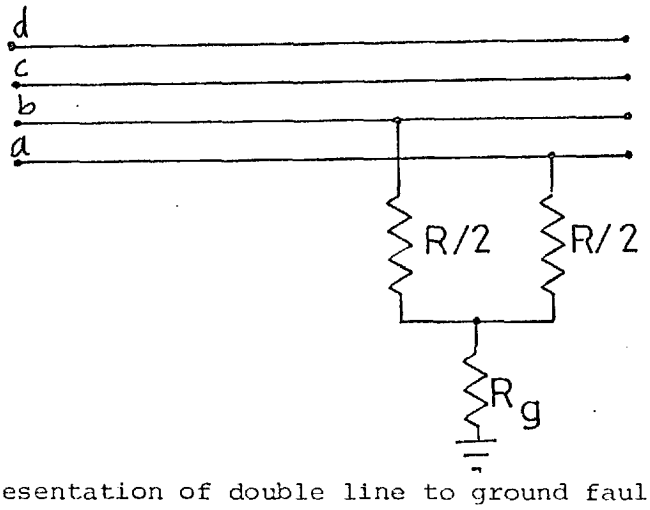

Fig. (3.7a) Representation of double line to ground fault.

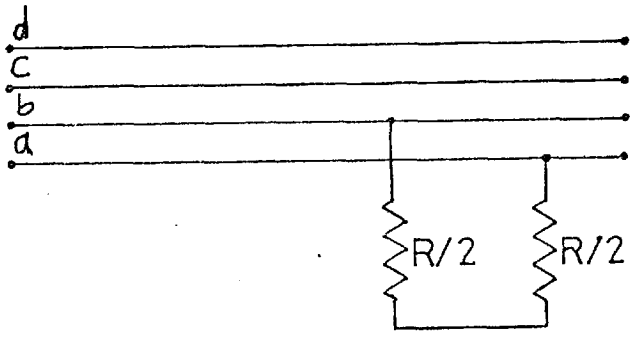

Fig. (3.7b) Representation of double line fault.

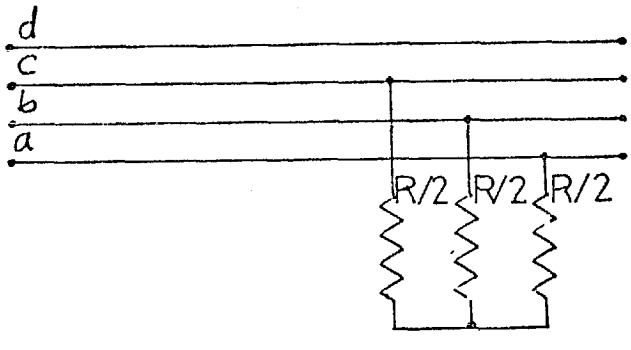

Fig. (3.8a) Representation of three phase fault.

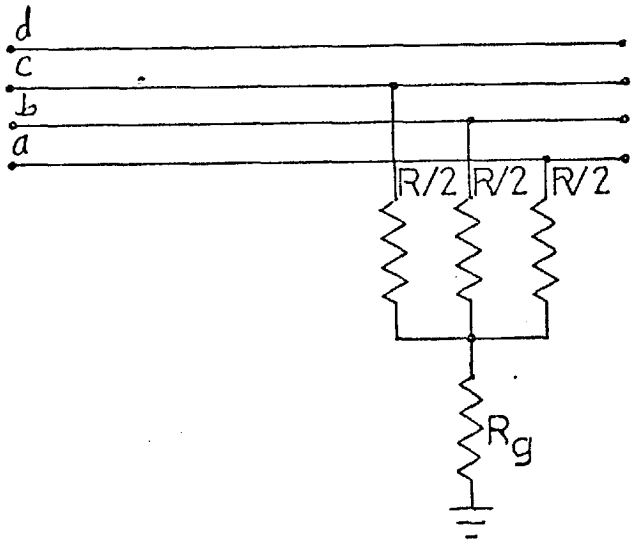

Fig. (3.8b) Representation of three phase to ground fault.

Putting $i_x = i_a + \frac{R_{mab}-R_{sb}}{R_{sa}-R_{mba}} i_b + \frac{R_{mac}-R_{mbc}}{R_{sa}-R_{mba}} i_c$

and $i_y = i_a + \frac{L_{mab}-L_{sb}}{L_{sa}-L_{mba}} i_b + \frac{L_{mac}-L_{mbc}}{L_{sa}-L_{mba}} i_c$

equation (3.28) becomes:

$$\upsilon_a-\upsilon_b = x(R_{sa}-R_{mba})\, i_x + x\,(L_{sa}-L_{mba}) \frac{d}{dt}\, i_y \qquad (3.29)$$

Similarly for a transposed line, using instantaneous values equation (3.27) may be written:

$$\upsilon_a-\upsilon_b = x\, R_1(i_a-i_b) + xL_1 \frac{d}{dt} (i_a-i_b) \qquad (3.30)$$

3.2.3 Three phase fault

For three phase faults, the fault impedance may be represented as in fig.(3.8a) or fig.(3.8b). Under this condition the voltage to ground of the three phases at the sending end are:

$$V_a = x(Z_{sa}I_a + Z_{mab}I_b + Z_{mac}I_c) + R\, I_a + RgI_o$$

$$V_b = x(Z_{mba}I_a + Z_{sb}I_b + Z_{mbc}I_c) + RI_b + RgI_o$$

$$V_c = x(Z_{mca}I_a + Z_{mcb}I_b + Z_{sc}I_c) + RI_c + RgI_o$$

Subtracting equation V_b from V_a gives:

$$V_a-V_b = x(Z_{sa}-Z_{mba}) \left[I_a + \frac{Z_{mab}-Z_{sb}}{Z_{sa}-Z_{mba}} I_b \right.$$

$$\left. + \frac{Z_{mac}-Z_{mbc}}{Z_{sa}-Z_{mba}} I_c \right] + \frac{R(I_a-I_b)}{Z_{sa}-Z_{mba}} \qquad (3.31)$$

Since this equation does not involve Rg it can also be applied to an isolated three-phase fault. Equation (3.31) is the same as equation (3.24) for a double phase fault, also in instantaneous form we obtain the same as equation (3.28), and hence this case is exactly the same as double-phase fault.

3.3 CALCULATION OF RESISTANCE AND INDUCTANCE

In the previous section, using phasor an equation of the form:

$$V = ZI \quad \ldots. \tag{3.32}$$

and in instantaneous values, an equation of the form:

$$\upsilon = Ri_x + L \frac{di_y}{dt} \tag{3.33}$$

was obtained for all fault conditions where the values of V, I, υ, i_x and i_y could be found by appropriate choice and combination of voltages and currents. From equation (3.32) or (3.33) the values of R and L can be calculated by several methods. These methods and their immunity to noise and dc offset will be studied in the following sections.

3.3.1 Peak determination method (ref. 21)

The peak determination method finds the line impedance by the predictive calculation of peak current and peak voltage in equation (3.32). The system voltages and currents are sampled continuously and the peaks calculated using these samples. Consider a typical voltage υ

$$\upsilon = V_p \sin\omega t \tag{3.34}$$

where V_p is the unknown peak voltage. Differentiating (3.34) with respect to t gives:

$$\upsilon' = \omega V_p \cos\omega t \tag{3.35}$$

where υ' is the first derivative of υ. If υ' can be determined, the peak voltage is given by

$$V_p^2 = \upsilon^2 + \left(\frac{\upsilon'}{\omega}\right)^2 \tag{3.36}$$

An equation similar to (3.36) also applies to the current samples and the peak current can similarly be determined. The modulus of the line impedance is obtained by division and, the phase difference λ between the voltage and current waveform is given by:

$$\lambda = \arctan\left(\frac{\omega i}{i'}\right) - \arctan\left(\frac{\omega v}{v'}\right) \qquad (3.37)$$

where i' is the first derivative of i. Knowing λ, the complete line impedance is determined.

This method relies on the fact that the dc offset in the primary current can be eliminated by loading the c.t. secondary with a corresponding mimic impedance. It can be shown that[21], if a c.t. secondary is loaded with the same $\frac{x}{R}$ ratio as the primary circuit, the exponential term vanishes, and the secondary voltage becomes a pure sinusoid. Exact cancellation of the dc offset, however, is not possible for all faults, because of the variation in x and R up to the fault. It is recommended[21] to match the secondary burden to a primary circuit composed of the source and 90% of the line impedance. In order to filter out the dc component, Rockefeller[22] suggested the use of first and second derivatives for the purpose of impedance calculation as follows:

$$Z = \frac{v'^2 + \left(\frac{v''}{\omega}\right)^2}{i'^2 + \left(\frac{i''}{\omega}\right)^2} \qquad (3.38)$$

The dc component of the current or voltage waveform has an exponential form such as $e^{-\beta t}$. The spectrum of this function is $\frac{1}{\sqrt{\beta^2+\omega^2}}$ which shows that $e^{-\beta t}$ contains both dc and low frequency components. Hence by differenciation an exponential dc component cannot be removed completely. The use of the second derivative has two main drawbacks; firstly the numerical errors in-

volved in calculating the second derivative are large and secondly, as will be seen in section (3.3.1.1), the amplification of high and low frequency components is greater than that occuring in euqation (3.36).

3.3.1.1 Immunity to noise and high frequency components

Using the basic central and backward difference expression for derivatives with either the first term only or the first plus second terms, the following difference expressions can be derived[21]. Here these equations are written for voltage samples, but it is clear that the results are general.

$$v'_k = \frac{1}{2T} (v_{k+1} - v_{k-1}) \tag{3.39}$$

or $$v'_k = \frac{1}{T} (-\frac{1}{12}v_{k+2} + \frac{2}{3}v_{k+1} - \frac{2}{3}v_{k-1} + \frac{1}{12}v_{k-2}) \tag{3.40}$$

or $$v'_k = \frac{1}{T} (v_k - v_{k-1}) \tag{3.41}$$

or $$v'_k = \frac{1}{2T} (v_k - v_{k-2}) \tag{3.42}$$

These four equations can be looked upon ds digital filters with the samples of voltage as input and the voltage derivative as output. By using the Z transform, the transfer function and hence the frequency spectrum for each of the above digital filters can be obtained from which the effects of noise and high frequency components can be studied. The transfer functions of equations (3.39) to (3.42) respectively are as follows:

$$H_1(Z) = \frac{1}{2T} (1 - \bar{Z}^2) \tag{3.43}$$

$$H_2(Z) = \frac{1}{12T} (\bar{Z}^2 - 1)(\bar{Z}^2 - 8\bar{Z}^1 + 1) \tag{3.44}$$

$$H_3(Z) = \frac{1}{T} (1 - \bar{Z}^1) \tag{3.45}$$

$$H_4(Z) = \frac{1}{2T} (1 - \bar{Z}^2) \tag{3.46}$$

Replacing Z with $e^{j\omega T}$ the frequency spectrum of the filters can be obtained as:

$$|H_1(f)| = 50N \left| \sin \frac{\pi f}{25N} \right| \tag{3.47}$$

$$|H_2(f)| = \frac{50N}{3} \left| (4-\cos \frac{\pi f}{25N}) \sin \frac{\pi f}{25N} \right| \tag{3.48}$$

$$|H_3(f)| = 100N \left| \sin \frac{\pi f}{50N} \right| \tag{3.49}$$

$$|H_4(f)| = 50N \left| \sin \frac{\pi f}{25N} \right| \tag{3.50}$$

where N is the number of S/C. We can see that from spectrum point of view the fourth and the first methods are the same and so only the first three methods will be studied. Also it can be seen that the spectrums not only depend on the frequency but they are also functions of sampling rate N. All methods have more or less a sinusoidal shape, but to have all frequency components attenuated with respect to 50HZ, they must have their maximum at 50HZ. In the first method the $|\sin \frac{\pi f}{25N}|$ has its maximum at 50HZ when:

$$\frac{\pi \cdot 50}{25 \cdot N} = \frac{\pi}{2}$$

or $N = 4$ S/C

Consequently in this method 4 S/C from filtering point of view is the optimum. By increasing the sampling rate the desired immunity becomes worse. Figs. (3.9) and (3.10) show the spectrums of the filter for 4 and 16 samples per cycle.

In the second method it can be shown that the maximum would occur when:

$$\cos \frac{\pi f}{25N} = 1 - \sqrt{1.5}$$

and for this maximum to be at 50Hz. N = 3.5 S/C which means that practically the 4 S/C is again the optimum sampling rate. The spectrum for 4 and 16 S/C are given in figures (3.11) and (3.12) which are slightly different from figures (3.9) and (3.10)

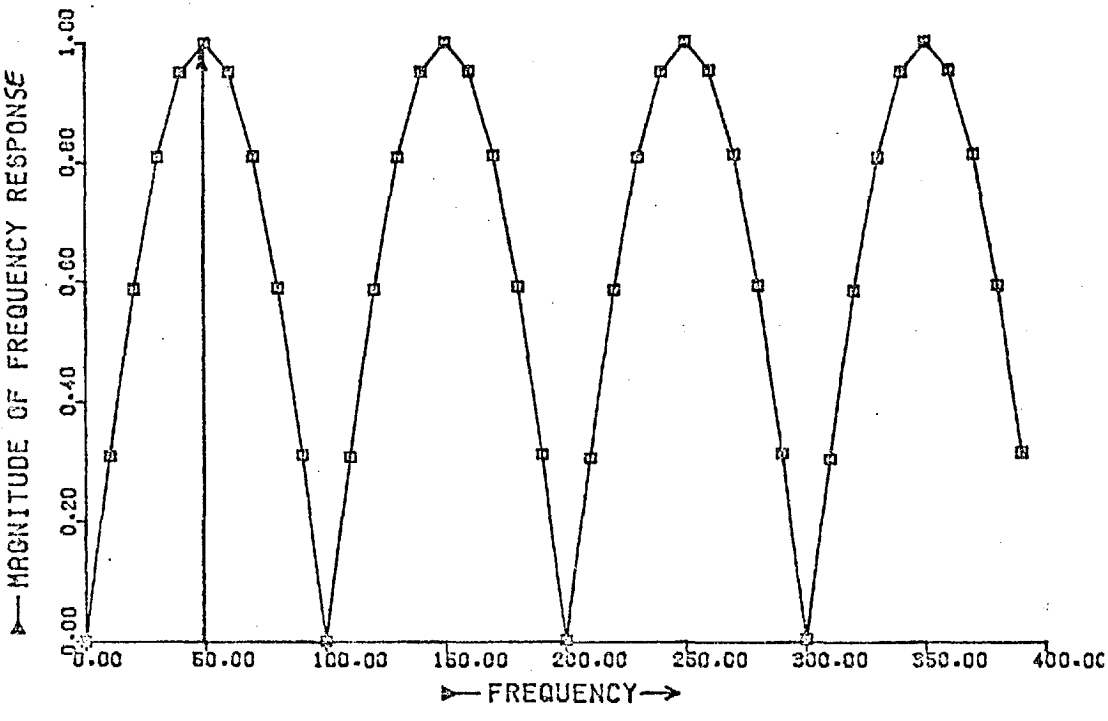

Fig. (3.9) Spectrum of $v_k = \frac{1}{2T} (v_{k+1} - v_{k-1})$ for 4 S/C

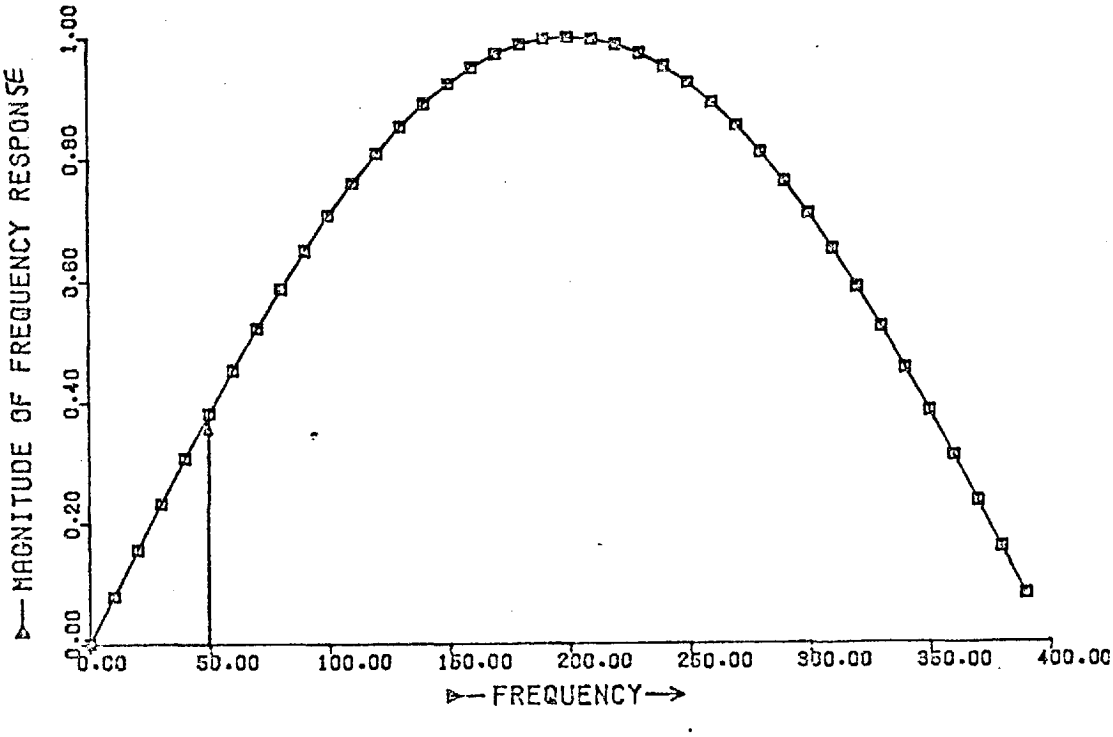

Fig. (3.10) Spectrum of $v'_k = \frac{1}{2T} (v_{k+1} - v_{k-1})$ for 16 S/C

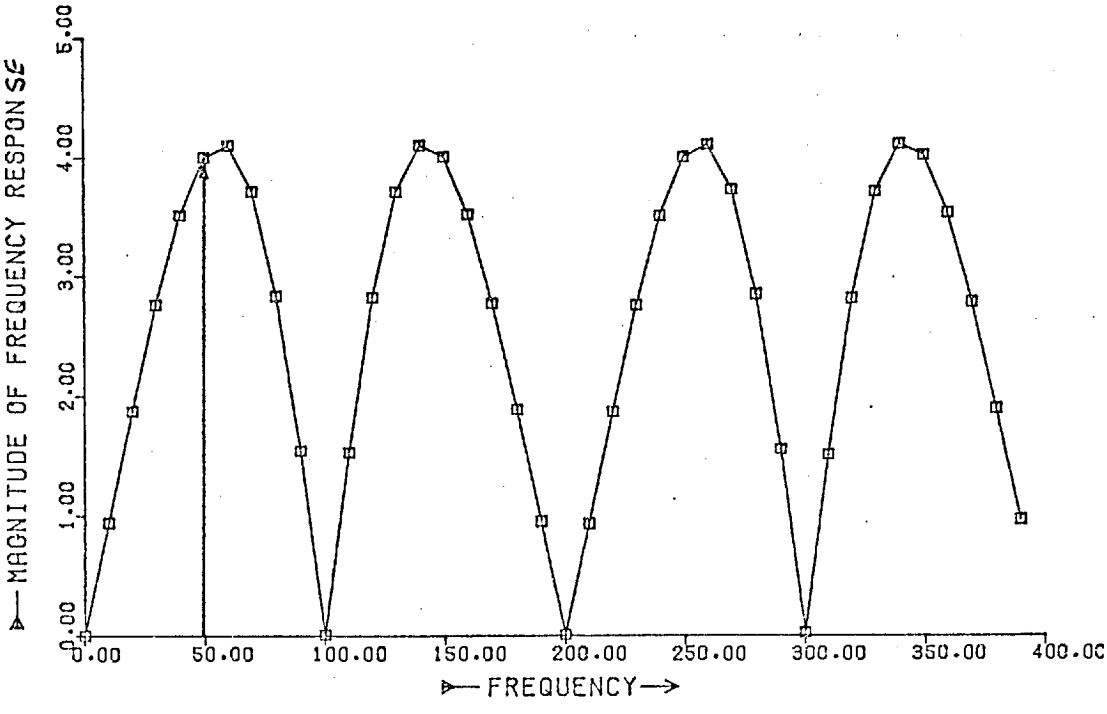

Fig. (3.11) Spectrum of $\upsilon'_k = \frac{1}{T}\left(-\frac{1}{12}\upsilon_{k+2} + \frac{2}{3}\upsilon_{k+1} - \frac{2}{3}\upsilon_{k-1} + \frac{1}{12}\upsilon_{k-2}\right)$ for 4 S/C

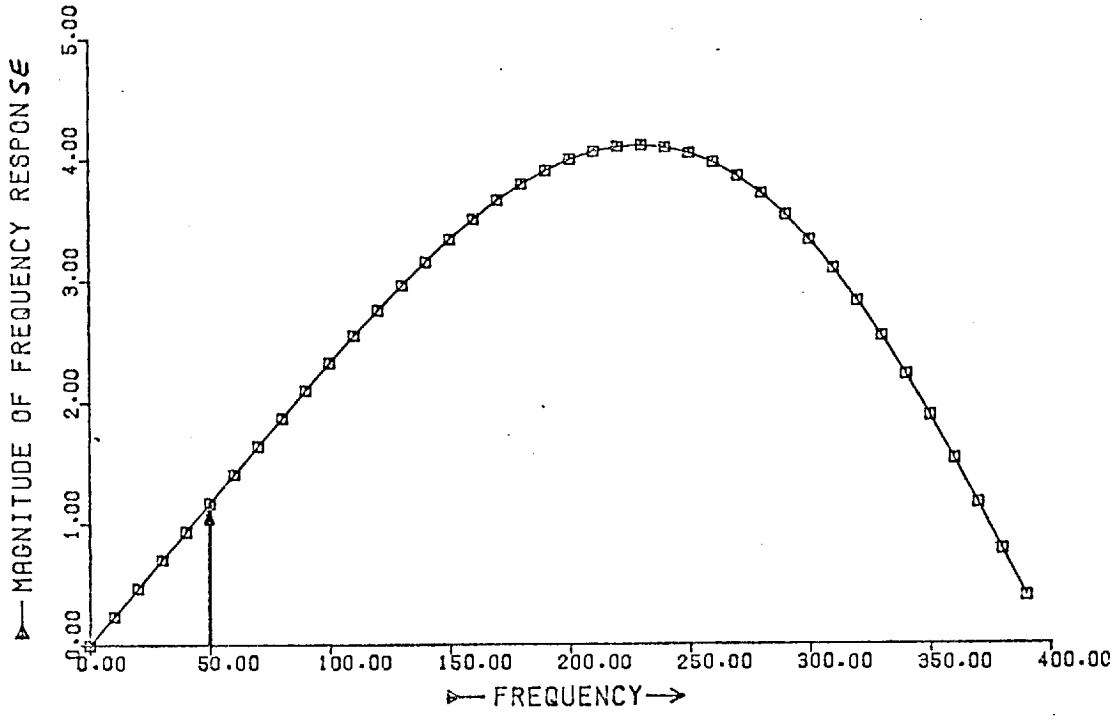

Fig. (3.12) Spectrum of $\upsilon'_k = \frac{1}{T}\left(-\frac{1}{12}\upsilon_{k+2} + \frac{2}{3}\upsilon_{k+1} - \frac{2}{3}\upsilon_{k-1} + \frac{1}{12}\upsilon_{k-2}\right)$ for 16 S/C

and from filtering point of view are worse than them. For the third method 2 S/C is the optimum sampling rate, which from the sampling theory point of view is impossible. In Figures (3.13) and (3.14) the spectrums of this method for 4 and 16 S/C can be seen. Hence from immunity to high frequency components the first method (equation 3.39) and the fourth method (equation 3.42) are the best. With these methods using 4 S/C all the high frequency components appear attenuated or at least unchanged. With a higher rate of sampling, say 16, it can be seen that many components larger than 50HZ are accentuated.

If the problem is looked at from a numerical point of view, the low rate of sampling will not be acceptable, because it gives large numerical errors[21] and consequently the peak determination method must be used with a high rate of sampling which will be involved by noise and harmonic amplification.

For the second derivative use can be made of the following equations:

$$\upsilon''_k = \frac{1}{4T^2} \left(\upsilon_{k+2} - 2\upsilon_k + \upsilon_{k-2}\right) \tag{3.51}$$

or

$$\upsilon''_k = \frac{1}{144T^2} \left(\upsilon_{k+4} - 16\upsilon_{k+3} + 64\upsilon_{k+2} + 16\upsilon_{k+1} - 130\upsilon_k + 16\upsilon_{k-1} + 64\upsilon_{k-2} - 16\upsilon_{k-3} + \upsilon_{k-4}\right) \tag{3.52}$$

or

$$\upsilon''_k = \frac{1}{T^2} \left(\upsilon_k - 2\upsilon_{k-1} + \upsilon_{k-2}\right) \tag{3.53}$$

or

$$\upsilon''_k = \frac{1}{4T^2} \left(\upsilon_k - 2\upsilon_{k-2} + \upsilon_{k-4}\right) \tag{3.54}$$

The transfer functions of these methods, respectively, are:

$$H_1(Z) = \frac{1}{4T^2} \left(1 - \bar{Z}^2\right)^2 \tag{3.55}$$

$$H_2(Z) = \frac{1}{144T^2} \left(\bar{Z}^2 - 1\right)^2 \left(Z^{-2} - 8Z^{-1} + 1\right)^2 \tag{3.56}$$

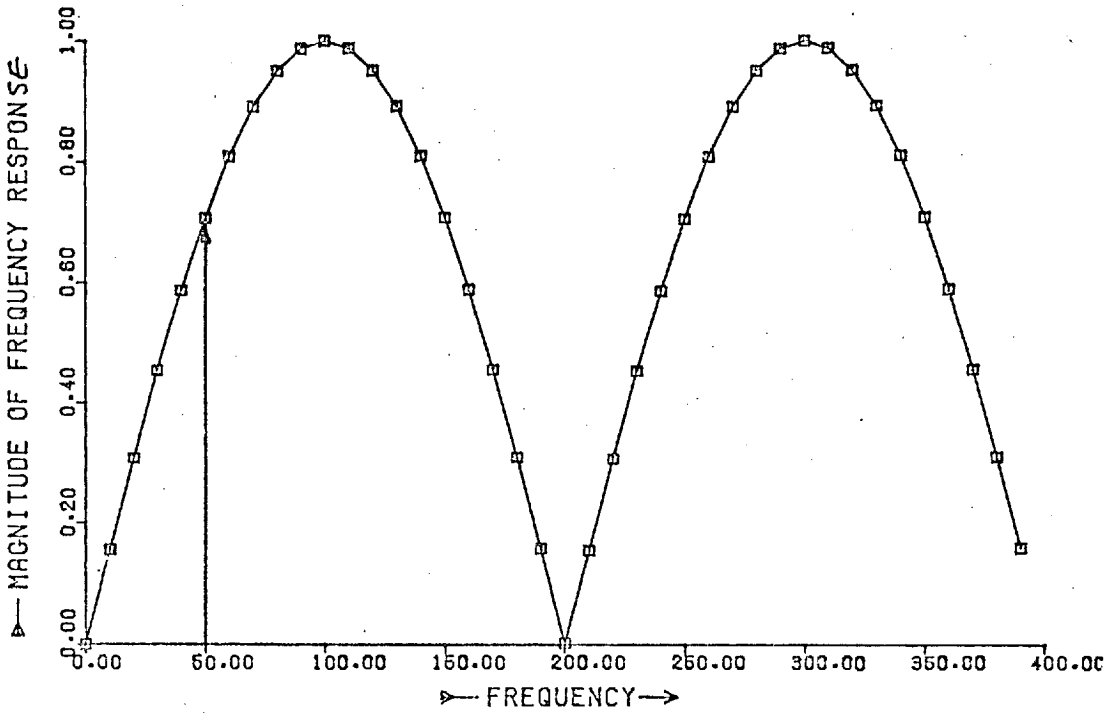

Fig. (3.13) Spectrum of $\upsilon'_k = \frac{1}{T}(\upsilon_k - \upsilon_{k-1})$ for 4 S/C

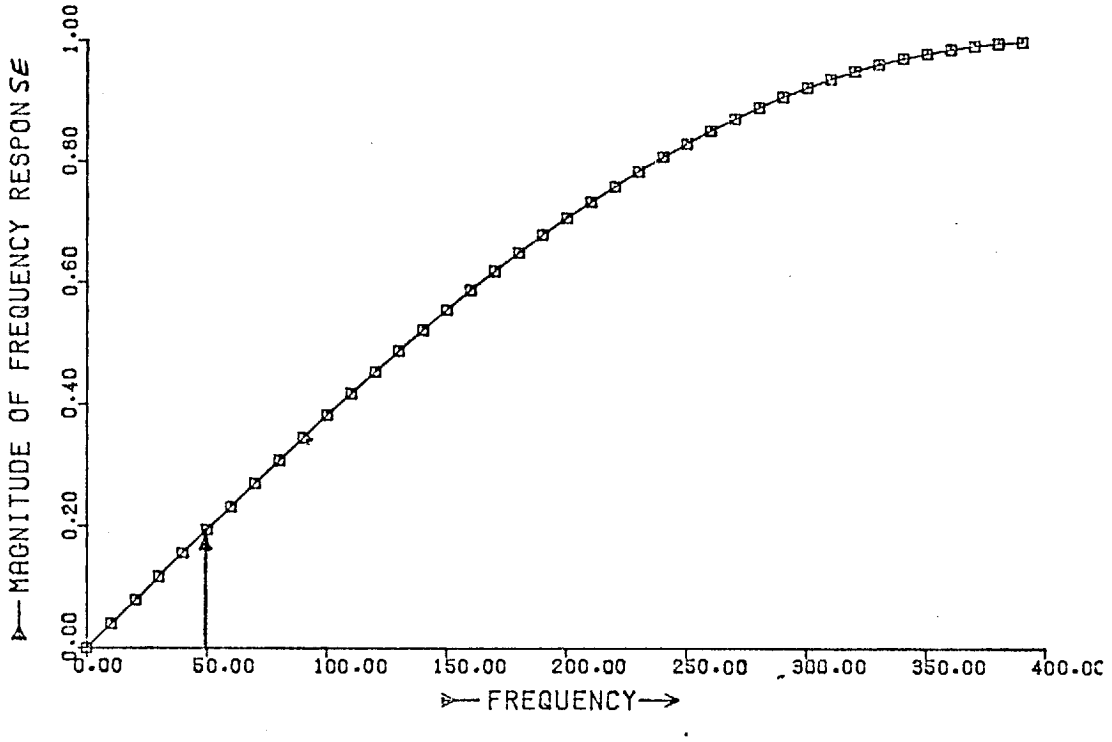

Fig. (3.14) Spectrum of $\upsilon'_k = \frac{1}{T}(\upsilon_k - \upsilon_{k-1})$ for 16 S/C

$$H_3(Z) = \frac{1}{T^2}(1-\bar{Z}^1)^2 \qquad (3.57)$$

$$H_4(Z) = \frac{1}{4T^2}(1-\bar{Z}^2)^2 \qquad (3.58)$$

And the frequency responses are:

$$H_1(f) = 2500N^2 \sin^2 \frac{\pi f}{25N} \qquad (3.59)$$

$$H_2(f) = \frac{2500N^2}{9}(4-\cos\frac{\pi f}{25N})^2 \sin^2 \frac{\pi f}{25N} \qquad (3.60)$$

$$H_3(f) = 10^4N^2 \sin^2 \frac{\pi f}{50N} \qquad (3.61)$$

$$H_4(f) = 2500N^2 \sin^2 \frac{\pi f}{25N} \qquad (3.62)$$

Study of these equations give the same results, as for the first derivative. In this case the amplification of the high frequency components is greater than previously.

It is concluded that the peak determination method must be used with a sampling rate other than 4 S/C and this will lead to amplification of the unwanted components larger than 50 Hz. Hence a high order analogue filter with very low cut-off frequency will be required to remove components near 50 Hz. Such a filter will have a long time delay. Also with this method, the calculation of resistance and inductance is difficult, and it is not easy to build an ideal characteristic.

3.3.2 FOURIER METHOD

Assume the fundamental components of voltage and current waveforms are:

$$\upsilon = V_p \sin(\omega t+\lambda+\delta) = A_v \sin\omega t + B_v \cos\omega t \ldots \qquad (3.63)$$

$$i = I_p \sin(\omega t+\delta) = A_i \sin\omega t + B_i \cos\omega t \ldots \qquad (3.64)$$

In complex form:

$$V = A_v + j\, B_v$$

$$I = A_i + j\, B_i$$

Hence from equation (3.32)

$$Z = \frac{V}{I} = R+jX = \frac{A_v A_i + B_v B_i}{A_i^2 + B_i^2} + j\, \frac{B_v A_i - A_v B_i}{A_i^2 + B_i^2}$$

or

$$R = \frac{A_v A_i + B_v B_i}{A_i^2 + B_i^2} \tag{3.65}$$

and

$$X = \frac{B_v A_i - A_v B_i}{A_i^2 + B_i^2} \tag{3.66}$$

It was Slemon et al[23] who proposed the application of the Fourier method to transmission line protection, but the algorithm was presented in a way which was not suitable for mini-computer or microprocessor application. They suggested calculation of the modulus and phase angle of transmission line impedance as follows:

$$Z = \sqrt{A_v^2 + B_v^2} \;/\; \sqrt{A_i^2 + B_i^2} \tag{3.67}$$

and

$$\lambda = \tan^{-1} \frac{B_v}{A_v} - \tan \frac{B_i}{A_i} \tag{3.68}$$

It is very difficult and time consuming to calculate Z from equation (3.67) by mini or micro processors. Also the calculation of arctangents is time consuming by exact means. An alternative is a program using a coarse look-up table. The new method of calculation for R and X from equations (3.65) and (3.66) has overcome all the difficulties and has made it possible to build an ideal characteristic easily.

If A_v, B_v, A_i and B_i are calculated for each phase the impedance of the transmission line seen from a single relaying point can be determined. Now, using Fourier analysis, the coefficients can be calculated as:

$$A_v = \frac{1}{\pi} \int_{\gamma}^{\gamma+2\pi} \upsilon \sin\omega t \, d(\omega t) \tag{3.69a}$$

$$B_v = \frac{1}{\pi} \int_{\gamma}^{\gamma+2\pi} \upsilon \cos\omega t \, d(\omega t) \tag{3.69b}$$

$$A_i = \frac{1}{\pi} \int_{\gamma}^{\gamma+2\pi} i \sin\omega t \, d(\omega t) \tag{3.69c}$$

$$B_i = \frac{1}{\pi} \int_{\gamma}^{\gamma+2\pi} i \cos\omega t \, d(\omega t) \tag{3.69d}$$

Where γ is an arbitrary angle from which to start the calculation. By using the trapezoidal rule (which requires less manipulation than Simpson's rule, but produces the same accuracy in this case) the coefficients can be calculated from N S/C as follows:

$$A_{vk} = \frac{1}{N} \left[\upsilon_{k-N} \sin\gamma + 2\upsilon_{k-N-1} \sin\left(\gamma + \frac{2\pi}{N}\right) + \ldots \right.$$

$$\left. \ldots + 2\upsilon_{k-1} \sin\left(\gamma + \frac{N-1}{N}2\pi\right) + \upsilon_k \sin(\gamma+2\pi) \right] \tag{3.70a}$$

and

$$B_{vk} = \frac{1}{N} \left[\upsilon_{k-N} \cos\gamma + 2\upsilon_{k-N-1} \cos\left(\gamma + \frac{2\pi}{N}\right) + \ldots \right.$$

$$\left. \ldots + 2\upsilon_{k-1} \cos\left(\gamma + \frac{N-1}{N}2\pi\right) + \upsilon_k \cos(\gamma+2\pi) \right] \tag{3.70b}$$

where υ_k, υ_{k-1}, ... are evenly spaced samples of voltage. Similar equations can be written for A_i and B_i. By calculating these four coefficients for each phase all other information about transmission line can be computed from:

$$V_p^2 = A_v^2 + B_v^2 \tag{3.71a}$$

$$I_p^2 = A_i^2 + B_i^2 \tag{3.71b}$$

$$\text{Active power} = \frac{1}{2} R I_p^2 = A_v A_i + B_v B_i \tag{3.72a}$$

$$\text{Reactive power} = \frac{1}{2} X I_p^2 = B_v A_i - A_v B_i \tag{3.72b}$$

Equations (3.70) show that samples taken over one cycle of the fundamental are required before R and X can be determined, but by adding the newest sample as it is measured into

A_v, B_v etc., and discarding the oldest, an updated value can always be readily obtained, and the change in R and X can be tracked. If a close up fault occurs, the new samples will be radically different from the old ones and R and X will move rapidly into the trip zone. Whereas a fault near the line far end might take about one cycle to be detected.

3.3.2.1 Immunity of Fourier method to noise and high frequency components

Equations (3.70) are two finite impulse response (FIR) digital filters with samples of voltage as inputs and the A_v and B_v as outputs. The Z transform of both sides of equation (3.70a) can be written as:

$$Z(A_{vk}) = \frac{1}{N}\left[\bar{Z}^N \sin\gamma + 2\bar{Z}^{N+1}\sin\left(\gamma+\frac{2\pi}{N}\right) + \ldots + 2\bar{Z}^{1}\sin\left(\gamma+2\pi-\frac{2\pi}{N}\right) + \sin(\gamma+2\pi)\right] \; Z(\upsilon_k) \tag{3.73}$$

from equation (3.73) the transfer function of the digital filter can be obtained as:

$$H_A(Z) = \frac{Z(A_{vk})}{Z(\upsilon_k)} = \frac{1}{N}\left[\sin\gamma\bar{Z}^N + 2\sin\left(\gamma+\frac{2\pi}{N}\right) Z^{-N+1} \ldots + 2\bar{Z}^{1}\sin\left(\gamma-\frac{2\pi}{N}\right) + \sin(\gamma+2\pi)\right] \tag{3.74}$$

Using the two relations:

$$\sum_{k=1}^{n-1} P^k \sin(kx) = \frac{P\sin(x) - P^n\sin(nx) + P^{n+1}\sin(n-1)x}{1-2P\cos(x)+P^2} \tag{3.75a}$$

and

$$\sum_{k=o}^{n-1} P^k \cos(kx) = \frac{1-P\cos(x) - P^n\cos(nx) + P^{n+1}\cos(n-1)x}{1-2P\cos(x)+P^2} \tag{3.75b}$$

it is possible to write equation (3.74) in closed form as:

$$H_A(Z) = \frac{1}{N}\,\frac{(1-\bar{Z}^N)(Z^2\sin\gamma - 2Z\sin\frac{2\pi}{N}\cos\gamma - \sin\gamma)}{1-2Z\cos\frac{2\pi}{N}+Z^2} \tag{3.76}$$

In the same way the transfer function of equation (3.70b) can be obtained as:

$$H_B(Z) = \frac{1}{N}\,\frac{(1-Z^{-N})(Z^2\cos\gamma + 2Z\sin\frac{2\pi}{N}\sin\gamma - \cos\gamma)}{1-2Z\cos\frac{2\pi}{N}+Z^2} \tag{3.77}$$

Putting $Z=e^{j2\pi fT}$ and $T = \frac{0.02}{N}$ Sec.the magnitude of the filter's spectrum is given by:

$$H_A(f) = \frac{2\sin\frac{\pi f}{50}}{N(\cos\frac{\pi f}{25N} - \cos\frac{2\pi}{N})} \sqrt{\sin^2\frac{2\pi}{N}\cos^2\gamma + \sin^2\gamma\sin^2\frac{\pi f}{25N}} \quad (3.78a)$$

and

$$H_B(f) = \frac{2\sin\frac{\pi f}{50}}{N(\cos\frac{\pi f}{25N} - \cos\frac{2\pi}{N})} \sqrt{\sin^2\frac{2\pi}{N}\sin^2\gamma + \cos^2\gamma\sin^2\frac{\pi f}{25N}} \quad (3.78b)$$

Equations (3.78) are the frequency responses of the Fourier method in its most general form, for N samples per cycle and with a starting angle equal to γ. From these two equations the property of the Fourier method with respect to high and low frequency components can be investigated.

For f = 50 Hz then:

$$H_A(50) = H_B(50) = 1 \quad (3.79)$$

Equation (3.79) implies that the filter passes a 50 Hz component without any change. The amplitutde of other components depend on three parametres namely: frequency (f), sampling rate (N) and starting angle (γ). For $\gamma = \frac{\pi}{4}$ the spectrum of the two FIR filters are the same, i.e.

$$H_A(f) = H_B(f) = \frac{\sqrt{2}\sin\frac{\pi f}{50}}{N(\cos\frac{\pi f}{25N} - \cos\frac{2\pi}{N})} \sqrt{\sin^2\frac{2\pi}{N} + \sin^2\frac{\pi f}{25N}} \quad (3.80)$$

For N=4 samples per cylce equation (3.78a) reduces to:

$$H_A(f) = \frac{2\sin\frac{\pi f}{50}}{4\cos\frac{\pi f}{100}} \sqrt{\cos^2\gamma + \sin^2\gamma\sin^2\frac{\pi f}{100}} \quad (3.81)$$

which for $\gamma=0$ $H_A(f) = \sin \frac{\pi f}{100}$ and for $\gamma = \frac{\pi}{2}$ $H_A(f) = \sin^2 \frac{\pi f}{100}$. These sine and squared sine characteristics are two extreme cases of equation (3.81). By choosing different starting points (γ) it is possible to obtain a variety of characteristics which lie between these extremes. By increasing the sampling rate the characteristic can be improved and more unwanted components filtered out. In figures (3.15) to (3.18) the magnitude characteristics of the Fourier method for 4,8,12 and 16 S/C is plotted against frequency. For all these figures γ has been chosen equal to $\pi/4$, and so they represent both $H_A(f)$ and $H_B(f)$. By choosing different starting angles (γ), slightly different characteristics will be obtained which from practical points of view, no important difference can be noted among them and so γ can have any value. Figure (3.19) shows the spectrums of Fourier method with 16 samples per cycle and $\gamma=0$, $\frac{\pi}{4}$ and $\pi/2$. From the magnitude characteristics of the Fourier technique with different rates of sampling (figures 3.15 to 3.18) it is apparent that, the part of the characteristic which lies between zero and 100 Hz is approximately independent of the sampling rate. This property implies that if components larger than 100 Hz can be filtered by analogue means, then the accuracy of the method would be independent of the sampling rate and hence there is no point in choosing too high a rate. A low sampling rate can result in hardware simplification and cost reduction and is very desirable in implementation. For this reason 4 S/C is chosen to see if a suitable analogue filter with a reasonable time delay which can effectively remove the components larger than 100 Hz can be found.

With a single pole Butterworth filter the overall characteristic of the algorithm can be seen in figures (3.20) and

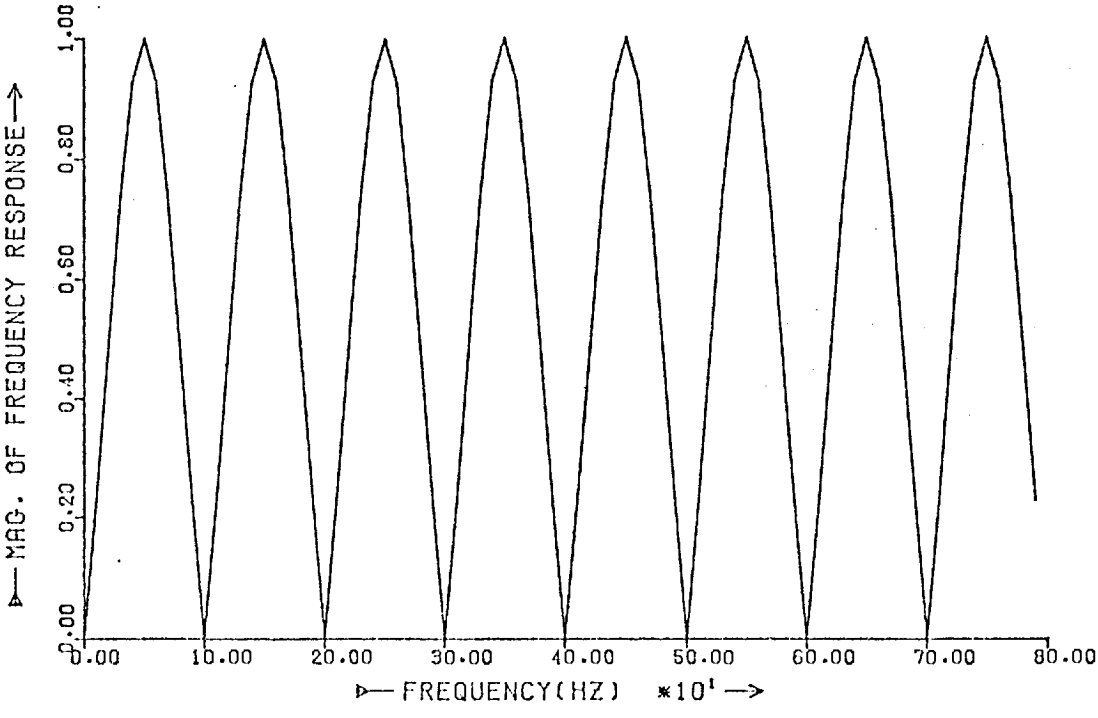

Fig. (3.15) Spectrum of the Fourier method with 4 samples per cycle.

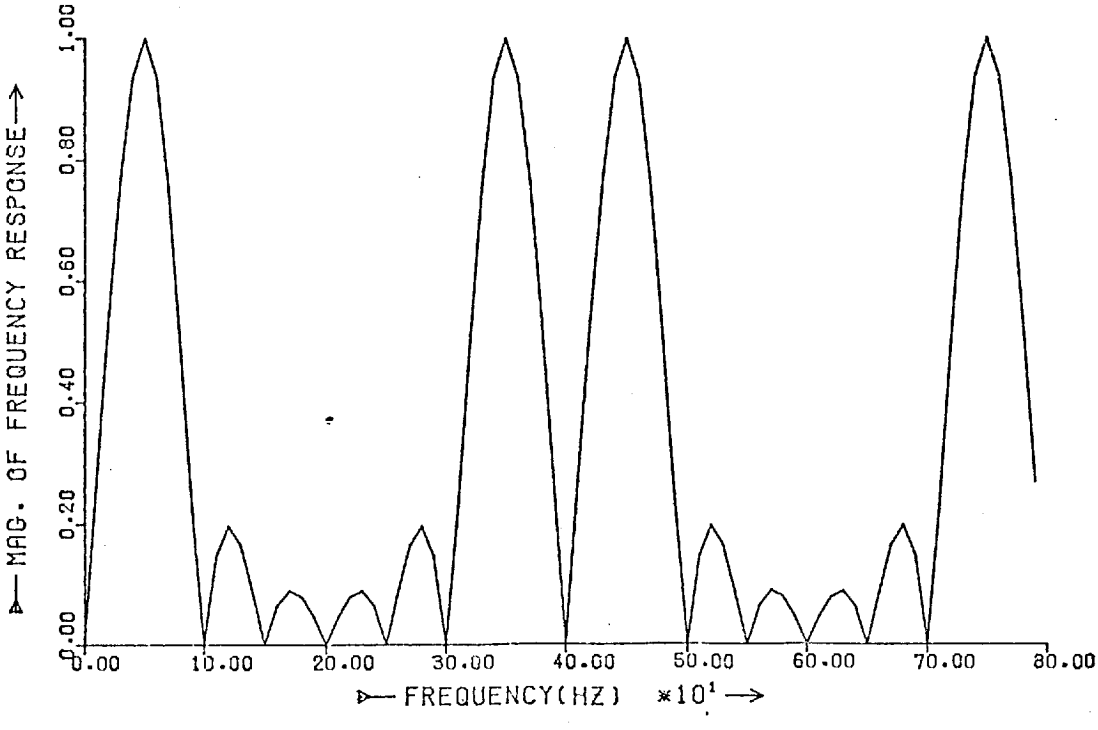

Fig. (3.16) Spectrum of the Fourier method with 8 samples per cycle.

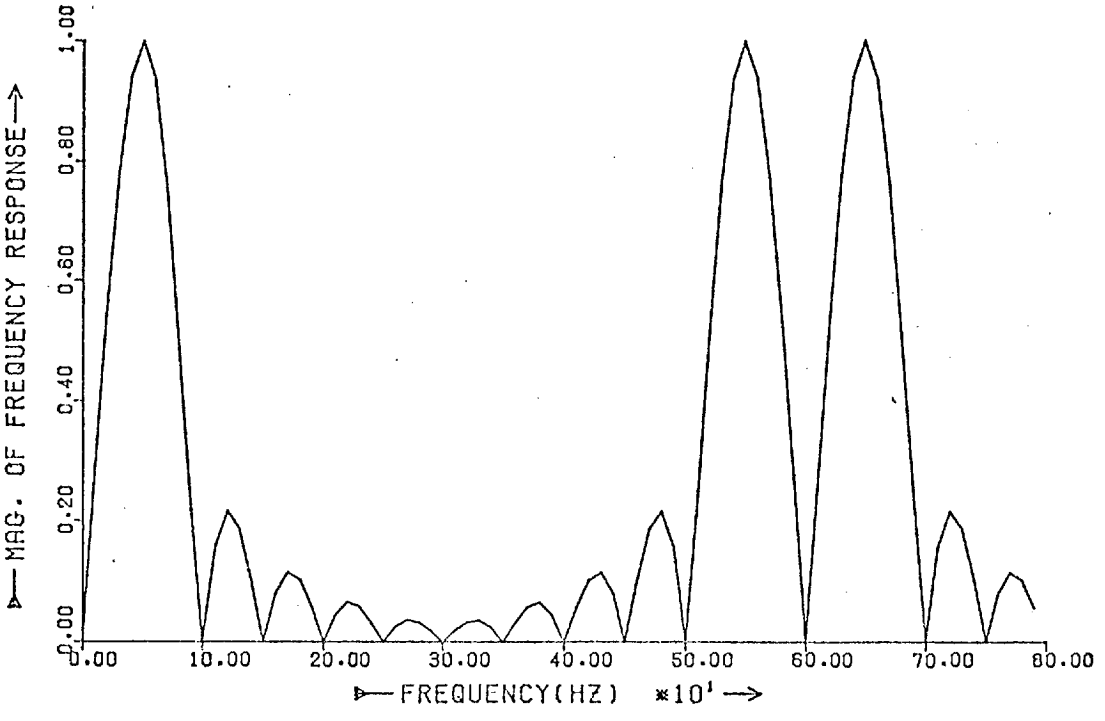

Fig. (3.17) Spectrum of the Fourier method with 12 samples per cycle

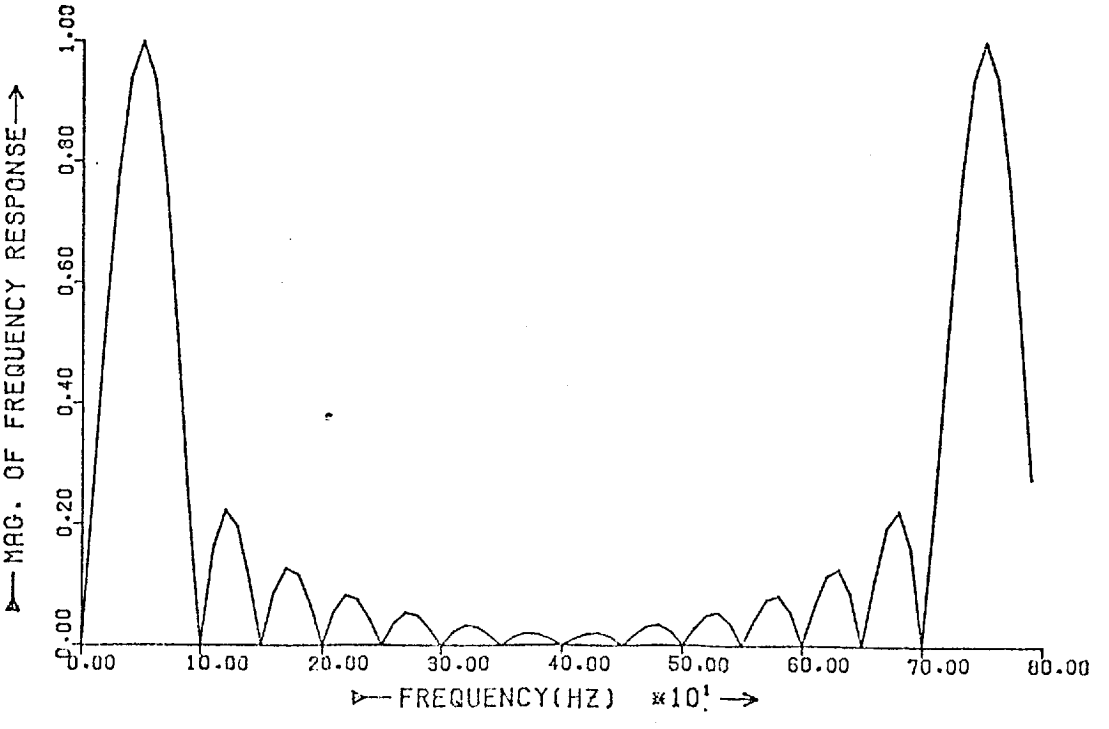

Fig. (3.18) Spectrum of the Fourier method with 16 samples per cycle

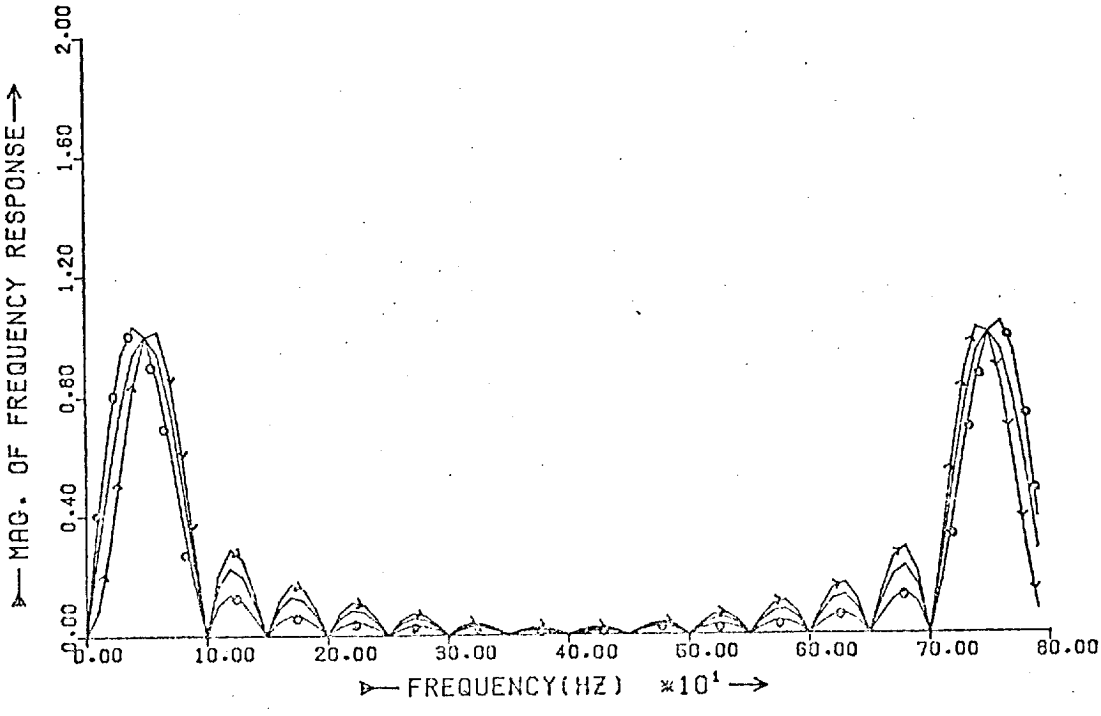

Fig. (3.19) Spectrum of the Fourier method with 16 samples per cycle for $\gamma = 0$, $\frac{\pi}{4}$ and $\pi/2$.

—o—o—o— $\gamma = 0$

——————— $\gamma = \pi/4$

—>—>—>— $\gamma = \pi/2$

(3.21) for 100 Hz and 60 Hz cut-off frequencies. Even with 60 Hz cut-off frequency such a filter cannot remove the components near the third and fifth harmonics effectively. Table (3.1) shows the time delays of a Butterworth filter with up to 4 poles with different cut-off frequencies. From this table it can be seen that a single pole Butterworth filter with 60 Hz cut-off frequency has a 5.3 msec.time delay. The characteristics with a two poles Butterworth filter for cut-off frequencies 100 Hz and 60 Hz can be seen in figures (3.22) and (3.23). With a two pole, 60 Hz cut-off this method gives satisfactory results. Also the result would be the same with a 80 Hz 3-pole filter. Both of these filters have a 6.37 ms time delay. From the foregoing, we see that a Fourier method with 4 S/C when used with a second order Butterworth filter having 60 Hz cut-off, from filtering point of view gives acceptable results. In this case the A_v and B_y can be written as:

$$A_{vk} = \frac{1}{4} (2\upsilon_{k-3} - 2\upsilon_{k-1}) \qquad (3.82a)$$

$$B_{vk} = \frac{1}{4} (\upsilon_{k-4} - 2\upsilon_{k-2} + \upsilon_k) \qquad (3.82b)$$

Table (3.1) Time delays of Butterworth filters

Cut-off frequency (Hz)	Time delay (ms)			
	one pole	two pole	three pole	four pole
60	5.31	6.37	8.49	14.85
80	3.98	4.77	6.37	11.14
100	3.18	3.82	5.09	8.91
150	2.12	2.55	3.40	5.94

During the resistance and reactance calculation the coefficient $\frac{1}{4}$ in equations (3.82) will be cancelled out and so it can be neglected from the beginning. These two equations can

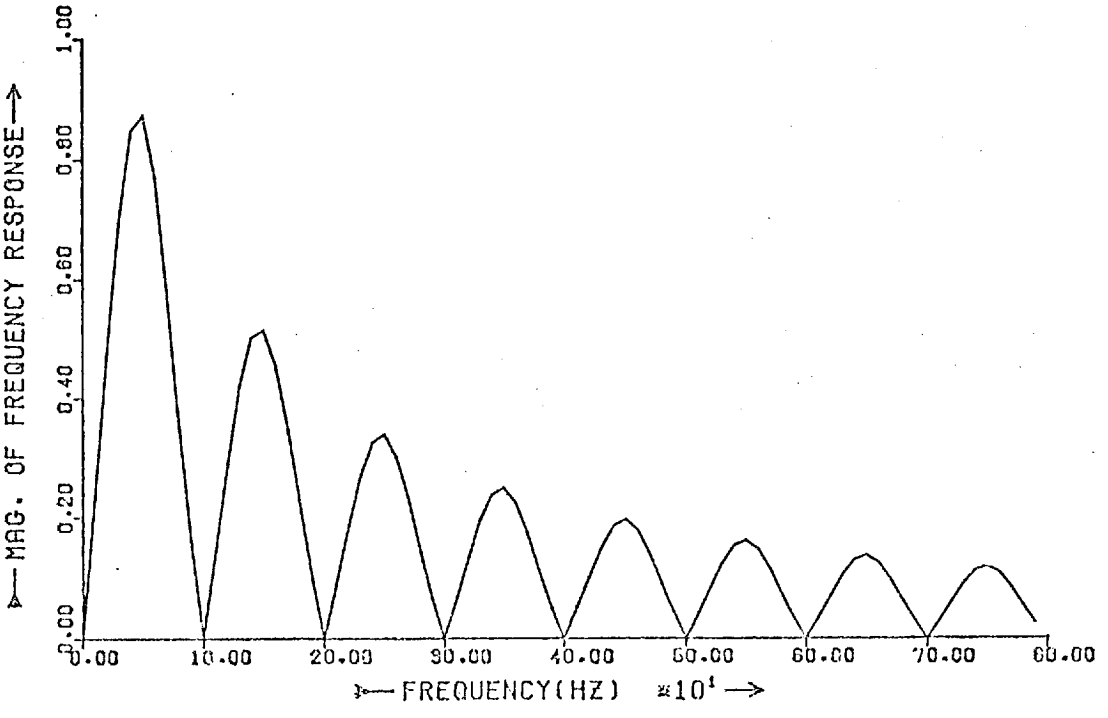

Fig. (3.20) Overall spectrum of the Fourier method with 4 samples per cycle and a single pole Butterworth filter with 90 Hz cut-off frequency

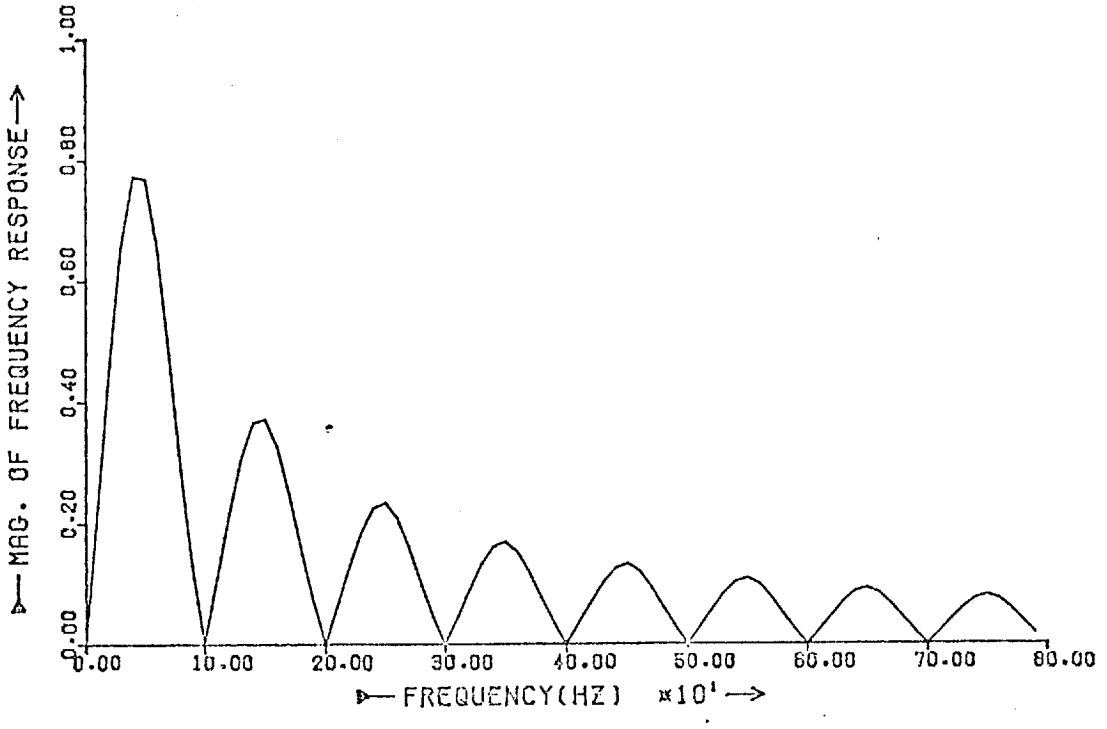

Fig. (3.21) Overall spectrum of the Fourier method with 4 samples per cycle and a single pole Butterworth filter with 60 Hz cut-off frequency.

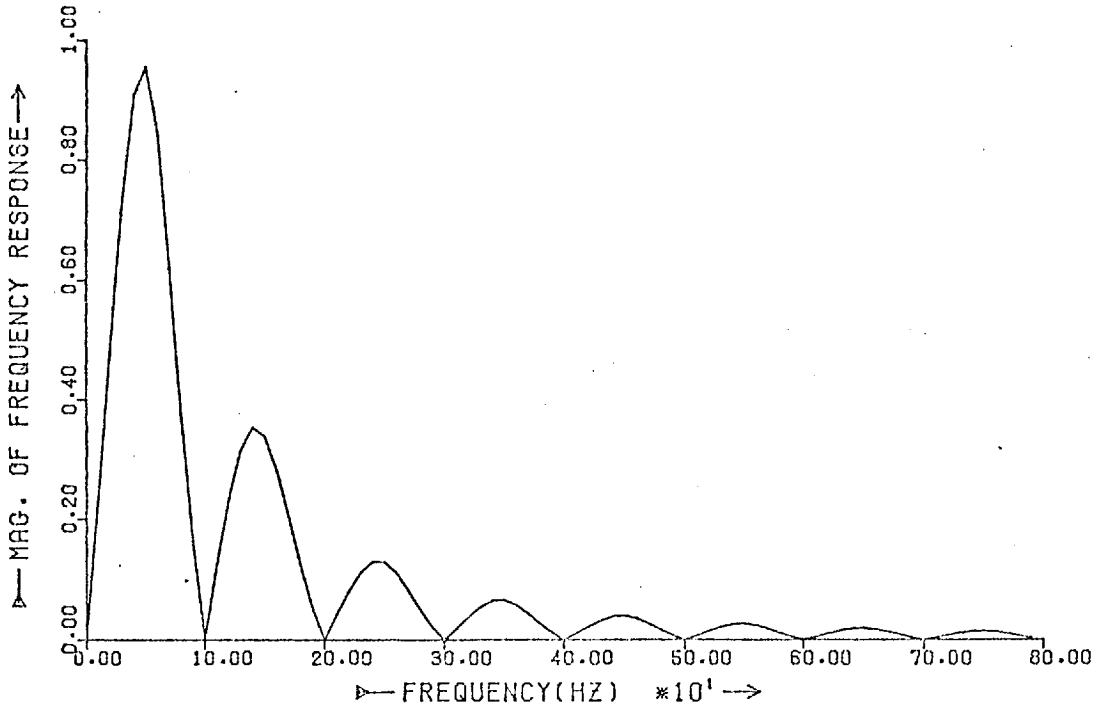

Fig. (3.22) Overall spectrum of the Fourier method with 4 samples per cycle and a two pole Butterworth filter with 100 Hz cut-off frequency

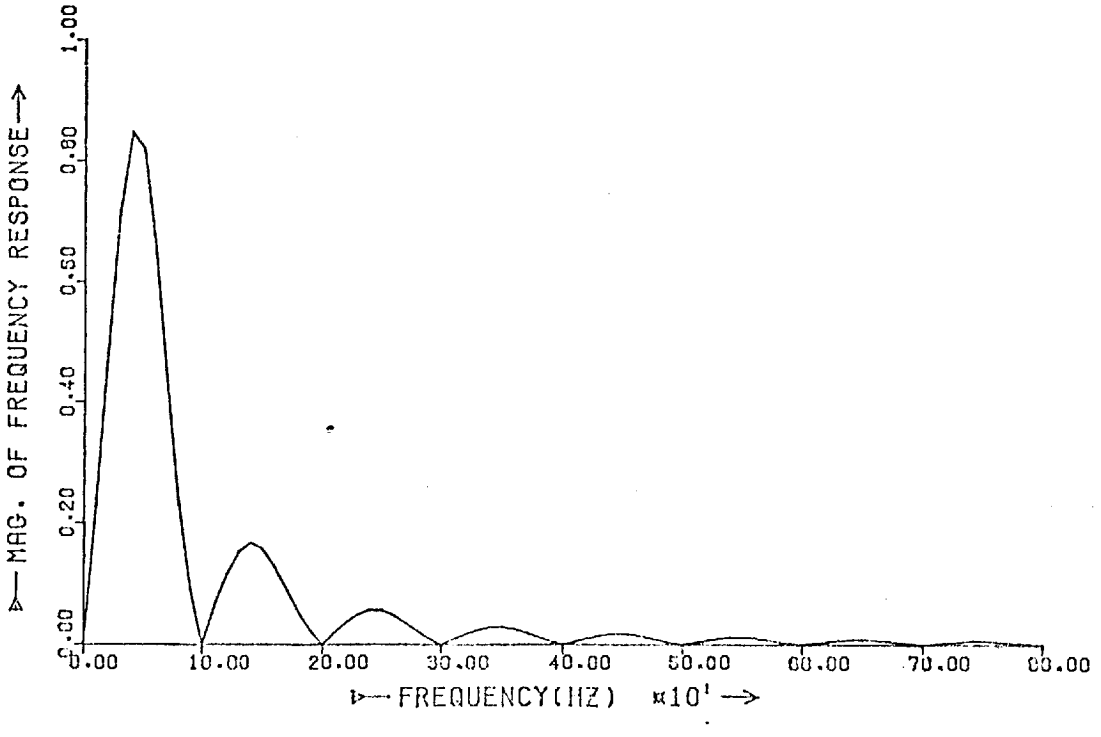

Fig. (3.23) Overall spectrum of the Fourier method with 4 samples per cycle and a two pole Butterworth filter with 60 Hz cut-off frequency.

be realized simply as in figure (3.24), which gives the A_{vk} and B_{vk} at its output. These two outputs can be used by a microprocessor or mini computer for the impedance calculation. Alternatively the calculation of A_{vk} and B_{vk} can be done by the computer as well. The realization of the Fourier method with 4S/C is simple, but it needs a filter with a time delay of about 6.37 ms. Another great disadvantage of using only 4 S/C is that to prevent false detection, at least 3 successive calculations are necessary to provide impedance values within the protected zone before a trip initiation signal can be reliably sent to the circuit breaker. Thus the relaying time in some cases, particularly for faults at the end of the line, might well become as large as two cycles. If faster fault detection is desired, the sampling rate must be increased. The spectrums with 8 samples per cycle can be seen in figures (3.25) to (3.27) for a 60 Hz single pole, 150 Hz double pole and 200 Hz three pole Butterworth filter. These cut-off frequencies are the highest which can be used to remove the unwanted components effectively. Both the two and three pole filter have 2.55 ms time delay, and they result in the same characteristic and so the second order filter is preferred. By increasing the sampling rate, studies have shown that the characteristic will improve, and it is possible to choose the analogue filter with the higher cut-off frequency. Table (3.2) shows approximately the highest cut-off frequencies for filters with different order, when used with 12 and 16 S/C. Although by increasing the sampling rate, the fault detection time slightly reduces the improvement that is obtained can not compensate for the complexity that involves the high rate of sampling, and hence no practical advantages can be obtained from it.

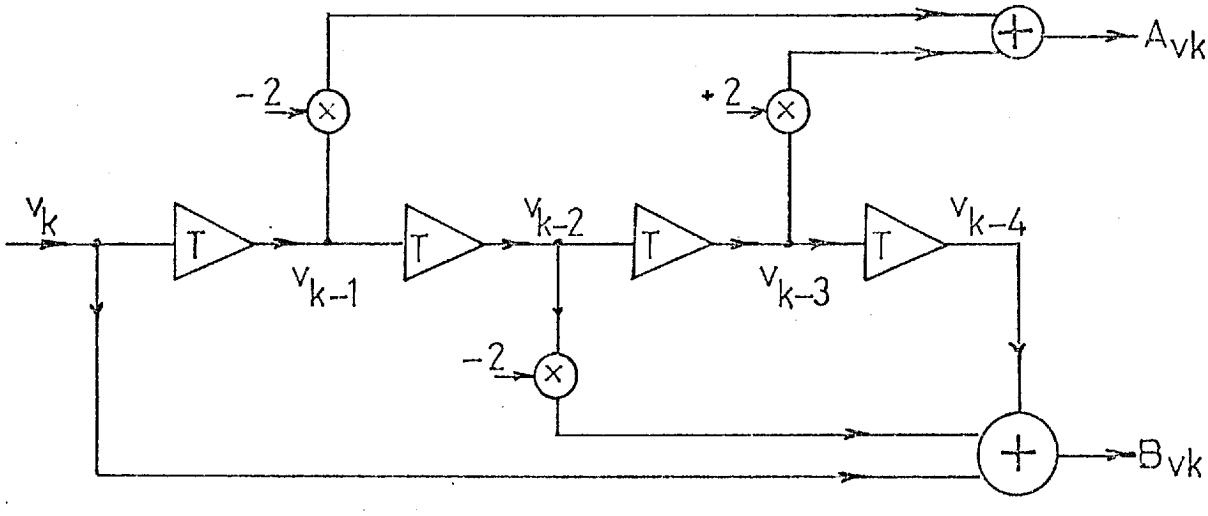

Fig. (3.24) Realization of the Fourier method with 4 samples per cycle

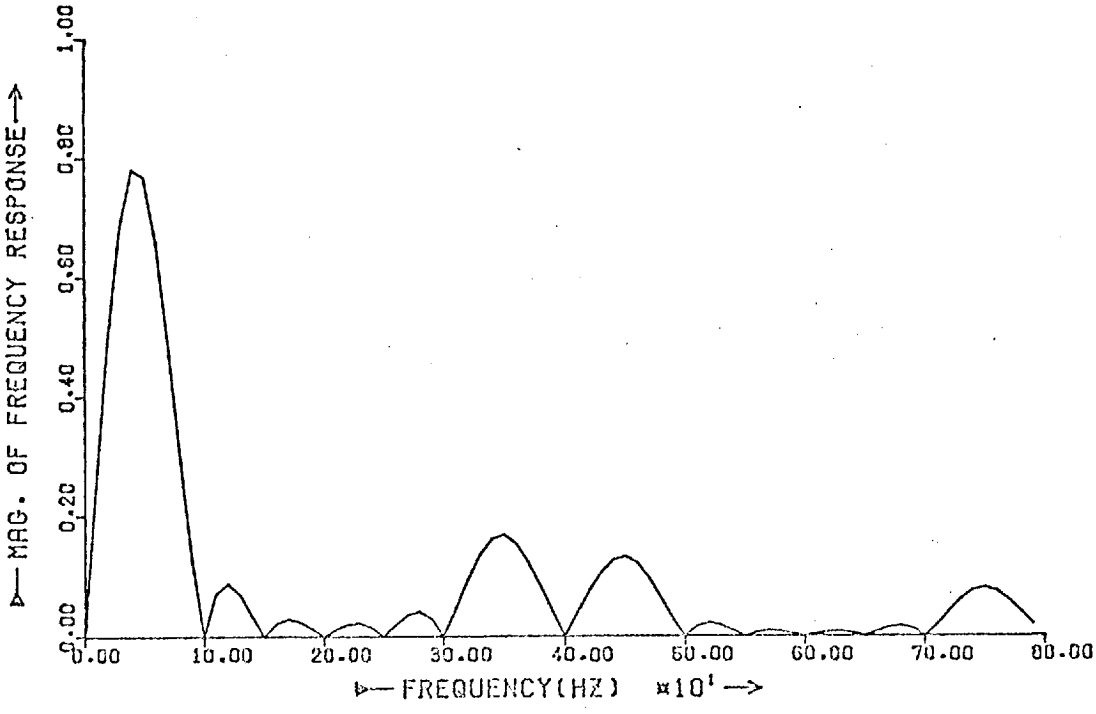

Fig. (3.25) Overall spectrum of the Fourier method with 8 samples per cycle and a single pole Butterworth filter with a 60 Hz cut-off frequency.

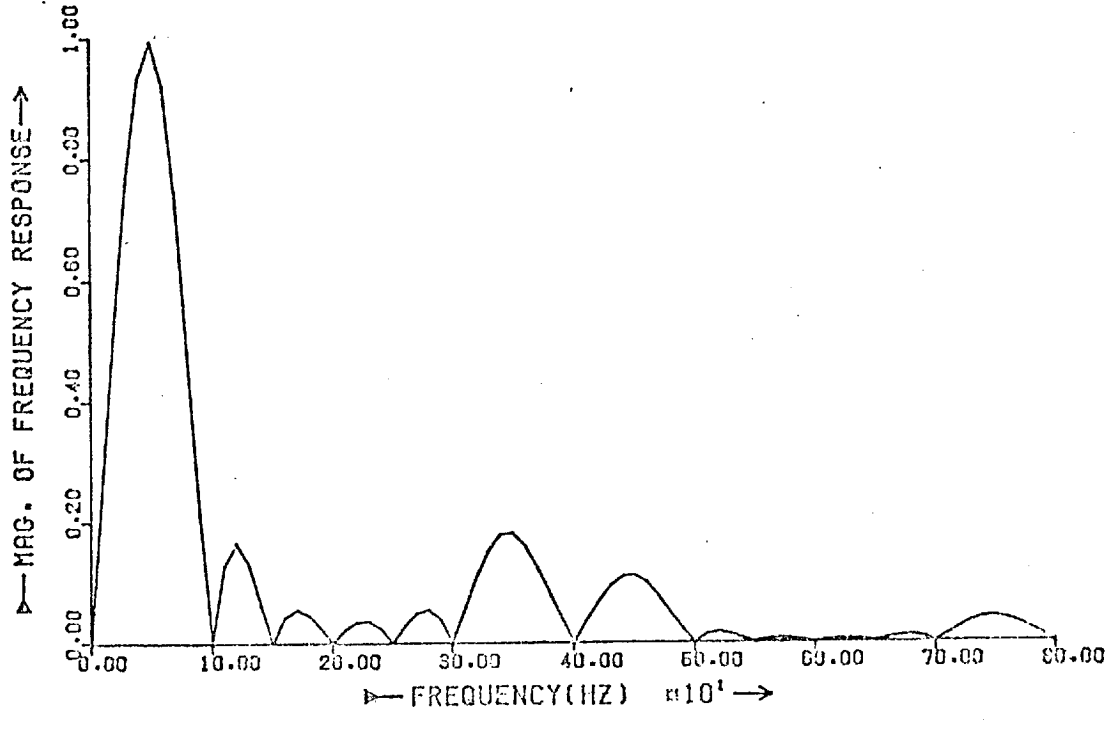

Fig. (3.26) Overall spectrum of the Fourier method with 8 samples per cycle and a two pole Butterworth filter with 150 Hz cut-off frequency.

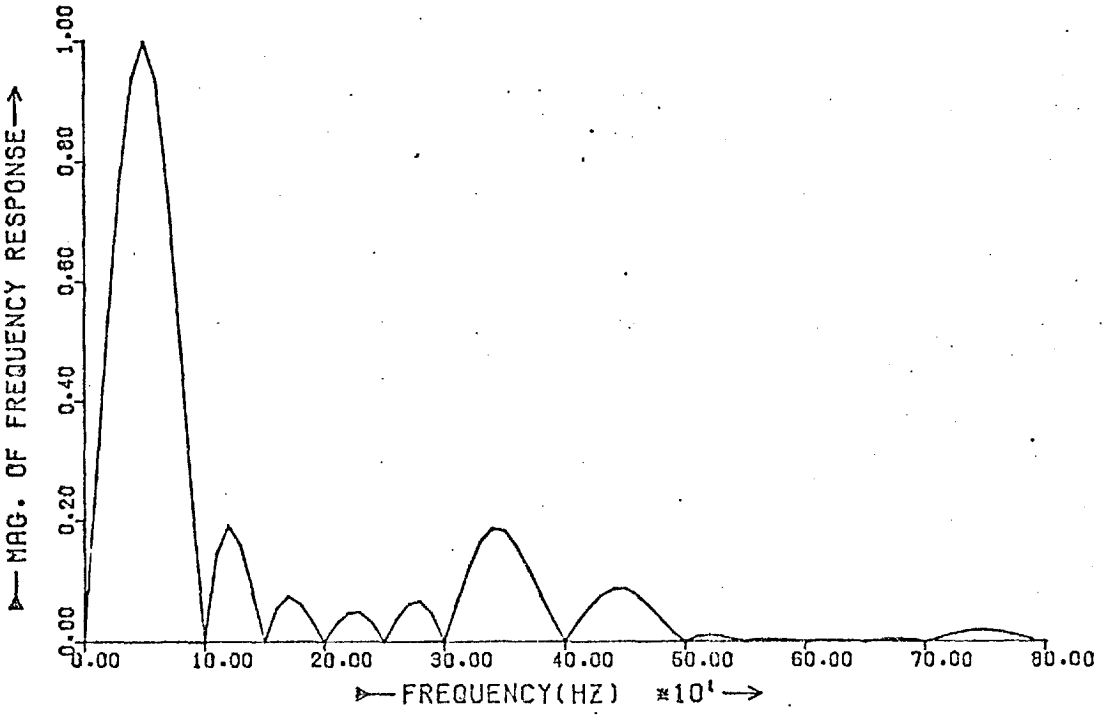

Fig. (3.27) Overall spectrum of the Fourier method with 8 samples per cycle and a three pole Butterworth filter with 200 Hz cut-off frequency

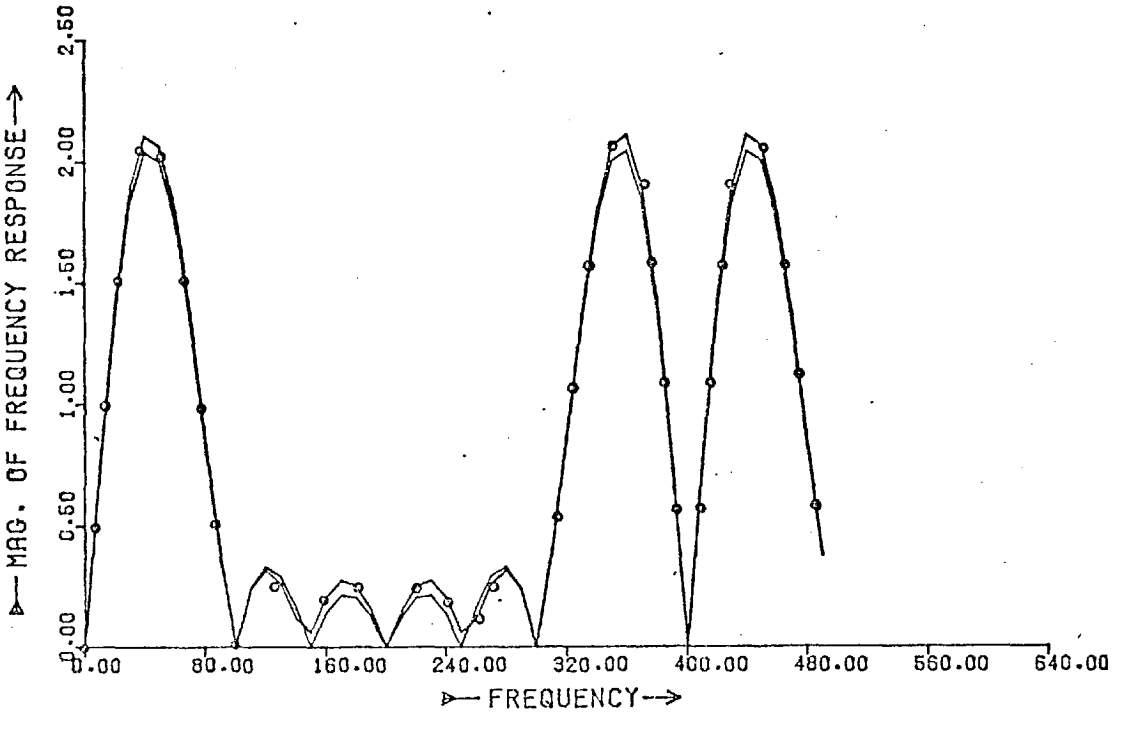

Fig. (3.28) Spectrum of the Fourier method with 8 samples per cycle

——————— Exact coefficients

—o—o—o— Approximated coefficient

Table (3.2) The highest cut-off frequency for 12 and 16 S/C

Sampling rate	Single pole cut-off	Double pole cut-off	Three pole cut-off
12 S/C	100	250	320
16 S/C	150	350	450

A Fourier method with 8 samples per cycle when used with a 150 Hz second order Butterworth filter can attenuate all unwanted components and at the same time is reasonably fast and simple. In this case A_{vk} and B_{vk} are calculated as:

$$A_{vk} = \frac{1}{8}\left[2(\upsilon_{k-6}-\upsilon_{k-2}) + \sqrt{2}\,(\upsilon_{k-7}+\upsilon_{k-5}-\upsilon_{k-3}-\upsilon_{k-1})\right] \quad (3.83a$$

$$B_{vk} = \frac{1}{8}\left[\upsilon_{k-8} -2\upsilon_{k-4}+\upsilon_{k}+\sqrt{2}\,(\upsilon_{k-7}-\upsilon_{k-5}-\upsilon_{k-3}+\upsilon_{k-1})\right] \quad (3.83b$$

In each equation only one multiplication is necessary. But even this can be avoided by approximating $\sqrt{2}$ with 1.5 and writing equations (3.8) as :

$$A_{vk} = 2(\upsilon_{k-6}-\upsilon_{k-2}) + 1.5(\upsilon_{k-7}+\upsilon_{k-5}-\upsilon_{k-3}-\upsilon_{k-1}) \quad (3.84a)$$

$$B_{vk} = \upsilon_{k-8}\ 2\upsilon_{k-4}+\upsilon_{k}+ 1.5(\upsilon_{k-7}-\upsilon_{k-5}-\upsilon_{k-3}+\upsilon_{k-1}) \quad (3.84b)$$

The coefficient $\frac{1}{8}$ has been omitted, because it will be cancelled out in the impedance calculation. These two equations can be calculated by only addition and shifting operation. They can also be realized as in figure (3.29). The frequency response of the method is:

$$H_A(f) = \frac{1}{2}\sin\frac{\pi f}{100}\,(1+\sqrt{2}\cos\frac{\pi f}{200}) \quad (3.85a)$$

and with 1.5 instead of $\sqrt{2}$ it becomes:

$$H_A(f) = \frac{1}{2}\sin\frac{\pi f}{100}\,(1 + 1.5\cos\frac{\pi f}{200}) \quad (3.85b)$$

Figure (3.28) shows these two spectrums. The maximum difference between them is less than 4% and for practical purposes they can be considered identical.

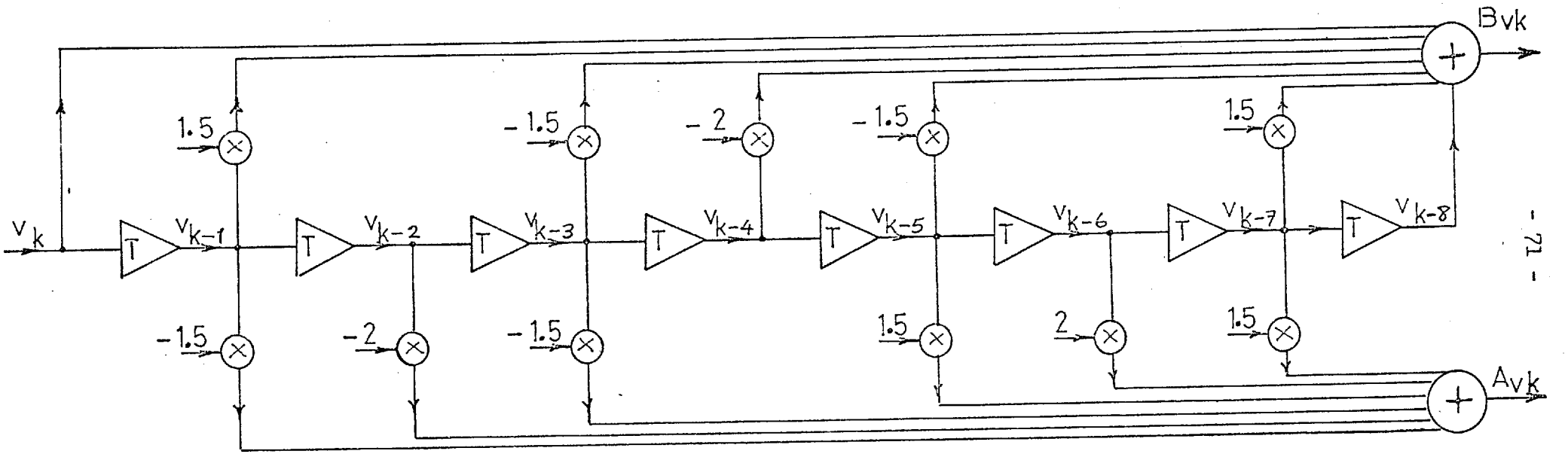

Fig. (3.29) Realization of the Fourier method with 8 samples per cycle

The accuracy of the Fourier method with any sampling rate is impaired by its inability to remove the exponential dc offset effectively. In the spectrum shown, it can be seen that a constant dc offset can be filtered out completely, but an exponential one which contains all low frequency components including 50 Hz, can not be removed. It can only be attenuated, and so the methods which can account directly for this component may be preferable.

3.3.3 SQUARE WAVE METHOD

To reduce arithmetical calculation of R and X in the Fourier method, orthogonal functions based on the square waves can be used[24]. (Note that the technique of section 3.3.2 employs sine and cosine waveforms as orthogonal functions). With square waves, the values of A_V and B_V can be calculated as:

$$A_v = \frac{1}{4}\int_{o}^{\pi} v\,d(\omega t) - \frac{1}{4}\int_{\pi}^{2\pi} v\,d(\omega t) \qquad (3.86a)$$

$$B_v = \frac{1}{4}\int_{o}^{\frac{\pi}{2}} v\,d(\omega t) - \frac{1}{4}\int_{\frac{\pi}{2}}^{\frac{3\pi}{2}} v\,d(\omega t) + \frac{1}{4}\int_{\frac{3\pi}{2}}^{2\pi} v\,d(\omega t) \qquad (3.86b)$$

By using the trapezoidal integration rule the values of A_V and B_V can be calculated from N samples per cycle as:

$$A_{vk} = \frac{\pi}{4N}\left[\left(v_{k-N}+2v_{k-N+1}+\ldots+2v_{k-\frac{N}{2}-1}+v_{k-\frac{N}{2}}\right)\right.$$

$$\left.-\left(v_{k-\frac{N}{2}}+2v_{k-\frac{N}{2}+1}+\ldots+2v_{k-1}+v_k\right)\right] \qquad (3.78a)$$

$$B_{vk} = \frac{\pi}{4N}\left[\left(v_{k-N}+2v_{k-N+1}+\ldots+2v_{k-\frac{3N}{4}-1}+v_{k-\frac{3N}{4}}\right)\right.$$

$$-\left(v_{k-\frac{3N}{4}}+2v_{k-\frac{3N}{4}+1}+\ldots+2v_{k-\frac{N}{4}-1}+v_{k-\frac{N}{4}}\right)$$

$$\left.+\left(v_{k-\frac{N}{4}}+2v_{k-\frac{N}{4}+1}+\ldots+2v_{k-1}+v_k\right)\right] \qquad (3.87b)$$

These two equations are non-recursive (finite impulse response) digital filters with samples of voltage as inputs and the A_{vk}

and B_{vk} as outputs. The Z-transform of A_{vk} can be written as:

$$Z(A_{vk}) = \frac{\pi}{4N}[(\bar{Z}^N+2\bar{Z}^{N+1}+\ldots+2Z^{-\frac{N}{2}-1}+Z^{-\frac{N}{2}}) - (Z^{-\frac{N}{2}}+2Z^{-\frac{N}{2}+1}+\ldots+2\bar{Z}^1+1)]\, Z(V_k)$$

or

$$Z(A_{vk}) = \frac{\pi}{4N}\left[\frac{(Z^{-\frac{N}{2}}-1)^2(1+\bar{Z}^1)}{Z^{-1}-1}\right] Z(\upsilon_k) \qquad (3.88)$$

From equation (3.88) the transfer function of the filter can be calculated:

$$H_A(Z) = \frac{Z(A_{vk})}{Z(V_k)} = \frac{\pi}{4N}\,\frac{(\bar{Z}^1+1)(Z^{-\frac{N}{2}}-1)^2}{Z^{-1}-1} \qquad (3.89)$$

The frequency response of the filter can be obtained by replacing Z with $e^{j\omega T}$:

$$H_A(\omega) = \frac{\pi}{N}\cot\frac{\omega T}{2}\sin^2\frac{N\omega T}{4}e^{-j(\frac{\pi}{2}+\frac{N\omega T}{2})} \qquad (3.90)$$

Putting $\omega=2\pi f$ and $T = \frac{0.02}{N}$ we obtain:

$$H_A(f) = \frac{\pi}{N}\cot\frac{\pi f}{50N}\sin^2\frac{\pi f}{100}\,e^{-j(\frac{1}{2}+\frac{f}{50})\pi} \qquad (3.91)$$

The magnitude of the frequency response is:

$$|H_A(f)| = \frac{\pi}{N}\sin^2\frac{\pi f}{100}\,\left|\cot\frac{\pi f}{50N}\right| \qquad (3.92)$$

Also the Z-transform of the B_{vk} is:

$$Z(B_{vk}) = \frac{\pi}{4N}[(\bar{Z}^N+2\bar{Z}^{N+1}+\ldots+2Z^{-\frac{3N}{4}-1}+Z^{-\frac{3N}{4}}) - (Z^{-\frac{3N}{4}}+2Z^{-\frac{3N}{4}+1}+\ldots$$
$$\ldots+2Z^{-\frac{N}{4}-1}+Z^{-\frac{N}{4}}) + (Z^{-\frac{N}{4}}+2Z^{-\frac{N}{4}+1}+\ldots+2\bar{Z}^1+1)]\, Z(\upsilon_k)$$

or

$$Z(B_{vk}) = \frac{\pi}{4N}\left[\frac{(Z+1)(1-Z^{-\frac{N}{4}})^2(1-Z^{-\frac{N}{2}})}{Z-1}\right] Z(\upsilon_k) \qquad (3.93)$$

From here:

$$H_B(Z) = \frac{Z(B_{vk})}{Z(\upsilon_k)} = \frac{\pi}{4N}\,\frac{(1+Z)(1-Z^{-\frac{N}{4}})^2(1-Z^{-\frac{N}{2}})}{Z-1} \qquad (3.94)$$

or in terms of f and N:

$$H_B(f) = \frac{2\pi}{N}\cot\frac{\pi f}{50N}\sin\frac{\pi f}{100}\sin^2\frac{\pi f}{200}\,e^{j(1-\frac{f}{50})\pi} \qquad (3.95)$$

and the magnitude of frequency response is:

$$|H_B(f)| = \frac{2\pi}{N} \sin^2 \frac{\pi f}{200} \left|\cot\frac{\pi f}{50N} \sin \frac{\pi f}{100}\right| \qquad (3.96)$$

The constant coefficients of A_{vk} and B_{vk} may be discarded.

By adding the newest sample as it is measured into A_v and B_v and discarding the oldest, both A_v and B_v can be written in recursive form as follows:

$$A_{vk+1}=A_{vk}+(-\upsilon_{k-N}-\upsilon_{k-N+1}+2\upsilon_{k-\frac{N}{2}}+2\upsilon_{k-\frac{N}{2}+1}-\upsilon_k-\upsilon_{k+1}) \qquad (3.97a)$$

$$B_{vk+1}=B_{vk}+(-\upsilon_{k-N}-\upsilon_{k-N+1}+2\upsilon_{k-\frac{3N}{4}}+2\upsilon_{k-\frac{3N}{4}+1}-2\upsilon_{k-\frac{N}{4}}$$

$$-2\upsilon_{k-\frac{N}{4}+1}+\upsilon_k+\upsilon_{k+1}) \qquad (3.97b)$$

The Z-transforms of these equations are:

$$Z(A_{vk+1})=\bar{Z}^1 Z(A_{vk})+(-\bar{Z}^{N-1}-\bar{Z}^N+2Z^{-\frac{N}{2}-1}+2Z^{-\frac{N}{2}}-\bar{Z}^1-1)\ Z(\upsilon_{k+1})$$

$$Z(B_{vk}+1)=\bar{Z}^1 Z(B_{vk})+(-\bar{Z}^{N-1}-\bar{Z}^N+2Z^{-\frac{3N}{4}-1}+2Z^{-\frac{3N}{4}}-2Z^{-\frac{N}{4}-1}-2Z^{-\frac{N}{4}}+\bar{Z}^1+1)$$

$$Z\ (\upsilon_{k+1})$$

From these two equations the transfer functions can be shown to be the same as equations (3.92) and (3.96), indicating that this method has the same frequency response in recursive or non-recursive form.

From equations (3.92) and (3.96) the spectrums of A_v and B_v have been plotted in Figures (3.30) to (3.37) with spectrums of the Fourier method for comparison. Comparison of the two methods shows that the square wave method accentuates some components and as a whole it has a poorer characteristic. For example in calculating A_v by it some components smaller than 50 Hz will be amplified (figures 3.29 to 3.32). This amplification of components between 30 and 40 Hz might reach 30% of the

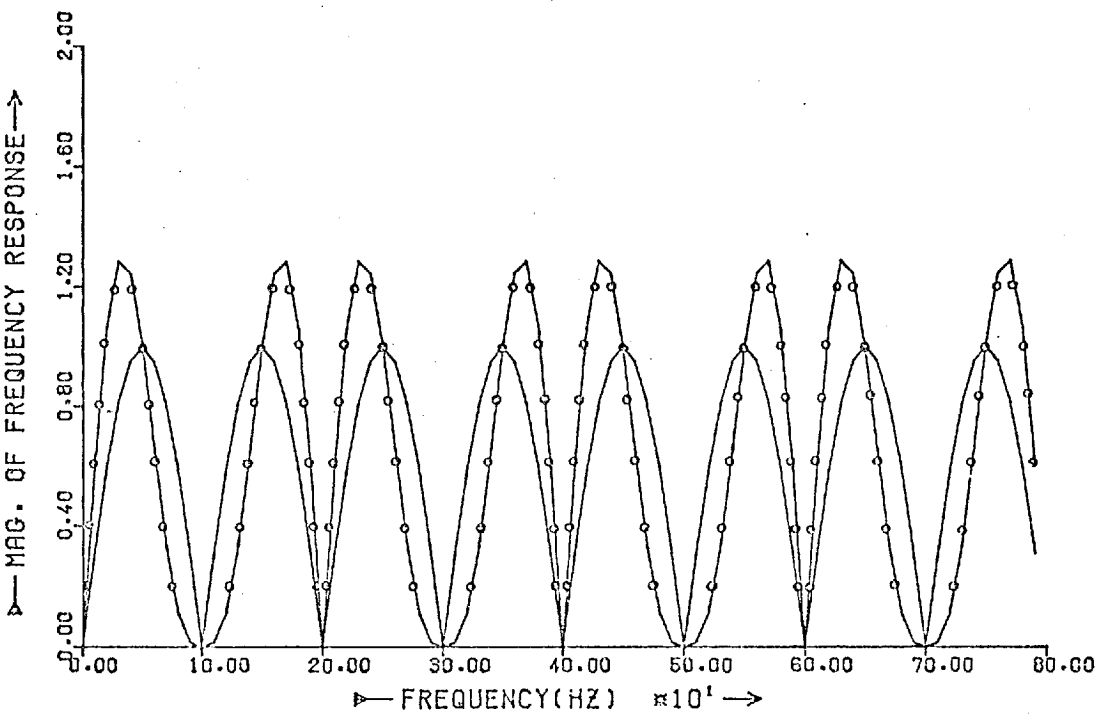

Fig. (3.30) Spectrums of the Fourier and square wave methods (A_{vk}) for 4 samples per cycle.

o—o—o—o— Square wave method

———— Fourier method

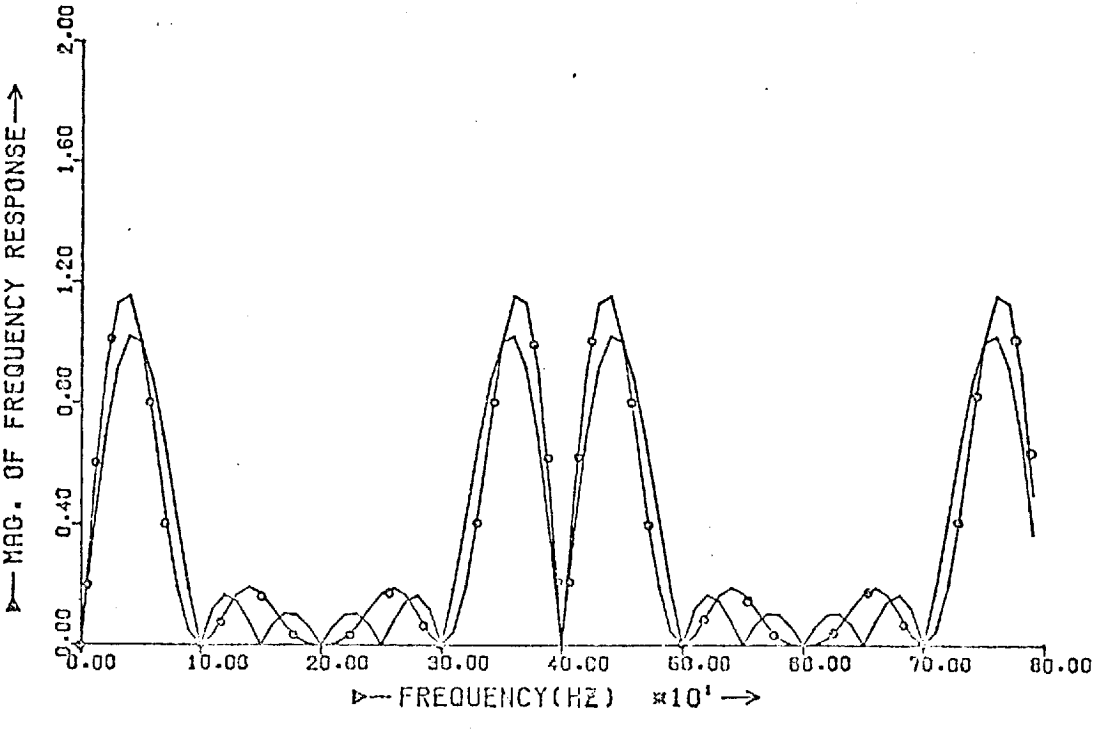

Fig. (3.31) Spectrums of the Fourier and square wave methods (A_{vk}) for 8 samples per cycle

—o—o—o— Square wave method

———— Fourier method

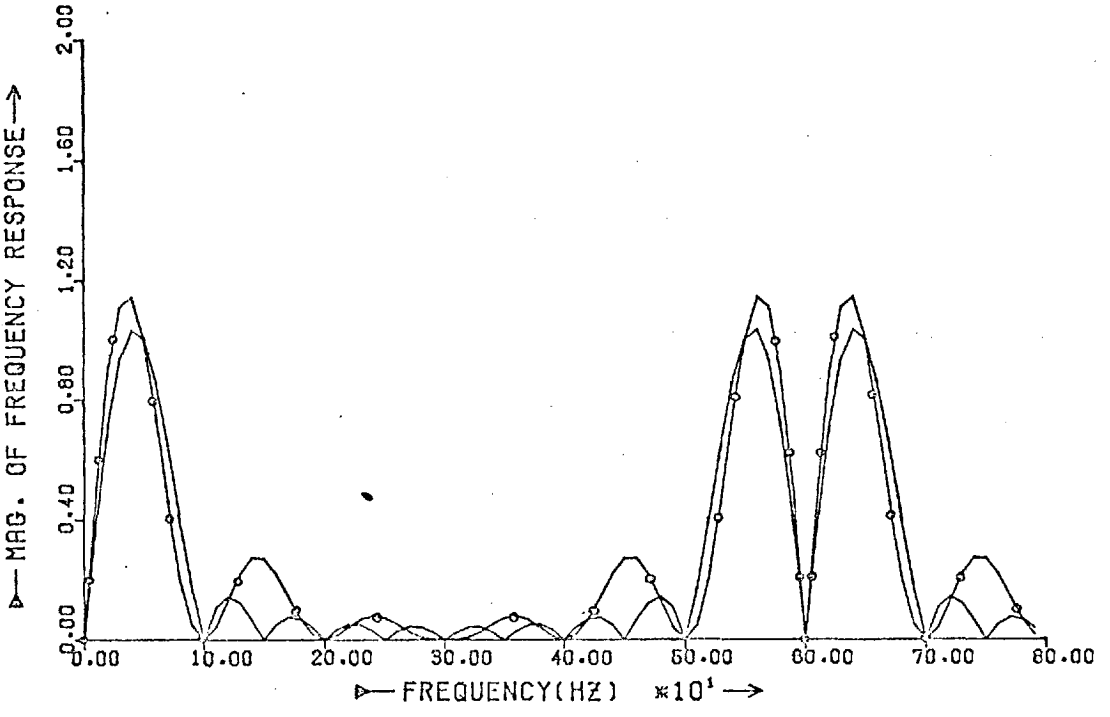

Fig. (3.32) Spectrums of the Fourier and square wave methods (A_{vk}) for 12 samples per cycle

—o—o—o— square wave method

——————— Fourier method

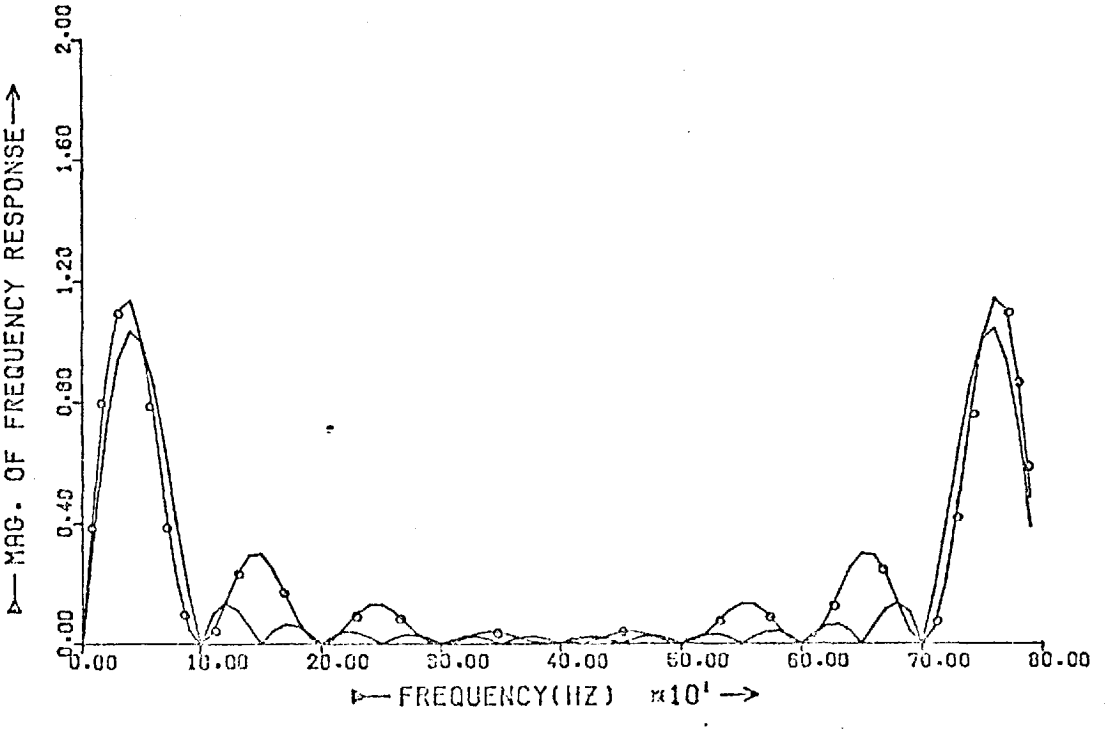

Fig.(3.33) Spectrums of the Fourier and square wave methcds (A_{vk}) for 16 samples per cycle

—o—o—o— square wave method

——————— Fourier method

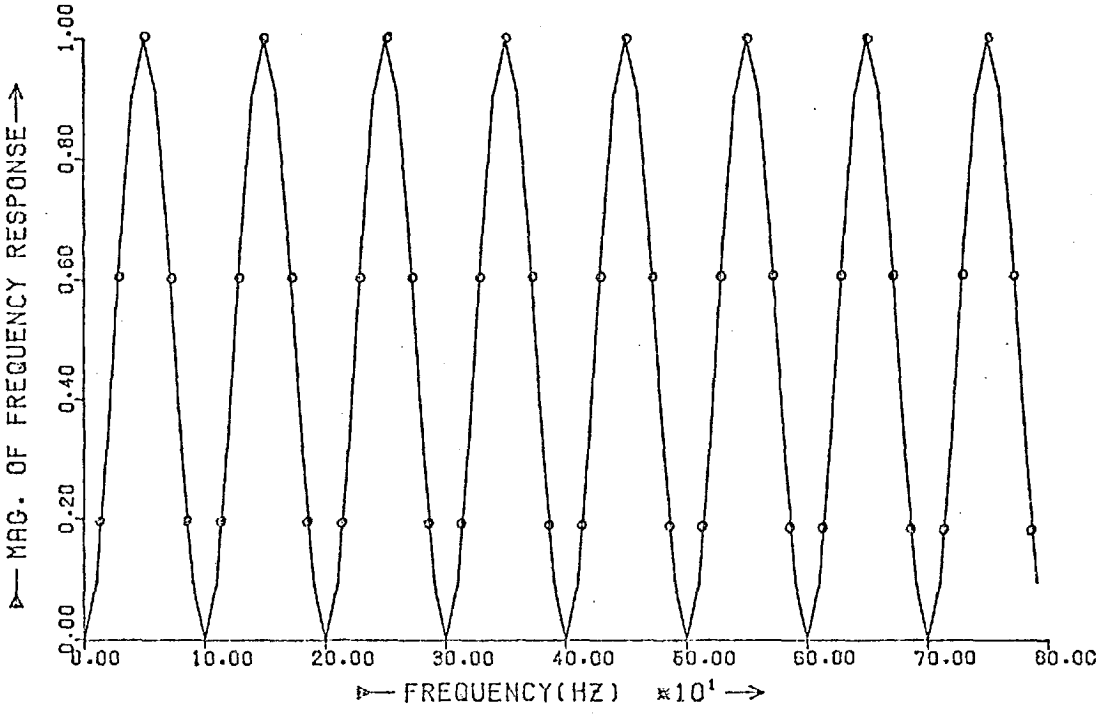

Fig. (3.34) Spectrums of the Fourier and square wave methods (B_{vk}) for 4 samples per cycle

—o—o—o— square wave method

———————— Fourier method

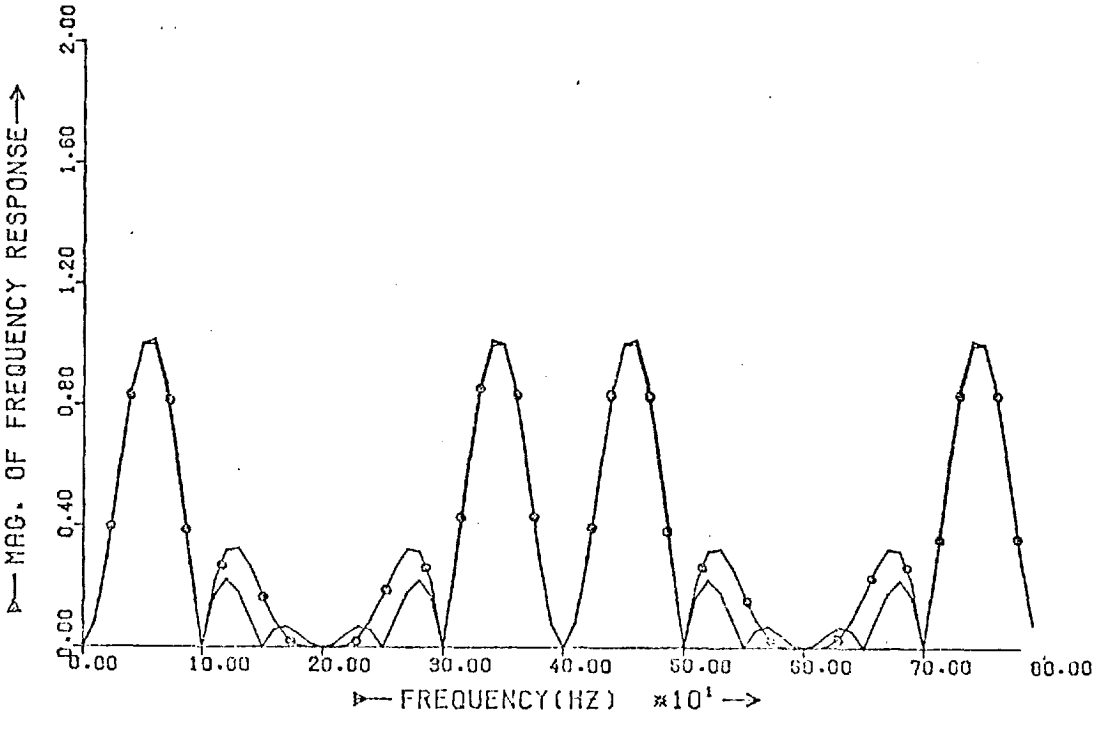

Fig. (3.35) Spectrums of the Fourier and square wave methods (B_{vk}) for 8 samples per cycle

—o—o—o— square wave method

———————— Fourier method

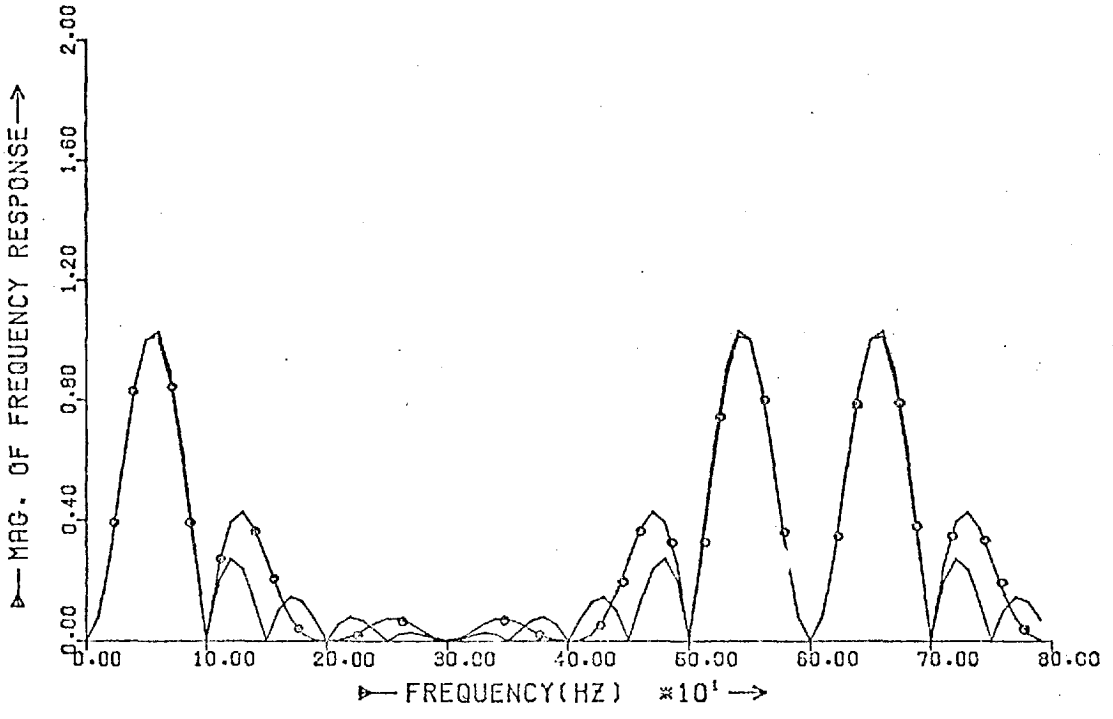

Fig. (3.36) Spectrums of the Fourier and square wave methods (B_{vk}) for 12 samples per cycle

—o—o—o— square wave method

——————— Fourier method

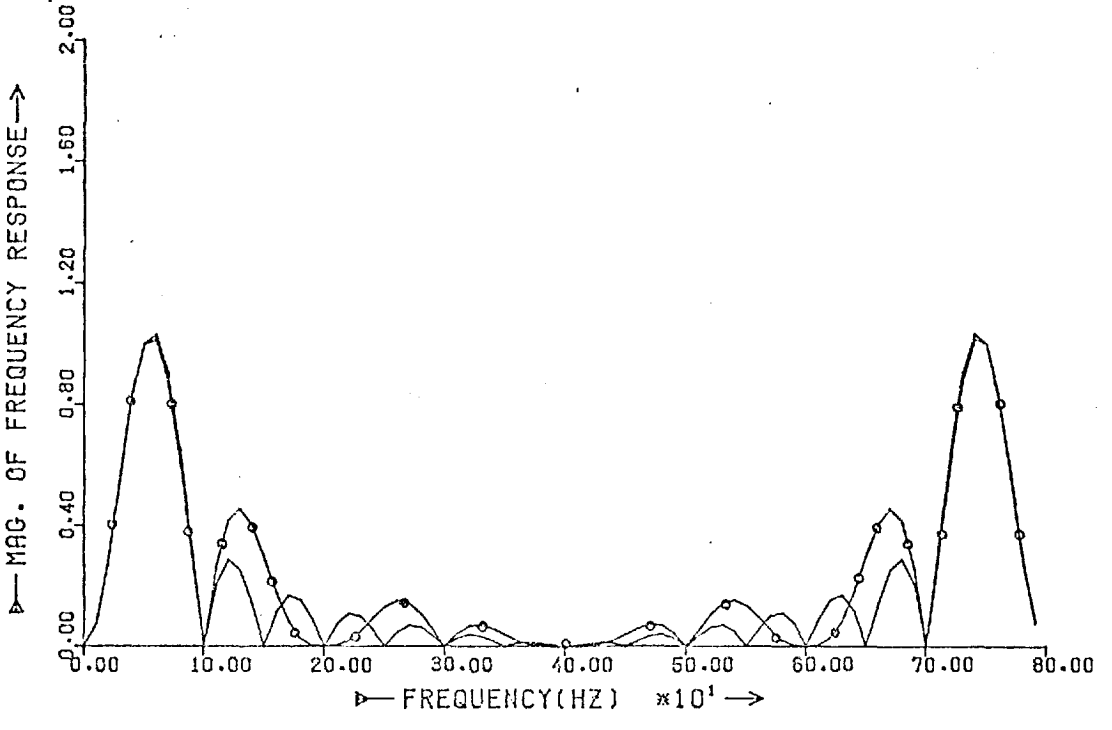

Fig. (3.37) Spectrums of the Fourier and square wave methods (B_{vk}) for 16 samples per cycle

—o—o—o— square wave method

——————— Fourier method

fundamental. The exponential dc offset of the current and voltage waveforms contain these sort of components which by this method will be accentuated. Consequently in dealing with exponential dc offset the behaviour of the square wave method is much poorer than the Fourier method. Also the attenuation of other unwanted components in the Fourier method is better than for the square wave method. For example in figure (3.36) the 130 Hz component has been attenuated 4 times by the Fourier method, but only 2.1 times by the square wave method. As a result of this comparison, no advantage is gained by use of the square wave method. Of course it can be argued that the calculation of A_v and B_v by this method does not need multiplications, but as seen earlier, by approximating the coefficients of the Fourier method, multiplication can be omitted, producing a characteristic which has negligible differences to the exact one.

3.3.4 McINNES METHOD[25]

The Fourier and square wave methods make use of equation (3.32) of section (3.3), to find the resistance and reactance of the transmission line. McInnes used equation (3.33) of that section for calculating resistance and reactance. By integrating equation (3.33) once over time instants (t_k) and (t_k+KT) and again over (t_{k+1}) and $(t_{k+1}+KT)$, the following two equations are obtained:

$$\int_{t_k}^{t_k+KT} \upsilon dt = R \int_{t_k}^{t_k+KT} i_x dt + L \int_{t_k}^{t_k+KT} di_y \qquad (3.98a)$$

$$\int_{t_{k+1}}^{t_{k+1}+KT} \upsilon dt = R \int_{t_{k+1}}^{t_{k+1}+KT} i_x dt + L \int_{t_{k+1}}^{t_{k+1}+KT} di_y \qquad (3.98b)$$

K is an arbitrary constant whose optimum value will be determined later on. These two equations can be written as:

$$SV_k = R\ SI_k + L\ DI_k \tag{3.99a}$$

$$SV_{k+1} = R\ SI_{k+1} + L\ DI_{k+1} \tag{3.99b}$$

where SV_k, SI_k, ... represent the integration terms in equations (3.98). From this pair of simultaneous equations, R and L can be calculated:

$$R = \frac{SV_{k+1}\ DI_k - SV_k\ DI_{k+1}}{SI_{k+1}\ DI_k - SI_k\ DI_{k+1}} = \frac{M_R}{D} \tag{3.100a}$$

$$L = \frac{T}{2}\ \frac{SV_k . SI_{k+1} - SV_{k+1}\ SI_k}{SI_{k+1} . DI_k - SI_k . DI_{k+1}} = \frac{M_L}{D} \tag{3.100b}$$

using the trapezoidal rule and N samples per cycle, SV_k and SI_k and DI_k can be written as:

$$\frac{2}{T}\ SV_k = \upsilon_{k+K} + \upsilon_k + 2 \sum_{n=1}^{k-1} \upsilon_{k+n} \tag{3.101a}$$

$$\frac{2}{T}\ SI_k = i_{k+K} + i_k + 2 \sum_{n=1}^{K-1} i_{k+n} \tag{3.101b}$$

$$DI_k = i_{k+K} - i_k \tag{3.101c}$$

where the υ_k and i_k ... are the instantaneous samples of voltage and current taken at equally spaced intervals. A similar equation can be written for SV_{k+1}, SI_{k+1} and DI_{k+1}. These equations are three non-recursive digital filters with the current and voltage samples as inputs and SI_k, ... as outputs. The transfer functions of SV_k and SI_k are the same and so only SV_k and DI_k will be considered. The Z-transform of DI_k is:

$$Z(DI_k) = (1-\bar{Z}^K)\ Z\ (i_k) \tag{3.102}$$

and so

$$H_{DI_k}(Z) = \frac{Z(DI_k)}{Z(i_k)} = 1-\bar{Z}^K \tag{3.103}$$

or in terms of frequency it will be:

$$H_{DI_k}(f) = 2 \sin \frac{K\pi f}{50N}\ e^{j(\frac{1}{2} - \frac{Kf}{50N})\pi} \tag{3.104}$$

and the magnitude of its spectrum is:

$$|H_{DI_k}(f)| = 2|\sin \frac{K\pi f}{50N}| \tag{3.105}$$

Equation (3.105) shows that the frequency response of this filter has a sine shape and is dependent on two parameters; N (sampling rate) and K representing the interval over which the integration is performed. If it is desired to attenuate the unwanted components with respect to the fundamental, the maximum of the sine characteristic must occur at 50 Hz. For this we must have

$$|\sin (\frac{50K\pi}{50N})| = 1 \tag{3.106}$$

or

$$\frac{K\pi}{N} = \frac{\pi}{2}, \frac{3\pi}{2}, \frac{5\pi}{2}, \ldots \tag{3.107}$$

or

$$K = \frac{N}{2}, \frac{3N}{2}, \frac{5N}{2}, \ldots \tag{3.108}$$

This is a very interesting result, since in order to have all components attenuated with respect to 50 Hz, the interval of integration must be half a cycle, $\frac{3}{2}$ cycles etc. and from this interval the smallest giving the fastest fault detection routine is the optimum. So if the integration interval is chosen to be half a cycle, independent of the sampling rate, the spectrum is as in figure (3.38). By increasing this interval, figure (3.39) is obtained and decreasing it, figure (3.40). In both figures the accentuation of the undesirable component can be seen.

The transfer function of SV_k is:

$$H_{SV_k} = \frac{T}{2} \frac{(1+\bar{Z}^{-1})(\bar{Z}^{K}-1)}{\bar{Z}^{1}-1} \tag{3.109}$$

giving the spectrum:

$$|H_{SV_k}(f)| = \frac{1}{N} |\sin \frac{K\pi f}{50N} \cot \frac{\pi f}{50N}| \tag{3.110}$$

Here again it can be shown that k equal to $\frac{N}{2}$ produces the optimum characteristic. For $k = \frac{N}{2}$ equation (3.110) becomes:

$$|H_{SV_k}(f)| = \frac{1}{N} \left|\sin \frac{\pi f}{100} \cot \frac{\pi f}{50N}\right| \qquad (3.111)$$

This spectrum, as is seen in figures (3.41) to (3.43) for 4, 8 and 16 samples per cycle is dependent on the sampling rate. Hence in this method the choice of cut-off frequency for the analogue filter depends upon the spectrum of DI_k, because this term is most vulnerable with respect to the harmonic and non-harmonic components. As stated, for optimizing the characteristic, the integration interval must be half a cycle, which gives the spectrum shown in figure (3.38). This spectrum is independent of the sampling rate, and is the same as the spectrum of Fourier with 4 samples per cycle, and like that method, as already discussed, for effective removal of the unwanted components a second order Butterworth filter with 60 Hz cut-off frequency is needed. The overall spectrum of Fig.(3.44) shows this combination. With this analogue filter, the spectrums of SV_k and SI_k with any rate of sampling equal or larger than 4 is acceptable, but from a numerical point of view the higher rate of sampling gives greater accuracy. For this reason 8 samples per cycle is suggested because it gives acceptable numerical accuracy and at the same time is low enough to allow for simple hardware. The overall characteristic of SV_k with a 60 Hz second order Butterworth filter and 8 samples per cycle is shown in Fig. (3.45). With this method, calculation of R and X requires samples of little more than half a cycle and so with a 6.37 ms time delay of the analogue filter, the overall fault detection time, even for the fault at the end of the line, is less than one cycle, Hence this method is faster than the Fourier method which needs the samples of one complete cycle for distant faults.

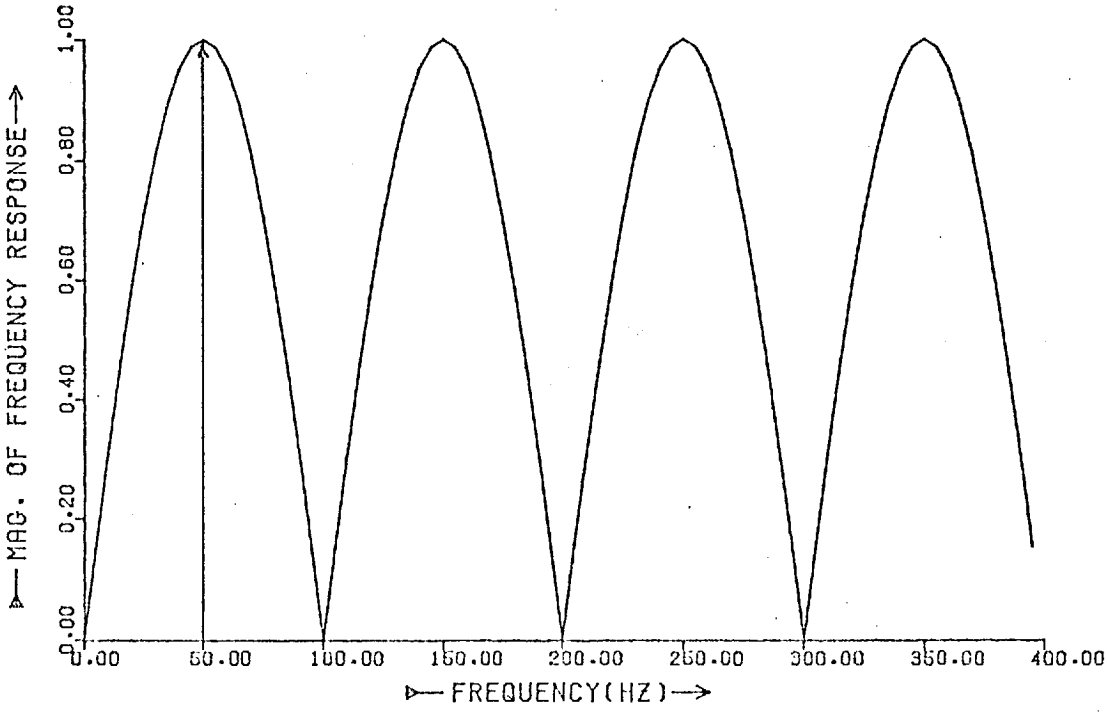

Fig. (3.38) Spectrum of DI_k when the interval of integration is half a cycle.

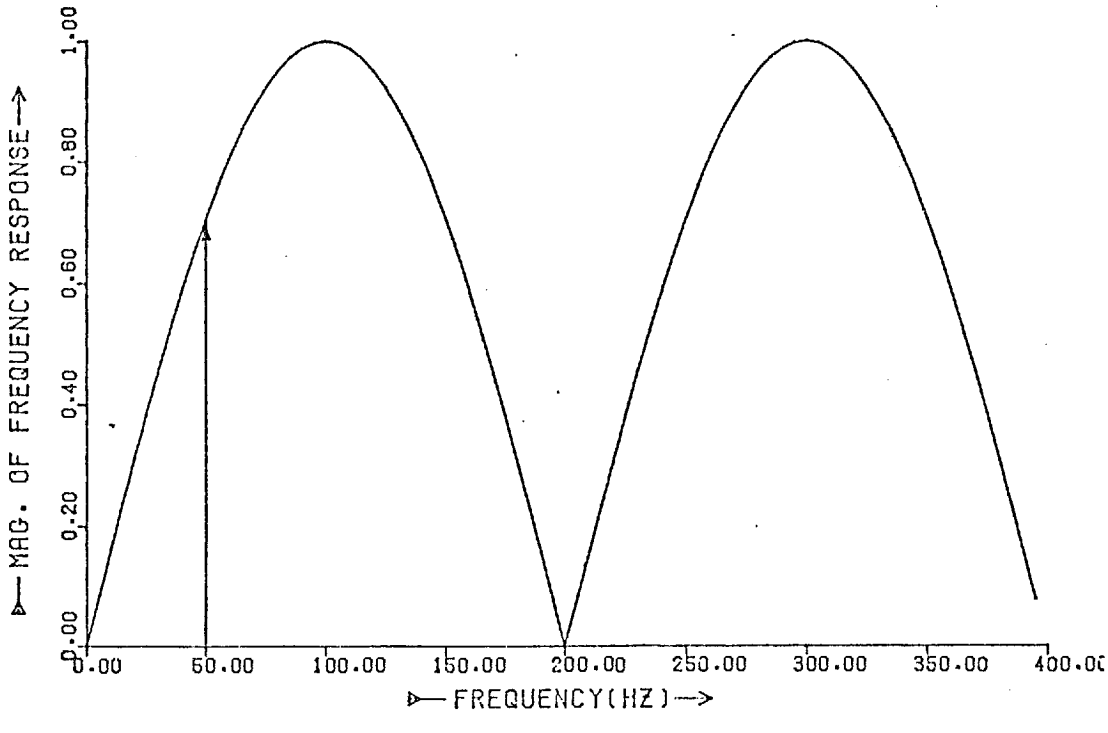

Fig. (3.39) Spectrum of DI_k when the interval of integration is more than half a cycle

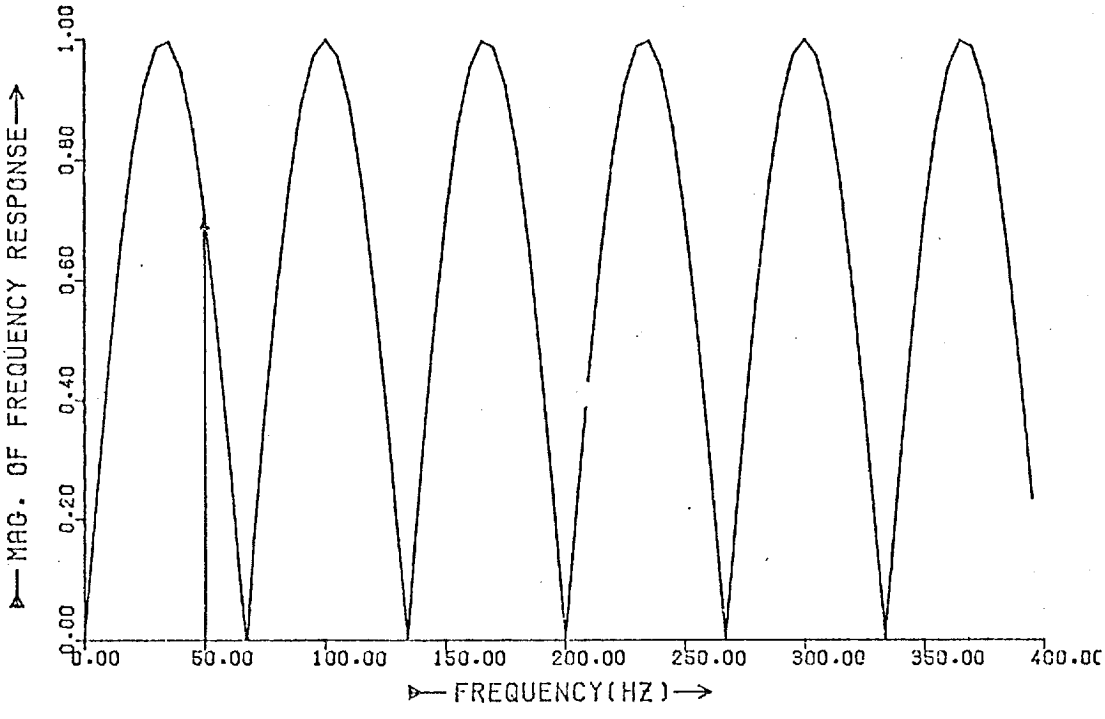

Fig. (3.40) Spectrum of DI_k when the interval of integration is less than half a cycle.

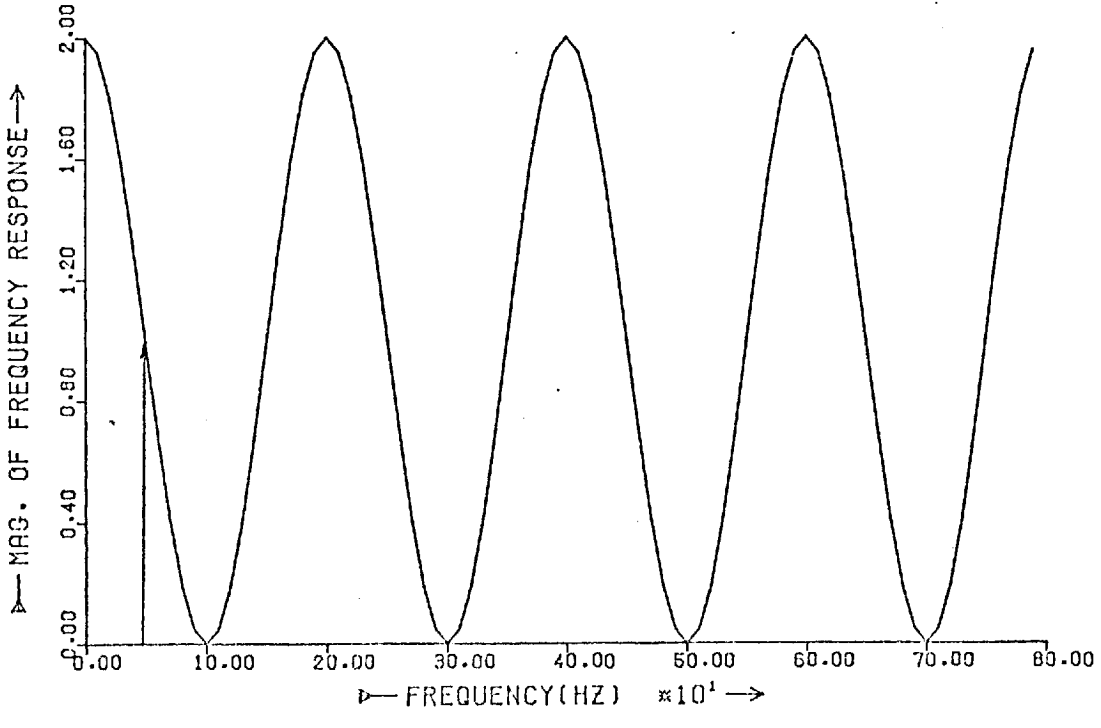

Fig. (3.41) Spectrum of SV_k for 4 samples per cycle

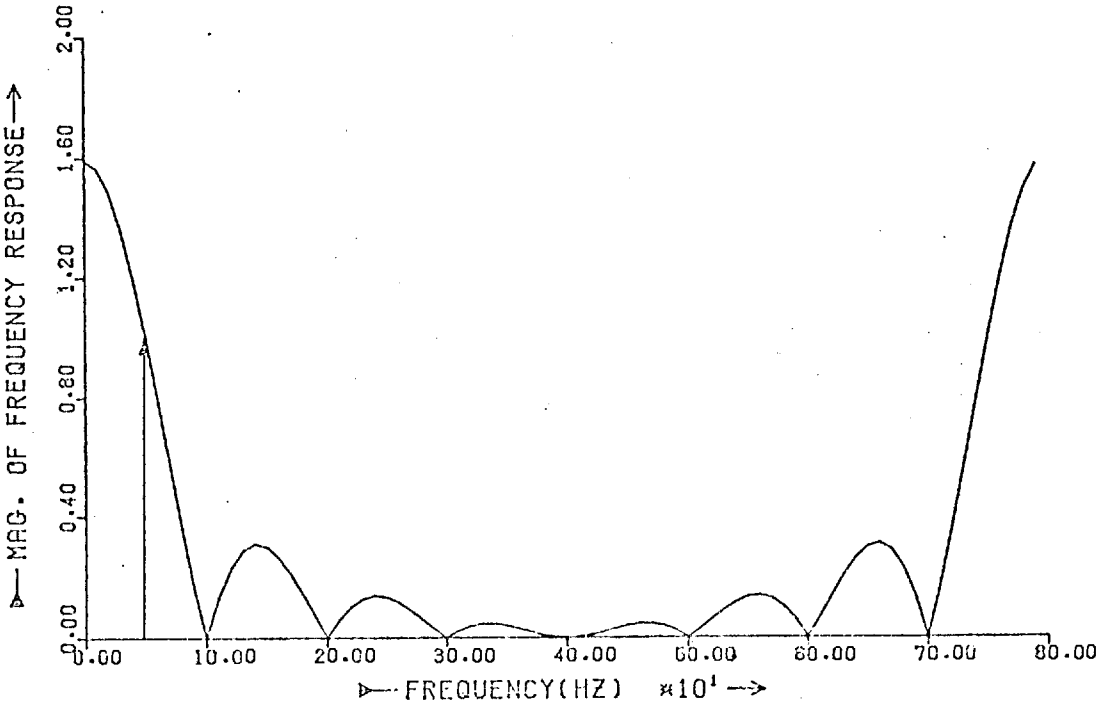

Fig. (3.42) Spectrum of SV_k for 16 samples per cycle

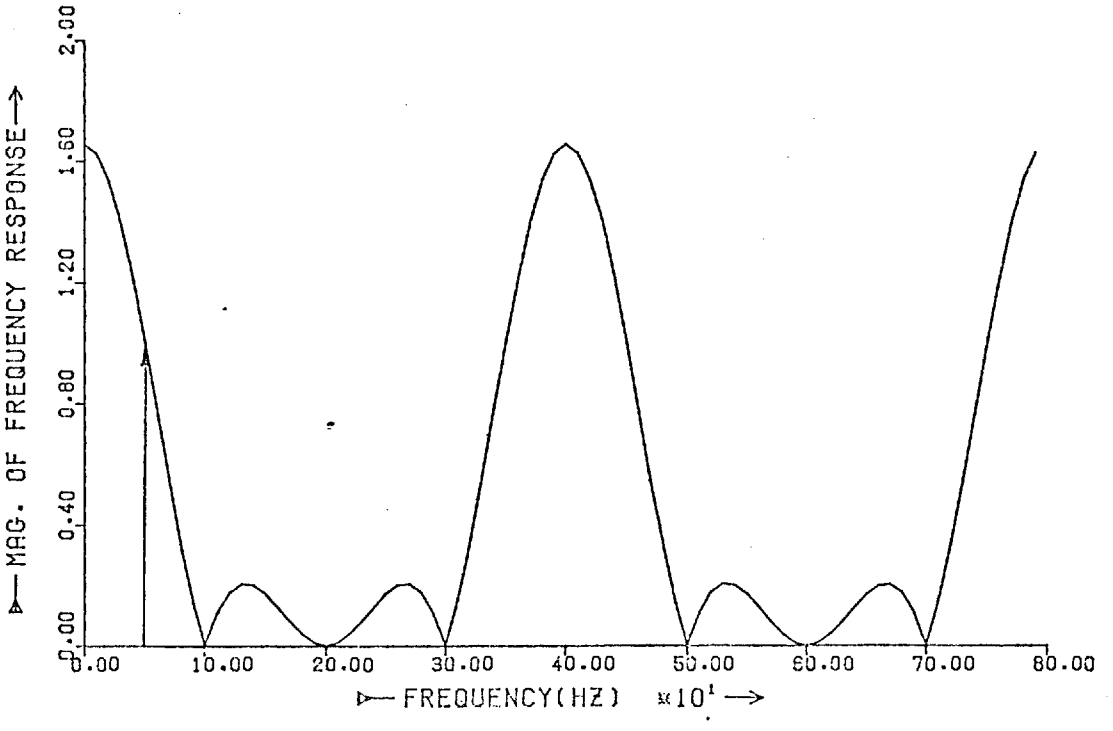

Fig. (3.43) Spectrum of SV_k for 8 samples per cycle

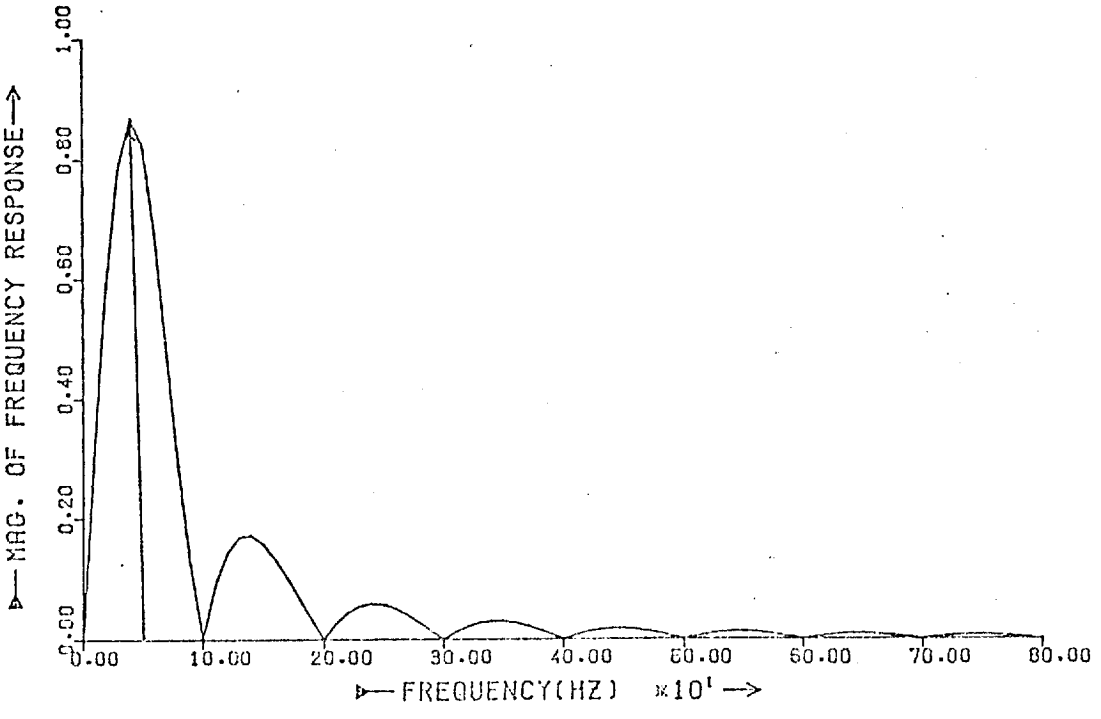

Fig. (3.44) Spectrum of DI_k with a 60 Hz second order Butterworth filter

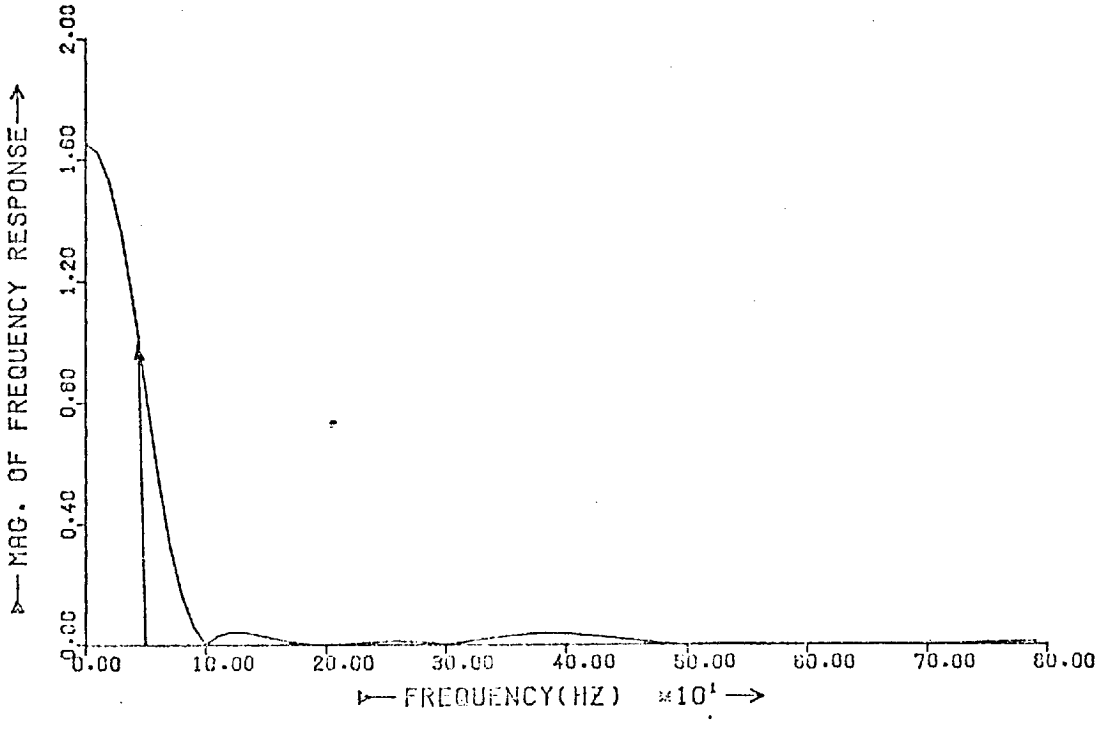

Fig. (3.45) Spectrum of SV_k with 8 samples per cycle and a 60 Hz second order Butterworth filter

3.3.5 MEAN SQUARE ERROR MINIMIZATION METHOD[26]

Equation (3.33) of section (3.3) can be rewritten as:

$$L \frac{di_y}{dt} + R\, i_x - \upsilon = e \tag{3.112}$$

where e is the error caused by shunt capacitance and noise effects

By integrating both sides over (O,t) we obtain:

$$L \int_o^t di_y + R \int_o^t i_x dt - \int_o^t \upsilon dt = e_t \tag{3.113}$$

The average of the square of the errors over the interval τ is given by:

$$e_m = \frac{1}{\tau} \int_o^\tau [L \int_o^t di_y + R \int_o^t i_x dt - \int_o^t \upsilon dt]^2 dt \tag{3.114}$$

We can choose L and R so that e_m is a minimum, for which the partial derivatives of e_m with respect to R and L should be zero. The following equations are obtained:

$$R \int_o^\tau (\int_o^t di_y)(\int_o^t i_x dt)dt + L \int_o^\tau (\int_o^t di_y)^2 dt = \int_o^\tau (\int_o^t \upsilon dt)(\int_o^t di_y)d$$

and (3.115a

$$R \int_o^\tau (\int_o^t i_x dt)^2 dt + L \int_o^\tau (\int_o^t di_y)(\int_o^t i_x dt)dt = \int_o^\tau (\int_o^t i_x dt)(\int_o^t \upsilon dt)dt$$

(3.115b

From these two equations R and L can be calculated. In comparison with the McInnes method better accuracy can be obtained, but the method is more complex and needs many more multiplications. For this reason it is discarded.

3.3.6 MINIMIZATION OF ERRORS OVER SEVERAL INTERVALS

In equation (3.113) the interval (O-t) can be divided into n parts by taking a sequence of samples[27]. This allows n equation of the type

$$R \int_{t_i}^{t_j} i_x dt + L(i_{yj} - i_{yi}) - \int_{t_i}^{t_j} \upsilon dt = e_j \tag{3.116}$$

to be written for the intervals t_i t t_j. Minimising $\sum_{j=1}^{n} e_j^2$ in re-

lation to R and L gives two equations from which R and L can be calculated as before. The accuracy of this method was found[26] to be less than the method 3.3.5 although the speed of computation was about the same.

3.3.7 DIGITAL HARMONIC FILTERING METHOD[26]

In general, it is possible to calculate R and L from equation (3.33) so that any number of harmonics can be eliminated. For example, to remove the third harmonic, equation (3.33) can be integrated once over $0,\beta$ (β is an arbitrary constant) and again over the intervals $\frac{\pi}{3}$, $(\beta + \frac{\pi}{3})$, the resulting equations, when added give:

$$L\left[\int_0^{\beta} di_y + \int_{\pi/3}^{\beta+\pi/3} di_y\right] + R\left[\int_0^{\beta} i_x dt + \int_{\pi/3}^{\beta+\pi/3} i_x dt\right] =$$

$$\int_0^{\beta} \upsilon dt + \int_{\pi/3}^{\beta+\pi/3} \upsilon dt \qquad (3.117)$$

In this equation the third harmonic is completely filtered. Also to remove the third and fifth harmonics equation (3.33) can be integrated once over $(o, \frac{2\pi}{5})$ and again over the interval $\frac{\pi}{3}$, $(\frac{\pi}{3} + \frac{2\pi}{5})$. The resulting equations, when added, give:

$$L\left[\int_0^{\frac{2\pi}{5}} di_y + \int_{\frac{\pi}{3}}^{\frac{2\pi}{5}+\frac{\pi}{3}} di_y\right] + R\left[\int_0^{\frac{2\pi}{5}} i_x dt + \int_0^{\frac{2\pi}{5}+\frac{\pi}{3}} i_x dt\right] =$$

$$\int_0^{\frac{2\pi}{5}} \upsilon dt + \int_{\frac{\pi}{3}}^{\frac{2\pi}{5}+\frac{\pi}{3}} \upsilon dt \qquad (3.118)$$

In general to remove two harmonics of order m and n the resulting equation will be:

$$L\left[\int_0^{\frac{2\pi}{m}} di_y + \int_{\frac{\pi}{n}}^{\frac{2\pi}{m}+\frac{\pi}{n}} di_y\right] + R\left[\int_0^{\frac{2\pi}{m}} i_x dt + \int_{\frac{\pi}{n}}^{\frac{2\pi}{m}+\frac{\pi}{n}} i_x dt\right] =$$

$$\int_0^{\frac{2\pi}{m}} \upsilon dt + \int_{\frac{\pi}{n}}^{\frac{2\pi}{m}+\frac{\pi}{n}} \upsilon dt \qquad (3.119)$$

This principle can be extended to any number of harmonics by making a sufficient number of integrations. For example, three harmonics of orders m,n and k can be eliminated by using:

$$L\ (\sum\int di_y) + R\ (\sum\int i_x dt) = \sum\int \upsilon dt \qquad (3.120)$$

where

$$\sum\int \upsilon dt = \int_0^{\frac{2\pi}{k}} \upsilon dt + \int_{\frac{\pi}{m}}^{\frac{2\pi}{k}+\frac{\pi}{m}} \upsilon dt + \int_{\frac{\pi}{n}}^{\frac{2\pi}{k}+\frac{\pi}{n}} \upsilon dt + \int_{\frac{\pi}{m}+\frac{\pi}{n}}^{\frac{2\pi}{k}+\frac{\pi}{m}+\frac{\pi}{n}} \upsilon dt$$

and $\sum\int di_y$ and $\sum\int i_x$ are calculated similarly. The spectrum of this method is better than that of McInnes (see discussion of reference 26) but it involves a little more calculation and also it needs more memory space, which is an important factor if it is intended to use a micro-processor for implementation.

3.3.8 GILBERT AND SHOVLIN METHOD[28]

Neglecting the exponential dc offset and other undesirable components of current and voltage waveforms, Gilbert and Shovlin showed that R and X can be calculated from:

$$R = \frac{2\upsilon_{k-1}\ i_{k-1} - \upsilon_k\ i_{k-2} - \upsilon_{k-2}\ i_k}{2(i_{k-1}^2 - i_{k-2}\ i_k)} \qquad (3.121a)$$

$$X = \frac{\upsilon_{k-1}\ i_k - \upsilon_k\ i_{k-1}}{i_{k-1}^2 - i_{k-2}\ i_k} \sin(\omega T) \qquad (3.121b)$$

This method is very sensitive to dc offset and noise and so only from an academic point of view it is of interest (see discussion on the method at the end of this thesis).

3.3.9 ORTHOGONAL NOTCH DIGITAL FILTERS METHOD[29]

Carr and Jackson[29] established a method involving two orthogonal notch digital filters with sine characteristics from which the magnitude and phase angle of the fundamental components of a waveform can be calculated from samples taken at four

equally spaced time intervals over a period. In this way they obtained the following equations:

$$4\ C_k\ \underline{/^{\phi}k} = (x_{k-4}-2X_{k-2}+X_k)-j(2X_{k-3}-2X_{k-1}) \tag{3.122a}$$

$$4\ C_{k+1}\ \underline{/^{\phi}k+1} = (-2X_{k-2}+2X_k)-j(X_{k-3}-2X_{k-1}+X_{k+1}) \tag{3.122b}$$

$$4\ C_{k+2}\ \underline{/^{\phi}k+2} = (-X_{k-2}+2X_k-X_{k+2})-j(-2X_{k+1}+2\ X_{k+1}) \tag{3.122c}$$

$$4\ C_{k+3}\ \underline{/^{\phi}k+3} = (-2X_{k+2}+2X_k)-j(-x_{k-1}+2X_{k+1}-X_{k+3}) \tag{3.122d}$$

The two-term brackets have a sine wave, and the three term brackets have a sine-squared wave characteristic. It can be shown that this method is the same as a Fourier method with 4 samples per cycle. By using a Fourier method the real and imaginary parts of a phasor quantity can be calculated as follows:

$$\text{Real} = \frac{1}{\pi}\int_{\pi/2}^{2\pi+\pi/2} x\ \sin(\omega t)\ d\ (\omega t) \tag{3.123a}$$

$$\text{Imag.} = \frac{1}{\pi}\int_{\pi/2}^{2\pi+\frac{\pi}{2}} x\ \cos\ (\omega t)\ d\ (\omega t) \tag{3.123b}$$

where x is the continuous function whose samples x_k, x_{k-1}, ... are the input of the digital filter. Using the trapezoidal rule with 4 intervals over a period, equations (3.123) can be rewritten as:

$$\text{Real} = \frac{1}{\pi}\cdot\frac{2\pi}{4}\cdot\frac{1}{2}\ (X_{k-4}\sin\frac{\pi}{2} + 2X_{k-3}\sin\pi + 2X_{k-2}\sin\frac{3\pi}{2} + 2\ X_{k-1}\ \sin 2\pi + x_k\ \sin\frac{5\pi}{2}$$

and

$$\text{Imag.} = \frac{1}{\pi}\cdot\frac{2\pi}{4}\cdot\frac{1}{2}\ (X_{k-4}\cos\frac{\pi}{2} + 2X_{k-3}\ \cos\pi + 2X_{k-2}\ \cos\frac{3\pi}{2} + 2X_{k-1}\ \cos 2\pi + x_k\ \cos\frac{5\pi}{2}\ )$$

or

$$\text{Real} = \frac{1}{4}\ (X_{k-4}\ -2\ X_{k-2} + X_k)$$

$$\text{Imag.} = \frac{1}{4}(-2X_{k-3}+2X_{k-1})$$

From here:

$$C_k \angle\phi_k = \frac{1}{4}(X_{k-4}-X_{k-2}+x_k) + \frac{j}{4}(-2X_{k-3}+2X_{k-1})$$

or

$$4C_k \angle\phi_k = (x_{k-4}-2X_{k-2}+x_k) - j(2X_{k-3}-2X_{k-1})$$

By moving ahead with new samples the interval of the integrations changes to $(\pi, 2\pi+\pi)$, $(\frac{3\pi}{2}, 2\pi+\frac{3\pi}{2})$ and $(2\pi, 4\pi)$ which give c_{k+1}, c_{k+2} and c_{k+3}. So there is no difference between the orthogonal notch digital filters method and the Fourier method with 4 samples per cycle (also see discussion at the end of this thesis).

3.3.10 CURVE FITTING METHOD[30]

By using the least square method, the samples can be fitted to an offset sine wave,and from which the real and imaginary part of the voltage and current can be calculated. The waveform is assumed to be as:

$$K_1 e^{-\xi t} + \sum_{m=1}^{M} (K_{2m}\sin m\omega t + K_{2m+1}\cos m\omega t) \qquad (3.124)$$

where M is the number of harmonics being considered, ξ is the decaying time constant and ω is the angular frequency of the fundamental. To fit the fault current or voltage to expression (3.124) the following function must be minimised:

$$E = \int_0^T \left[I - K_1 e^{-\xi t} - \sum_{m=1}^{M} (K_{2m}\sin m\omega t + K_{2m+1}\cos m\omega t)\right]^2 dt$$

where I is the current or voltage waveform and T is the sampling period. After minimisation we obtain:

$$K_r = \int_0^T I\, f_r(t)\,dt \quad \text{for } r = 1, 2, \ldots, 2N+1$$

where the $f_r(t)$ are weighting functions which can be calculated

off-line. In this method ξ and $m\omega$ have to be predetermined. The method seems interesting and it is simple enough for on-line application, but it has two main drawbacks, namely:

(i) In general, the $\frac{X}{R}$ ratio for the source is different from that of the line, so different ξ values for faults at different points on the line are necessary. Also ξ depends on the fault resistance which might change widely for different fault and so ξ cannot be predetermined accurately.

(ii) During the fault there are a large variety of harmonics and non-harmonics generated. Analogue filters can remove high frequency components, but the algorithm should account for low frequency ones. Practically expression (3.124) can account only for 1 or 2 of these components, otherwise the off-line calculation of $f_r(t)$ becomes very complicated.

3.4 CONCLUSION

In this chapter we obtained the following results:

(i) The cut-off frequency of the analogue filter which is used in filtering the noise and high frequency components, depends on;type of algorithm, order of the filter and sampling rate.

(ii) In peak determination methods, in order to have all high frequency components attenuated with respect to 50 Hz the sampling rate should be 4S/C, which from a numerical point of view is not acceptable. Also this method is unable to cope with exponential dc components.

(iii) The Fourier method, with 8 S/C and a 150 Hz, two pole Butterworth filter, from the filtering point of view is quite acceptable, but its accuracy might be impaired by its inability to remove the exponential dc offset effectively. In this

method by approximating the coefficients, multiplication in real and imaginary parts of a phasor can be avoided, without any practical changes in the spectrum.

(iv) Square wave method accentuates some components and as a whole it has a poorer characteristic than the Fourier method. Also in dealing with the exponential dc off-set its behaviour is worse than that.

(v) In the McInnes method, the interval of integration must be half a cycle, otherwise the fault generated high frequency components will be accentuated. It directly accounts for exponential dc offset and this is its great advantage over other methods. If it is used with a 60 Hz, two pole Butterworth filter, it will filter out all noise and fault generated high frequency components.

In the next chapter these algorithms, in the presence of exponential dc off-set and fault generated high frequency components, are used to calculate R and X in a test model, and then the results are compared.

CHAPTER 4

OFF-LINE TESTS

In this chapter the effect of exponential dc offset and fault generated high frequency components on the accuracy of Fourier, Square wave and McInnes methods with different rate of sampling are studied. The typical system which was used for this purpose is described in Appendix A1. This system has a high $\frac{X}{R}$ ratio, and consequently for fault inception angles about zero radian, results in a high exponential dc offset. Many high frequency components are generated when fault inception angle is about $\pi/2$ radians. The waveforms obtained (Figs. 4.7) and (4.8) tend to be idealistic and neglect the effects of random and non-predictable parametres such as arc-resistance variations, sensitivity of zero-sequence impedance to earth resistivity and changes in mutual coupling between parallel circuits due to varying power flows. However, the simulation does allow the merits of different algorithms to be compared on the same basis.

4.1 D.C. OFF-SET STUDIES. TEST SERIES 1

The aim was to study the effect of the transient dc offset on the accuracy of the algorithm, and so at this stage the shunt capacitance of the line was discarded. To obtain the most severe dc off-set, the line was considered to be unloaded[31] and opened at point B (Fig.A1.1 in Appendix A1). For faults at the end of the line AB, the impedance seen at point A was calculated using different algorithms. The end of the line was chosen for fault study because the accuracy of the impedance calculation with a fault at this point is the most important one. In this model, the overall $\frac{\bar{X}}{R}$ ratio was about 23.8 which for some fault

inception angle results in a high transient dc off-set. The highest dc off-set was obtained for a zero fault inception angle and this component completely disappeared when the angle was equal to the overall system impedance (source + line) angle. The system impedance angle was near to $\pi/2$ and at this angle the dc component was negligible.

4.1.1 Fourier method

The impedance seen at point A was calculated for different sampling rates and different fault inception angles. Some typical results for 8 and 16 samples per cycle for 3 different fault inception angles can be seen in figure (4.1). From these the accuracy of the Fourier method is more or less independent of the sampling rate and a low rate of sampling (8 S/C) is preferred. The maximum errors of R and X are given in table (4.1) Col. A where it can be seen that for a fault inception angle near to $\pi/2$ the maximum error for X is less than 0.5% and for R less than 4%. For fault inception angles near zero, the errors increase and reach about 80% for R and 6% for X. The large error for zero fault inception angle is due to the exponential dc off-set in fault current and the inability of the Fourier method in removing this component effectively. The Fourier method attenuates this component but such attenuation is not enough.

The errors for R and X change periodically and the maximum errors reduce exponentially as the calculation continues. When the exponential dc off-set disappears the errors become negligible. This effect can be shown also mathematically: If in the presence of an exponentially dc off-set the peak of the current waveform is calculated by the Fourier method, the result would be:

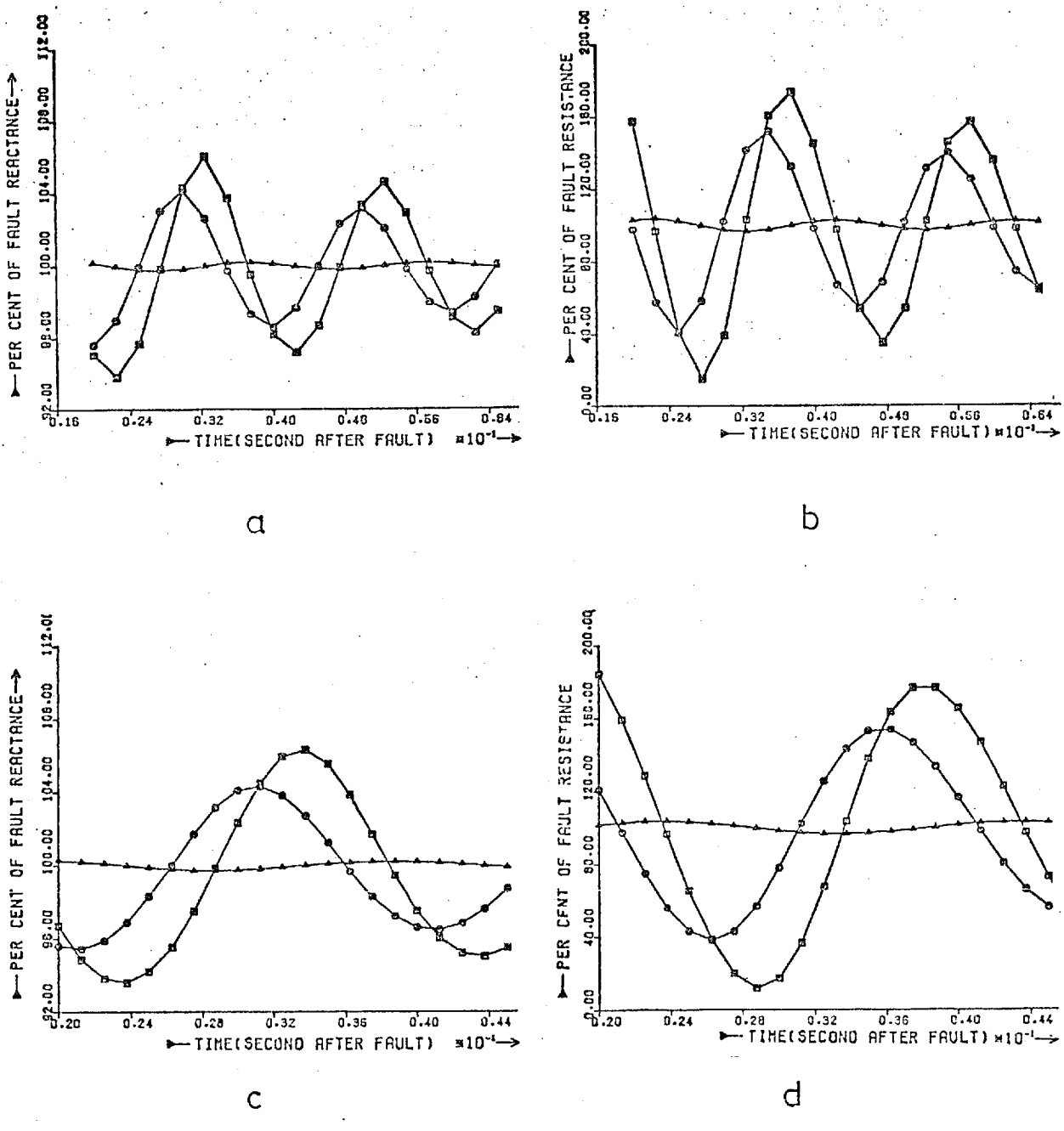

Fig. (4.1) Results of resistance and reactance calculation by the Fourier method. (Shunt capacitance is discarded).

a and b : calculated resistance and reactance with 8 samples per cycle

c and d : calculated resistance and reactance with 16 samples per cycle

zero fault inception angle

$\pi/4$ fault inception angle

$\pi/2$ fault inception angle

$$\frac{\text{Calculated current peak}}{\text{Actual current peak}} = \left(1+C_1 e^{\frac{-2}{\tau}t} + C_2 e^{\frac{-1}{\tau}t} \cos(\omega t+\gamma)\right)^{\frac{1}{2}} \quad (4.1)$$

where C_1, C_2 and γ are constant coefficients and τ is the time constant of the exponential dc component of the current waveform. Equation (4.1) shows that the calculated current peak changes periodically and its error decreases exponentially until it becomes (in the steady state) equal to the actual current peak.

Figure (4.2) shows the accuracy of the Fourier method with 8 samples per cycle with exact and approximated coefficient ($\sqrt{2}$ and 1.5), and no difference is descernable between them. In the previous chapter it was seen that from filtering point of view they are also identical.

It can be concluded that the Fourier coefficients can be approximated without practically affecting accuracy or spectrum.

Table (4.1) Maximum error (in %) for different methods
Shunt capacitance is discarded

Sampling rate	Fault inception angle (FIA)	R and X	Fourier method A	Square Wave method B	McInnes method trapezoidal rule C	McInnes method Simpson rule D
8 S/C	0	R	73.76	115.75	14.23 (142.1)	0.79 (1.66)
		X	6.08	8.54	5.75 (8.82)	0.28
	$\pi/2$	R	3.79	5.20	0.17	0.00
		X	0.26	0.35	5.21	0.00
16 S/C	0	R	87.88	111.20	4.14 (23.57)	0.41
		X	6.38	8.17	1.47 (2.41)	0.03
	$\pi/2$	R	3.95	5.00	0.14	0.00
		X	0.27	0.35	1.29	0.00

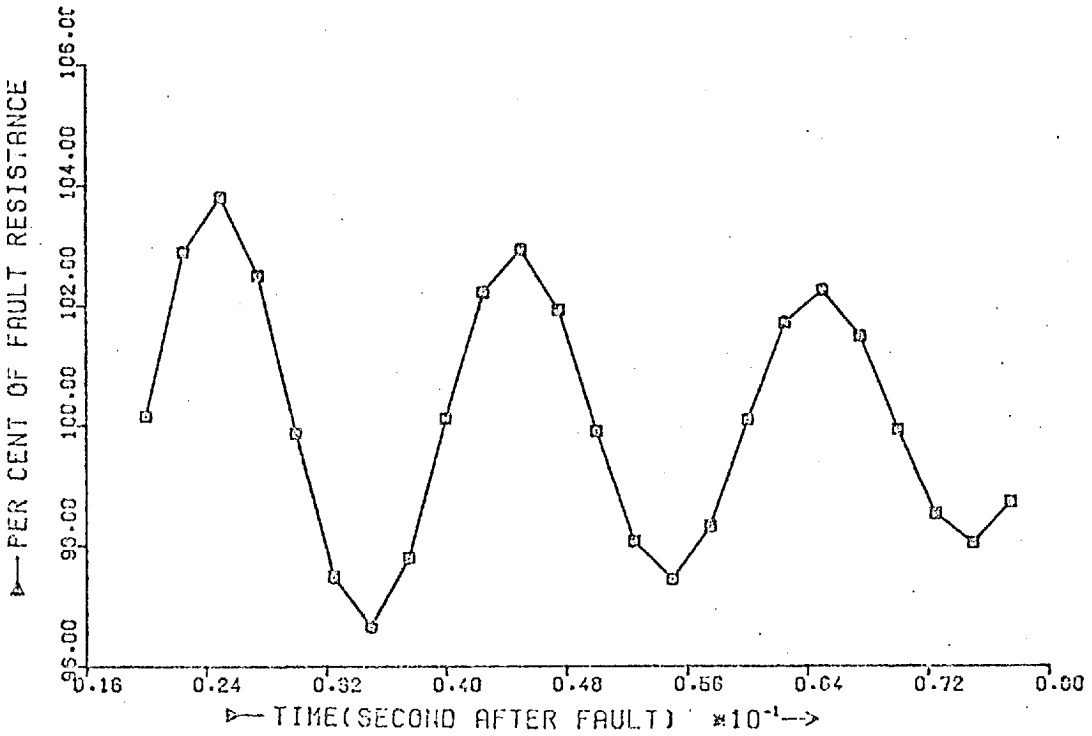

Fig. (4.2) The results of resistance calculation with the Fourier method and 8 samples per cycle.

Exact coefficients

Approximated coefficients

4.1.2 Square wave method

Some typical results for this method with 8 16 S/C and for 3 different fault inception angles can be seen in figure (4.3). Like the Fourier method, the accuracy is the same for different rates of sampling. Also the errors change periodically and decreases exponentially. The maximum error for resistance changes from about 5% (when FIA = $\pi/2$) to about 115% (when FIA = 0) and for reactance it changes from about 0.5% (FIA = $\pi/2$) to about 8.5% (FIA = 0). As a whole the overall accuracy is less than the Fourier method. Hence a modified Fourier method with 8 samples per cycle is preferable, because it gives greater accuracy with similar simplicity.

4.1.3 McInnes method

The integration terms SV_k, SI_k,... in the McInnes method can be calculated by using either the trapezoidal or Simeson's rule. The trapezoidal rule is simpler but it gives less accuracy than Simpson's rule. From a spectrum point of view both of them produce almost identical results. Typical results can be seen in figures (4.4). Also the maximum errors are given in table (4.1) Col. C. In contradistinction to the Fourier and square wave methods, increasing the sampling rate improves the accuracy. With 8 S/C, the error for R is less than 15% and for X is less than 6%. With 16 samples per cycle, these errors reduce to 5 and 1.5% respectively. Figure (4.4) shows that at some point the error is large. These large errors, which appear only at two or three points have been shown in brackets in the table (4.1). These errors are due to the exponential dc offset in current waveforms. When there is no exponential dc off-set the numerators and denominators in the equation (3.100a) and (3.100b) are constant, but

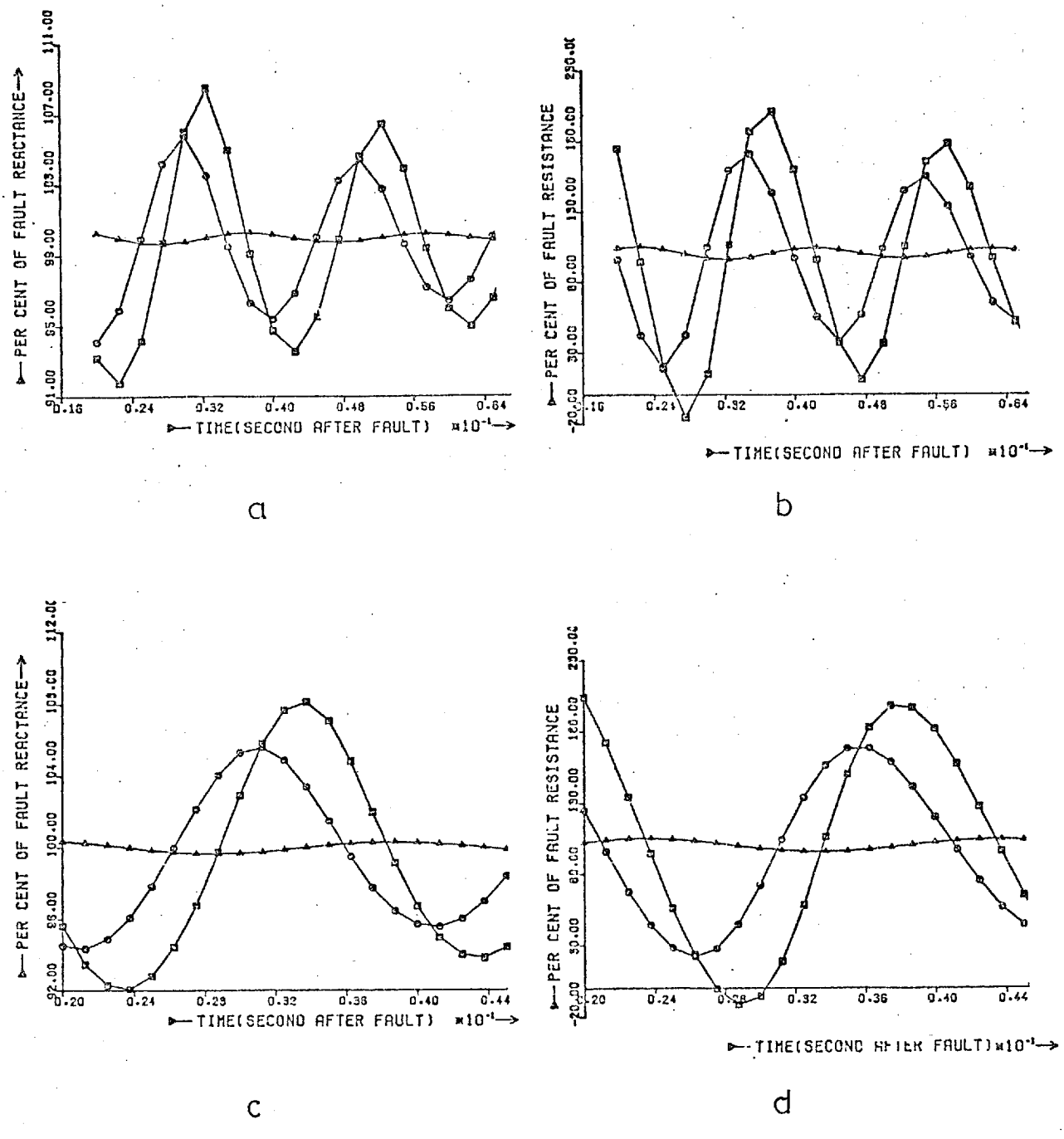

Fig. (4.3) The results of resistance and reactance calculation by the square wave method. (Shunt capacitance is discarded).

a and b : calculated resistance and reactance with 8 samples per cycle

c and d : calculated resistance and reactance with 16 samples per cycle

—□—□—□—□— zero fault inception angle

—○—○—○—○— π/4 fault inception angle

—△—△—△—△— π/2 fault inception angle

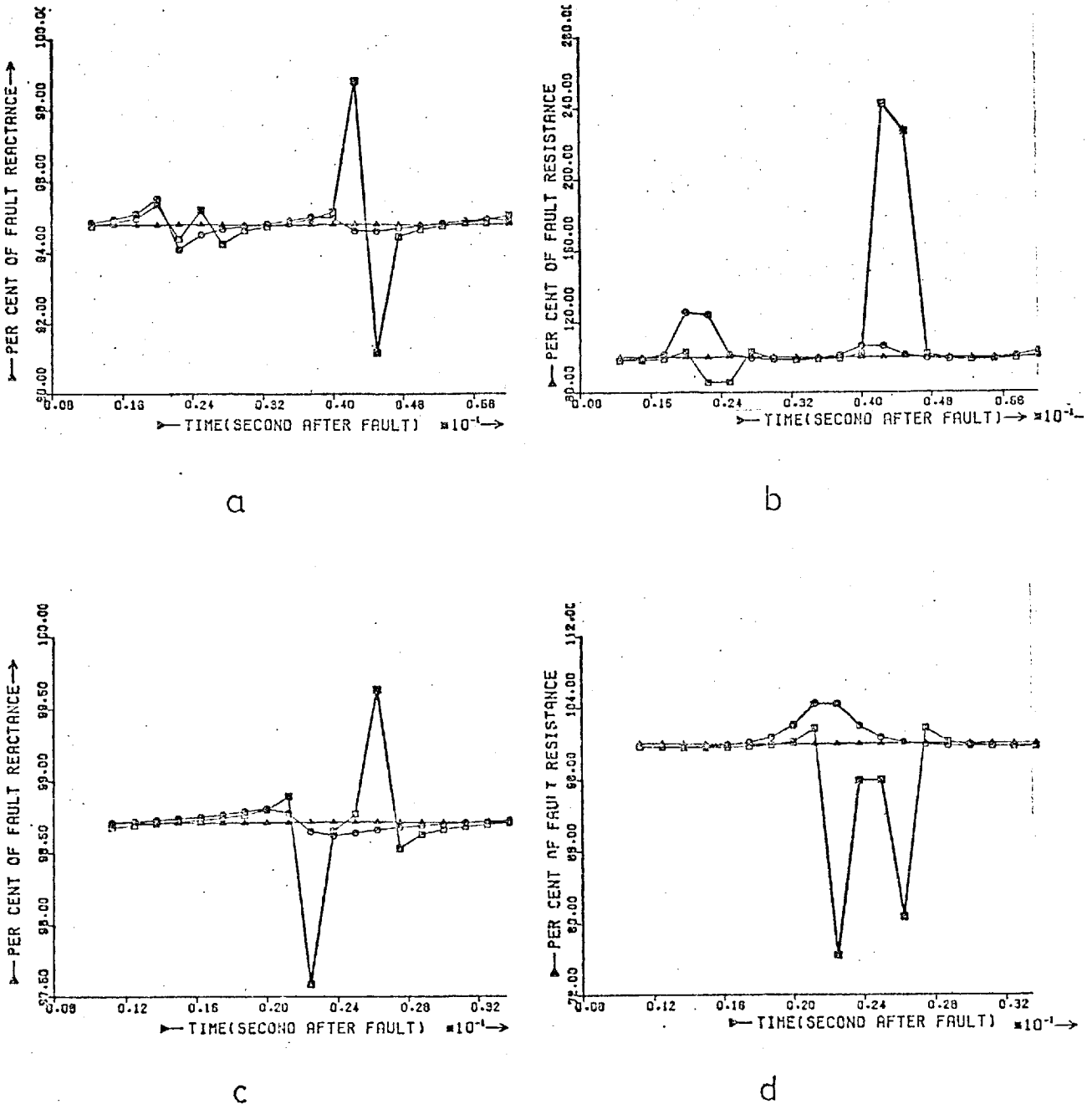

Fig. (4.4) The results of resistance and reactance calculation by the McInnes method (trapezoidal rule). Shunt capacitance is discarded.

a and b: calculated resistance and reactance with 8 samples per cycl
c and d: calculated resistance and reactance with 16 samples per cycle

—□—□—□—□— zero fault incepction angle

—○—○— π/4 fault inception angle

—△—△—△—△— π/2 fault inception angle

if these terms are plotted in the presence of exponential dc off-set, figure (4.5) is obtained. It is seen that these terms change periodically (as the calculation continues) and reduce exponentially to their final value. At some point such as A the numerators and denominators are large and so they are not sensitive to the numerical errors. As a result of this, the accuracy of the calculated resistance and reactance at these points is very good, but sometimes it happens that at some points, e.g. B, the values of the numerators and denominators become very small, and the terms are very sensitive to numerical errors. As a result the error in R and X at these points becomes large. This problem does not necessarily impair the practicability of the McInnes method with the trapezoidal rule, because it happens only at two or three points which are usually reached after the fault has been detected. However, these errors can be predicted very easily by checking the values of the numerator and denominator terms. If these terms are very small, the error could be large and R and X for that particular point or points should be discarded to await for the next samples.

Figures (4.6) show some typical results for McInnes' method with the Simpson rule. The maximum errors for this method also can be seen in table (4.1) col. D. The results are very encouraging. The maximum error for reactance is less than 0.3% and for the resistance is about 1%. These errors are with 8 samples per cycle. With 16 samples per cycle the results are more accurate. In this case even for small values of numerator and denominator of R and X, the maximum errors are less than 0.3 and 1.66% respectively. In fact the numerical error in using Simpson's rule is much less than the trapezoidal rule and because of this, even with a very small numerator and denominator, the errors of R and X are very small.

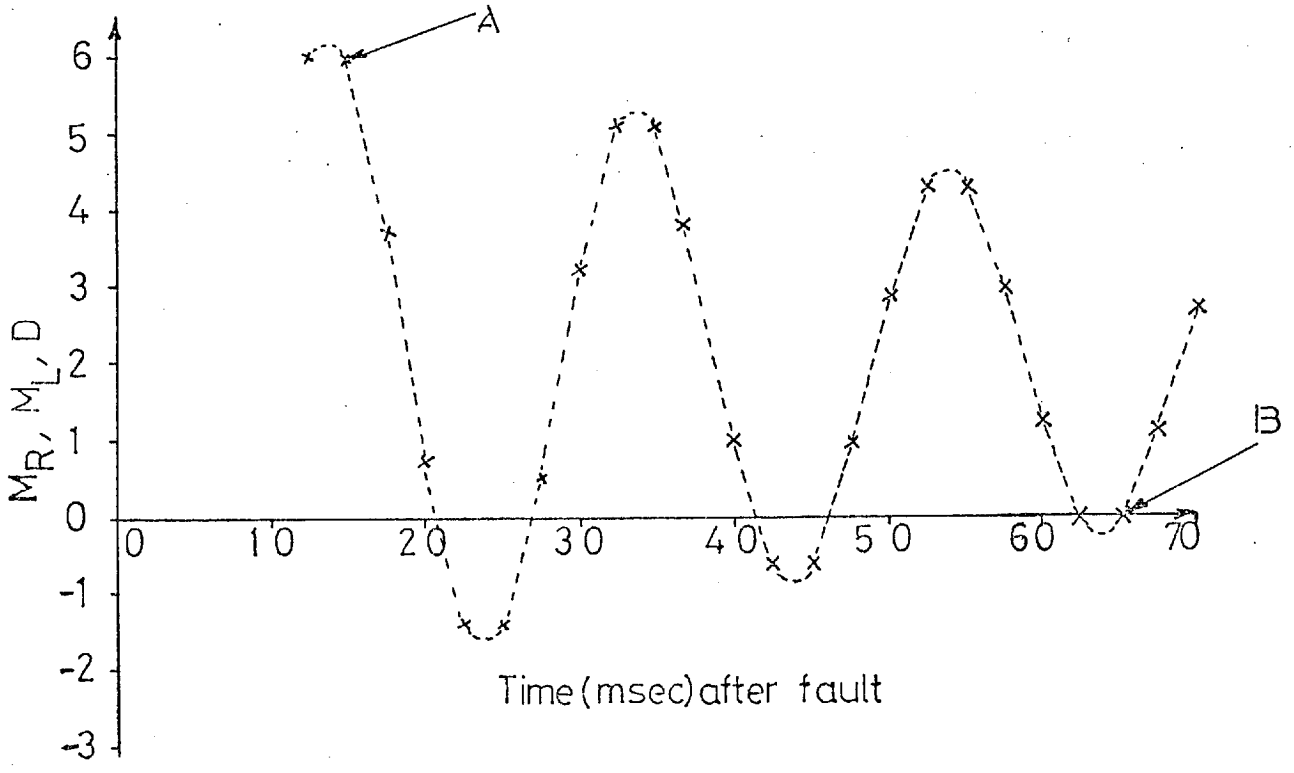

Fig. (4.5) The numerator and denominator of resistance and inductance in the McInnes method

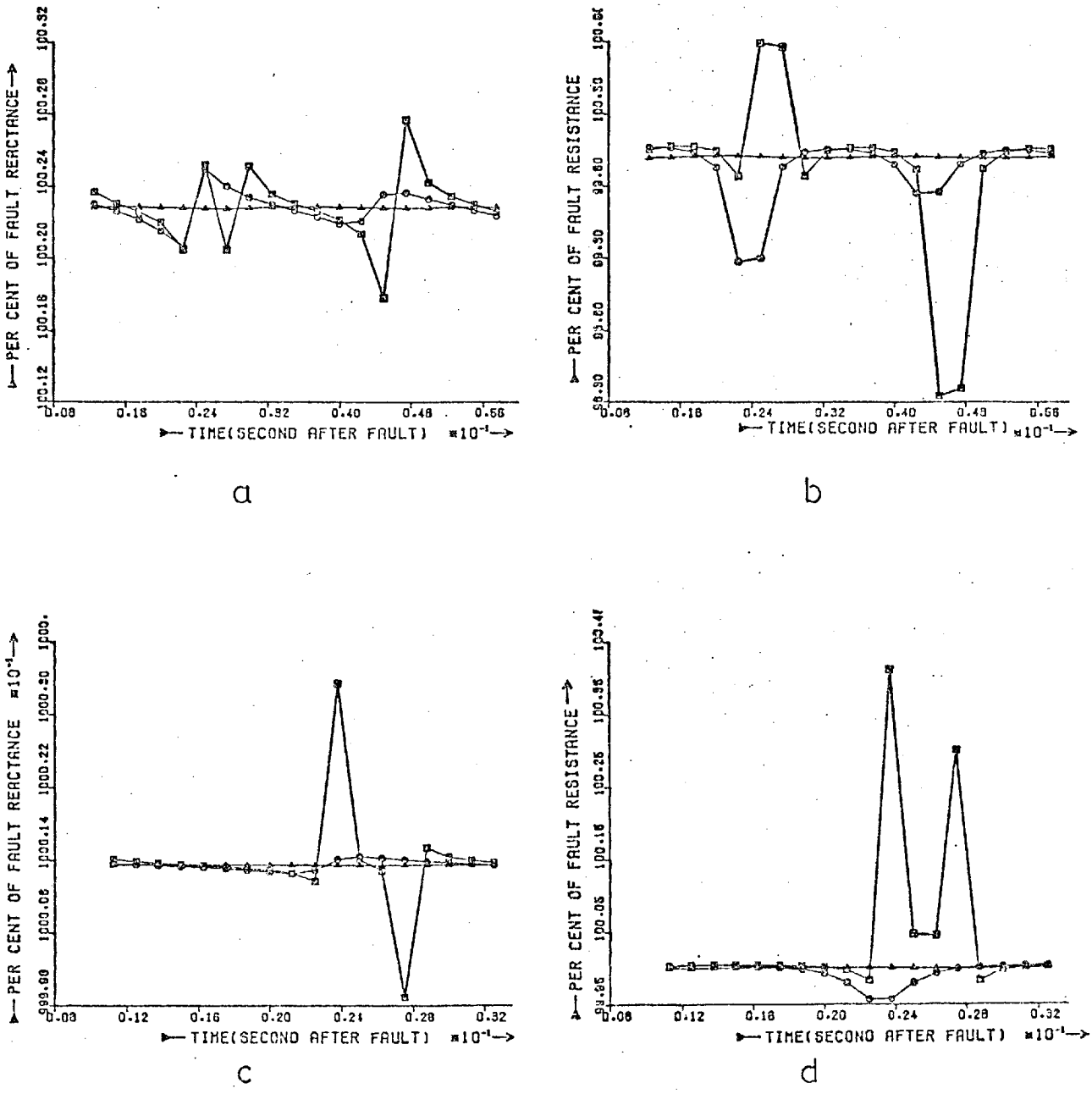

Fig. (4.6) The results of resistance and reactance calculation by the McInnes method (Simpson rule). Shunt capacitance is discarded.

a and b : calculated resistance and reactance with 8 samples per cycle

c and d : calculated resistance and reactance with 16 samples per cycle

—□—□—□— zero fault inception angle

—o—o—o— $\pi/4$ fault inception angle

—△—△—△— $\pi/2$ fault inception angle

4.2 FAULT GENERATED HIGH FREQUENCY COMPONENTS TEST SERIES 2

The aim of these tests was to study the accuracy of different algorithms against fault generated harmonics and non-harmonics when the shunt capacitance of the transmission line was taken into account. The representation of transmission line was obtained by a multi section lumped parameter model consisting of 10 cascaded T sections[23] in which self and mutual impedances and shunt capacitance were included. In previous sections the spectrums of different methods were studied to determine the necessary analogue filters and their associated cut-off frequencies. For the McInnes method with any sampling rate, at least a second order Butterworth filter with 60 Hz cut-off frequency was necessary, and for the Fourier or square wave method, with 8 samples per cycle, a second order, 150 Hz Butterworth filter was needed.

The voltage and current waveforms of the test model were passed through the necessary filters and then the output of the filters were used for R and X calculation by the different methods. The Butterworth filters were simulated digitally (see next chapter) by the bilinear transformation for 60 Hz cut-off frequency:

$$u_{k+2} = 0.000537(\upsilon_{k+2}+2\upsilon_{k+1}+\upsilon_k) + 1.933\, u_{k+1} - 0.935\, u_k$$

For 100 Hz cut-off frequency:

$$u_{k+2} = 0.00146(\upsilon_{k+2}+2\upsilon_{k+1}+\upsilon_k) + 1.889\, u_{k+1} - 0.895\, u_k$$

and for 150 Hz cut-off frequency:

$$u_{k+2} = 0.0032(\upsilon_{k+2}+2\upsilon_{k+1}+\upsilon_k) + 1.834\, u_{k+1} - 0.846\, u_k$$

where υ_k is the k^{th} input sample to the filter and u_k is the k^{th} output sample from the filter. The same filters must be applied

to current samples (the sampling rate for the digital filters was 8000 samples per second). Some typical current and voltage waveforms before and after filtering can be seen in figures (4.7 and (4.8). For a fault inception angle equal to $\pi/2$ radians the voltage waveform is very distorted. The field oscillograms which have been recorded in high voltage substation are smoother than waveforms in figures (4.8). This is because the recorders have a poor frequency response at high frequencies and they filter out many components.

In tables (4.2) and (4.3) some typical results for the Fourier method with 8 and 16 samples per cycle are recorded. Here again for zero fault inception angle, for which there is a large exponential dc offset, the error for the resistance is large and for the reactance is about 10%. For $\pi/2$ fault inception angle, although there are a large number of harmonics and non-harmonics components, the errors are acceptable, because in this case, no d.c. off-set is present. These results and also the results of section (4.1) show how the Fourier method is vulnerable to the presence of an exponential d.c. component.

Tables (4.4) and (4.5) show some typical results for the McInnes method with Simpson's rule. The results have been obtained with a second order, 60 Hz Butterworth filter. With 8 samples per cycle the maximum error for reactance is about 3% (for zero fault inception angle, at one point the error reaches about 6%, but at this point the numerators and denominators of R and X are small and the value could be discarded, also before this point is reached, the fault actually has been detected). For the R the maximum error is about 20% but this is quite acceptable, because in building the relay characteristic, to

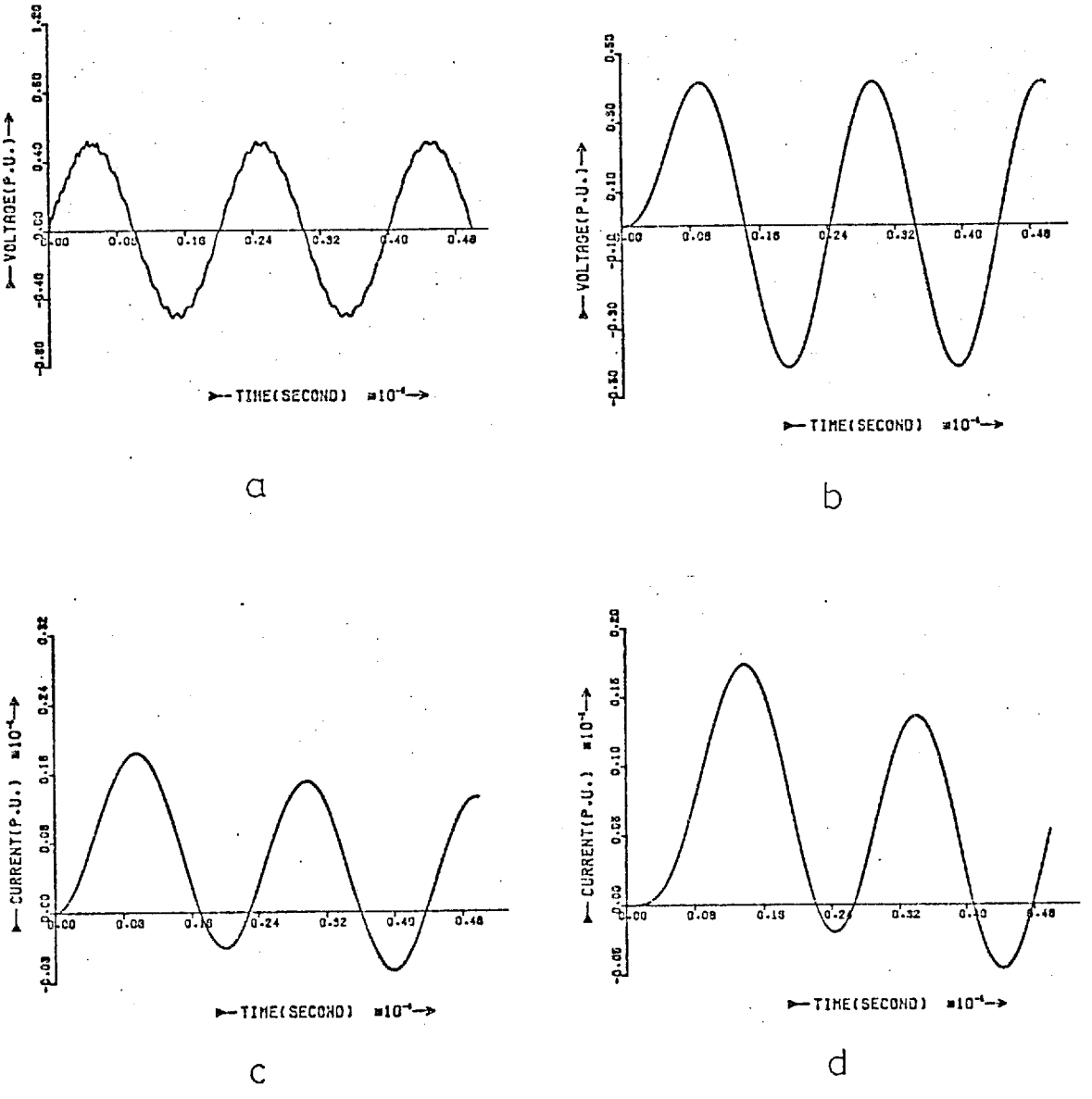

Fig. (4.7) The inputs and outputs of second order 60 Hz Butterworth filter (fault inception angle = 0)

a - Input voltage waveform

b - Output voltage waveform

c - Input current waveform

d - Output current waveform

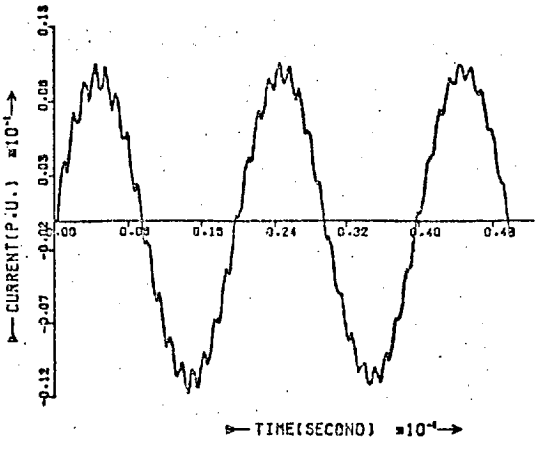

a

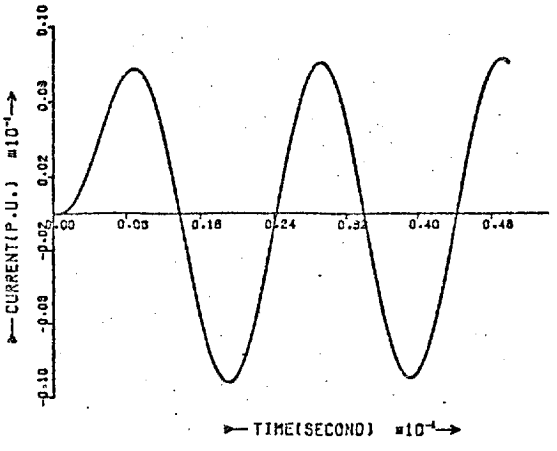

b

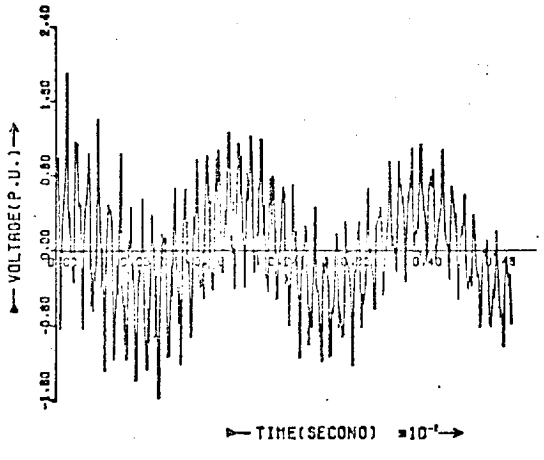

c

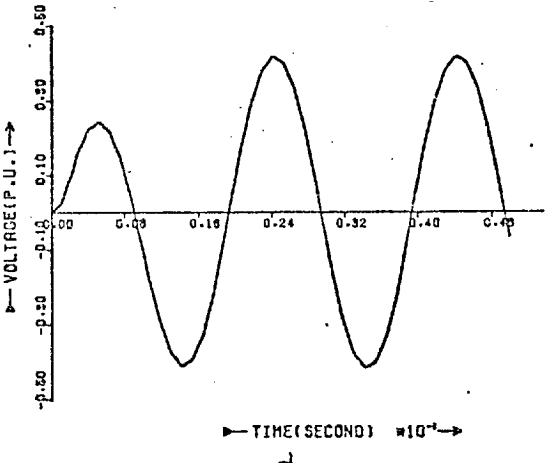

d

Fig. (4.8) The inputs and outputs of second order 60 Hz Butterworth filter (fault inception angle = $\pi/2$ radians)

a - Input current waveform

b - Output current waveform

c - Input voltage waveform

d - Output voltage waveform

Table (4.2) Off-line test results with the Fourier method.
Fault inception angle = 0.
Shunt capacitance is considered.
The results are with a two-pole, 150 Hz Butterworth filter.

Time (ms) after fault	100 R/RF*		100 X/XF*	
	8 S/C	16 S/C	8 S/C	16 S/C
20.00	227.40	247.90	95.28	99.31
21.25		234.43		94.83
22.50	146.72	193.68	90.74	91.83
23.75		146.90		90.37
25.00	60.18	101.05	91.23	90.12
26.25		58.29		90.91
27.50	- 3.94	20.85	95.62	92.71
28.75		- 8.01		95.45
30.00	-18.69	-24.15	102.75	98.97
31.25		-23.34		102.87
32.50	37.08	- 3.01	108.83	106.56
33.75		35.19		109.23
35.00	128.33	83.71	108.11	110.20
36.25		130.89		109.26
37.50	179.51	166.02	103.53	106.80
38.75		183.65		103.58
40.00	167.75	183.95	97.75	100.33
41.25		170.53		97.57
42.50	119.70	147.92	94.66	95.57

* RF = Actual fault resistance

XF = Actual fault reactance.

Table (4.3) Off-line test results with the Fourier method.
Fault inception angle = $\pi/2$.
Shunt capacitance is considered.
The results are with a two pole 150 Hz Butterworth filter.

Time (msec) after fault	100 R/RF*		100 X/XF*	
	8 S/C	16 S/C	8 S/C	16 S/C
20.00	70.58	74.08	97.46	92.34
21.25		69.65		98.81
22.50	87.02	83.87	100.36	100.62
23.75		88.62		100.31
25.00	79.21	85.40	99.54	99.77
26.25		79.63		99.47
27.50	66.02	72.64	99.77	99.46
28.75		65.52		99.72
30.00	58.27	59.93	100.96	100.23
31.25		57.18		100.93
32.50	62.54	58.12	102.35	101.72
33.75		62.25		102.41
35.00	75.19	68.31	103.05	102.88
36.25		75.36		103.11
37.50	86.72	81.98	103.07	103.13
38.75		87.03		103.06
40.00	93.81	90.73	102.88	102.96
41.25		93.77		102.86
42.50	101.22	96.99	102.68	102.74

* RF Actual fault resistance

XF Actual fault reactance

cover fault resistance, a large tolerance for R must be considered. With 16 samples per cycle more accuracy can be obtained, if desired.

The accuracy of square wave method, and the McInnes method with trapezoidal rule, also were investigated. Square wave method was the worst one. McInnes' method with trapezoidal rule was less accurate than the one with Simpson's rule and more accurate than the Fourier method.

Table (4.4) Off-line test results with the McInnes Method (Simpson's rule). Fault inception angle = 0. Shunt capacitance is considered. The results are with a two-pole 60 Hz Butterworth filter

Time (msec) after fault	100 R/RF*		100 X/XF*	
	8 S/C	16 S/C	8 S/C	16 S/C
11.25	100.65	100.47	99.86	100.08
12.50		99.50		100.25
13.75	99.02	99.11	100.52	100.38
15.00		99.08		100.44
16.25	99.58	99.28	100.62	100.45
17.50		99.39		100.41
18.75	99.81	99.39	100.42	100.32
20.00		99.05		100.17
21.25	97.15	97.96	99.61	99.90
22.50		94.54		99.30
23.75	113.10	61.79	102.78	94.43
25.00		115.69		102.16
26.25	104.42	108.17	100.80	100.92
27.50		106.35		100.43
28.75	103.74	106.53	99.97	99.95
30.00		111.55		98.76
31.25	81.03	54.10	106.10	108.59
32.50		91.54		101.87
33.75	96.18	94.56	101.35	101.21

* RF = Actual fault resistance
XF = Actual fault reactance

Table (4.5) Off-line test results with the McInnes method (Simpson's rule). Fault inception angle = $\pi/2$ Shunt capacitance is considered. The results are with a two-pole 60 Hz Butterworth filter.

Time (msec) after fault	100 R/RF*		100 X/XF*	
	8 S/C	16 S/C	8 S/C	16 S/C
11.25	78.88	65.22	97.25	98.19
12.50		65.49		99.10
13.75	76.49	71.37	98.67	99.85
15.00		79.10		100.16
16.25	83.42	85.01	99.85	100.10
17.50		87.36		99.88
18.75	88.69	86.79	100.01	99.74
20.00		85.03		99.74
21.25	88.14	83.81	100.03	99.98
22.50		83.85		100.20
23.75	86.18	84.89	100.39	100.33
25.00		86.18		100.37
26.25	86.68	86.73	100.54	100.31
27.50		85.68		100.20
28.75	87.35	83.10	100.58	100.16
30.00		79.90		100.24
31.25	83.90	77.33	100.63	100.50
32.50		76.57		100.87
33.75	81.66	77.98	100.93	101.22

* RF = Actual fault resistance

XF = Actual fault reactance

4.3 FAULT DETECTION SPEEDS. TEST SERIES 3

The aim of these tests was to study the fault detection speed of the Fourier and McInnes method(Simpson's rule) with 8 samples per cycle. Many tests were carried out, showing that the McInnes method was faster than the Fourier method. For faults at the end of the line the fault detection time for the Fourier method was about 20 (ms) and for the McInnes method about 12.5 (ms). Faults not far from the relaying point were detected sometimes faster, but this was not true for all cases. Figures (4.9) to (4.12) show the trace of resistance and reactance for some typical results.

4.4. VARIATION OF FAULT RESISTANCE. TEST SERIES 4

During a fault, the fault resistance might change because of the cross-winds, ionization etc. To investigate the effect of this variation on the accuracy of the reactance calculation, the resistance of the model was changed linearly with a rate equal to 10% per cycle or 5 times per second. With the McInnes method, the maximum errors were found to be around 2% and 0.3% for zero and $\frac{\pi}{2}$ fault inception angles respectively.

4.5 CONCLUSION

It has been shown that the McInnes method with Simpson's rule gives the most accurate and encouraging results among all the algorithms. Two conditions apply as:

i) The integration terms in the method must be performed on half a cycle of samples.

ii) The method must be used with a second order analogue filter at least, with 60 Hz cut-off frequency.

It was shown also that 8 samples per cycle is quite acceptable. With this sampling rate the different terms in the

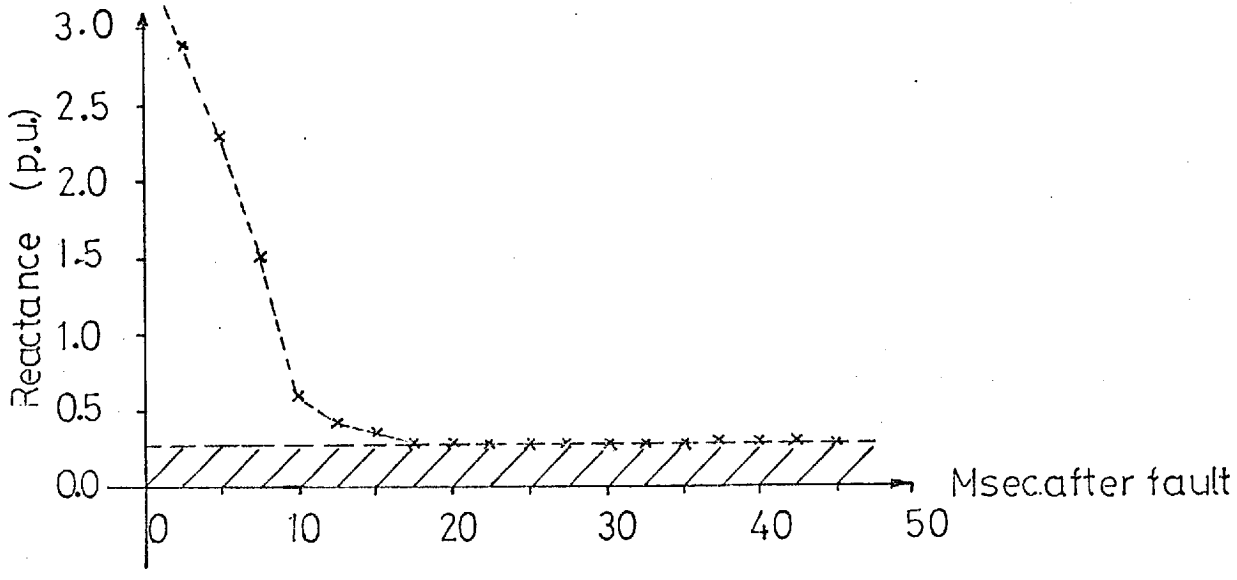

a

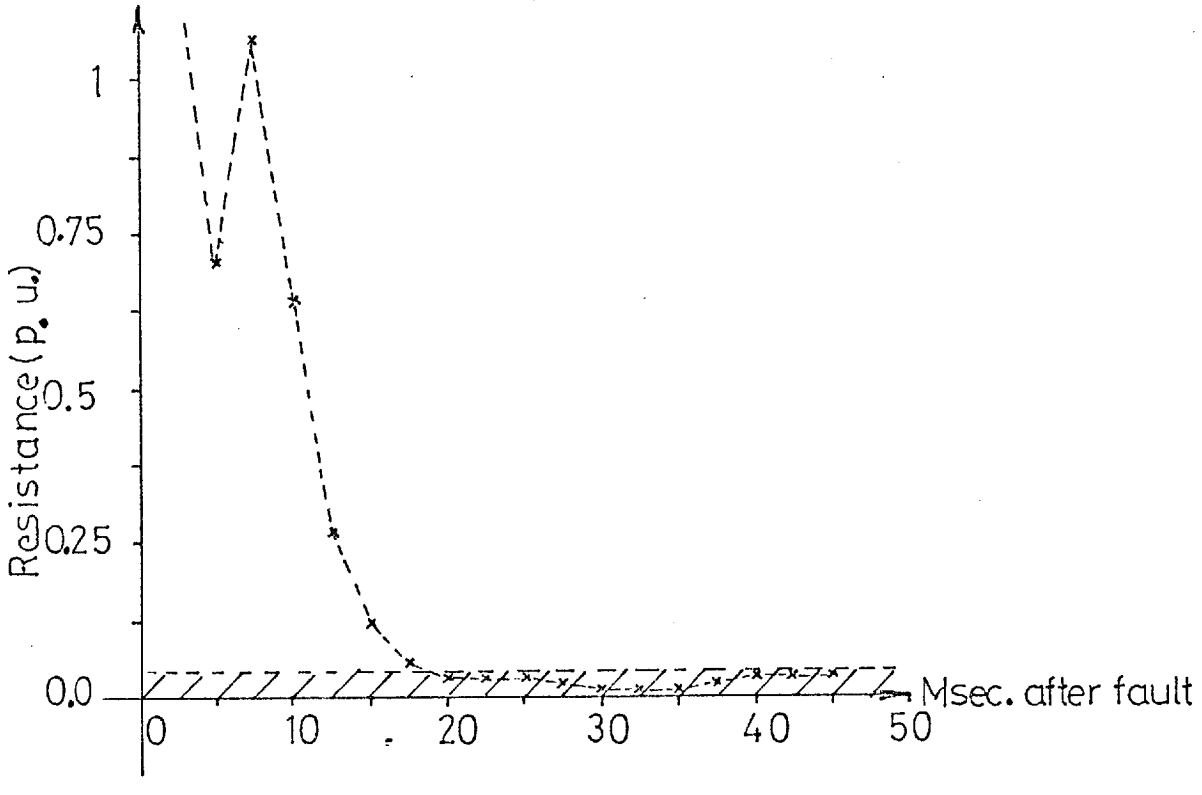

Fig. (4.9) Traces of calculated resistance and reactance with the Fourier method.
Fault at the end of the line
$\alpha = \pi/2$ (FIA)

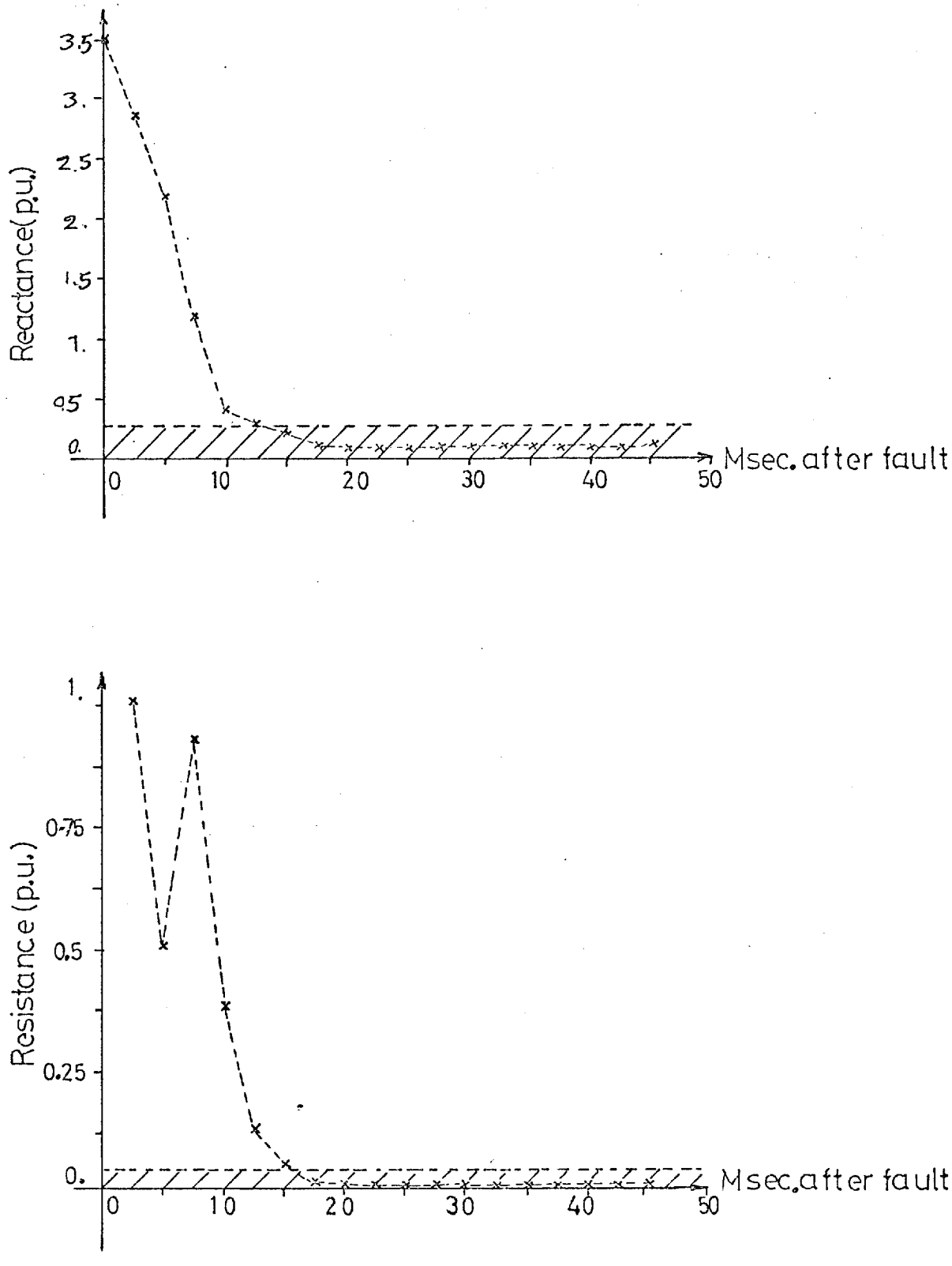

Fig. (4.10) Traces of the calculated resistance and reactance with the Fourier method.
Fault 25 miles far from relaying point.
$\alpha = \pi/2$ (FIA)

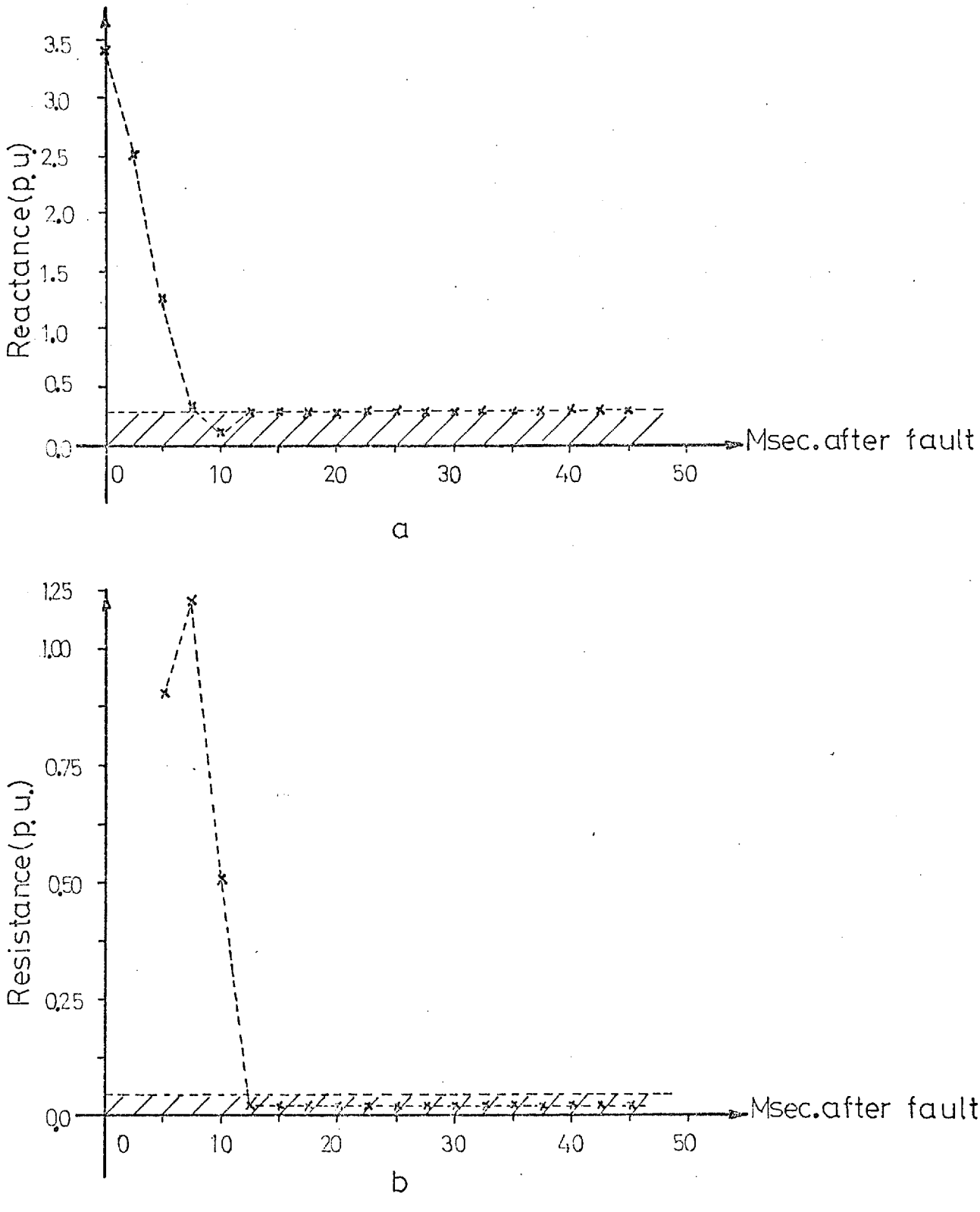

Fig. (4.11) Traces of the calculated resistance and reactance with the McInnes method.
Fault at the end of the line
$\alpha = \pi/2$(FIA)

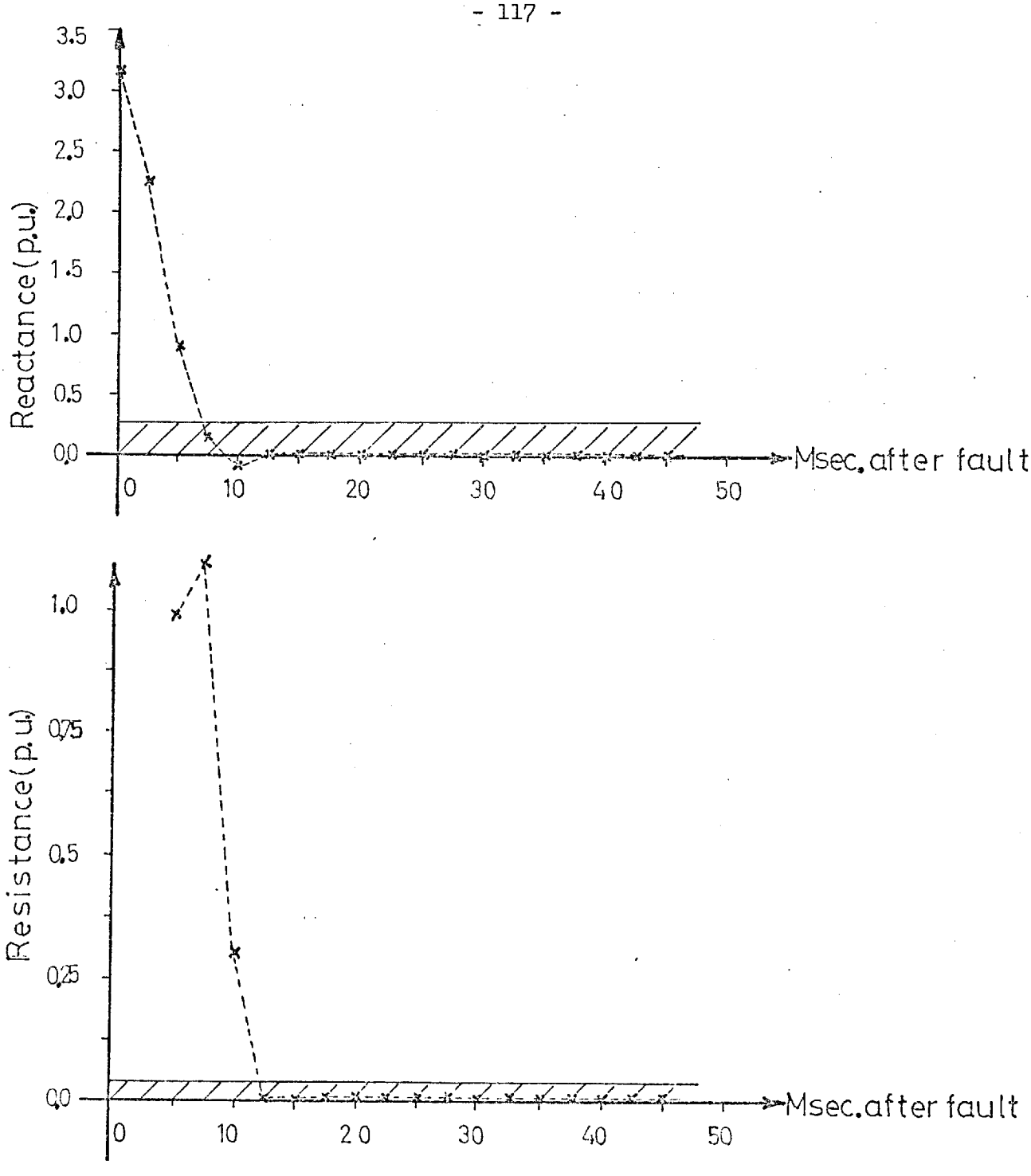

Fig. (4.12) Traces of the calculated resistance and reactance with the McInnes method.
Fault 12.5 miles far from relaying point
$\alpha = \pi/2$ (FIA)

McInnes method are as follows:

$$\begin{aligned} SI_k &= i_{k-4}+4i_{k-3}+2i_{k-2}+4i_{k-1}+i_k \\ SV_k &= \upsilon_{k-4}+4\upsilon_{k-3}+2\upsilon_{k-2}+4\upsilon_{k-1}+\upsilon_k \\ SI_{k+1} &= i_{k-3}+4i_{k-2}+2i_{k-1}+4i_k+i_{k+1} \\ SV_{k+1} &= \upsilon_{k-3}+4\upsilon_{k-2}+2\upsilon_{k-1}+4\upsilon_k+\upsilon_{k+1} \\ DI_k &= i_k - i_{k-4} \\ DI_{k+1} &= i_{k+1} - i_{k-3} \end{aligned} \qquad (4.2)$$

The criterion for the fault to be inside the zone is that:

$$DI_k\ (SV_{k+1}-K_1 SI_{k+1}) < DI_{k+1}(SV_k-K_1\ SI_k)\ \ldots \qquad (4.3a)$$

and

$$SI_k(SV_{k+1}-K_2 DI_{k+1}) > SI_{k+1}(SV_k-K_2\ DI_k)\ \ldots \qquad (4.3b)$$

where

$K_1 = R_z$ and $K_2 = \frac{3}{T} X_z$, and R_z , X_z are the positive sequence resistance and reactance of the zone. In equations (4.3) there are 8 multiplications with no division.

The terms SI_k, ... can be calculated very easily by computer or can be realized outside the computer by simple hardware as in figure (4.13). In this case, after each sample, only SI_k, ... are read into the computer and it checks only the inequalities (4.3).

Throughout chapter 3 and this chapter, analogue Butterworth filters have been employed to filter out unwanted frequencies. There are other kinds of analogue filter, e.g. Chebyshev, Bessel, etc. that might be used. Also instead of analogue, digital filters could be used. In the next chapter a study of Butterworth and possible alternatives from spectrum and transient time response point of view will be undertaken to decide which kind of filter is most suitable for line protection.

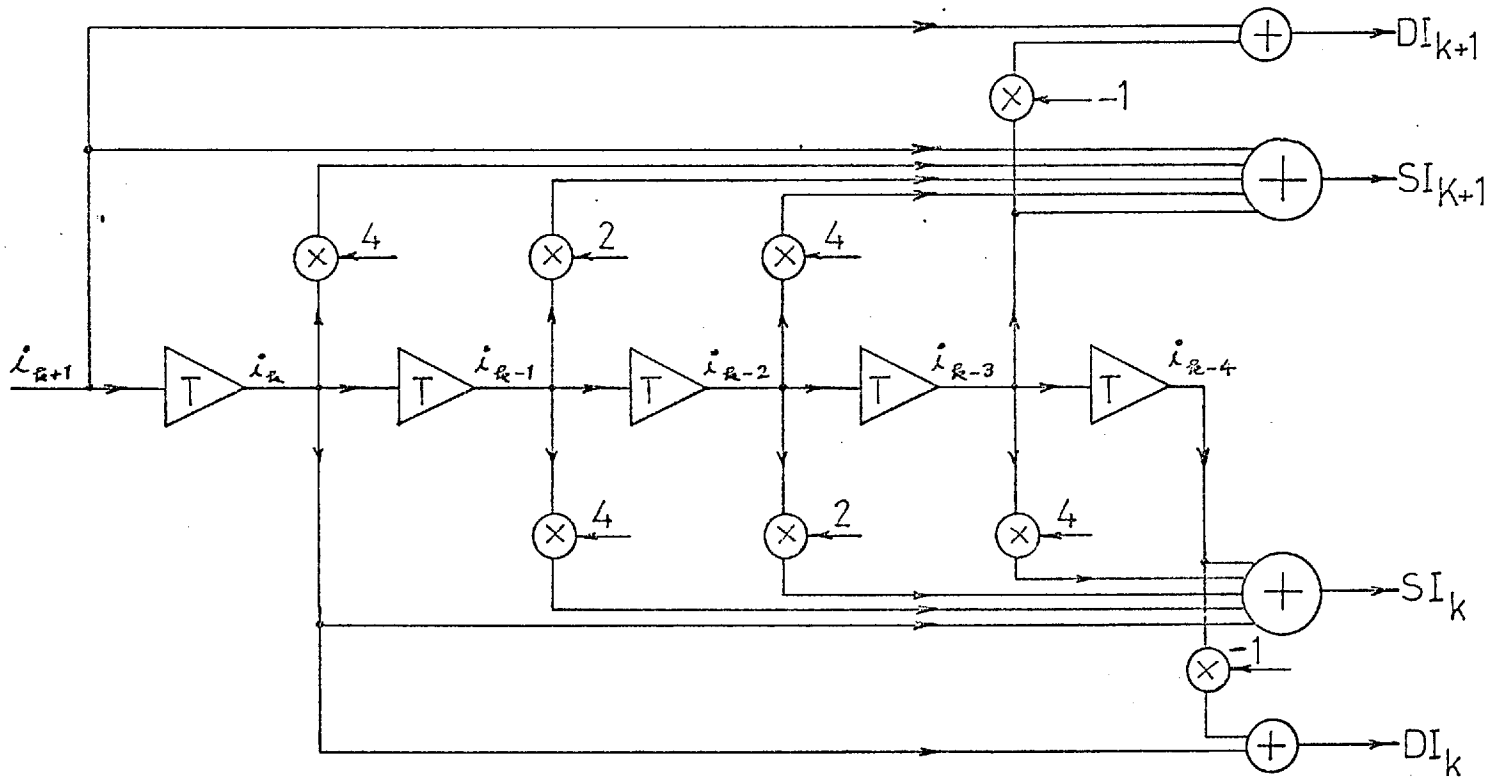

Fig. (4.13) Realization of integration terms in the McInnes method

CHAPTER 5

ANALOGUE AND DIGITAL FILTERING

In the previous chapter we saw that with every method of impedance calculation a low pass filter should be used to remove undesirable harmonic components for which either analogue or digital filters could be used. Analogue filters are cheaper and simpler and so unless there are some clear advantages in using digital filters from transient time response or spectrum point of view, the analogue filter is to be preferred.

In this chapter, both kinds of filters will be reviewed, their spectrums and step responses will be compared and recommendations for digital protection purposes will be made.

5.1 ANALOGUE FILTERS

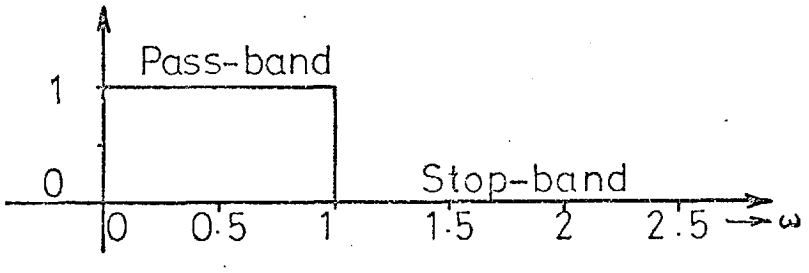

Fig. (5.1) Ideal low-pass filter characteristic.

It is well known that a filter with an ideal characteristic (a filter which passes all components in pass band without any attenuation and removes all components in stopband completely) is unrealizable by a physical network and so it becomes necessary to approximate it. In order to build a practical filter, only certain types of function are physically realizable, known as rational functions. In modern filter theory, approximation theory is used to find a realizable rational function which gives a magnitude or phase characteristic as near to the ideal as possible. Butterworth and Chebyshev are the two most

common types of filters which have been established in this way. Modern filters do not possess a definite cut-off frequency, as in classical filter theory, but are usually normalized at a convenient point, specified by the designer. Butterworth filters are usually normalized at the 3db point and in the Chebyshev filter this is taken as the last point of interest in the passband

The basic design procedure for these filters is to choose a function H(s) whose squared magnitude when $s = j\omega$ gives the desired filter function. The poles of this function are then determined from which the filter design is synthesized.

5.1.1 Butterworth filter

One approximating function which gives the flattest magnitude characteristic at $\omega=o$ has been suggested by Butterworth[5] as

$$H(S)\ H(-S) = |H(S)|^2 = \frac{1}{1+\omega^{2n}} \qquad (5.1)$$

The function H(S) is called the Butterworth function, of n^{th} order and its denominator the Butterworth polynomial. The network realization of this function is the Butterworth filter. The characteristic of the Butterworth filter is called a maximally flat one, and it is monotonic in both, the passband and the stopband. For a transfer function whose numerator is a constant and whose magnitude is monotonic in the passband, the Butterworth filter for a fixed n, gives the flattest possible curve at the origin. It should also be clear that the higher the value of n (or what is equivalent, the larger the number of elements required in the network realization), the greater the degree of maximal flatness possible. The approximation to an ideal characteristic close to $\omega=o$ is very good but there is an increased attenuation at the higher passband frequencies,

because the approximation is of the Taylor-series type, i.e. it is an approximation about a point. The poles of the Butterworth filter are given by the left half plane roots of:

$$\left(\frac{S}{j}\right)^{2n} + 1 = o \tag{5.2}$$

or

$$S_k = -\sin \frac{2k-1}{2n}\pi + j \cos \frac{2k-1}{2n}\pi \tag{5.3}$$

where k is integer 1,2,...,n. From these poles the filters can be synthesized and the answers obtained are then scaled to give the exact physical values of the practical filter. Sketches of the first ten orders of Butterworth approximation to low pass filter can be seen in Fig. (5.2).

5.1.2 Chebyshev filter

If some ripple is allowed in the passband or stopband a Chebyshev filter with the following transfer function can be used:

$$H(S).\ H(-S) = |H(S)|^2 = \frac{1}{1+\varepsilon^2 C_n^2(\omega)} \tag{5.4}$$

where $C_n(\omega)$ is the Chebyshev polynomial of order n and is defined as:

$$C_n(\omega) = \cos(n \arccos \omega) \quad \text{for } o \leq \omega \leq 1$$

and $$C_n(\omega) = \cosh(n \operatorname{arccosh} \omega) \quad \text{for } \omega > 1$$

Of all possible transfer functions with constant numerator, the transfer function obtained by the use of Chebyshev polynomials is optimum in the sense that it is the function of lowest order for achieving a prescribed deviation in the passband and the fastest possible rate of cut-off outside the passband. In this case the filter characteristic has ripples only in the passband. When the transfer function is permitted to have finite zeros, the optimum function becomes the Chebyshev rational function. For this case the characteristic has equal

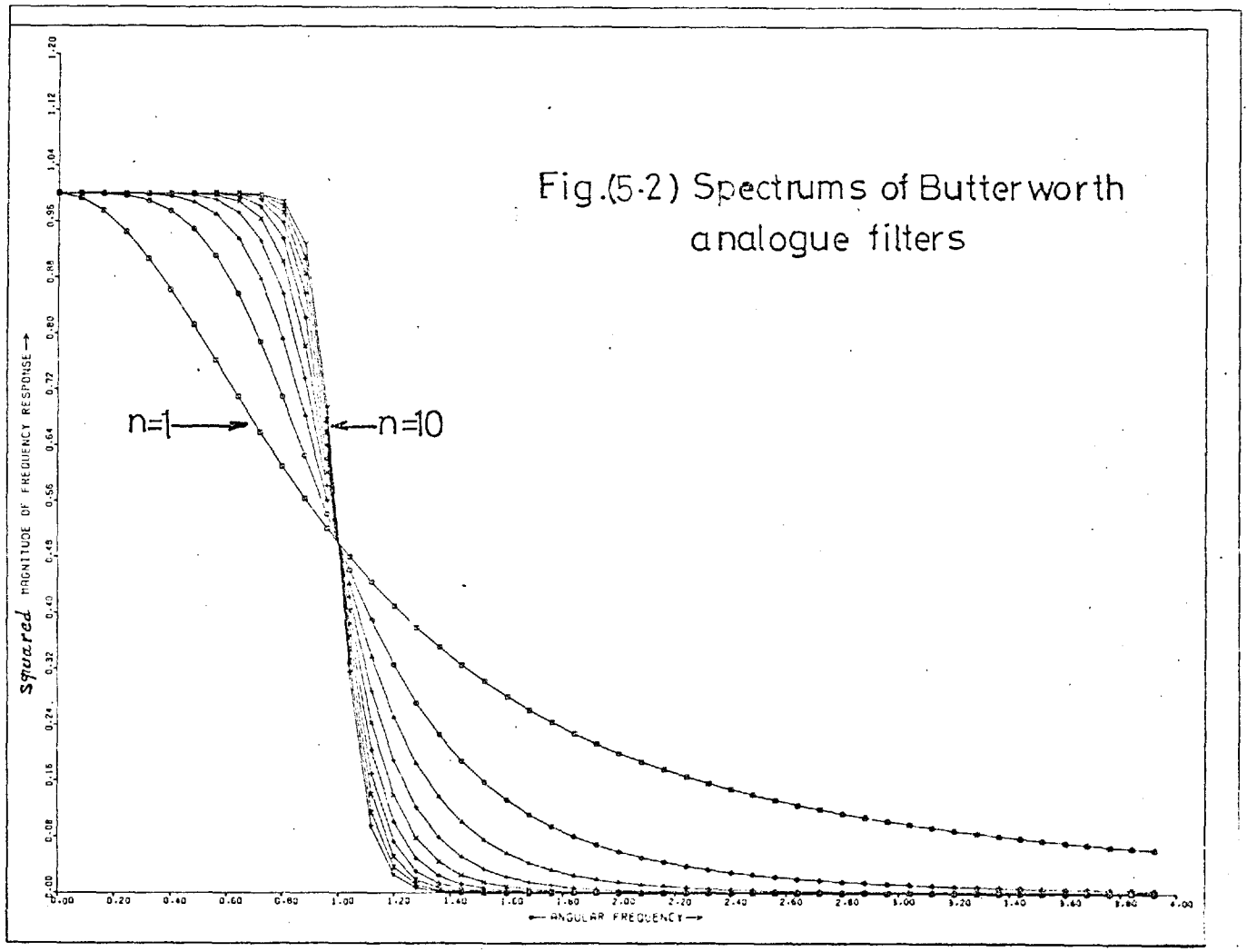

Fig.(5-2) Spectrums of Butterworth analogue filters

ripples in both the passband and stopband. These polynomials and rational functions are unique. No other polynomials and rational functions with the same optimum properties exist. Knowledge of these upper bounds on performance is extremely valuable, because it shows the futility of searching for other approximating polynomials that will give better performance than Chebyshev polynomials of the same degree.

The definition of the Chebyshev polynomials may easily be put into recognizable polynomial form if we let

$$\xi = \cos^{-1} \omega$$

so that $\omega = \cos \xi$

Substitution of this change of variable in $C_n(\omega)$ and subsequent manipulation leads to:

$$C_n(\omega) = \text{Real } (\omega + j\sqrt{1-\omega^2})^n \qquad (5.5)$$

Also it can be shown that:

$$C_{n+1}(\omega) = 2\,\omega\, C_n(\omega) - C_{n-1}(\omega) \qquad (5.6)$$

By inspection of (5.5) we can see that $c_o=1$ and $C_1= \omega$. Other Chebyshev polynomials can be calculated from (5.6):

$$C_2(\omega) = 2\,\omega^2 - 1$$

$$C_3(\omega) = 4\,\omega^3 - 3\omega$$

$$C_4(\omega) = 8\,\omega^4 - 8\,\omega^2 + 1$$

$$C_5(\omega) = 16\omega^5 - 20\omega^3 + 5\omega$$

$$C_6(\omega) = 32\omega^6 - 48\omega^4 + 18\omega^2 - 1$$

The poles of the Chebyshev filter are given by:

$$1 + \varepsilon^2\, C_n^2\, (\frac{S}{j}) = o$$

which after necessary manipulation gives

$$S_K = \sin\gamma \sinh\beta + j \cos\gamma \cosh\beta \qquad (5.7)$$

where

$$\gamma = \frac{2k+1}{2n}\,\pi \qquad k=1,2,\ldots,n$$

$$\beta = \frac{1}{n} \sinh^{-1} \frac{1}{\varepsilon}$$

It can be shown that these poles lie on an ellipse. Sketches of first ten orders of the Chebyshev approximation to low pass filters with 1 and 3 db ripples can be seen in figures (5.3) and (5.4) respectively. Allowing larger ripples in the pass-band enables the filter characteristic to become sharper.

5.1.3 Transient response of filters

The impulse response function of both Butterworth and Chebyshev filters can be expressed in the form:

$$H(S) = \frac{A}{P(S)} \tag{5.8}$$

where P(S) is the corresponding polynomial in s and A is a constant whose value depends on the type and order of P(s). Upon expansion into partial fractions, this system function becomes:

$$H(s) = A \sum_{i=1}^{n} \frac{U_i}{s+s_i} \tag{5.9}$$

where U_i is the residue of the pole at $-s_i$. The residues can be computed from (5.8) and (5.9) by standard methods.

The step response is the integral of the impulse response, i.e.

$$G(s) = \frac{H(s)}{s} = A \sum_{i=1}^{n} \frac{U_i}{s(s+s_i)}$$

or

$$G(s) = A \sum_{i=1}^{n} \left(\frac{U_i/s_i}{s} - \frac{U_i/s_i}{s+s_i} \right) \tag{5.10}$$

By using the inverse Laplace transform the impulse and step response of filters can be calculated in the time domain as follows:

$$h(t) = A \sum_{i=1}^{n} e^{-Re(s_i)t} [Re(U_i)\cos Im(s_i)t + Im(u_i) \sin Im(s_i)t] \tag{5.11}$$

and

$$g(t) = A \sum_{i=1}^{n} \frac{u_i}{s_i} - A \sum_{i=1}^{n} e^{-Re(s_i)t} [Re(u_i/s_i)\cos Im$$

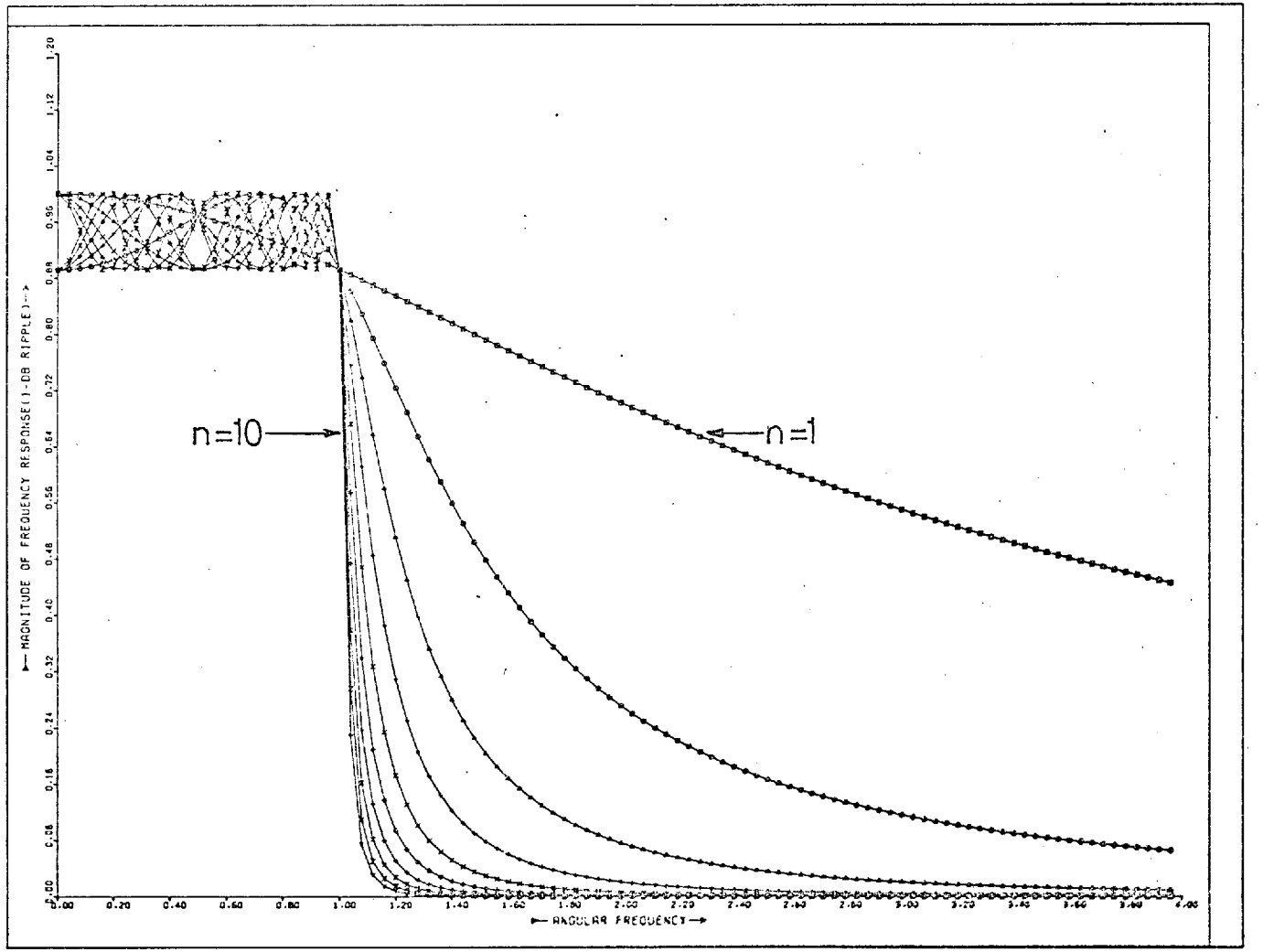

Fig.(5·3) Spectrums of Chebyshev filters with 1db ripple

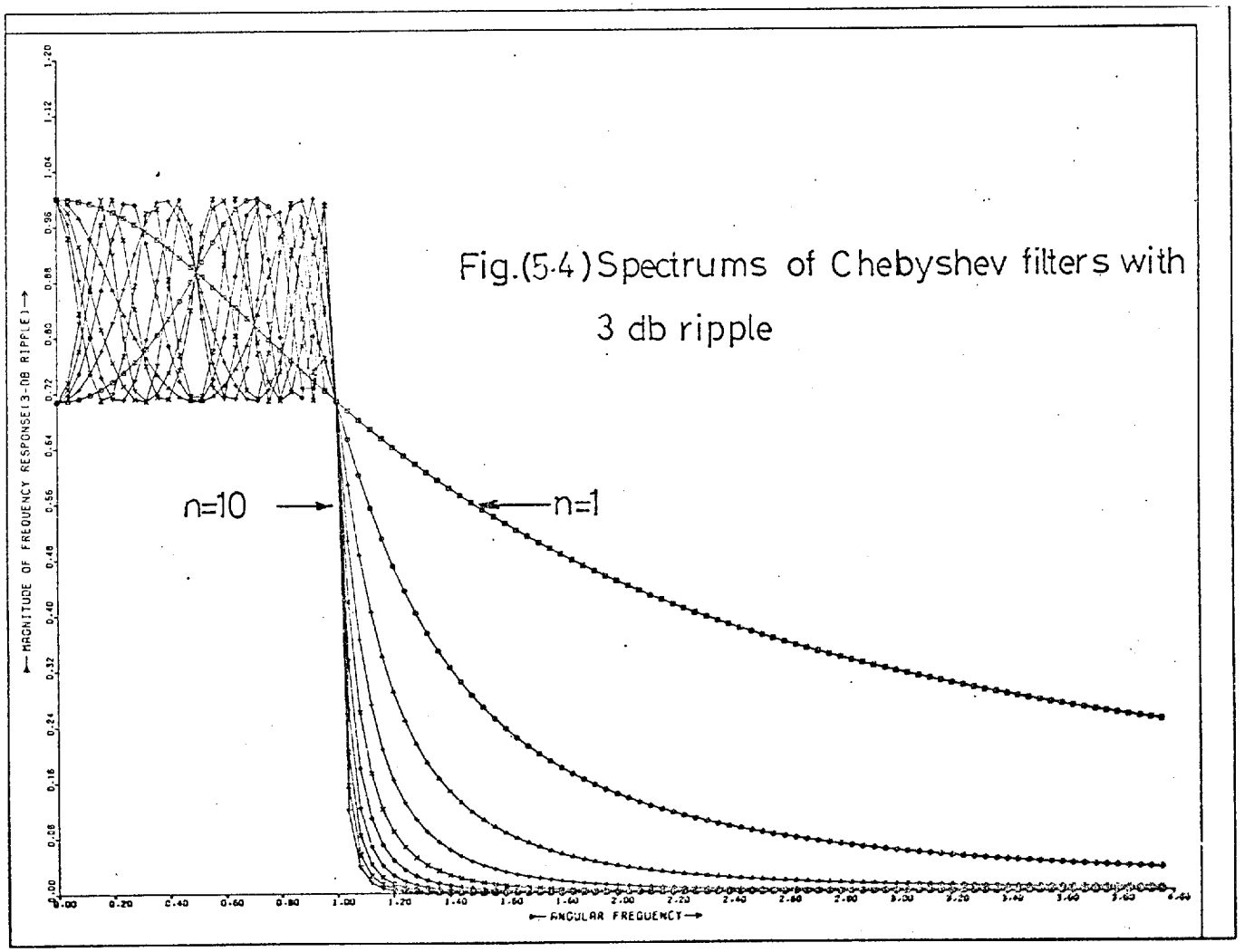

Fig.(5.4) Spectrums of Chebyshev filters with 3 db ripple

$$(s_i)t + Im(u_i/s_i)\ \sin Im(s_i)t] \qquad (5.12)$$

Figures (5.5) and (5.6) show the impulse and step responses of Butterworth filters for first ten orders. Also figures (5.7) and (5.8) show the step responses for the first ten orders of Chebyshev filter with 1 and 3 db ripple. We can see that by increasing the ripple the transient time delay of the Chebyshev filter increases and also the final steady state value of the filter with the odd number of poles is different from that of the filter with an even number of poles

5.1.4 Comparison of analogue filter types

The loss of the Butterworth filter (in db) for $\omega >> 1$ is

$$\text{Loss} = 20 \log \omega^n = 20n \log\omega$$

and for Chebyshev filter it is:

$$\text{Loss} = 20 \log 2^{n-1}\ \varepsilon\ \omega^n = 20n\log\omega + 20\log\varepsilon + 6.02(n-1)$$

It can be seen that the fall-off for Butterworth filter is 20n db/decade but for the Chebyshev filter it is larger and depends on ε and n. For a larger amount of ripple, the fall-off is sharper.

From a transient time response point of view, the Chebyshev filter is worse than Butterworth's. By increasing the ripple in the passband of Chebyshev filter its spectrum becomes sharper but its time delay also increases. Since in the protection field both the spectrum and time delay are important, no advantage can be discerned in the Chebyshev over the Butterworth filter.

There are other types of filter which have been suggested by different authors. One class of filter was developed by Papoulis[36] with an odd number of poles and later on by Fukada[37] with an even pole number. This class of filter is

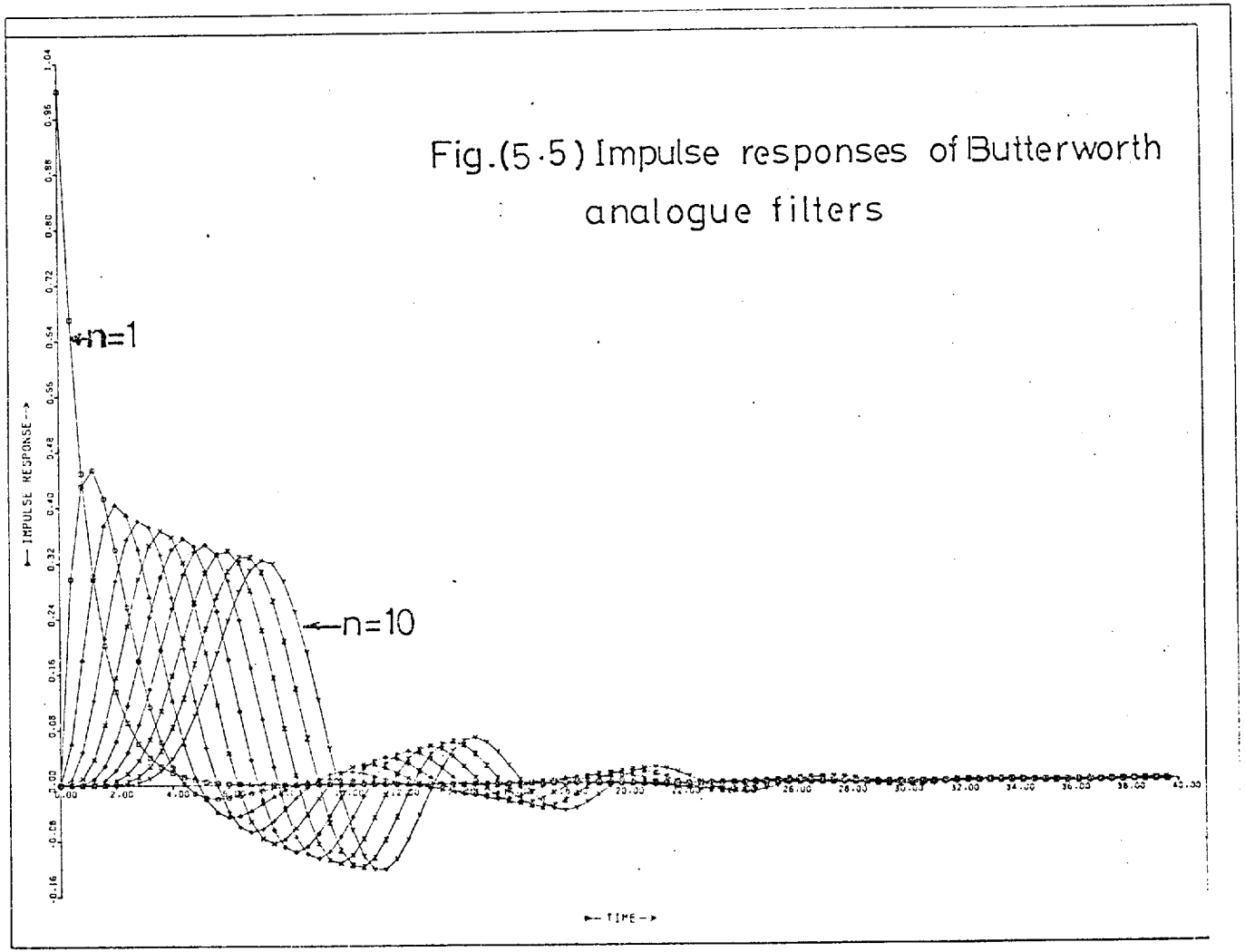

Fig.(5·5) Impulse responses of Butterworth analogue filters

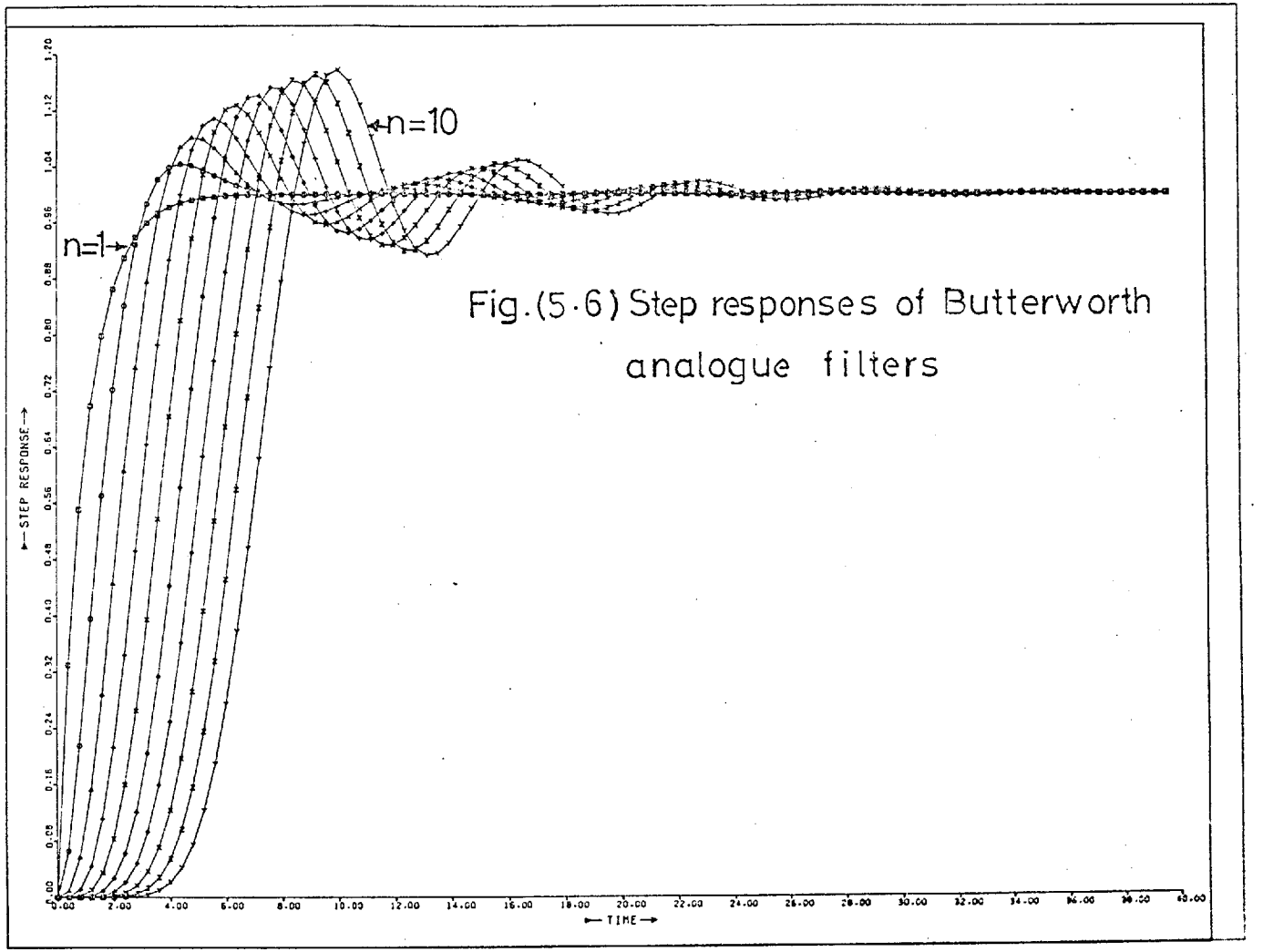

Fig.(5·6) Step responses of Butterworth analogue filters

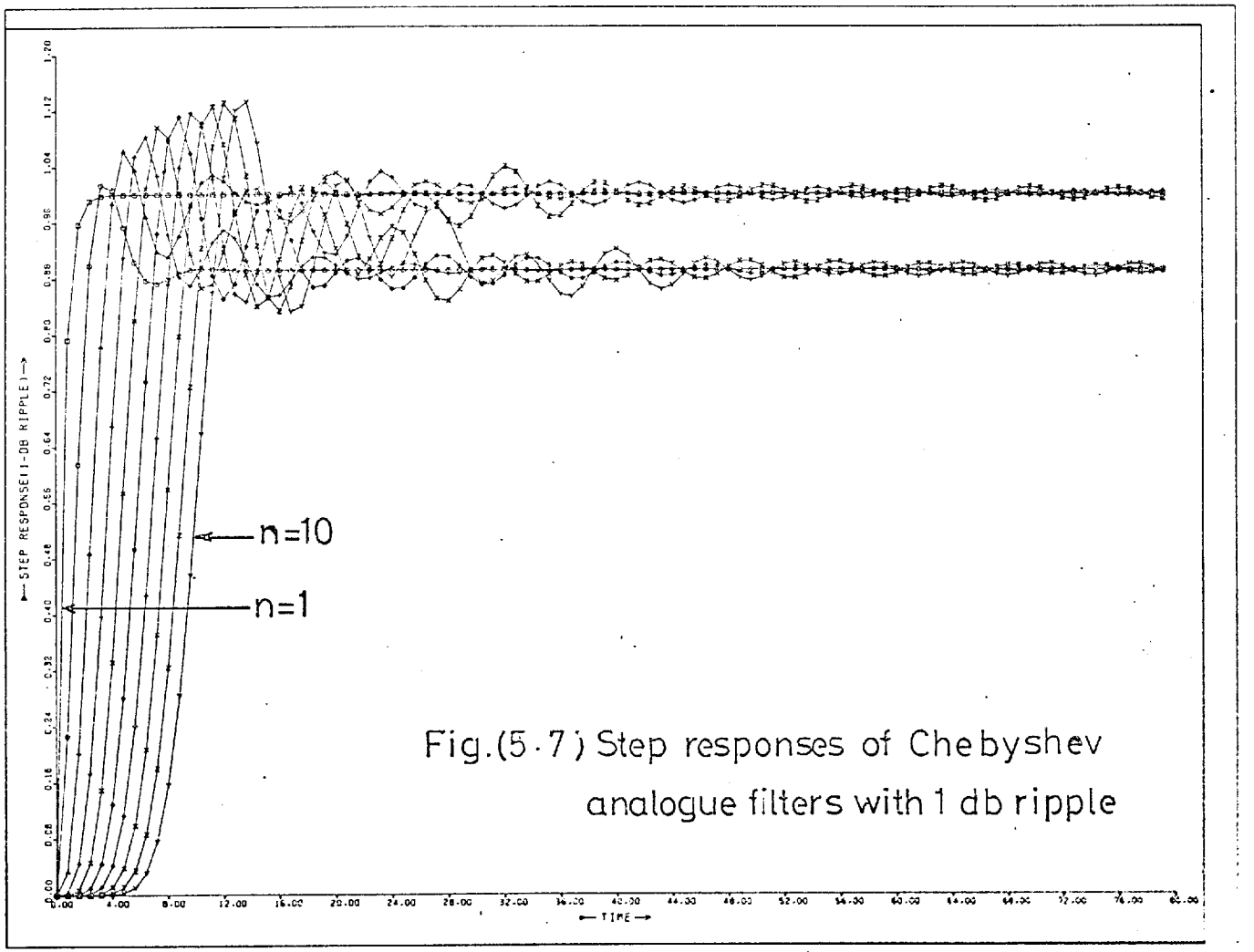

Fig.(5·7) Step responses of Chebyshev analogue filters with 1 db ripple

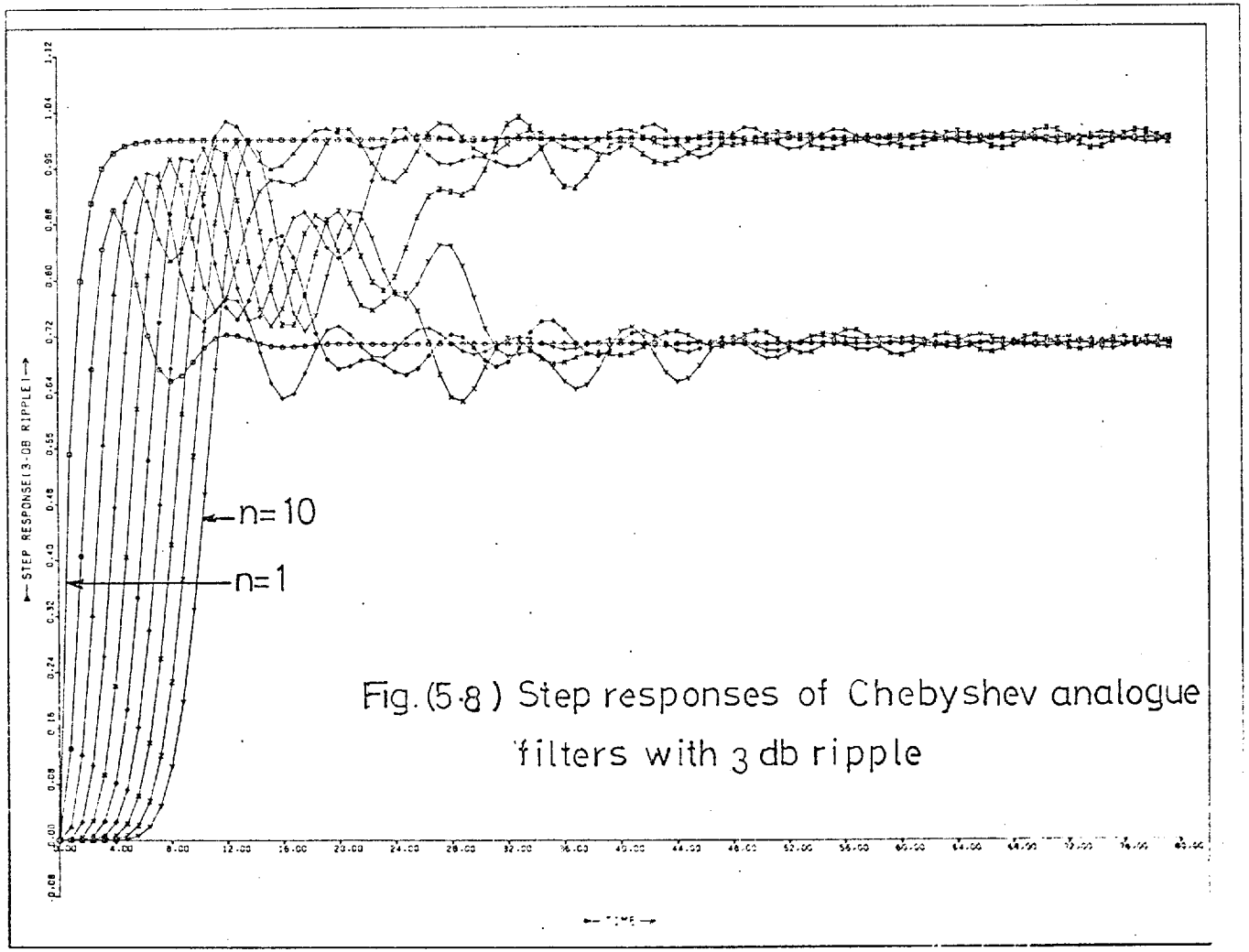

Fig. (5.8) Step responses of Chebyshev analogue filters with 3 db ripple

called L or optimum filter. Since its amplitude characteristic has no ripple in the pass band and a high rate of attenuation in the stop band, it combines the desirable features of both the Butterworth and Chebyshev response. Among all filters of a given order this new class has the maximum cut-off rate under the condition of a monotonically decreasing response. Comparing this filter with the Butterworth filter for the same order, it is sharper than the Butterworth at cut-off frequency, but its time delay is larger. For protection, there is thus no advantage of L filters over the Butterworth type.

Another class worth considering are the Bessel filters which have a small transient time delay, but their spectrums from sharpness point of view are worse than Butterworth filters. The phase response of these filters are more linear than Butterworth and because of this they have some application in communication systems but not for protection purposes.

5.1.5 Realization of Butterworth and Chebyshev filters

All filters can be realized by an active Rc network in which the active element is an operational amplifier. If the transfer function is written as the multiplication of first and second order transfer functions as:

$$H(s) = \frac{A}{P(s)} = A \left(\frac{1}{s+s_1} \times \frac{1}{s+s_2} \times \ldots \times \frac{1}{s^2+as+b} \times \frac{1}{s^2+cs+d} \times \ldots\right) \tag{5.13}$$

then each of these functions can be realized by an active network, containing a single operational amplifier.

The transfer function with one pole such as:

$$H(s) = \frac{K}{s+s_1} \tag{5.14}$$

can be realized either by a simple network as in fig. (5.9)a, or by an active network as in fig. (5.9)b. In using the simple

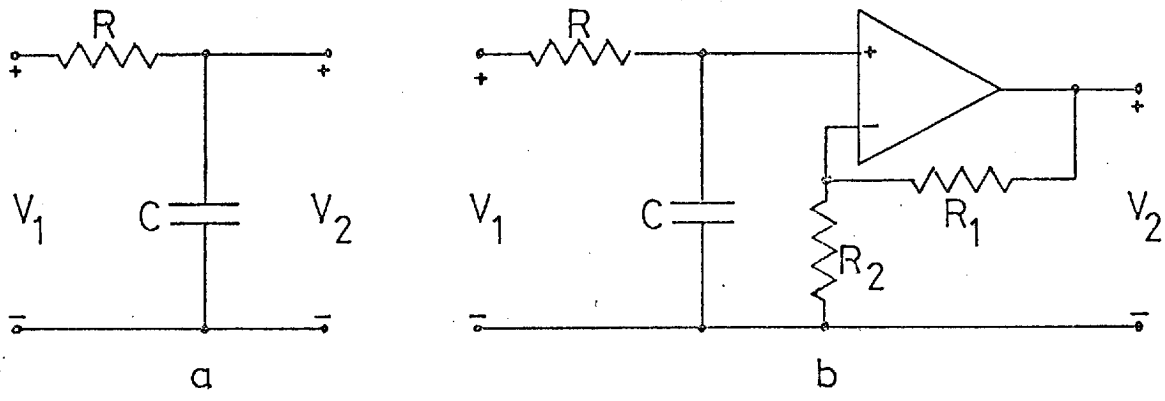

Fig.(5.9) First order low-pass filter

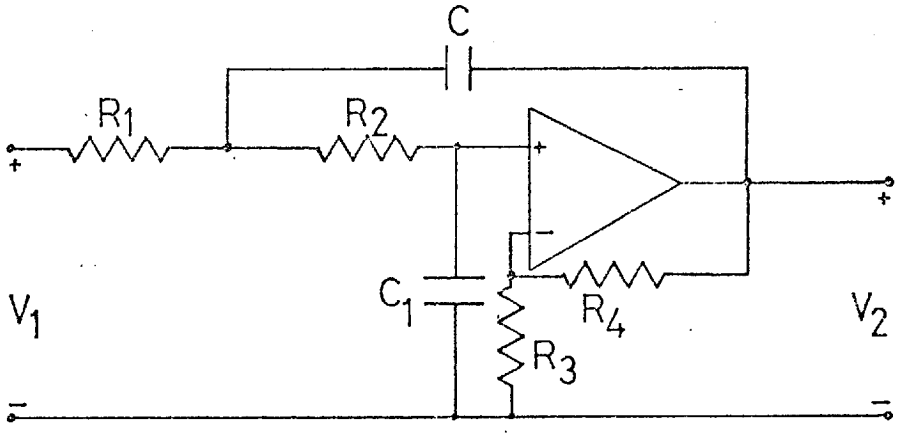

Fig.(5.10) Sallen and Key second order low-pass filter

network of fig. (5.9)a, a buffer might be necessary when this circuit is connected to other circuits. But the output of circuit (5.9)b can be connected to other circuits directly, because the operational amplifier acts as an isolator for the filter. In order that the circuit (5.9)b can represent equation (5.14), the following relations must be satisfied:

$$\frac{1}{RC} = s_1 \text{ and } \frac{1}{c}\left(1 + \frac{R_1}{R_2}\right) = K \tag{5.15}$$

A transfer function with two conjugate poles such as:

$$H(s) = \frac{K}{s^2+as+b} \tag{5.16}$$

can be realized by different schemes. One commonly used, suggested by Sallen and Key[38,60] is shown in figure (5.10). The elements of this circuit must satisfy the following relations:

$$\begin{aligned} &\frac{r}{R_1R_2CC_1} = K \\ &\frac{1}{R_2C}(1-r) + \frac{1}{R_1C} + \frac{1}{R_2C} = a \\ &\frac{1}{R_1R_2CC_1} = b \\ &1 + \frac{R_4}{R_3} = r \end{aligned} \tag{5.17}$$

These 4 equations have 7 unknown parameters and so 3 of them can be chosen arbitrarily. These arbitrary elements are determined to minimize the sensitivity[62] of filter poles with respect to all elements. The sensitivity of a pole $S_p = \sigma_p + j\omega_p$ with respect to an element X is defined as:

$$\text{sensitivity} = \frac{\partial\sigma_p/\sigma_p}{\partial X/X} + j\,\frac{\partial\omega_p/\omega_p}{\frac{\partial X}{X}} \tag{5.18}$$

In table (5.1), for second order Butterworth filter, the elements of fig. (5.10) which have been calculated for different cut-off frequencies can be seen.

Table (5.1) Elements of second order Butterworth filter

cut-off frequency HZ	R1 KΩ	R2 KΩ	R3 KΩ	R4 KΩ	C PF	C1 PF
60	3.8	23.0	30	260	0.2	0.4
100	4.8	27.5	36	320	0.1	0.2
150	4.8	27.5	36	320	0.068	0.136
200	5.2	30.0	40	350	0.047	0.094
250	4.0	24.0	30	270	0.047	0.094

5.2 DIGITAL FILTERING

Digital filtering is the process of spectrum shaping using digital methods and is defined by the following equation:

$$y_k = \sum_{i=o}^{r} L_i x_{k-i} - \sum_{i=1}^{m} K_i y_{k-i} \qquad (5.19)$$

where x_k is the k^{th} input sample to the filter and y_k is its k^{th} output sample.

The design of a digital filter consists of finding the coefficients L_i and k_i to fulfill a given filtering requirement.

The filter is a recursive one unless all the K_i coefficients are zero in which case it is called non-recursive.

Equation (5.19) can be realized either as figure (5.11) or in canonic form as figure (5.12).

5.2.1 Z-transform

The basic mathematical tool of digital filters is z-transform calculus. The z-transform of a sequence x_{k-i} $i = o,1,2,\ldots$ is defined as:

$$X(Z) = \sum_{i=o}^{\infty} x_{k-i} \bar{Z}^i \qquad (5.20)$$

and the inverse z-transform is:

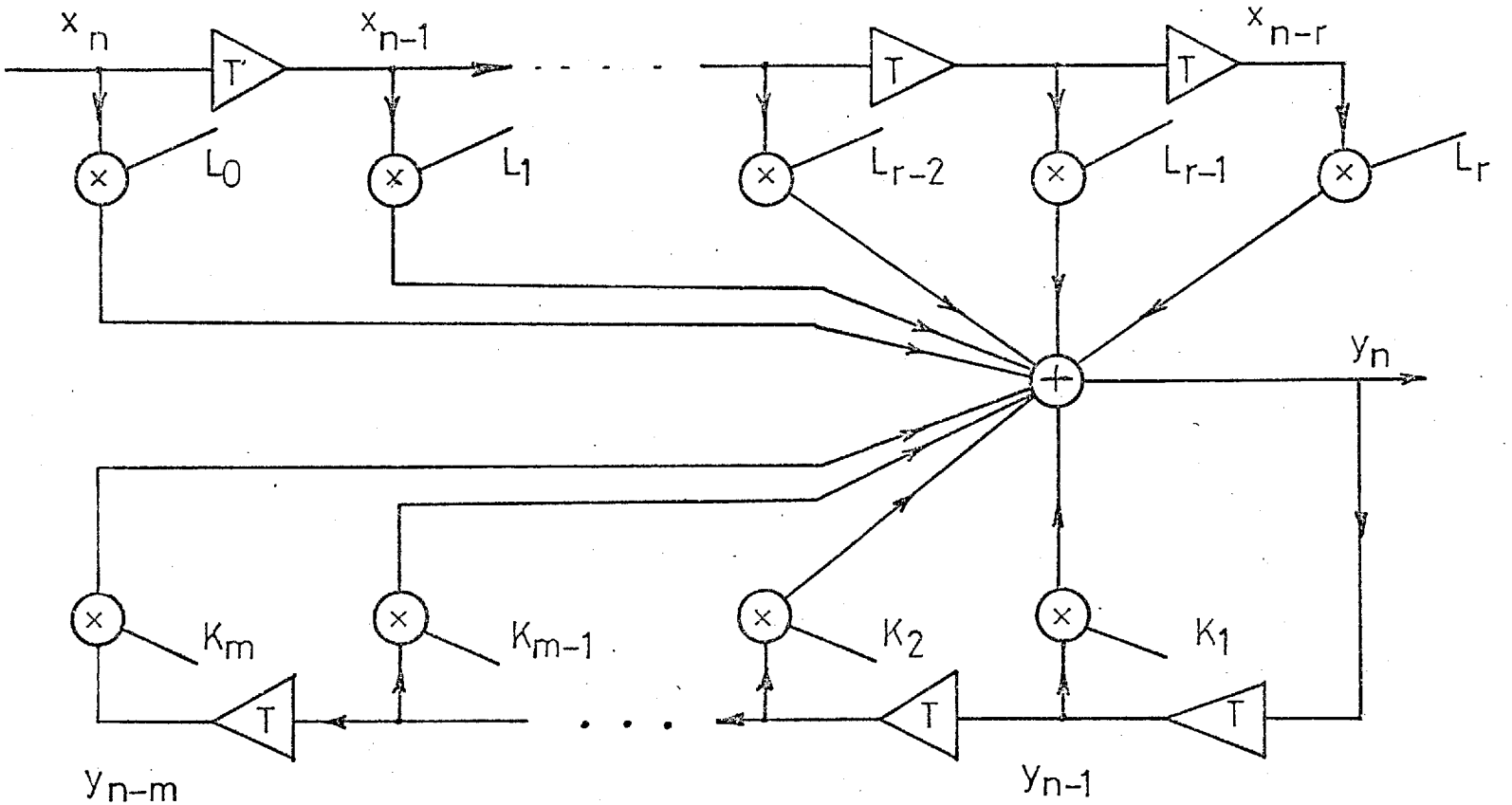

Fig. (5.11) Representation of an m-order recursive filter

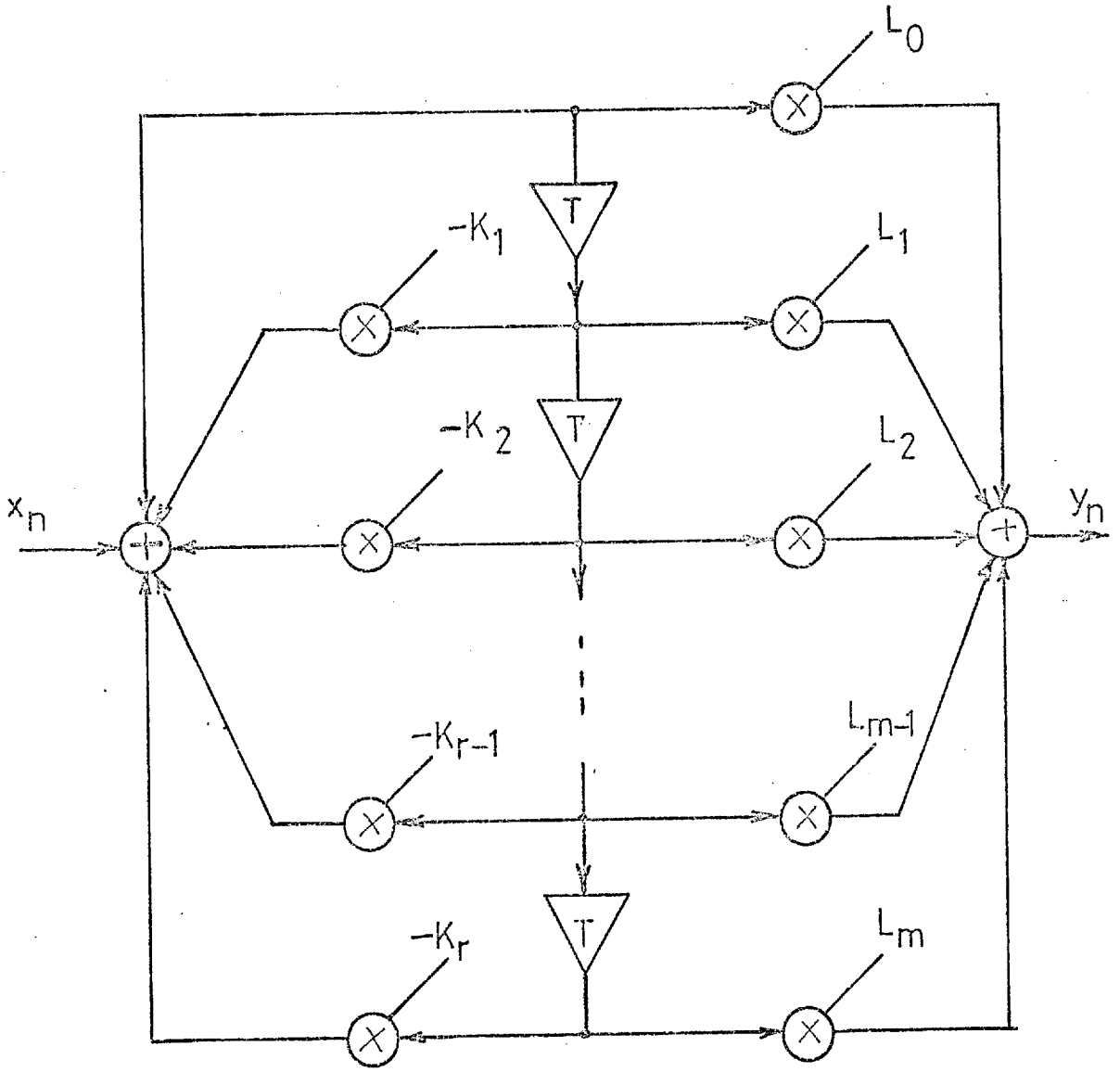

Fig.(5.12) Canonic representation of digital filter

$$x_k = \frac{1}{2\pi j} \oint X(Z) Z^{i-1} \, dz \qquad (5.21)$$

The integration is performed around any closed curve which encloses all the singular points of X(Z) and the origin.

5.2.2 Transfer function of digital filters

The Z-transform of both sides of equation (5.19) can be calculated as follows:

$$Y(Z) = \left(\sum_{i=o}^{r} L_i \bar{Z}^i \right) X(Z) - \left(\sum_{i=1}^{m} K_i \bar{Z}^i \right) Y(Z)$$

or

$$Y(Z) = \frac{\sum_{i=o}^{r} L_i \bar{Z}^i}{\sum_{i=o}^{m} K_i \bar{Z}^i} X(Z) \qquad (5.22)$$

Putting:

$$\frac{\sum_{i=o}^{r} L_i \bar{Z}^i}{\sum_{i=o}^{m} K_i \bar{Z}^i} = H(Z) \qquad (5.23)$$

equation (5.22) becomes:

$$Y(Z) = H(Z) \; X \; (Z) \qquad (5.24)$$

Analogous to continuous analogue filtering, H(Z) is called the transfer function of the digital filter. In analogue filters by replacing s by jω, the frequency response of the filter can be obtained. In digital filtering Z must be replaced by $e^{j\omega T}$, if the frequency response function is needed[39]. Also, as in analogue filtering, H(Z) is called the impulse response of the digital filter.

5.2.3 Recursive digital filter

There are two common methods for designing a recursive digital filter; one valid method is to design it from an analogue filter. For many years efforts have been made to

improve and optimize such filters. This technique enables use to be made of the efforts in this field.

Assume that a stable analogue filter is chosen, e.g. Butterworth or Chebyshev, with a transfer function $H_A(s)$. If, in this transfer function, s is replaced by $\frac{Z-1}{Z+1}$, we would obtain the transfer function[39], $H_D(Z)$ of the Butterworth or Chebyshev digital filter.

If the angular frequency of the digital filter is ω_D and its corresponding analogue one is ω_A, they are related to each other as follows:

$$s = \frac{Z-1}{Z+1}$$

$$j\omega_A = \frac{e^{j\omega_D T} - 1}{e^{j\omega_D T} + 1} = j \tan \frac{\omega_D T}{2}$$

or
$$\omega_A = \tan \frac{\omega_D T}{2} \qquad (4.25)$$

Now assume that we wish to design a third order Butterworth digital filter with a cut-off frequency equal to ω_{DC}. First we design a third order Butterworth analogue filter with a cut-off frequency of ω_{AC}, where:

$$\omega_{AC} = \tan \frac{\omega_{DC} T}{2}$$

and then in the designed transfer function s is replaced by $\frac{Z-1}{Z+1}$ producing the transfer function of the desired digital filter. Some typical Butterworth and Chebyshev digital filters which have been designed in this way are given in Appendix A2.

Another method for designing a recursive digital filter is the optimization method[40]. The problem of choosing the coefficients K_i and L_i of the digital filter (equation 5.19) to suit an arbitrary specified frequency response may be considered as a classical approximation problem. In this approach, the coefficients are chosen such that the square of the

difference (error) between the designed and desired coefficients is minimum. Minimization of this square error in the frequency domain is done using the non-linear optimization algorithm described by Fletcher and Powell[42]. A general recursive filter transfer function can be written either in cascade form as

$$H(Z) = A \prod_{k=1}^{K} \frac{1 + a_k \bar{Z}^1 + b_k \bar{Z}^2}{1 + c_k \bar{Z}^1 + d_k \bar{Z}^2} \tag{5.26}$$

or in parallel form as

$$H(Z) = A \sum_{k=1}^{K} \frac{1 + a_k \bar{Z}^1 + b_k \bar{Z}^2}{1 + c_k \bar{Z}^1 + d_k \bar{Z}^2} \tag{5.27}$$

In the parallel form for high order filters it is both difficult to find the zeroes and increase the number of filter sections (K) produces negligible improvement in the desired characteristic. This form is not usually used.

In the cascade form assume that the desired magnitude at angular frequencies $\omega_1, \omega_2, \ldots \omega_p$ are $y_1, y_2, \ldots, y_\ell$. $\omega_1, \ldots$ corresponds to values of the variable Z as, $Z_i = e^{j\omega_i T}$. The square of the error is

$$Q(\theta) = \sum_{i=1}^{\ell} \left| |H(Z_i)| - Y_i \right|^2 \tag{5.28}$$

where θ is a vector of (4K+1) unknown coefficients:

$$\theta = (a_1, b_1, c_1, d_1, a_2, b_2, c_2, d_2, \ldots, A)'$$

The problem is to find a value of θ, say θ^* such that for all θ

$$Q(\theta^*) \leq Q(\theta)$$

By using Fletcher's and Powell's method, digital filters with any sections can be designed. For example for a low pass filter with a cut-off frequency at $\frac{1}{20}$th sampling frequency, the two following digital filters have been designed in this way. With one section only (second order digital filter):

$$H(Z) = 0.121 \frac{Z^2-1.64Z+1}{Z^2-1.79Z+0.836} \tag{5.29}$$

or

$$u_k = 0.121(\upsilon_k-1.64\upsilon_{k-1}+\upsilon_{k-2})+1.79u_{k-1}-0.836u_{k-2} \tag{5.30}$$

and with two sections (4th order digital filter);

$$H(Z) = 0.0249 \frac{Z^2-1.85Z+1}{Z^2-1.86Z+0.944} \times \frac{Z^2-1.22Z+1}{Z^2-1.729Z+0.765} \tag{5.31}$$

or

$$H(Z) = 0.0249 \frac{Z^4-3.07Z^3+4.26Z^2-3.07Z+1}{Z^4-3.59Z^3+4.93Z^2-3.057Z+0.722} \tag{5.32}$$

or in time domain:

$$u_k = 3.591u_{k-1}-4.93u_{k-2}+3.057u_{k-3}-0.72u_{k-4}$$

$$+ \quad 0.0249(\upsilon_k-3.07\upsilon_{k-1}+4.26\upsilon_{k-2}-3.07\upsilon_{k-3}+\upsilon_{k-4}) \tag{5.33}$$

In all recursive filters for stability all the poles, on the complex plane must be inside the unit circle[59].

5.2.4 Non-recursive digital filter

In a non-recursive digital filter, the value of an output, u_k is related to the input sequency by:

$$u_k = \sum_{i=o}^{M-1} L_i \quad \upsilon_{k-i} \tag{5.34}$$

Although this filter needs more storage and a greater number of arithmetic operations in comparison with recursive types, it has also a number of advantages. Stability is always ensured, and particularly it can be designed with a linear phase characteristic. This property is valuable in communication systems. For protection purposes it does not offer any particular advantage.

The transfer function of the equation (5.34) can be written as:

$$H(Z) = \sum_{i=o}^{M-1} L_i \quad \bar{Z}^i \tag{5.35}$$

There are a number of ways for designing nonrecursive digital filters, but only two are useful here.

5.2.4.1 Fourier method design of non-recursive filters

Assume that the design of a non-recursive digital filter with a characteristic $|H(j\omega)|$ as in fig. (5.13) is required.

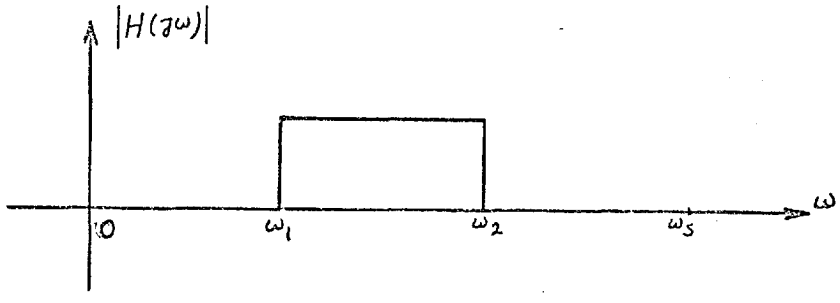

Fig.(5.13) Desired characteristic of a non-recursive digital filter

In this figure $\omega_s = 2\pi f_s$ and f_s is the sampling frequency. By using the Fourier series the real and imaginary parts of $H(j\omega)$ can be expressed as follows:

$$Re(\omega) = a_o + \sum_{n=1}^{\infty} a_n \cos n\omega T \qquad (5.36a)$$

$$Im(\omega) = \sum_{n=1}^{\infty} b_n \sin n\omega T \qquad (5.36b)$$

where

$$H(j\omega) = Re(\omega) + j\, Im(\omega) \qquad (5.37)$$

But

$$\cos n\omega T = \frac{e^{jn\omega T} + \bar{e}^{jn\omega T}}{2} = \frac{Z^n + \bar{Z}^n}{2} \qquad (5.38a)$$

and

$$\sin n\omega T = \frac{e^{jn\omega T} - \bar{e}^{jn\omega T}}{2j} = \frac{Z^n - \bar{Z}^n}{2j} \qquad (5.38b)$$

Putting $\cos n\omega T$ and $\sin n\omega T$ from equations (5.38) into (5.36) and (5.37) we obtain:

$$H(Z) = a_o + \sum_{n=1}^{\infty} a_n \frac{Z^n + \bar{Z}^n}{2} + \sum_{n=1}^{\infty} b_n \frac{Z^n - \bar{Z}^n}{2}$$

or

$$H(Z) = a_o + \frac{1}{2} \sum_{n=1}^{\infty} [(a_n + b_n) Z^n + (a_n - b_n) \bar{Z}^n] \qquad (5.39)$$

The series is truncated at a finite number of terms and then by comparison with equation (5.35), the coefficients L_i are obtained. In figure (5.14a)the spectrum of a digital filter with 20 terms which have been designed in this way can be seen. This filter in the stop band has some undesirable oscillation caused by truncation of the Fourier series, called Gibbs oscillation. Multiplication of the impulse response of the filter by a window function results in a smoothing of the frequency characteristic with significant reduction in ripple. There are a wide variety of window functions[43]. One of them is Hamming's window function[43]. Using this window we obtain an improved characteristic as in figure (5.14b).

5.2.4.2 Linear-phase non recursive digital filter[45]

In order that a non recursive digital filter has a linear phase, one of the two following relations must exist between its impulse response coefficients.

$$L_i = L_{M-i-1} \tag{5.40a}$$

or

$$L_i = -L_{M-i-1} \tag{5.40b}$$

where M is the length of the filter. In the first case digital filter has positive and in the second, it has negative symmetry. Also the filter might have odd or even length, and so linear phase digital filters can have one of the following 4 cases:

a) Positive symmetry and odd length. Spectrum is given by

$$G(f) = \sum_{k=o}^{n} a(k) \cos 2\pi kf \tag{5.41a}$$

where $n=(M-1)/2$, $a(o)=L_n$ and $a(k)=2L_{n-k}$, for $k=1,\ldots,n$;

b) Positive symmetry and even length. Spectrum is given by

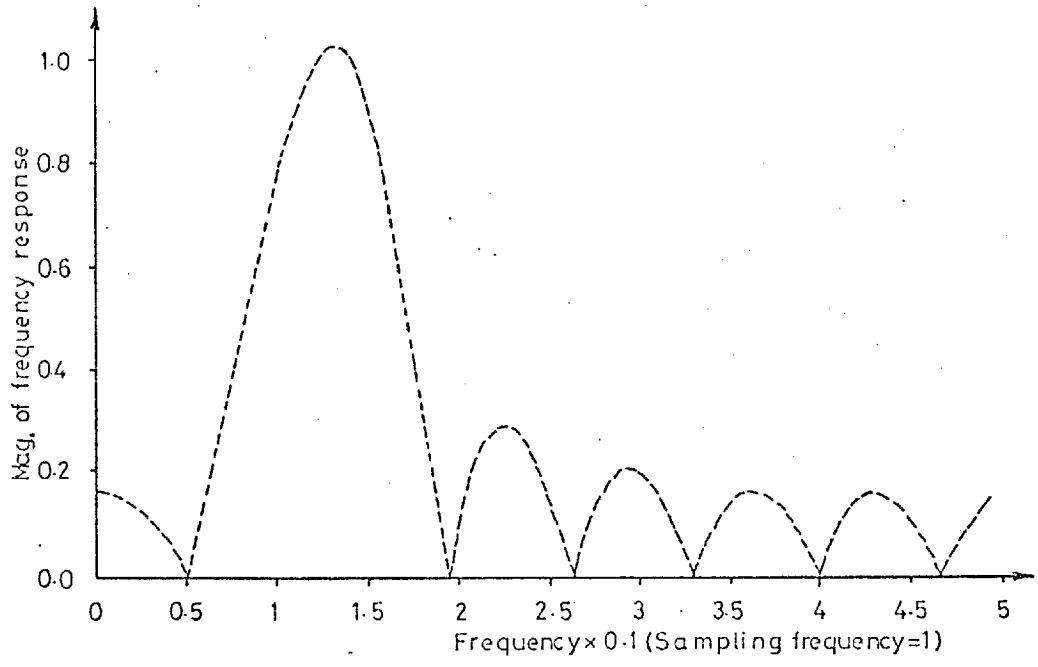

Fig. (5.14)a Spectrum of a non-recursive band-pass digital filter with 20 terms designed by Fourier method.

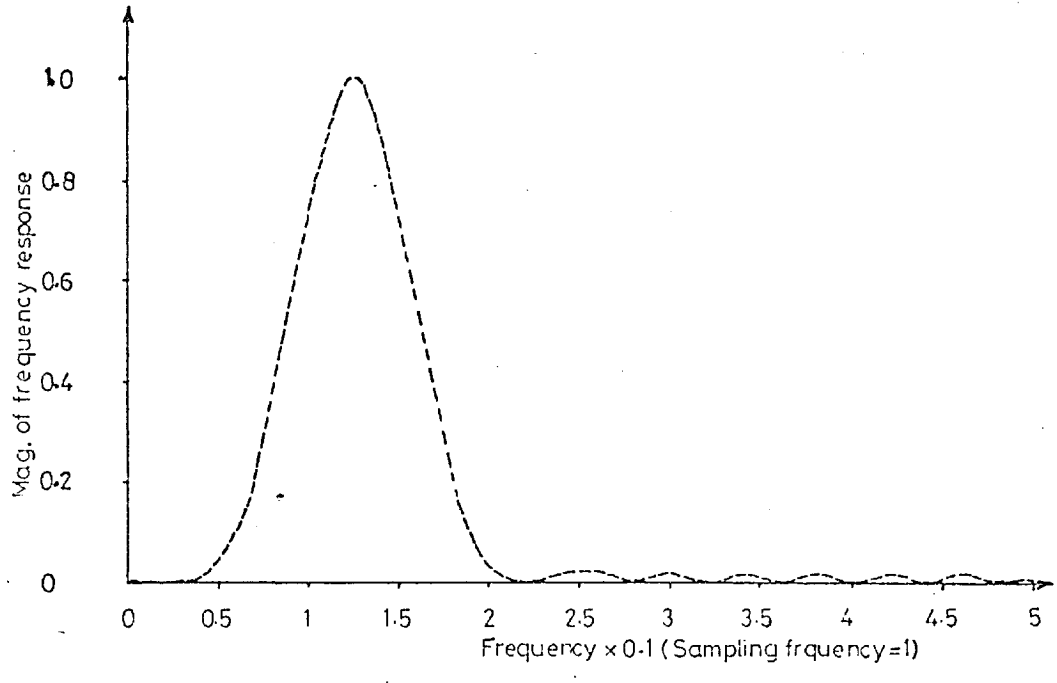

Fig. (5.14)b Spectrum of a non-recursive band-pass digital filter with 20 terms designed by Fourie method and with Hamming's window function.

$$G(f) = \sum_{k=1}^{n} b(k) \cos 2\pi (k-\tfrac{1}{2}) f \qquad (5.41b)$$

where $n=M/2$, and $b(k)=2L_{n-k}$, for $k=o,1,\ldots n$

c) Negative symmetry and odd length. Spectrum is given by

$$G(f) = \sum_{k=1}^{n} c(k) \sin 2\pi k f \qquad (5.41c)$$

where $n=(M-1)/2$, and $c(k)=2L_{n-k}$ for $k=1,2,\ldots n$

d) Negative symmetry and even length. Spectrum is given by

$$G(f) = \sum_{k=1}^{n} d(k) \sin 2\pi (k-\tfrac{1}{2}) f \qquad (5.41d)$$

where $n=M/2$ and $d(k) = 2L_{n-k}$, for $k=1, \ldots n$

McClellan[45] has shown that cases (b),(c) and (d) can be put in the form of case (a) and treated in a unified way. Then by using the Remez exchange method[46,48,44] filters with minimum weighted Chebyshev error in approximating a desired frequency response can be designed.

5.2.5 Transient time response of digital filters

In a digital filter as in an analogue one the output of the filter for a unit step input is used as a measure to represent the time delay which a filter may introduce during the transient state.

A unit step function in discrete form can be defined as:

$$x_k = 1 \quad \text{for } k = o,1,2,\ldots$$

and

$$x_k = o \quad \text{for } k < o$$

where x_k is the k^{th} sample of a continuous unit step function at equally spaced intervals.

The Z-transform of this function can be obtained in a closed form as:

$$Z(x_k) = X(Z) = \frac{1}{1-Z^{-1}} = \frac{Z}{Z-1} \qquad (5.42)$$

Now assume that the impulse response of the digital filter is H(Z) and its output for a unit step input y_k, with a Z-transform equal to Y(Z), we can write:

$$Y(Z) = H(Z)\ X(Z) \qquad (5.43)$$

Putting X(Z) from (5.42) into (5.43) we will obtain:

$$Y(Z) = \frac{Z}{Z-1}\ H(Z)$$

By using inverse Z-transform we can calculate the output of the filter in time domain:

$$Y_k = \frac{1}{2\pi j} \oint Y(Z)\ Z^{k-1}\ dZ = \frac{1}{2\pi j} \oint \frac{Z}{Z-1}\ Z^{k-1}\ H(Z)dZ$$

By using the Residue Theorem we can write:

$$y_k = \sum \left(\text{Residue of } \frac{Z^k H(Z)}{Z-1}\right) \qquad (5.44)$$

From equation (5.44) the output of any digital filter for a unit step input can be calculated.

5.2.6 Comparison between analogue and digital filters

Nonrecursive digital filters can be designed to have exact linear phase and an approximating ideal characteristic, but they suffer from the drawback that they must have many terms , 32 terms or even more . These large number of terms require a long time delay for computation which is unacceptable. Also the linearity of the phase characteristic is not important in protection.

A recursive digital filter with fewer terms can give a sharp characteristic. In figures (5.15) to (5.17) the spectrums of 1st, 2nd and 5th order Butterworth digital filters which have been designed by the bilinear transformation method can be seen. In these figures for comparison the corresponding spectrums of analogue filters have also been plotted. The

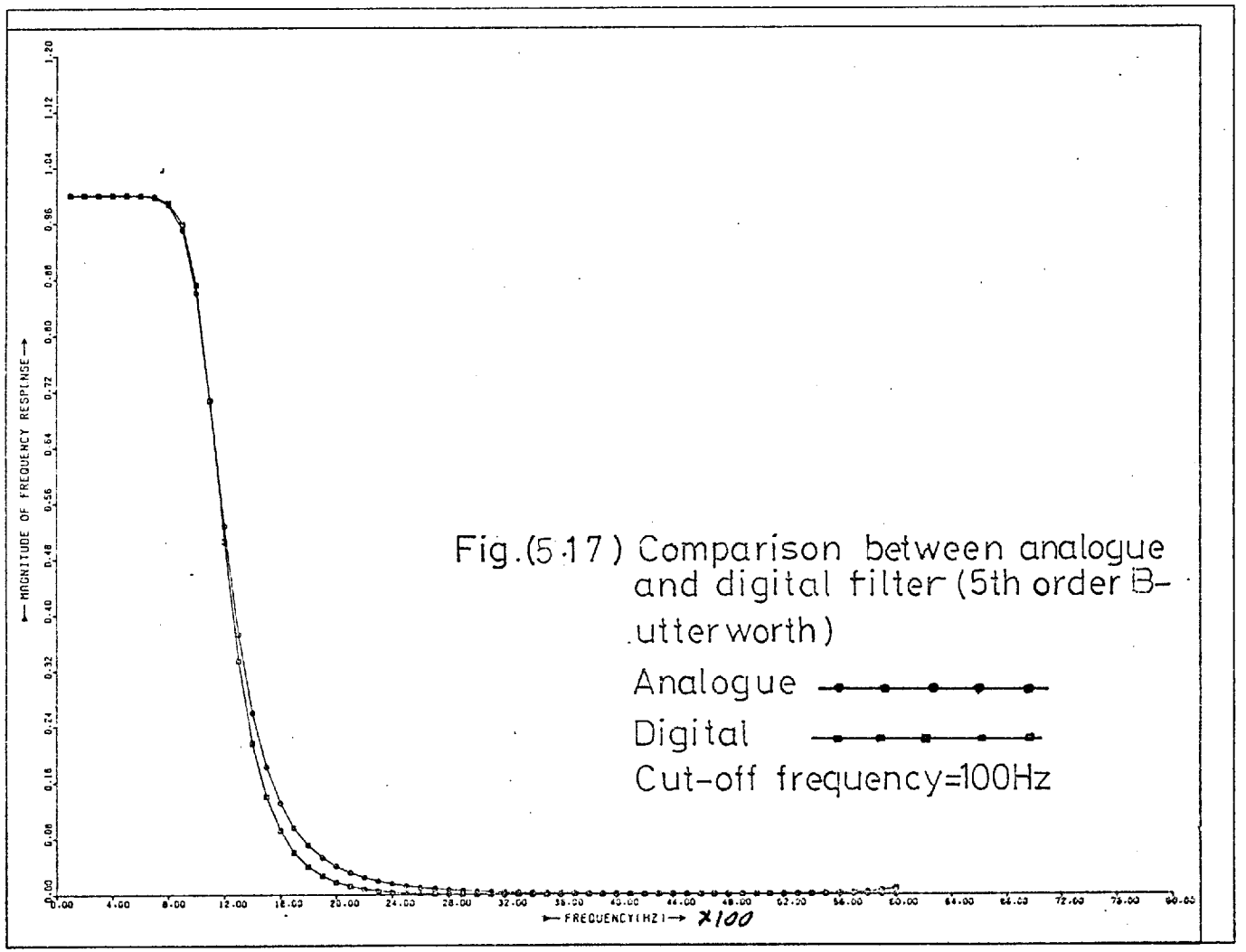

Fig.(5.17) Comparison between analogue and digital filter (5th order Butterworth)

Analogue

Digital

Cut-off frequency=100Hz

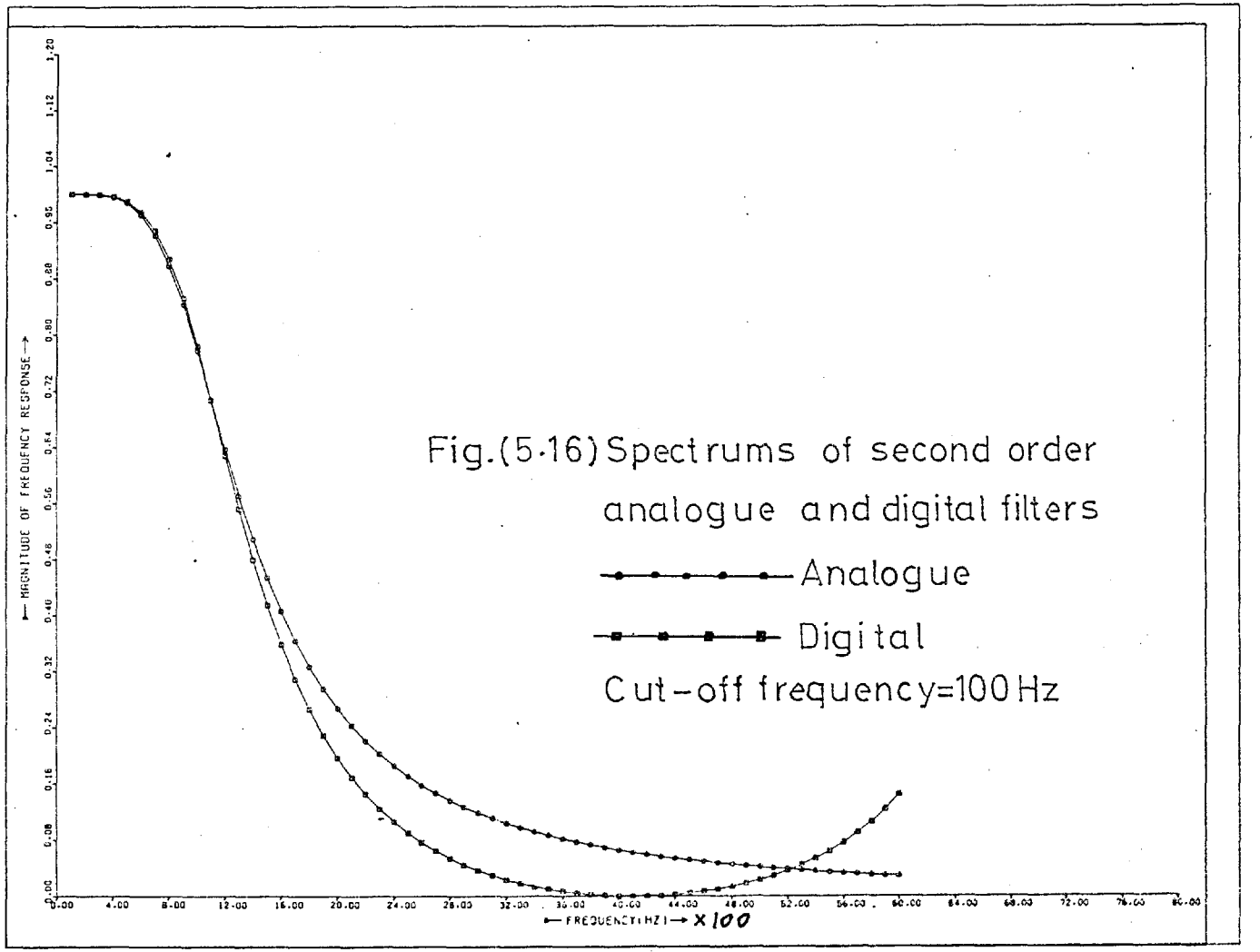

Fig.(5.16) Spectrums of second order analogue and digital filters

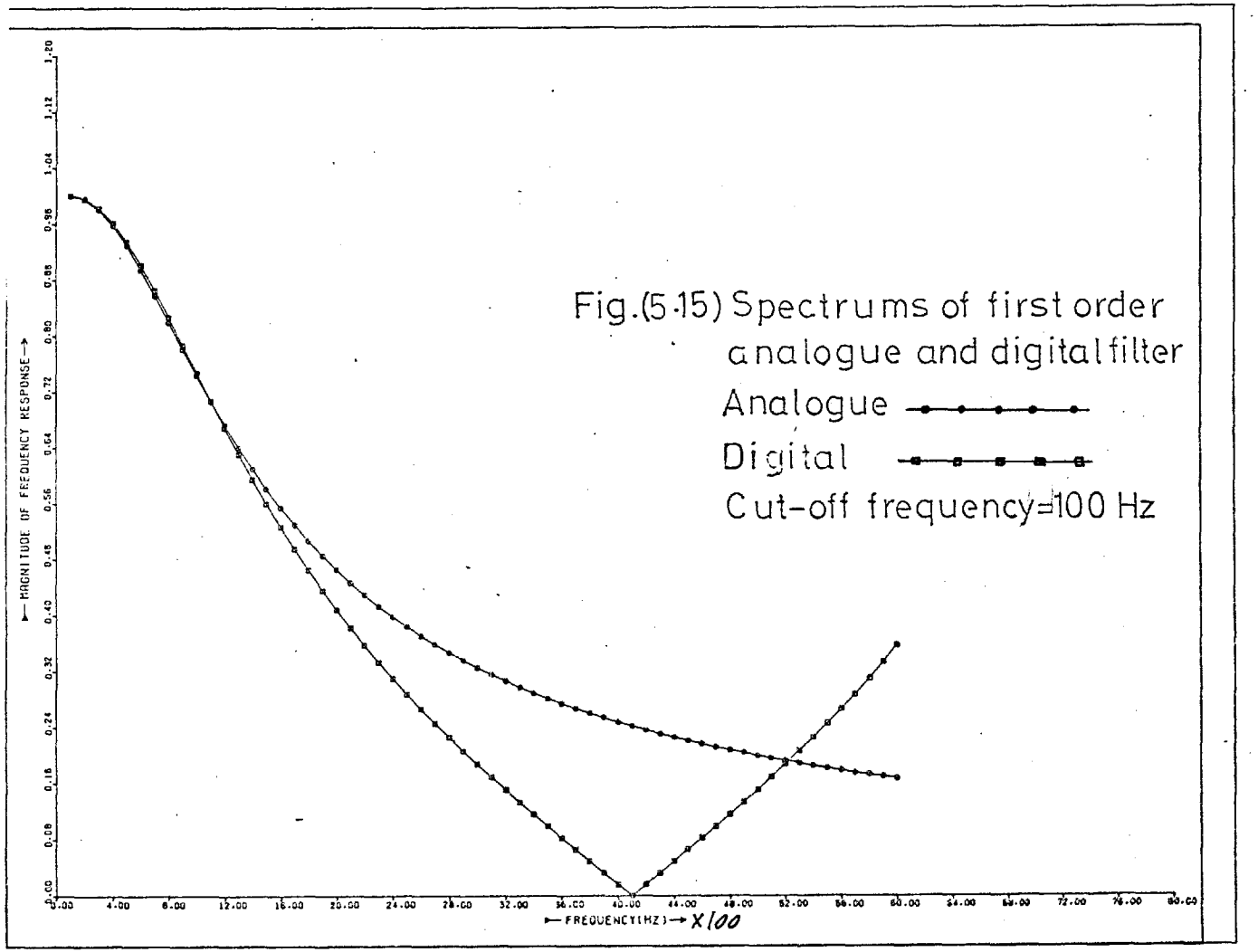

Fig.(5.15) Spectrums of first order analogue and digital filter

digital filter spectrums are periodic and for the frequencies around half the sampling frequency and below them are better than analogue filters, but at higher frequencies, the spectrums of analogue filters are better. Figure (5.18) shows the unit step responses of 2nd, 5th and 8th order digital and analogue Butterworth filters, and we can see that the transient time delay of both types of filters are the same. The spectrums of the 2nd and 4th order digital filters which have been designed by Fletcher and Powell optimization method (equation 5.30 and 5.33) are depicted in figures (5.19) and (5.20) and the unit step response of the 4th order filter is given in figure (5.21). The corresponding Butterworth analogue filter curves, again have been replotted for comparison. We can see that the digital filters obtained in this way have sharper spectrums, but they also have longer time delays in the transient state. Hence for protection purposes the digital filters again do not offer any advantages over analogue types.

It is argued that digital filters are more accurate and drift free, but since sample and hold circuits, analogue to digital converters etc, which might have offset and drift are required before the digital filters, it is unlikely for the overall digital filter to be more accurate than analogue one.

Another important point in the power system, in which a low rate of sampling is used, digital filters must be accompanied by analogue ones, otherwise the high frequency components cannot be removed.

5.3 CONCLUSION

In this chapter the analogue and digital filters have been compared and it is concluded that for protection purposes analogue filters are preferred, for the following reasons:

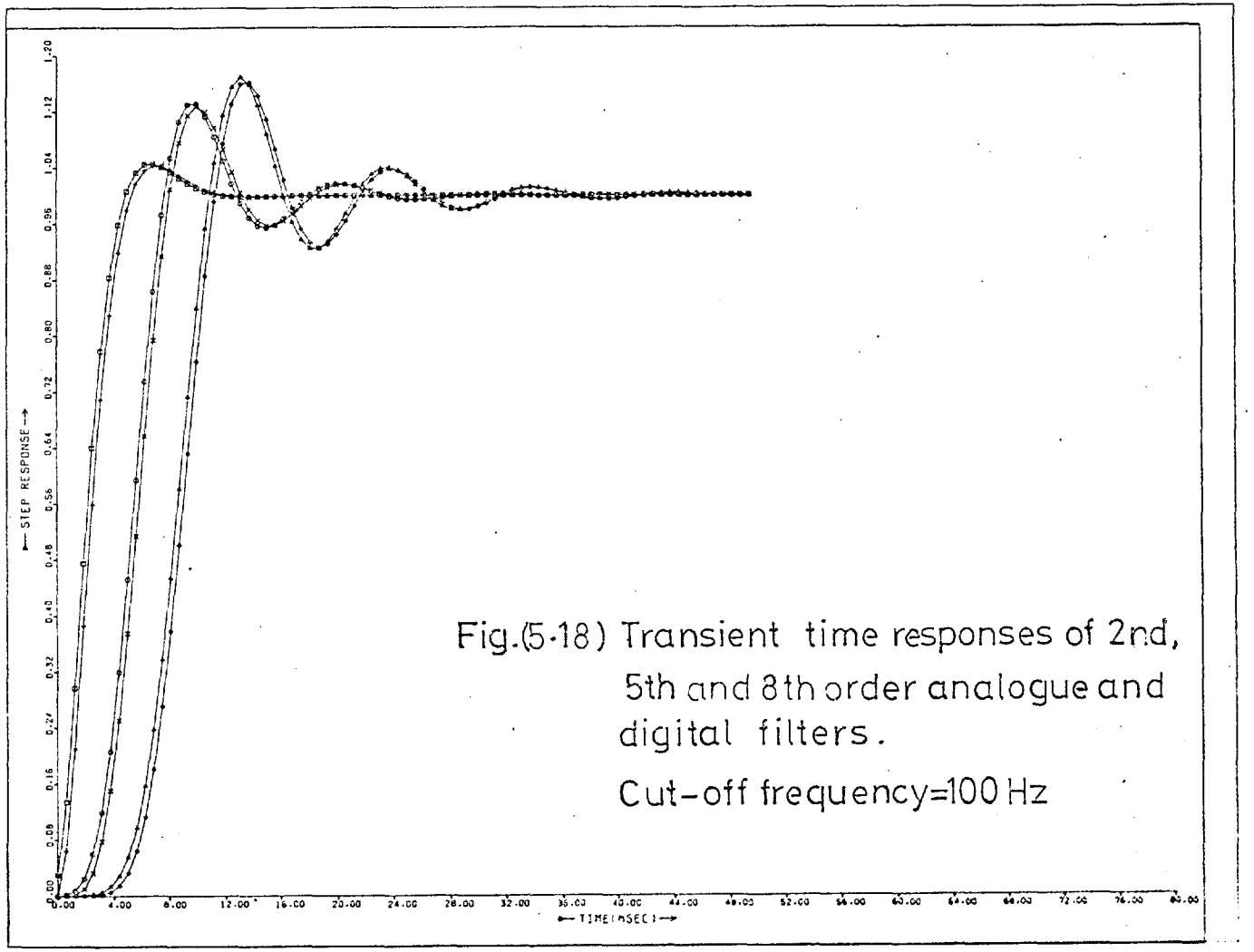

Fig.(5-18) Transient time responses of 2nd, 5th and 8th order analogue and digital filters.

Cut-off frequency=100 Hz

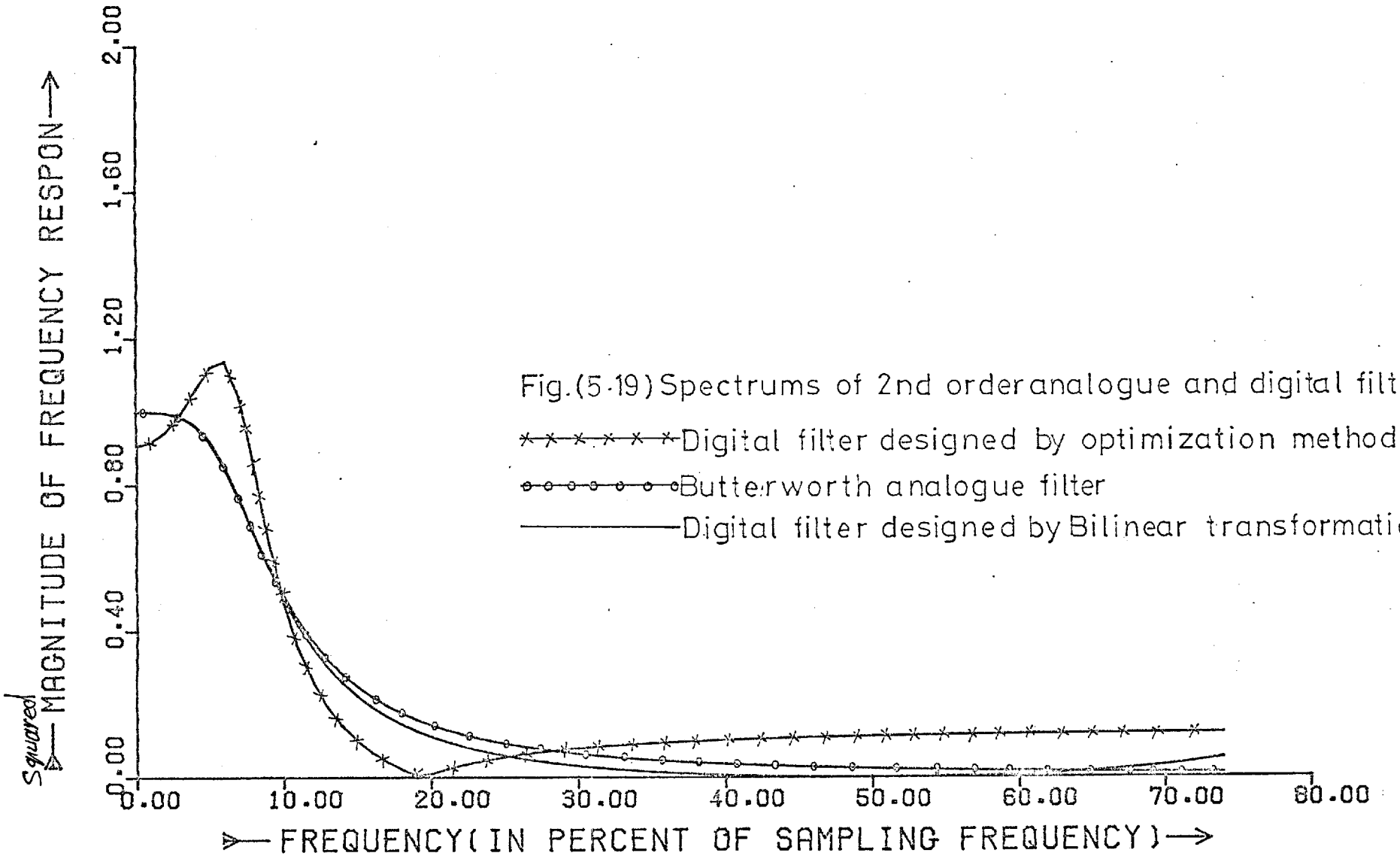

Fig.(5-19) Spectrums of 2nd order analogue and digital filters

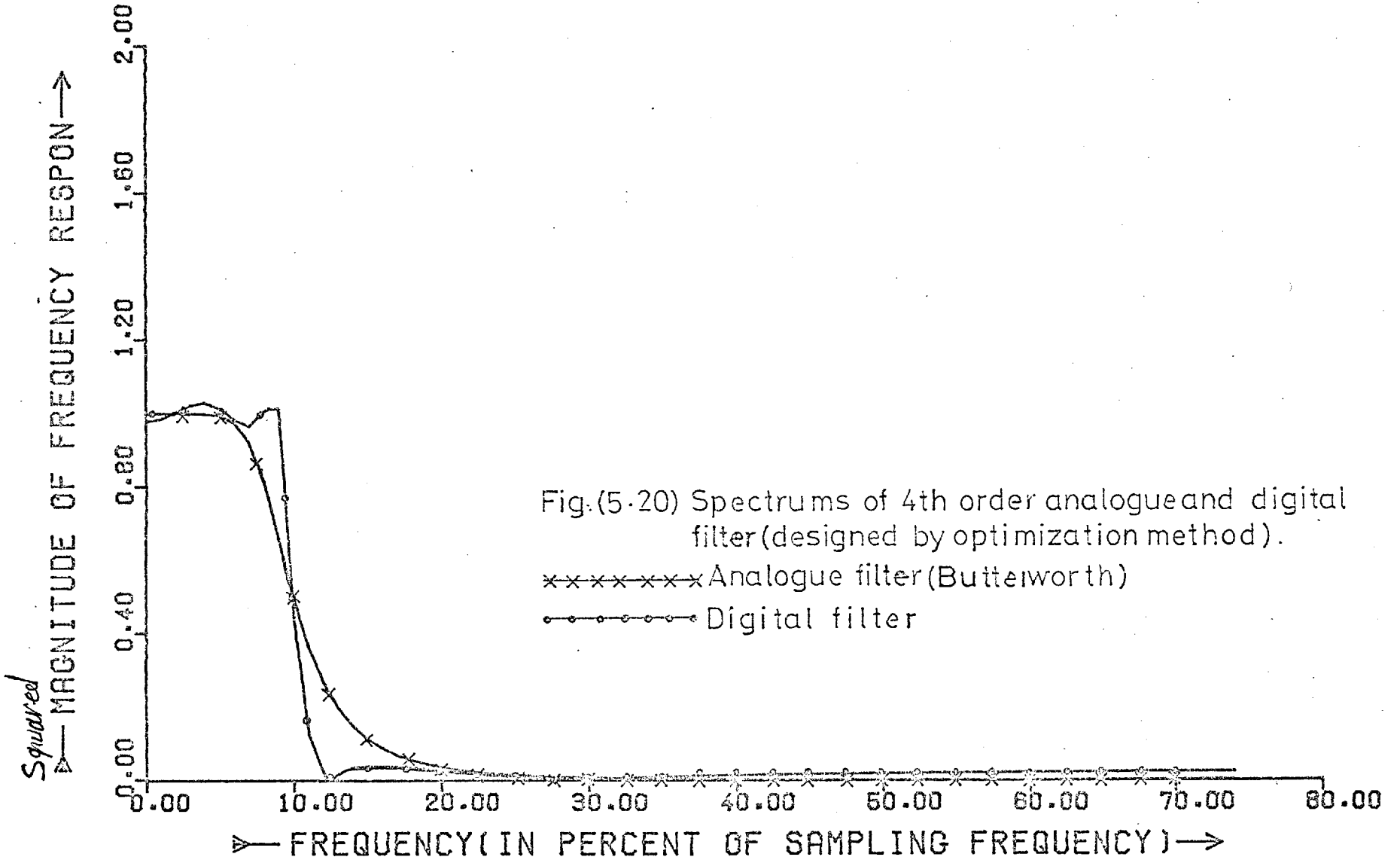

Fig.(5·20) Spectrums of 4th order analogue and digital filter (designed by optimization method).

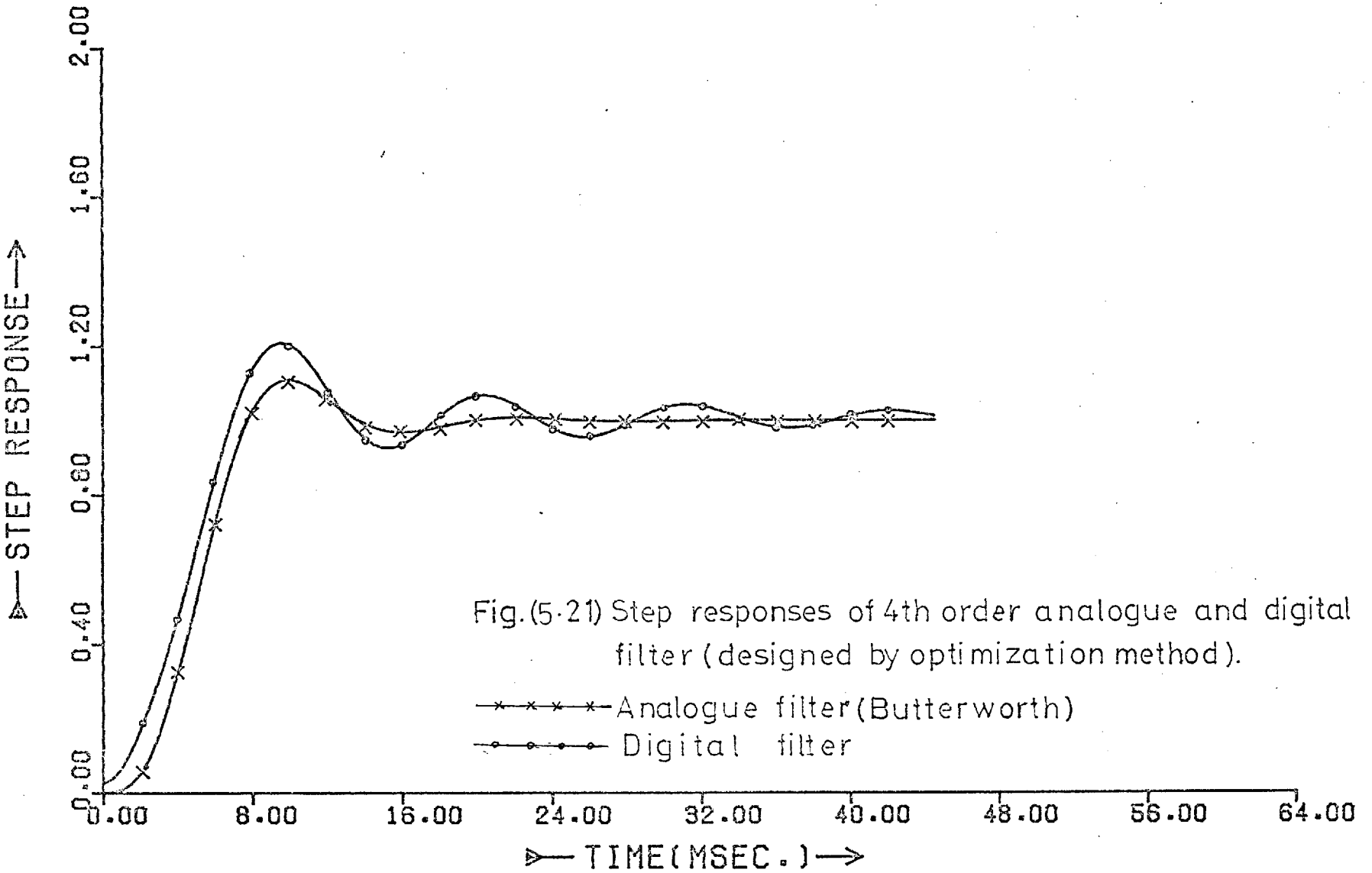

Fig.(5·21) Step responses of 4th order analogue and digital filter (designed by optimization method).

(I) Analogue filters are cheaper. They are simple to design and to construct;

(II) Digital filters must be used with analogue, otherwise high frequency components will not be removed;

(III) From the transient time delay and spectrum point of view no clear advantage can be seen in either filter type;

(IV) For frequencies higher than half the sampling rate analogue filters have the better spectrums for digital protection purposes.

From the choice of analogue filters the Butterworth filter is recommended. For protection purposes, other filters such as L or Chebyshev filters do not offer any advantages over the Butterworth filter. The Chebyshev filter designed with a large ripple together with the L filter both have sharper characteristics, but unfortunately they have longer time delays than the Butterworth filters.

In chapter 3 it was shown that among Butterworth analogue filters, second order, can give a satisfactory result. This filter can be realized by only one operational amplifier.

CHAPTER 6

CLOSE-UP FAULTS AND DOUBLE CIRCUIT LINE PROBLEMS

Close up faults and double circuit lines present problems in distance measurement and must be dealt with carefully. These problems are studied in this chapter.

6.1 CLOSE-UP FAULTS

The correct operation of protective systems using distance relays depends on the determination of the direction in which the fault current is flowing with reference to the voltage at the relaying point.

In conventional analogue relaying, this is generally achieved by using either directional relays in conjunction with impedance relays or mho relays in which both the directional and measuring characteristics are combined. In these relays, close-up faults present a problem, since the voltage collapses to a point at which there is insufficient voltage to provide the required operation. In polarised mho relay, this problem has been solved by selecting a suitable polarising voltage derived from the fault voltage through a resonant circuit tuned to system frequency (memory) or from an unfaulted phase through a suitable phase shifting circuit (sound-phase polarising); alternatively, a combination of part sound-phase and part faulted-phase polarising[54] is used. The last two methods do not solve the problem in the case of 3-phase faults, because an unpolarised mho characteristic is obtained, and operation for close-up faults becomes indeterminate. Most transmission systems have additional earth wire protection for a certain distance out from the switching station or generating station[64], so that a three-phase flashover due to a lightning stroke in this region is considered

unlikely. Flashover for other reasons in this region is likely to affect one or two phases and not three phases, and it is only enough for the fault to remain as a phase-fault or earth-fault for about 1.5 cycles before developing into a three phase fault in order that the operation of distance protection is ensured. One possible cause of terminal three-phase faults is the failure to remove temporary earthing connections on a line after completion of maintenance work. In some instances, where earthing switches are used for this purpose, interlocking with the main circuit breaker is possible and the risk of closing on to a three-phase fault is remote. Because of the foregoing, the requirements for protection against instantaneous three-phase faults are subject to some difference of opinion. For example in Great Britain[64], the risk involved is not considered to be great and the protection for three phase close-up faults is provided only in the third zone of the relay. For zone 3 an off-set mho relay is normally used which also initiates the starting and timing relays, and it is set with the backwards reach about 10% of the forwards reach and so covers the region near to the relaying point. For the first zone a polarized mho distance relay is used. In computer relaying, for close-up faults small values of resistance and reactance of the faulty line will be obtained, but numerical and other errors may make the computed results unreliable in determining the fault direction. In such a case, as in analogue relays, the directional information must be obtained either by using memory voltage or sound-phase voltage principles.

6.1.1 Memory voltage principle

Holden and Morrison[65] have shown that transmission line impedances calculated using prefault voltage values can be

related to the positive sequence impedance of the source behind the relay and are of sufficient magnitude that the directional information obtained would give directional discrimination for all types of faults. To establish the fault as close-up, the voltage samples could be used. Depending on sampling rates, 3 to 5 small samples within a predefined tolerance could indicate that the voltage is sufficiently small to preclude its use in reliably ascertaining the direction of the fault. In this case, a memory voltage would be substituted for normal relaying voltage in subsequent impedance calculation. The selection of the appropriate memory voltage is based on the type of the fault. The criterion for operation is that the calculated reactance (by using the last prefault cycle of the memory voltage) becomes positive. There is no need for the resistance to be calculated. Having established that the fault is close-up. Table (6.1) summarises the relaying quantities to be chosen when the fault has been classified into one of the six fault types.

Table (6.1) Relay quantities and criteria for operation

Fault classified as	Relay currents	Prefault voltage
ab	I_a-I_b	V_a-V_b
bc	I_b-I_c	V_b-V_c
ca	I_c-I_a	V_c-V_a
ad	I_a+KI_o	V_{ad}
bd	I_b+KI_o	V_{bd}
cd	I_c+KI_o	V_{cd}

By using the Fourier method, the reactance is calculated from equation (3.66) of chapter 3. In this equation the

denominator is always positive and so it can be omitted, which reduces the criterion for operation to:

$$A_i B_v > A_v B_i \qquad (6.1)$$

For the McInnes method, the criterion becomes:

$$SI_{k+1}(SV_k - DI_k) > SI_k(SV_{k+1} - DI_{k+1}) \qquad (6.2)$$

In equations (6.1) and (6.2) only two multiplications are required and computation can be fast.

6.1.2 Sound-phase voltage principle

When the fault is established as close-up, a sound phase voltage can be substituted for the normal relay voltage in subsequent impedance calculations. With this method all unbalanced close-up faults can be discriminately detected.

Holden[66] has shown that by substituting the sound phase voltage for relaying voltage the criterion for operation reduces to

$$R > 0 \qquad (6.3)$$

Table (6.2) summarises the new criteria for operation.

Table (6.2) Relay quantities and criteria for operation

Fault classifed as	Relay currents	Sound phase voltage
ab	$I_a - I_b$	$-V_c$
bc	$I_b - I_c$	$-V_a$
ca	$I_c - I_a$	$-V_b$
ad	$Ia + K I_o$	$V_b - V_c$
bd	$Ib + K I_o$	$V_c - V_a$
cd	$Ic + K I_o$	$V_a - V_b$

For the McInnes method the criterion becomes:

$$DI_k \ (SV_{k+1}-SI_{k+1}) > DI_{k+1}(SV_k-SI_k) \qquad (6.4)$$

and for the Fourier method it reduces to:

$$A_v \ A_i > B_v \ B_i \qquad (6.5)$$

Equations (6.4) and (6.5) again have only two multiplications.

The sound phase voltage principle is easier to use since it does not need prefault samples. Its main drawback is that it cannot give directional information for three-phase close-up faults, but as mentioned earlier, three phase faults are unlikely to occur and can be accounted for in the third zone calculation.

6.2 DOUBLE CIRCUIT LINE

A double circuit line may have one or more earth wires bonded to earth at short intervals. The voltage gradients along the earth and earth wires can generally be assumed the same and thus they can be replaced by an equivalent conductor having the necessary self and mutual impedances with the various phase conductors (figure 6.1). For circuit 1 the voltage drop per unit length may be written as

$$\frac{d}{dX} V = ZI \qquad (6.1)$$

where

$$Z = \begin{vmatrix} Z_{aa} & Z_{ab} & Z_{ac} & Z_{aA} & Z_{aB} & Z_{aG} \\ Z_{ab} & Z_{bb} & Z_{bc} & Z_{bA} & Z_{bB} & Z_{bG} \\ Z_{ac} & Z_{bc} & Z_{cc} & Z_{cA} & Z_{cB} & Z_{cG} \end{vmatrix}$$

$$V = \begin{vmatrix} V_a & V_b & V_c \end{vmatrix}'$$

$$I = \begin{vmatrix} I_a & I_b & I_c & I_A & I_B & I_G \end{vmatrix}'$$

These relations account for intercircuit mutual

terms and will be used for the derivation of suitable relaying quantities which can account for the mutual effects.

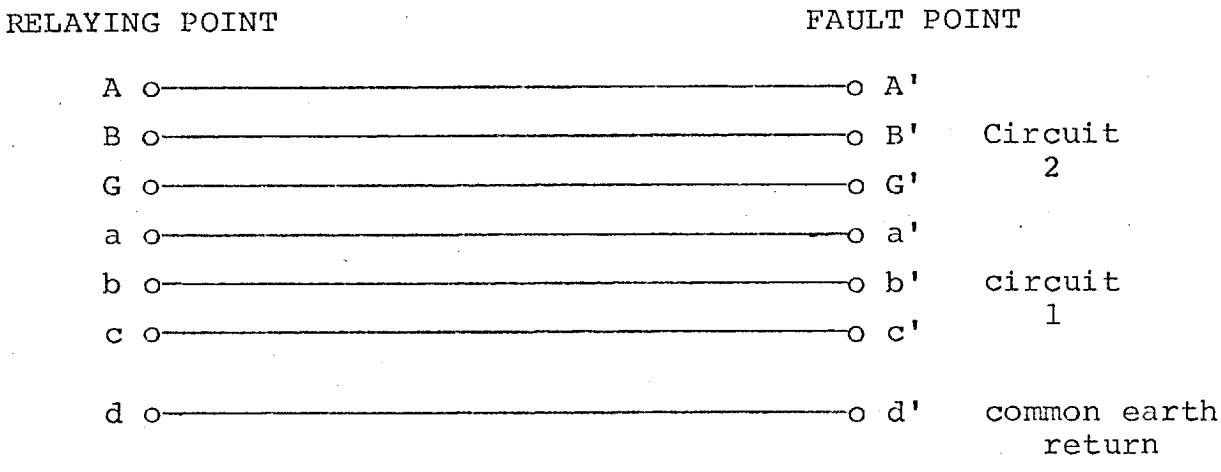

Fig. (6.1) Equivalent double circuit lines.

If circuit 1 is transposed its self and mutual impedances each become balanced and can in turn be expressed in terms of positive and zero sequence impedances as follows:

$$Z_{aa} = Z_{bb} = Z_{cc} = \frac{1}{3}(Z_o + 2Z_1)$$

$$Z_{ab} = Z_{bc} = Z_{ac} = \frac{1}{3}(Z_o - Z_1) \qquad (6.2)$$

If circuit 2 is also transposed its self and mutual impedances would become balanced and if each conductor of circuit 1 in turn occupies every spatial position with respect to every conductor of circuit 2 and vice versa, all the inter-circuit mutual terms become equal. As a result the positive and negative sequence mutual coupling between two circuits vanishes, leaving only zero sequence mutual coupling. For example consider three major types of transposed double circuit overhead lines construction in the United Kingdom. Their positive and zero sequence impedances, given[56] in table (6.3), shows that the positive sequence mutual impedances are about 3 to 5% of the positive sequence self impedances, but the zero sequence mutual impedances are abo ut 50 to 55% of the zero-

sequence self impedances. For practical purposes the positive sequence mutual impedances can be neglected, and only zero sequence coupling need to be accounted as follows:

$$Z_{aA} = Z_{bB} = Z_{cG} = Z_{aB} = Z_{bA} = \frac{1}{3} Z_{mo}$$

$$Z_{aG} = Z_{cA} = Z_{bG} = Z_{cB} = \frac{1}{3} Z_{mo} \qquad (6.3)$$

Using these equations together with equations (6.2), the equations (6.1) may be simplified as:

$$\frac{d V_a}{dX} = Z_1 I_a + (Z_o - Z_1) I_{o1} + Z_{mo} I_{o2} \qquad (6.4a)$$

$$\frac{d V_b}{dX} = Z_1 I_b + (Z_o - Z_1) I_{o1} + Z_{mo} I_{o2} \qquad (6.4b)$$

$$\frac{d V_c}{dX} = Z_1 I_c + (Z_o - Z_1) I_{o1} + Z_{mo} I_{o2} \qquad (6.4c)$$

From equations (6.1) and (6.4) the voltage drop can be calculated for any given fault condition. Such conditions will now be considered in turn.

Table (6.3) Impedances of double circuit overhead lines

circuit construction	400KV quad. 0.4 in^2 copper equivalent	275KV twin 0.4 in^2 copper equivalent	132KV single 0.175 in^2 copper equivalent
positive sequence self-impedance Z_1 Ω/mile	0.032+J0.446	0.063+J0.510	0.286+J0.647
positive sequence mutual-impedance Z_m Ω/mile	J0.023	J0.021	J0.019
zero-sequence self-impedance Z_o Ω/mile	0.167+J1.27	0.222+J1.38	0.589+J1.64
zero-sequence mutual-impedance Z_{mo} Ω/mile	0.136+J0.68	0.174+J0.74	0.304+J0.80

6.2.1 Single Phase to Earth Faults

When a solid single phase to earth fault occurs on phase a of circuit 1 at a distance x along the line from the transducer, the phase to earth voltage V_a can be calculated by use of equations (6.1) for an untransposed line or by equations (6.4) for a transposed and balanced double circuit line.

For an untransposed line the voltage drop may be written

$$V_a = xZ_{aa}(I_a + \frac{Z_{ab}}{Z_{aa}} I_b + \frac{Z_{ac}}{Z_{aa}} I_c + \frac{Z_{aA}}{Z_{aa}} I_A + \frac{Z_{aB}}{Z_{aa}} I_B + \frac{Z_{aG}}{Z_{aa}} I_G) \ \ldots \quad (6.5)$$

which is in the form

$$V_a = x\, Z_{aa} \cdot I_x \quad (6.6)$$

where

$$I_x = I_a + \frac{Z_{ab}}{Z_{aa}} I_b + \frac{Z_{ac}}{Z_{aa}} I_c + \frac{Z_{aA}}{Z_{aa}} I_A + \frac{Z_{aB}}{Z_{aa}} I_B + \frac{Z_{aG}}{Z_{aa}} I_G \ \ldots \quad (6.7)$$

For a transposed line the voltage drop is:

$$V_a = x\, Z_1 (I_a + \frac{Z_o - Z_1}{Z_1} I_{o1} + \frac{Z_{mo}}{Z_1} I_{o2}) \quad (6.8)$$

which is in the form

$$V_a = x\, Z_1\, I_y \quad (6.9)$$

where

$$I_y = I_a + \frac{Z_o - Z_1}{Z_1} I_{o1} + \frac{Z_{mo}}{Z_1} I_{o2} \quad (6.10)$$

Equations (6.6) and (6.9) are in a form similar to equation

(3.32) of chapter 3. The resistance and inductance can be calculated by the methods described previously. The current I_x and I_y are calculated from equation (6.7) and (6.10). The phase angle of coefficients $\frac{Z_{ab}}{Z_{aa}}$, $\frac{Z_{ac}}{Z_{aa}}$, ..., $\frac{Z_{o-}Z_1}{Z_1}$, $\frac{Z_{mo}}{Z_1}$ can be neglected and I_x and I_y may be rewritten as follows:

$$I_x = I_a + K_b I_b + K_c I_c + K_A I_A + K_B I_B + K_G I_G \qquad (6.11)$$

$$I_y = I_a + K_{o1} I_{o1} + K_{om} I_{o2} \qquad (6.12)$$

where now the K_b, K_c,...K_{o1}, K_{om} are scalar values.

Using instantaneous values of voltage and current equation (6.5) may be written:

$$\upsilon_a = xR_{aa}\left(i_a + \frac{R_{ab}}{R_{aa}} i_b + \frac{R_{ac}}{R_{aa}} i_c + \frac{R_{aA}}{R_{aa}} i_A + \frac{R_{aB}}{R_{aa}} i_B + \frac{R_{aG}}{R_{aa}} i_G\right) + X\, L_{aa} \frac{d}{dt}\left(i_a + \frac{L_{ab}}{L_{aa}} i_b + \frac{L_{ac}}{L_{aa}} i_c + \frac{L_{aA}}{L_{aa}} i_A + \frac{L_{aB}}{L_{aa}} i_B + \frac{L_{aG}}{L_{aa}} i_G\right) \qquad (6.13)$$

Putting

$$i_a + \frac{R_{ab}}{R_{aa}} i_b + \frac{R_{ac}}{R_{aa}} i_c + \frac{R_{aA}}{R_{aa}} i_A + \frac{R_{aB}}{R_{aa}} i_B + \frac{R_{aG}}{R_{aa}} i_G = i_x \qquad (6.14a)$$

$$i_a + \frac{L_{ab}}{L_{aa}} i_b + \frac{L_{ac}}{L_{aa}} i_c + \frac{L_{aA}}{L_{aa}} i_A + \frac{L_{aB}}{L_{aa}} i_B + \frac{L_{aG}}{L_{aa}} i_G = i_y \qquad (6.14b)$$

equation (6.13) becomes

$$\upsilon_a = x\, R_{aa}\, i_x + x\, L_{aa} \frac{d}{dt} i_y \qquad (6.15)$$

For a transposed and balanced double circuit line from equations (6.4) the voltage drop using instantaneous value may be written:

$$\upsilon_a = x\, R_1 \left(i_a + \frac{R_{o-}R_1}{R_1} i_{o1} + \frac{R_{mo}}{R_1} i_{o2}\right) + x\, L_1 \frac{d}{dt}\left(i_a + \frac{L_{o-}L_1}{L_1} i_{o1} + \frac{L_{mo}}{L_1} i_{o2}\right) \qquad (6.16)$$

which again can be written in the form of equation (6.15). In this case i_x and i_y are

$$i_x = i_a + \frac{R_o - R_1}{R_1} i_{o1} + \frac{R_{mo}}{R_1} i_{o2} \qquad (6.17a)$$

$$i_y = i_a + \frac{L_o - L_1}{L_1} i_{o1} + \frac{L_{mo}}{L_1} i_{o2} \qquad (6.17b)$$

From equations (6.15) or (6.16) the resistance and reactance can be calculated by the McInnes method. Hence, the single circuit line analysis can be extended to account for the presence of a mutually coupled line by adding extra terms that require knowledge of the currents flowing in the phases of the coupled line. The accuracy of the impedance computation may be maintained by this compensation but greater computation time would be required. In order to obtain the correct faulted line impedance the various line currents and also the self and mutual line impedance terms must not change over the entire distance between the transducers and the fault point. In practical power systems it will be seen that the line current varies and special care might be needed in the application of mutual compensation methods.

6.2.2 Phase faults

For double phase faults between conductors a and b and a three phase fault involving all three conductors of circuit 1, the voltage between the faulty phases for an untransposed line can be written as:

$$V_a - V_b = x\,(Z_{aa} - Z_{ab})\Big[\, I_a + \frac{Z_{ab} - Z_{bb}}{Z_{aa} - Z_{ab}} I_b + \frac{Z_{ac} - Z_{bc}}{Z_{aa} - Z_{ab}} I_c + \frac{Z_{aA} - Z_{bA}}{Z_{aa} - Z_{ab}} I_A + \frac{Z_{aB} - Z_{bB}}{Z_{aa} - Z_{ab}} I_B + \frac{Z_{aG} - Z_{bG}}{Z_{aa} - Z_{ab}} I_G \Big] \qquad (6.18)$$

which is in the form

$$V_a - V_b = x\,(Z_{aa} - Z_{ab}).\ I_x \tag{6.19}$$

where

$$I_x = I_a + \frac{Z_{ab}-Z_{bb}}{Z_{ad}-Z_{ab}} I_b + \frac{Z_{ac}-Z_{bc}}{Z_{aa}-Z_{ab}} I_c + \frac{Z_{aA}-Z_{bA}}{Z_{aa}-Z_{ab}} I_A$$

$$+ \frac{Z_{aB}-Z_{bB}}{Z_{aa}-Z_{ab}} I_B + \frac{Z_{aG}-Z_{bG}}{Z_{aa}-Z_{ab}} I_G \tag{6.20}$$

For a transposed line the voltage between faulty phases is:

$$V_a - V_b = xZ_1\ (I_a - I_b) \tag{6.21}$$

Hence, in this case no extra terms are required to account for the effects of intercircuit mutual coupling, and the conventional delta relaying current $(I_a - I_b)$ and voltage $(V_a - V_b)$ may be used to find the positive sequence impedance xZ_1 of the line using one of the methods described in chapter 3.

Using instantaneous values of voltage and current for an untransposed line equation (6.18) can be written:

$$\upsilon_a - \upsilon_b = x\,(R_{aa}-R_{ab})\Big[\ i_a + \frac{R_{ab}-R_{bb}}{R_{aa}-R_{ab}} i_b + \frac{R_{ac}-R_{bc}}{R_{aa}-R_{ab}} i_c$$

$$+ \frac{R_{aA}-R_{bA}}{R_{aa}-R_{ab}} i_A + \frac{R_{aB}-R_{bB}}{R_{aa}-R_{ab}} i_B + \frac{R_{aG}-R_{bG}}{R_{aa}-R_{ab}} i_G\Big]$$

$$+ x\,(L_{aa}-L_{ab})\,\frac{d}{dt}\Big[\ i_a + \frac{L_{ab}-L_{bb}}{L_{aa}-L_{ab}} i_b + \frac{L_{ac}-L_{bc}}{L_{aa}-L_{ab}} i_c$$

$$+ \frac{L_{aA}-L_{bA}}{L_{aa}-L_{ab}} i_A + \frac{L_{aB}-L_{bB}}{L_{aa}-L_{ab}} i_B + \frac{L_{aG}-L_{bG}}{L_{aa}-L_{ab}} i_G\Big] \tag{6.22}$$

Putting

$$i_a + \frac{R_{ab}-R_{bb}}{R_{aa}-R_{ab}} i_b + \frac{R_{ac}-R_{bc}}{R_{aa}-R_{ab}} i_c + \frac{R_{aA}-R_{bA}}{R_{aa}-R_{ab}} i_A$$

$$+ \frac{R_{aB}-R_{bB}}{R_{aa}-R_{ab}} i_B + \frac{R_{aG}-R_{bG}}{R_{aa}-R_{ab}} i_G = i_x \tag{6.23a}$$

$$i_a + \frac{L_{ab}-L_{bb}}{L_{aa}-L_{ab}} i_b + \frac{L_{ac}-L_{bc}}{L_{aa}-L_{ab}} i_c + \frac{L_{aA}-L_{bA}}{L_{aa}-L_{ab}} i_A + \frac{L_{aB}-L_{bB}}{L_{aa}-L_{ab}} i_B + \frac{L_{aG}-L_{bG}}{L_{aa}-L_{ab}} i_G = i_y \qquad (6.23)$$

equation (5.22) becomes:

$$v_a - v_b = x\,(R_{aa}-R_{ab})\, i_x + x(L_{aa}-L_{ab})\, \frac{d}{dt}\, i_y \qquad (6.24)$$

Similarly for a transposed double circuit line, using instantaneous values, equation (6.21) may be written:

$$v_a - v_b = xR_1(i_a-i_b) + xL_1 \frac{d}{dt}(i_a-i_b) \qquad (6.25)$$

in which no extra terms are required to account for the effects of intercircuit mutual coupling. Equations (6.24) and (6.25) can be solved by the McInnes method.

6.3 BEHAVIOUR OF DISTANCE RELAYS UNDER EARTH FAULT CONDITIONS ON DOUBLE-CIRCUIT LINES

It has been shown that compensation for the effect of mutual coupling between circuits on the impedance measurement may be made for both balanced and unbalanced circuits. When the circuits are unbalanced the amount of computation required in the impedance measurement is far more than for the balanced line, the latter requiring compensation only for ground faults. It may, however, be possible to use the simpler zero sequence compensation for an unbalanced circuit, and allow for or accept the errors that arise. If the inter-circuit mutual coupling is neglected, from equation (6.8) it can be seen that the earth fault relay will overreach when the zero sequence currents in the two circuits are of the opposite sign and it will underreach when the zero sequence currents are of the same sign. If the intercircuit mutual coupling is accounted for, acceptable results are only possible if the amount of mutual coupling and the values of the current flowing in the coupled

circuit are the same over the entire distance between the relaying and fault points. Since the relay relies on information obtained at the relaying point only, this will not be true if the fault is beyond the busbar of the next substation, or on the adjacent mutually coupled line. This can lead to non-selective interruption of the sound line and so it is not always desirable to provide such compensation. On the whole compensation has more drawbacks than advantages and in general it is not applied.

The advantages and drawbacks of intercircuit mutual compensation has been studied by Davison and Wright[67]. Their results are shown in figures (6.3) and (6.4). These figures indicate, that if no attempt is made to compensate distance relays against the effects of inductive mutual coupling on double circuit lines, the effective operating zone of such a relay will be modified to a moderate degree owing to the presence of the second line. There is no risk of a non-selective interruption of the sound line. With mutual compensation applied to normal distance protection, the relays would perform correctly for faults on the circuit with which they are associated. They would, however, measure incorrectly for faults on the adjacent circuit, and would lead to non-selective interruption of it. Hence, if mutual compensation is to be applied, it would have to be applied selectively and for this the peak of the relaying currents in the two circuits might be calculated and compared. If one of the currents is significantly greater in magnitude than the other, the fault would appear to be on that circuit with the greater current, and mutual compensation would be permissible for that circuit but should be avoided on the other. However, for faults at the end

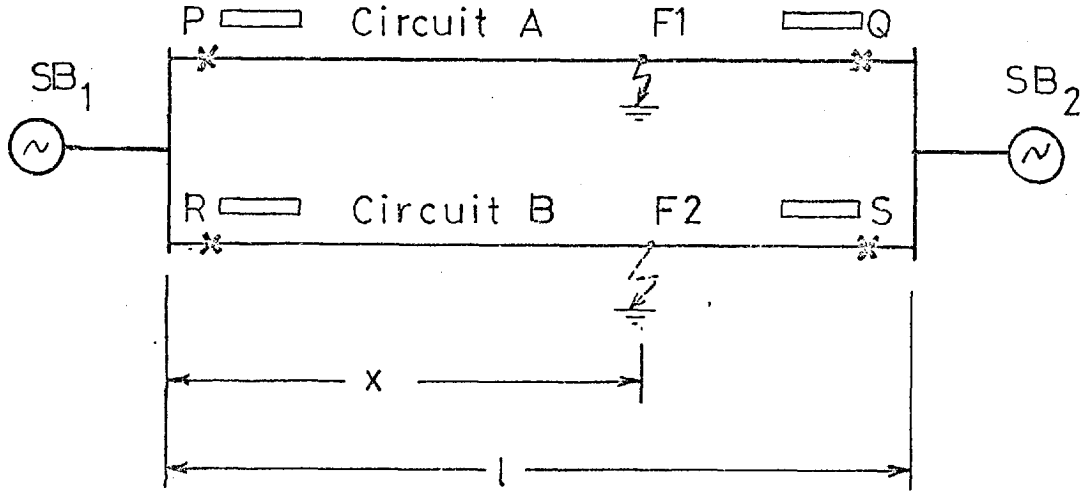

Fig.(6.2) Single line representation of faulted double circuit line

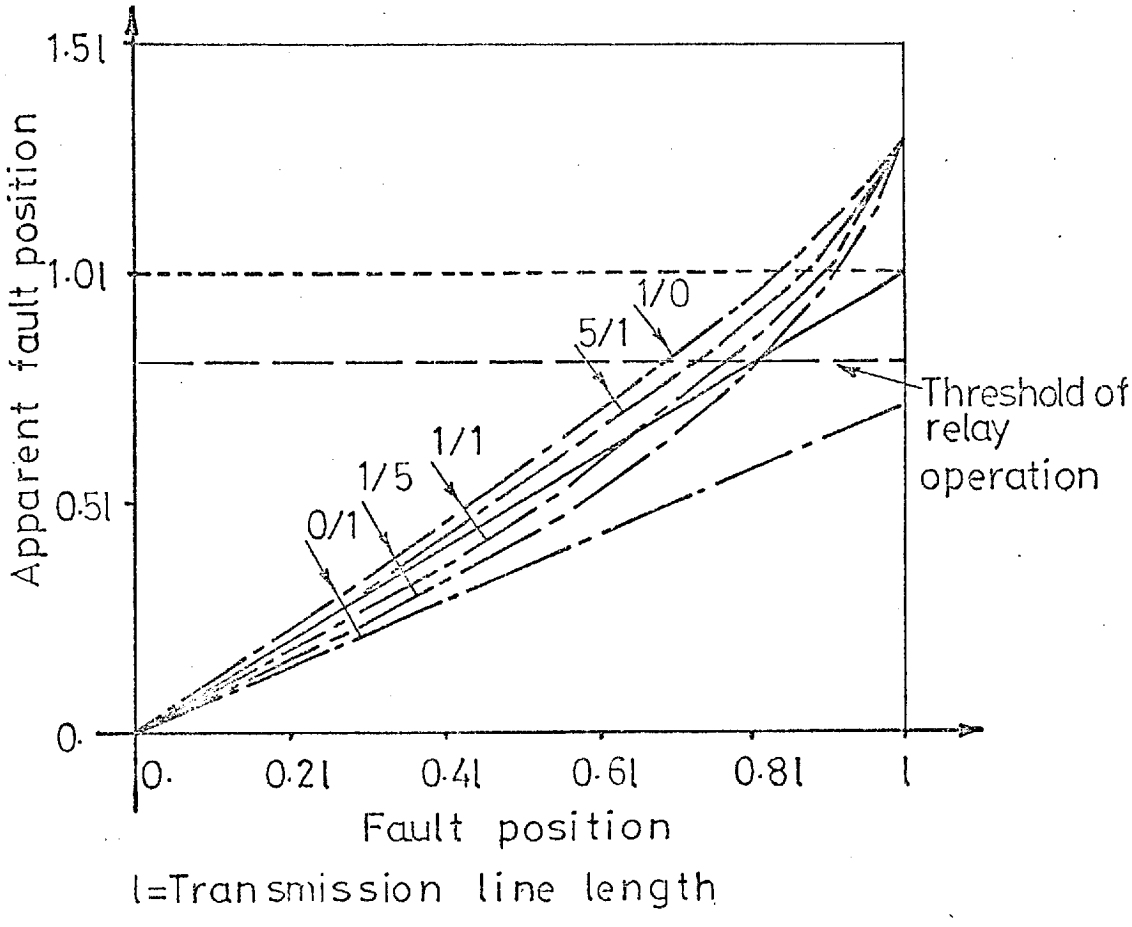

Fig. (6.3) Curves illustrating the distances measured by relay P when fault is on circuit A

———— Ideal relationship and mutually compensated relays

—·—·— Relays without mutual compensation

Numbers on curves indicate the source MVA ratios.

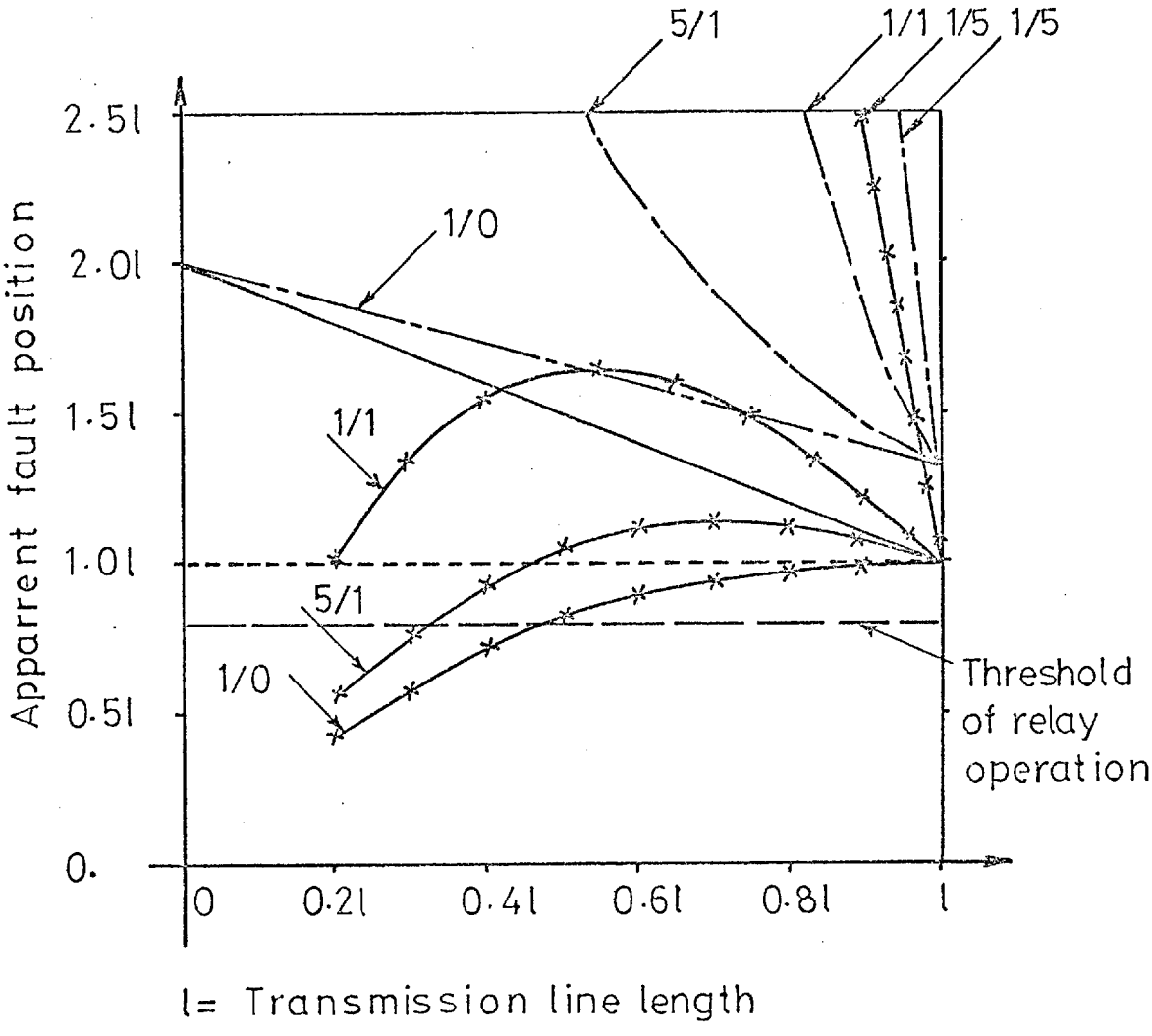

Fig. (6.4) Curves illustrating the distances measured by relay when fault is on circuit A

——————— Ideal relationship

-x-x-x-x-x-x Mutually compensated relays

——·——·——·—— Relays without mutual compensation

Numbers on curves indicate the source MVA ratios.

of the line, the two currents would appear to be approximately equal and in such a case mutual compensation could be safely applied to both circuits. The calculation of the peak of the relaying current in the two circuits would add to the amount of computation required in the impedance measurement and it would make the system more complicated. For this reason, as in analogue relays, neglecting the intercircuit mutual compensation, reducing the zone-reach and using the inter-tripping signal to avoid delay which could be caused by zone-reduction, might be preferable.

6.4 CONCLUSION

For close-up fault protection the sound phase voltage principle was found to be more convenient for digital protection.By this method all types of unsymmetrical close-up faults can be discriminately detected by simple computation involving only two multiplications. A three phase close-up fault ought to be accounted for in the third zone.

For double circuit lines it is better to neglect the intercircuit mutual coupling. In this case the zone length must be reduced, and for the fast removal of the fault at the end of the line, inter-tripping principles should be applied.

CHAPTER 7

ON-LINE TESTS

For research and development purposes,[33,63] the requirement for data acquisition and control of a typical 400 KV mesh substation on the CEGB networks has been chosen. As indicated in figure (7.1), one corner of such a substation has been modelled by setting up 220 V, 3-phase circuits in the laboratory in which the circuit breakers and isolators have been simulated by a three-phase contactor. These are slugged electronically to provide realistic operating times and the control circuitry enables them to be operated from a digital processor. In the mesh corner, full instrumentation is applied by means of voltage and current transducers, but in the remainder of the substation only the status of breakers and isolators is modelled by single phase relays so that the substation configuration can be determined.

In this chapter only the hardware and software which are relevant to the transmission line protection are described and some typical results of the on-line tests are presented.

7.1 HARDWARE

The schematic diagram of the interface, which was used for the tests is depicted in figure (7.2). In the following sections a brief description is given.

7.1.1 Transducers

Signals which are monitored by the computer are current and voltage. The current signals are measured by air cored current transformers (linear couplers). The sensitivity of the linear coupler is about 6mv pp/amp r.m.s. The voltage is

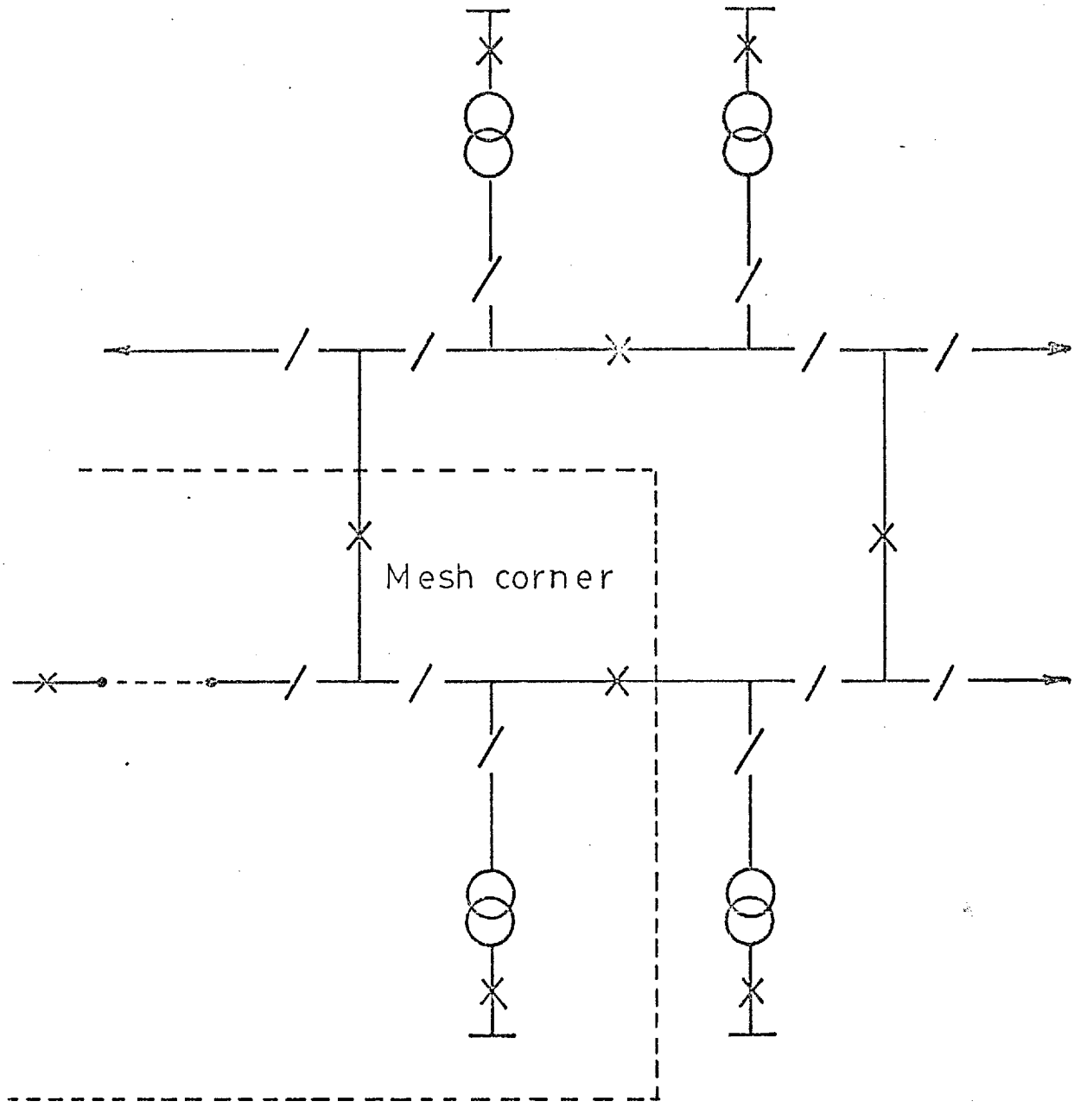

Fig.(7· 1) Mesh type substation layout

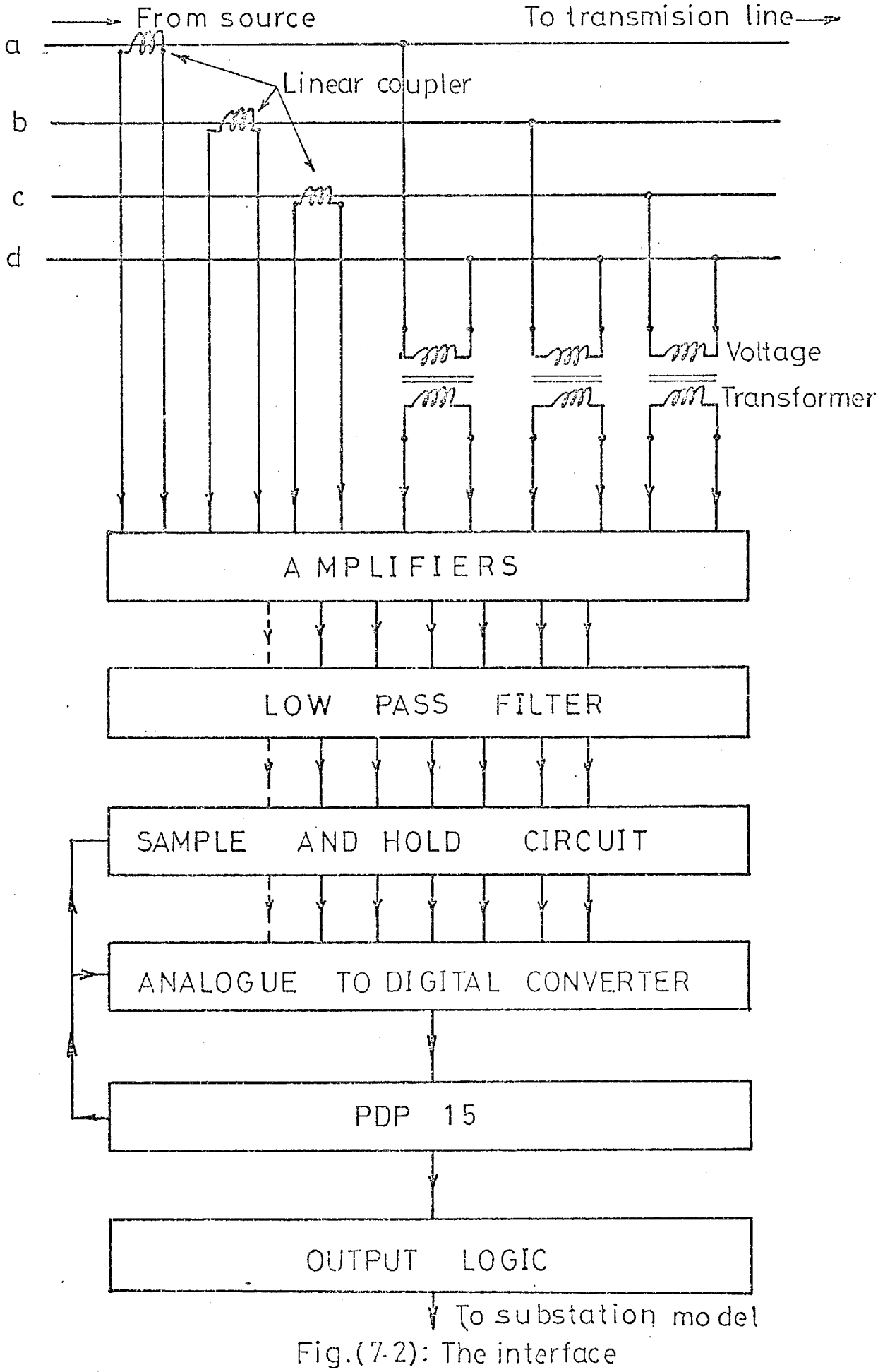

Fig.(7-2): The interface

measured between each phase and neutral as shown in figure (7.2). Since the linear coupler output is proportional to the rate of change of input current, such differentiation leads to the amplification of noise and high frequency components, producing distortion on the output voltage of the linear coupler.

7.1.2 Amplifiers

The maximum voltage that can be applied to the A/D converter is ± 10 volt. It is desired to scale up the signals up to this voltage because in this case more accuracy can be obtained. The fault current on the transmission line is limited to about 10 amp r.m.s. At higher currents the transmission line inductors become saturated and consequently the current becomes distorted. For this maximum current the output of the linear coupler is about 60 mv peak to peak, and so the gain of the amplifier for the linear coupler was chosen to be about 300. Because of improper design, the linear couplers outputs were different for exactly the same inputs. The amplifiers were designed to have variable gains which could be adjusted so that all the linear couplers had the same outputs for the same inputs. The same is true for the voltage transformers for which the amplifier gains was about 1.1 and was mainly used to adjust the inequality in the turn-ratios of the transformers.

7.1.3 Low-pass filters

The low pass filters which are used for current and voltage filtering must be exactly the same, otherwise the phase shift between corresponding voltages and currents would be variable producing a large error in R and X calculations. Linear couplers have been mounted unsymmetrically in the model and because of this the effect of mutual coupling on the yellow phase is

different from the other two phases. This causes the linear couplers to produce slightly different phase shifts which increases the errors of R and X. The filters which were used are simple RC Butterworth filters with single pole and 130 Hz cut-off frequency. The filter resistances are variable and are adjusted until all the linear couplers outputs have the same phase shift.

In chapter 3 it was shown that a second order Butterworth filter with 60 Hz and 150 Hz cut-off are required for the McInnes and Fourier methods respectively. The interface was designed and built before that analysis. At that stage by inspection it was found that a single pole filter with 130 Hz cut-off frequency was necessary to smooth the distorted waveforms of the linear couplers outputs during normal operations. No other criterion was involved in choosing the filter. In this chapter the results of on-line tests with this filter are presented.

7.1.4 Sample and hold circuits[63]

The instantaneous voltage level of the signal was stored in a capacitor before being scanned by the computer. This function was performed by the sample and hold circuit consisting of an analogue switch, a capacitor and a buffer (fig. 7.3). A 1000 pf capacitor was used to store the voltage level and the analogue switch was closed for 5 microseconds to allow the capacitor to acquire the instantaneous voltage level. The capacitor was buffered from the output by a dual FET, and an 741 operational amplifier set at unity gain.

The operation of the analogue switch was synchronised to the scanning of the computer, both controlled by the phase

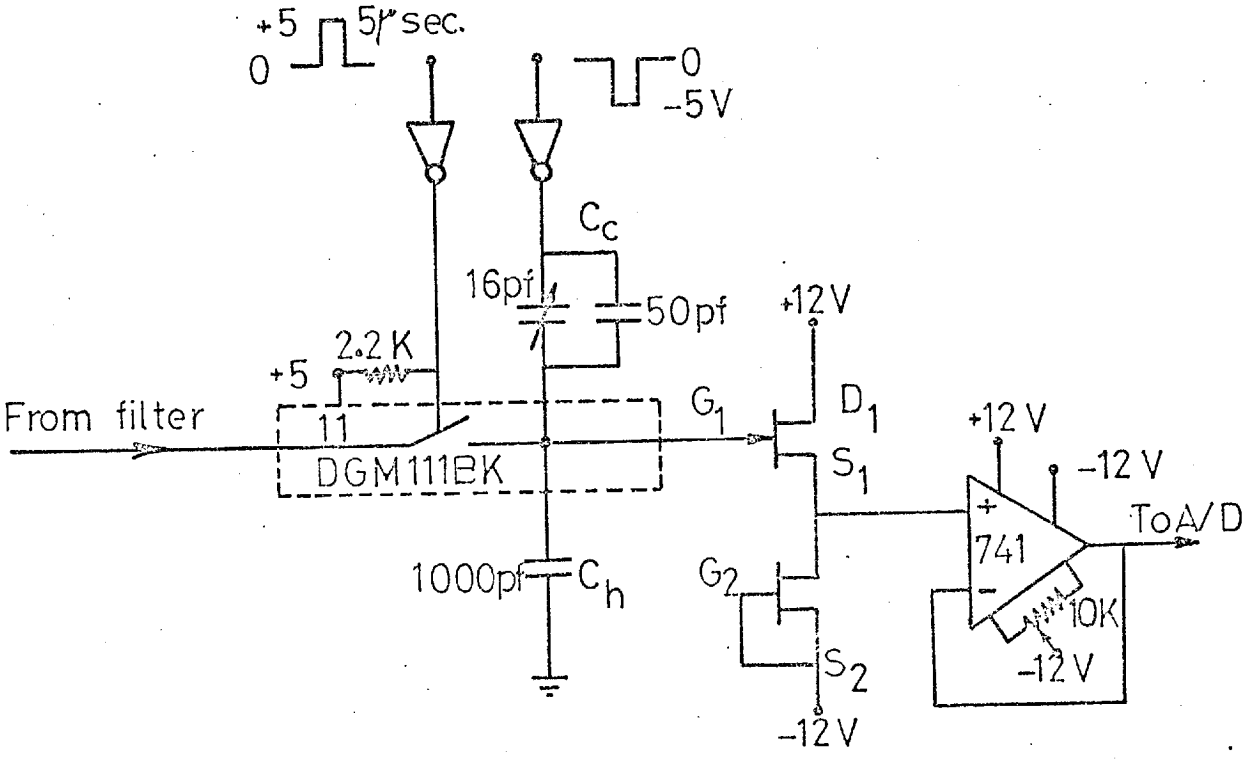

Fig.(7.3) Sample and hold circuit

locked oscillator in the interface. The sampling pulse from the phase locked oscillator was used to trigger a monostable wired to give a 5 microsecond pulse, applied to close the analogue switches. Because there is some capacitance from the gate to the source of the switch, a portion of the gate signal to the switch was coupled through the device on to the holding capacitor c_h. Thus, a slight offset voltage was added to the output when switching from sample to hold. A particular advantage of the operational sample and hold is[63] that the a.c. offset is independent of the analogue signal level. This offset can be compensated by removing a fixed amount of the charge from the holding capacitor upon switching into the hold mode. In Fig. (7.3) the offset is cancelled out by an opposing signal, coupled by C_c from the sample pulse input onto the holding capacitor. The variable capacitor C_c can be adjusted to obtain a zero offset at c_h.

7.1.5 Phase locked oscillator and frequency multiplier

The function of the phase locked oscillator and frequency multiplier (fig. 7.4) is to synchronise the sampling and programmed data transfer to the system frequency. Pulses, which are synchronised (locked) to the system frequency, set the computer program interrupt flag for data transfer and trigger the sampling circuit for system current and voltage sampling.

This circuit consists essentially of a basic phase locked loop (National semeconductors LM565ON phase locked loop) and a frequency multiplier. The filter used in the phase locked loop was a simple low pass filter. The frequency multiplier chain consisted of a binary counter. The counting process

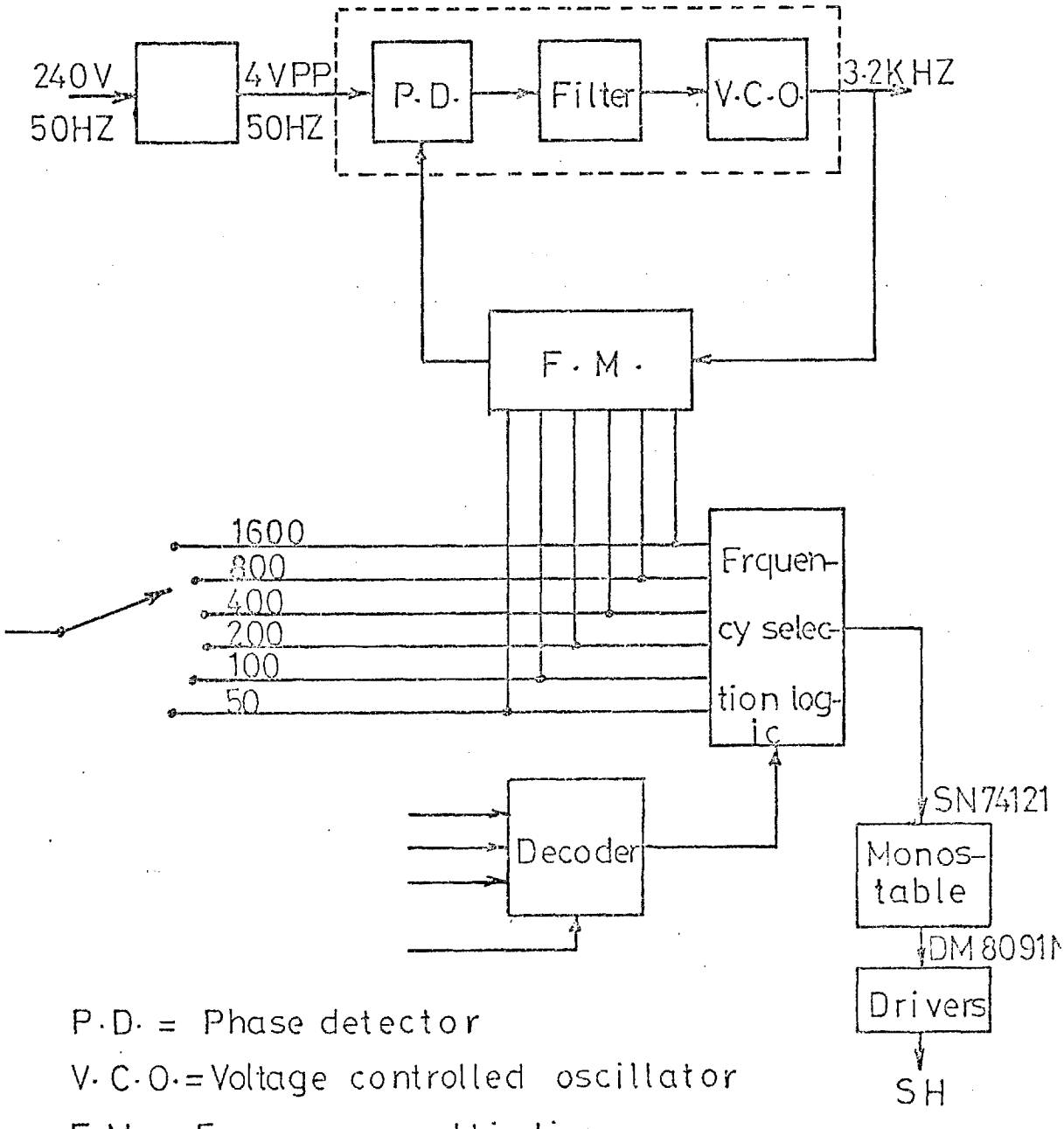

P.D. = Phase detector

V.C.O. = Voltage controlled oscillator

F.M. = Frequency multiplier

Fig.(7.4) Phase locked loop and frequency multiplier

was such that for every 2^6 pulses going into the chain, 1 pulse comes out at the other end of the chain. The phase detector compares the feedback waveform with the reference and produces a voltage signal proportional to their phase difference. The ac component of this signal was removed by the low pass filter and the resulting signal used to control the frequency of the voltage controlled oscillator. The system operated with a steady-state phase error, because the voltage controlled oscillator required a finite input control voltage for its operation. The control voltage at the voltage controlled oscillator changes the frequency in a direction that tends to reduce the phase difference between the reference and feedback signal. The frequency of the voltage controlled oscillator was thus exactly 2^6 times the average frequency of the reference.

Waveforms at 3200 Hz, 1600 Hz, 800 Hz, 400 Hz, 200 Hz, 100 Hz and 50 Hz from the frequency multiplier could be made available through manual or computer controlled switches. These waveforms, through a monostable both operated the analogue switches of the sample and hold and at the same time interrupted the computer program to carry out the pre-programmed functions (for example, data transfer). The computer could be interrupted by setting the interrupt flag by grounding the interrupt line.

7.1.6 Analogue to digital converters

The analogue to digital converter in the PDP15 provided a fast multichannel scanning and conversion facility under program control. Channel selection occured under program control by giving a channel address to the multiplexer control. Conversion accuracy could be pre-selected by setting a 7

position rotary switch. The variation of conversion errors and conversion time with word length is listed in table (7.1) and 10 bit word length was chosen with a conversion time of 18 μsec and conversion accuracy of ±0.1%.

Table (7.1) Conversion time and accuracy of A/D converter

Word lengths No. of bits	Max. conversion error %	Conversion time μs
6	± 1.6	9.
7	± 0.8	10.5
8	± 0.4	12.
9	± 0.2	13.5
10	± 0.1	18.
11	± 0.05	25.
12	±0.025	35.

The A/D converter accepts inputs in the range of -10 +10 volt. Analogue inputs were converted to numbers in the TWO's complement representation.

7.2 SOFTWARE

The sampling rate and interrupt were controlled by programs prepared in Macro 15 language and calculations have deen done in 18 bit TWO's complement integer arithmetic. Both single and double precision arithmetic could be used.

In the multiply and divide subroutines, numbers were entered in two's complement representation and converted to one's complement representation before processing. When multiplication or division was completed, numbers were converted back to two's complement representation before exit.

With the PDP15, two's complement addition of two numbers takes about 1.6 microseconds. Although this computer

has hardware multiplication and division which can perform, the multiplication or division of two integer numbers (in one's complement) in about 3 microseconds, in order to put the numbers in the appropriate address and to convert them to one's complement, and after processing back to two's complement, between 21.3 to 26.1 microseconds to multiply two numbers is required and about 24.8 to 29.6 microseconds to divide them. Multiplication by 2 or 4 is done by shifting the number in the accumulator one or two bits to the left. This takes only 0.8 microseconds. Division by these numbers can be performed by shifting the number one or two bits to the right. As a typical example in Macro 15 programming the subroutine for signed multiplication of two numbers is depicted on the next page.

```
                        /SUBROUTINE FOR MULTIPLICATION OF TWO INTEGERS
                        /HANDLES +VE AND -VE NUMBERS
                        /EXECUTION TIME 21.3 TO 26.1 MICROSECS.
                        /
                        /       C=A.B
                        /
                        /CALLING SEQUENCE
                        /
                        /       LAC A
                        /       JMS* MULT
                        /       LAC B
                        /       DAC C


                                .TITLE MULT
                                .GLOBL MULT
00000 R 000000 A    MULT    Ø
                        /GET SIGN AND MAGNITUDE OF AC (I.E. OF A)
00001 R 664000 A            GSM
                        /SKIP IF LINK = Ø,I.E. A +VE
00002 R 741400 A            SZL
                        /A -VE, ADD 1 TO COMPLETE 2'S COMPLEMENT
00003 R 340017 R            TAD (1
                        /STORE A'S MAGNITUDE(SIGN IN LINK)
00004 R 040012 R            DAC AA
                        /LOAD AC WITH B
00005 R 420000 R            XCT* MULT
                        /INCREMENT MULT SO THAT RETURN IS TO 'DAC C'
00006 R 440000 R            ISZ MULT
                        /SKIP IF AC(=B) +VE
00007 R 741100 A            SPA
                        /B IS -VE AND IN 2'S COMPLEMENT
                        /CHANGE TO 1'S COMPLEMENT(LINK IS UNCHANGED)
00010 R 300020 R            ADD (-2
                        /MULTIPLY
00011 R 657122 A            MULS
                        /A'S MAGNITUDE IS STORED HERE
00012 R 000000 A    AA      Ø
                        /LOAD PRODUCT FROM MQ REGISTER.
00013 R 641002 A            LACQ
                        /SKIP IF +VE
00014 R 741100 A            SPA
                        /-VE CHANGE TO 2'S COMPLEMENT.
00015 R 340017 R            TAD (1
00016 R 620000 R            JMP* MULT
      000000 A              .END
00017 R 000001 A *L
00020 R 777776 A *L
SIZE=00021      NO ERROR LINES
```

7.2.1 Main program

Fig. (7.5) shows the flowchart of the main program which was used for on-line tests. In this program, detection of system abnormalities is achieved by comparing samples of the current cycle with corresponding samples of the previous cycle. Samples of a complete cycle must be stored before this process is initiated.

The program starts with setting counters and API addresses, after which it turns on the program interrupt facility and waits for the first program interrupt. When this interrupt occurs, the system voltages and currents are sampled and stored. Then it waits for the next interrupt. It remains in this phase until samples of a complete cycle are stored. After this the computer is ready to start detection of system abnormalities. Upon receiving the next program interrupt, it samples the system voltages and currents, then compares the voltage samples with the corresponding samples in the previous cycle. If these samples differ by an amount larger than the predefined tolerance limit, the associated fault counters are incremented. If not, the associated fault counters are decremented if they are not already zero. Then the fault counters are examined, and if one of them equals or exceeds 3, the fault classification routine is initiated, otherwise the program waits for the next interrupt. Fault classification is accomplished by analysing the fault counters. A fault diagnostic code is constructed, consisting of 3 binary digits each of which is associated with a fault counter. If a fault counter is equal to or greater than 2, the corresponding bit of the code is set. In this way for each type of fault a unique code is established.

The actual construction of the diagnostic code is as follows. After clearing the accumulator, the fault counters are examined sequentially. If the fault counter under examination equals or exceeds 2, the link is set, otherwise the link is cleared. The content of the link is moved into the least significant bit of the accumulator by rotating the link and accumulator one place to the left. In this way, when all the fault counters are examined, the diagnostic code is formed in the accumulator.

The diagnostic code is micro-programmed into a JMS instruction (jump to subroutine). Execution of the resulting instruction effectively calls the appropriate fault service subroutine to service the fault. After classifying the fault and calling the appropriate fault service subroutine the computer is ready to enter the impedance calculation.

In the fault service subroutine the corresponding terms such as SV,SI ,... or A_V,B_V,... are calculated and then the R and X from the appropriate algorithms are obtained. If these are equal to or smaller than the predifined resistance and reactance of the protected zone, the associated zone counter is incremented, otherwise decremented if it is not already zero. The zone counter is examined and if it exceeds or equals 3 the fault is assumed to exist inside the zone and so the C.B. trip signal is sent, otherwise the program waits for the next interrupt.

In this way after each set of samples the fault is classified repeatedly, and so random false classifications do not cause a wrong decision, but lengthens the overall time delay.

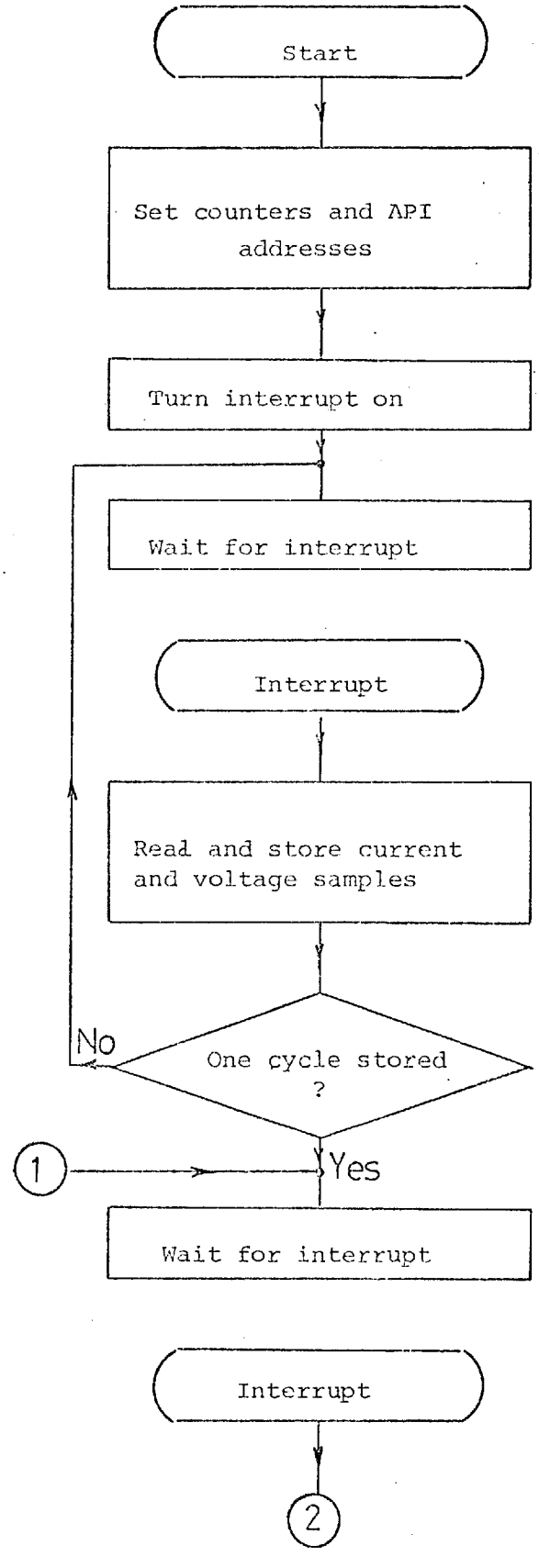

Fig. (7,5) Main program

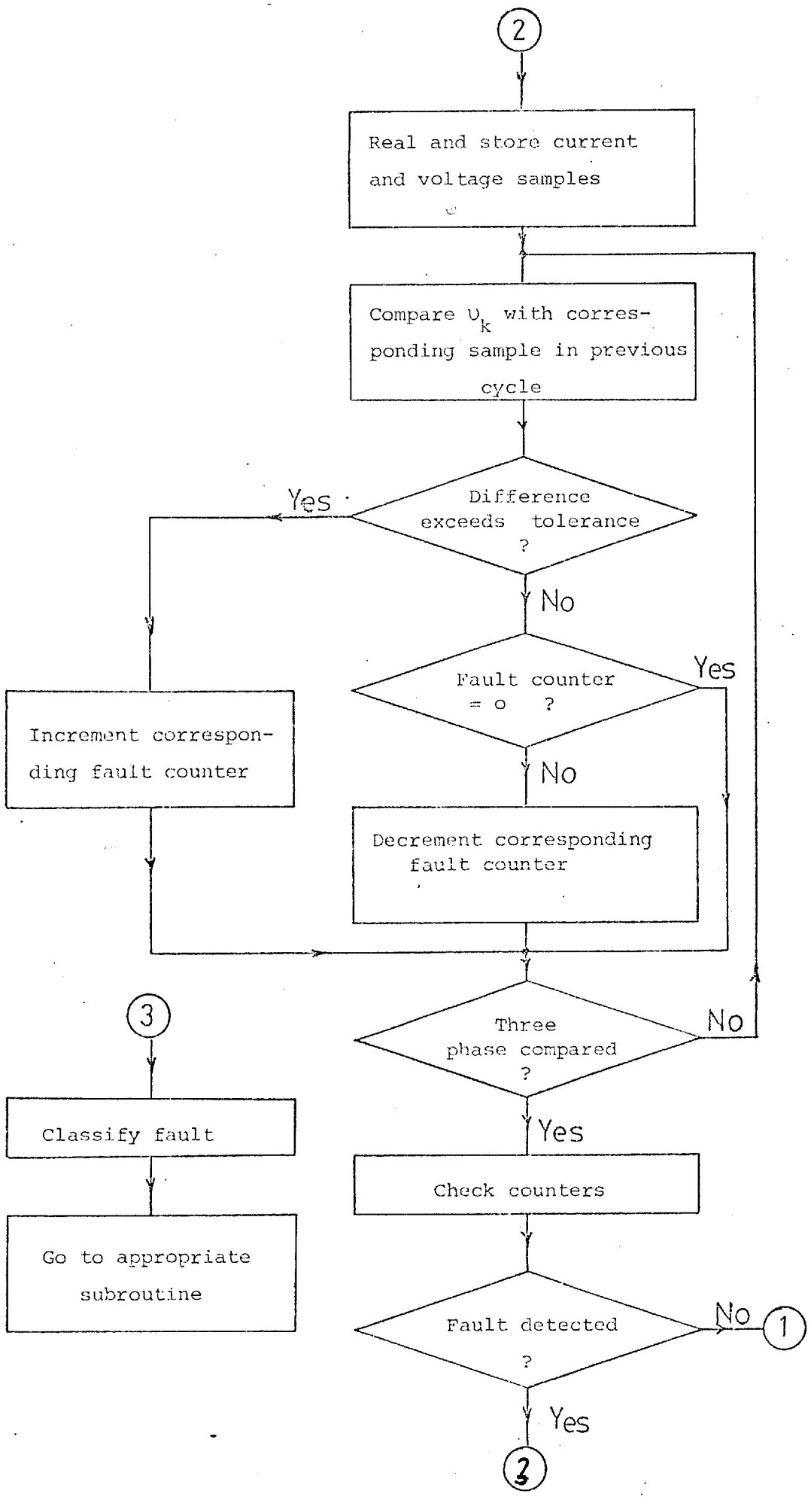

Fig. (7.5) (cont.) Main program

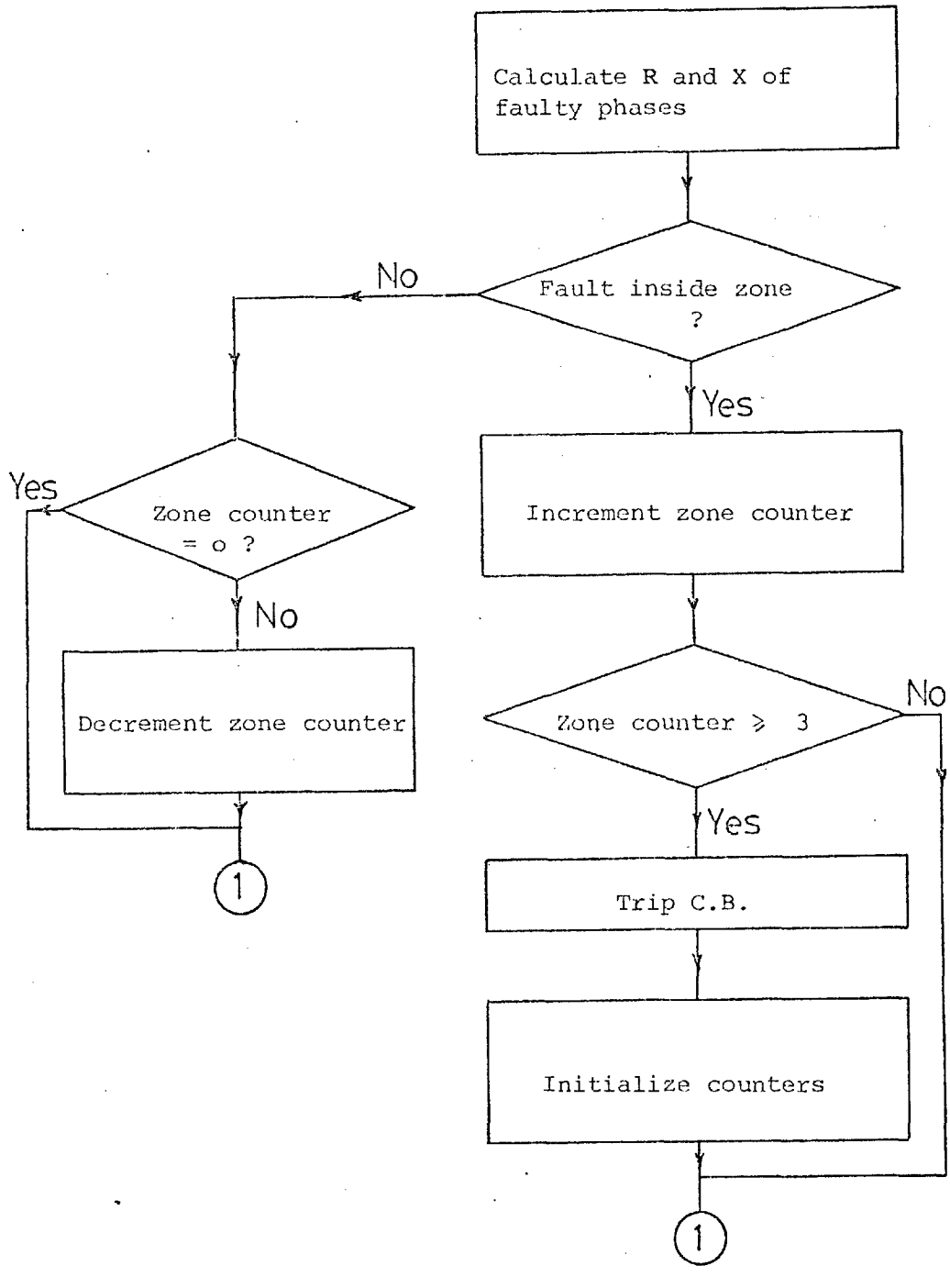

Fig. (7.5) (cont.) Main program
Fault service subroutine

If, after each set of samples, the impedances between each two phases and also between each phase and ground are calculated and compared with predetermined zone impedances, there is no need for voltage monitoring and fault classification. Fig. (7.6) shows the flowchart for this method of protection. The main problem of this method is the lengthy process of calculating 6 impedances which is time consuming and requires a fast hardware and a low sampling rate on this computer. As a typical example table (7.2) shows the calculation time distribution of the impedance calculation by McInnes' method with Simpson's rule and 16 S/C. For single phase faults, the calculation of R and X with their associated terms takes 517.3 microseconds and for phase faults 468.3μS but if the R and X are calculated for all types of faults, the time needed is about 2898μS. To this the necessary time for data acquisition and fault classification and house keeping must be added. Although the A/D conversion time for the 10 bits range is 18 μS the program for conversion and storing every single item of analogue data takes about 46μS. Fault classification takes another 40μS and so with the PDP15 the fault must be classified, and the faulty phase or phases must be found. In this manner only one R and one X needs to be calculated.

Table (7.2) Calculation time (μS) in the McInnes method (Simpson's rule)

Type of fault	SI_1	SI_2	SV1	SV2	R and X	Total
Single phase to earth	107.7	107.7	24	24	253.9	517.3
Phase faults	53.6	53.6	53.6	53.6	253.9	468.3

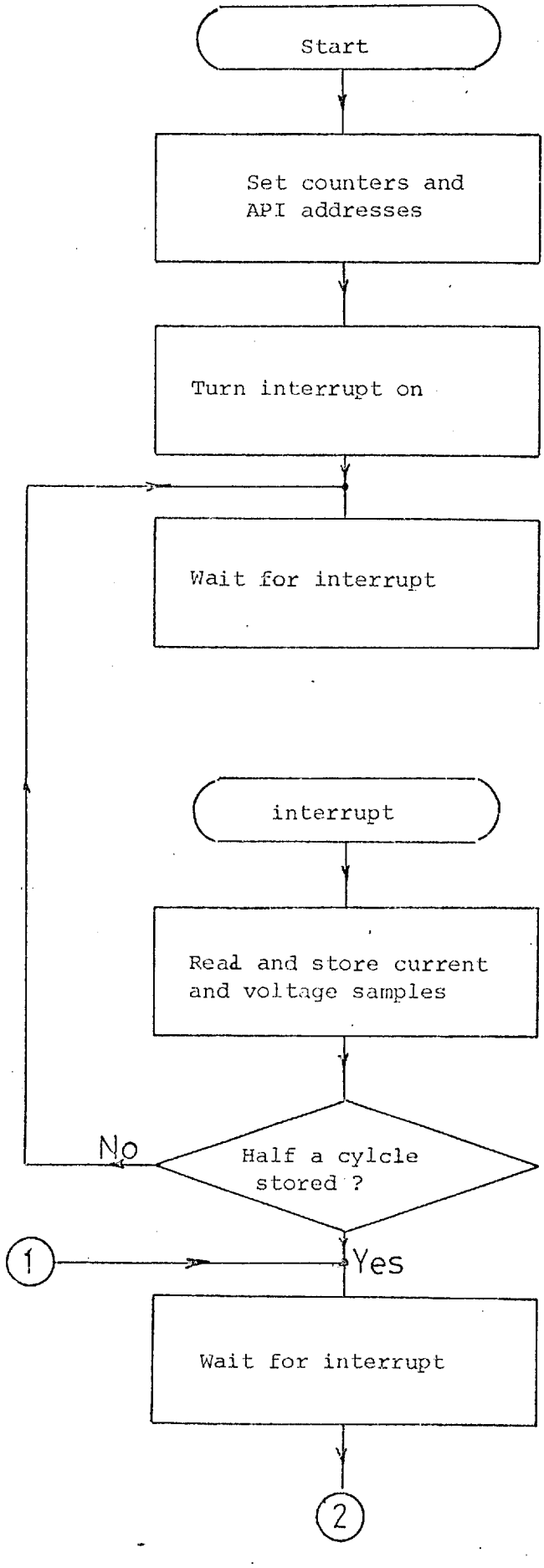

Fig. (7.6) Ideal program

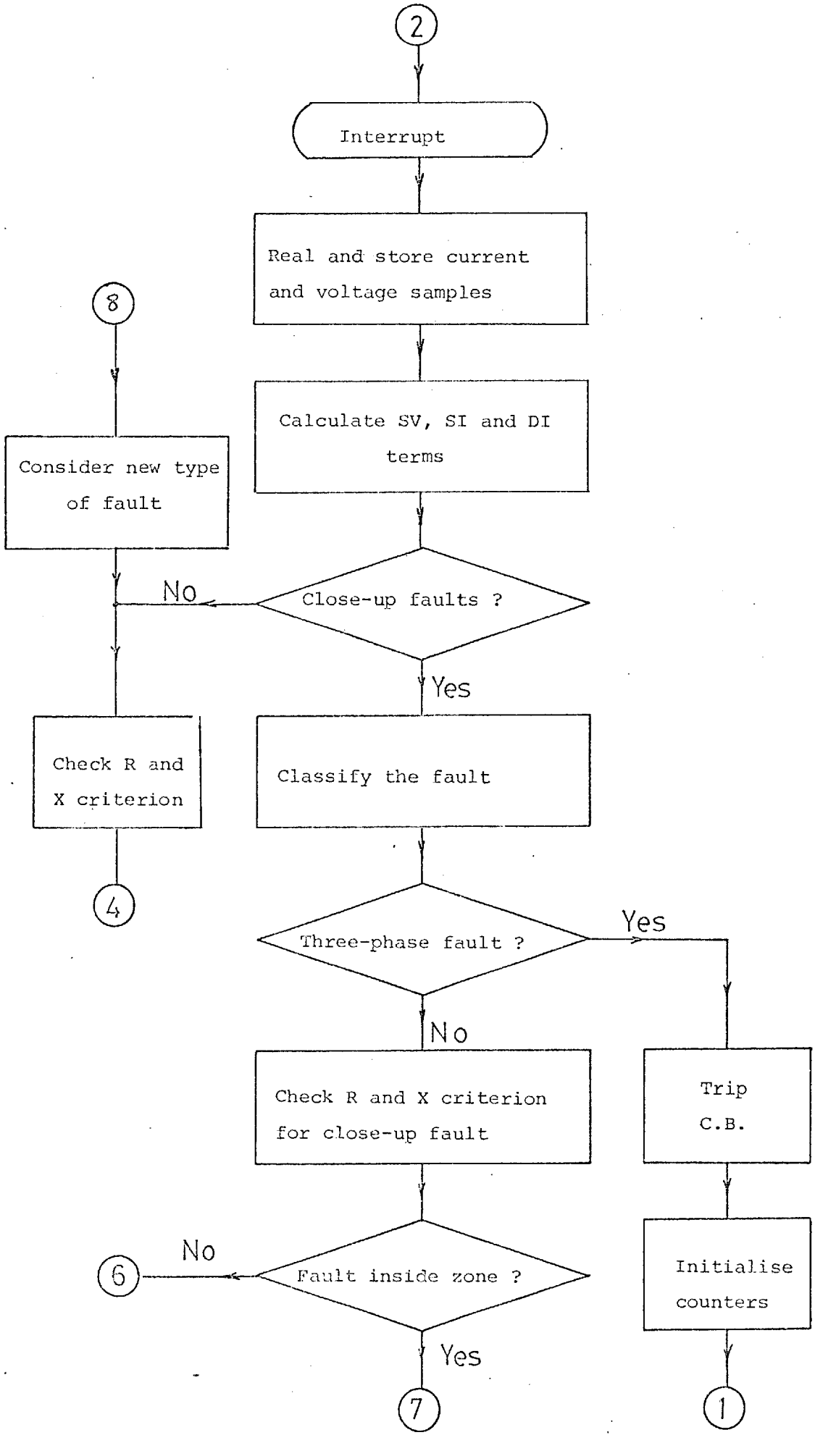

Fig. (7.6) (Cont.) Ideal program

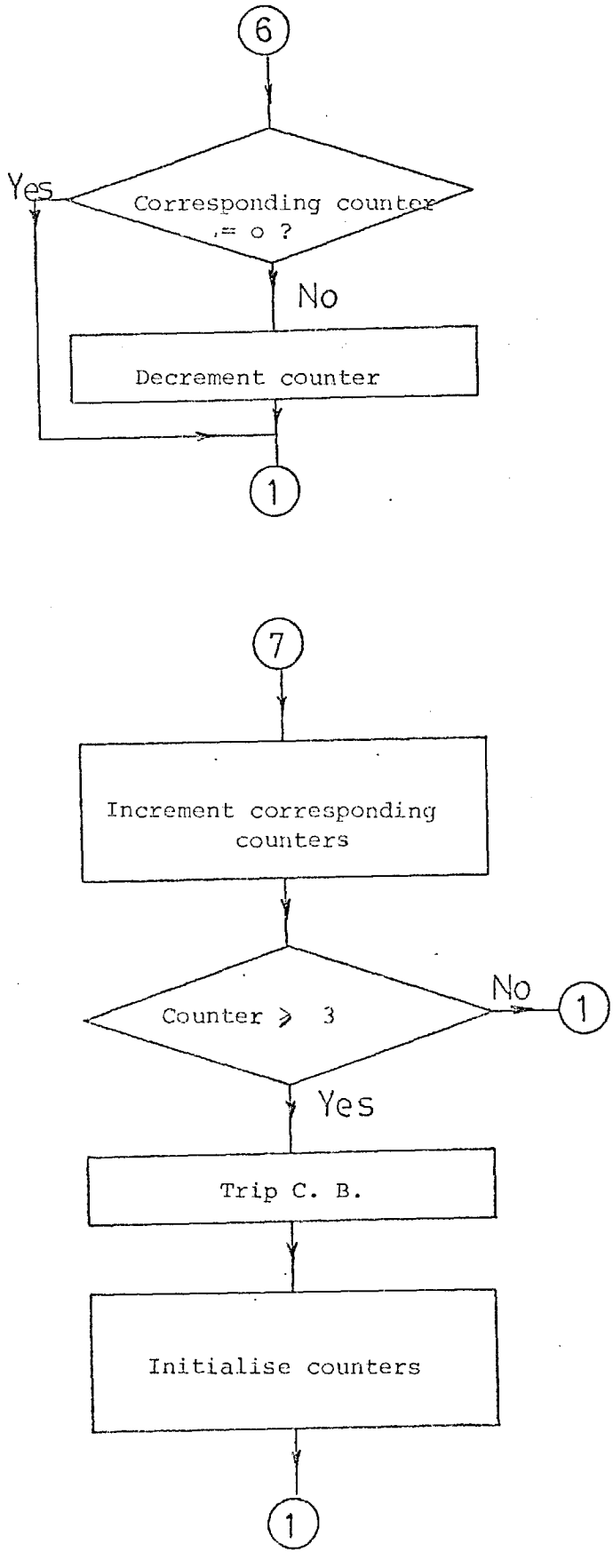

Fig. (7.6) (cont.) Ideal program

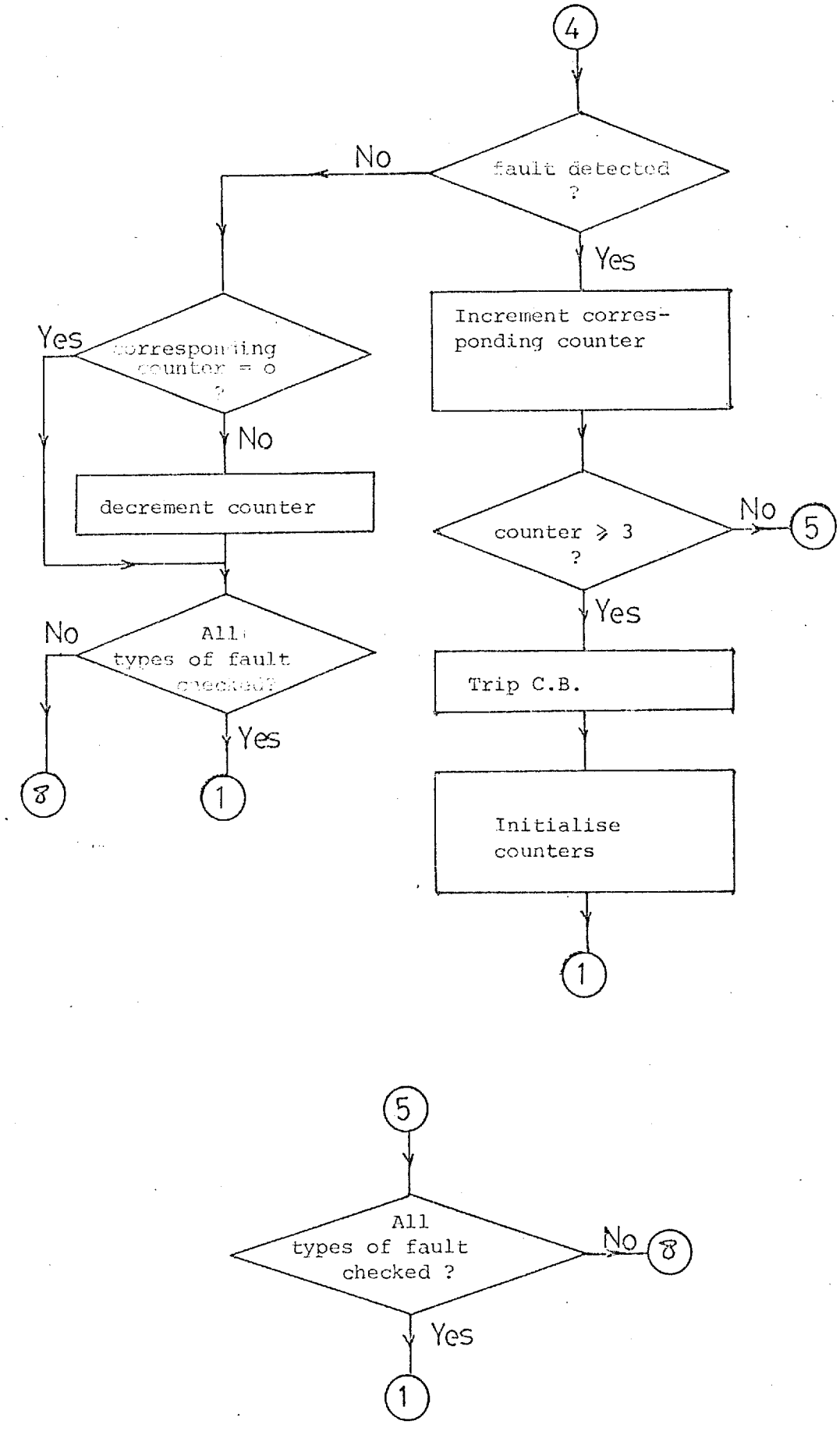

Fig. (7.6) (Cont.) Ideal program

7.3 ON-LINE TEST RESULTS

The model described in Appendix A1 was used to investigate the accuracy of different algorithms on-line. The hardware and software described in this chapter were used to detect the abnormalities on the transmission line and to calculate the reactance and resistance of the faulty phase or phases. Many tests for different types of faults were carried out. Not only were the algorithms tested off-line in chapter 4, re-examined again, but also tests were carried out on the algorithm described by Gilbert and Shovlin[28] who claimed that their method used with a linear coupler could give acceptable accuracy.

Three main sources of error in the impedance calculation, were common for all the algorithms, namely:

i) The reactances of the transmission line model saturated at about 10 amps r.m.s. and made the waveform distorted. These reactances have been assembled quite close together and have a strong mutual effect on each other. This mutual coupling affects the accuracy of R and X calculations in single phase to earth more than in other types of faults.

ii) The linear couplers have been assembled unsymmetrically and very close to each other and so they are affected differently by mutual coupling which causes the model to act as an untransposed transmission line.

iii) The interface shifts both the currents and the voltages. These phase shifts must be the same for all signals, otherwise the ratio between calculated R and X will be changed.

Another very important source of error in the McInnes method (and also Gilbert and Shovlin method) is the d.c. shift

of the current and voltage signals due to the amplifiers and sample and hold circuits etc. Fourier or square wave methods filter out the constant d.c. component in these waveforms and they are therefore not sensitive to any d.c. shifts.

In almost all the tests which were carried out the Fourier method from an accuracy point of view gave the best results. McInnes' method was more accurate than the square wave one. The results of Gilbert's and Shovlin's method were unacceptable.

There were three main reasons why the Fourier method produced greater accuracy than the McInnes method.

i) McInnes' method must be used with a second order, 60 Hz, low pass filter, if good accuracy is desired. A first order, 130 Hz is not suitable for this method.

ii) The linear coupler attenuates the exponential d.c. offset considerably, and consequently removes the main drawback of the Fourier method.

iii) The current and voltage signals had a d.c. shift due to the improper design of the interface. Sample and hold circuits were imperfect and it was not possible to adjust to zero their d.c. off-set. One section of the interface which is used as a part of a larger interface for frequency control research purposes was not under the control of the author. This part of the interface was also responsible for the d.c. offset in the current and voltage signals. The Fourier method can cope with this d.c. shift successfully, but in the McInnes method, this component is integrated and consequently causes the accuracy to be decreased. This d.c. shift can be calculated and accounted for by software, but this increases the computation of impedance.

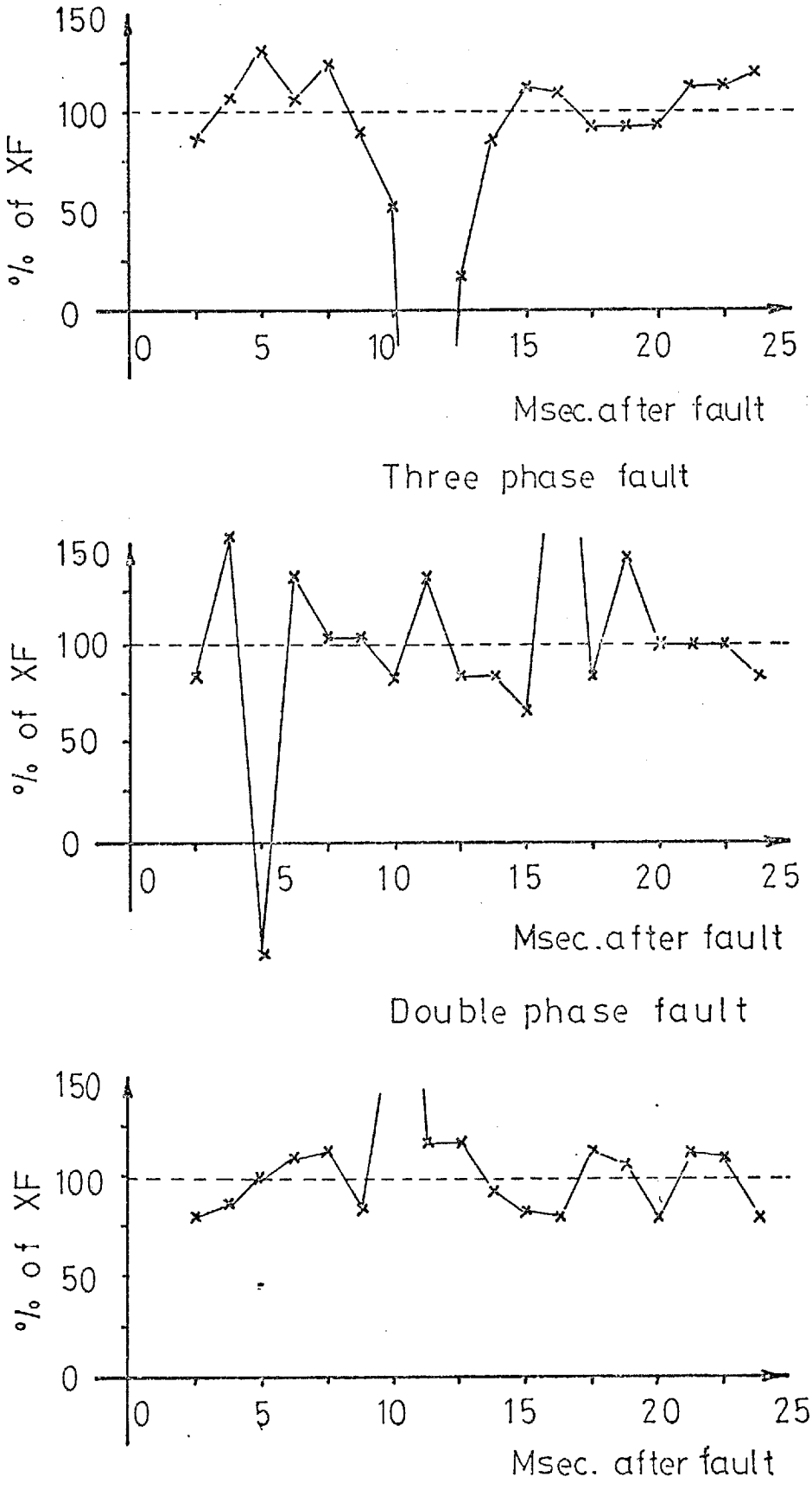

Fig.(7.7) On-line calculated reactance by Shovline method

XF= Actual fault reactance

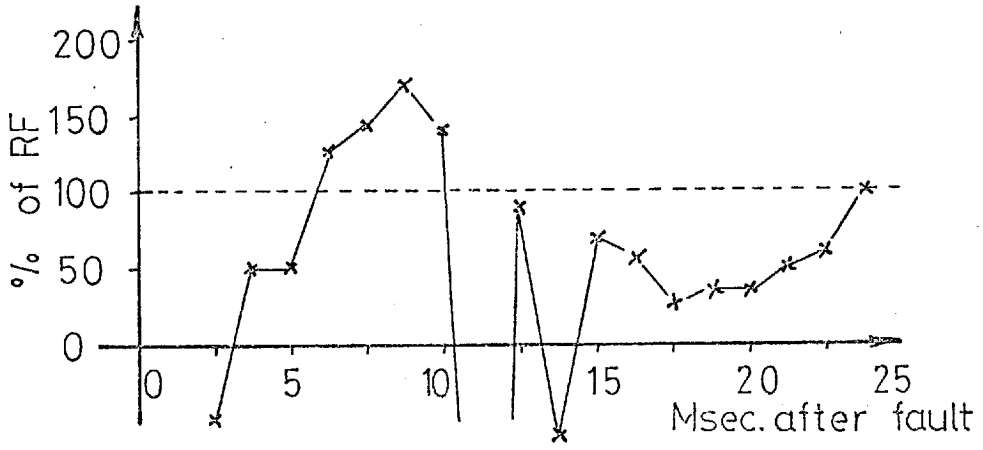

a

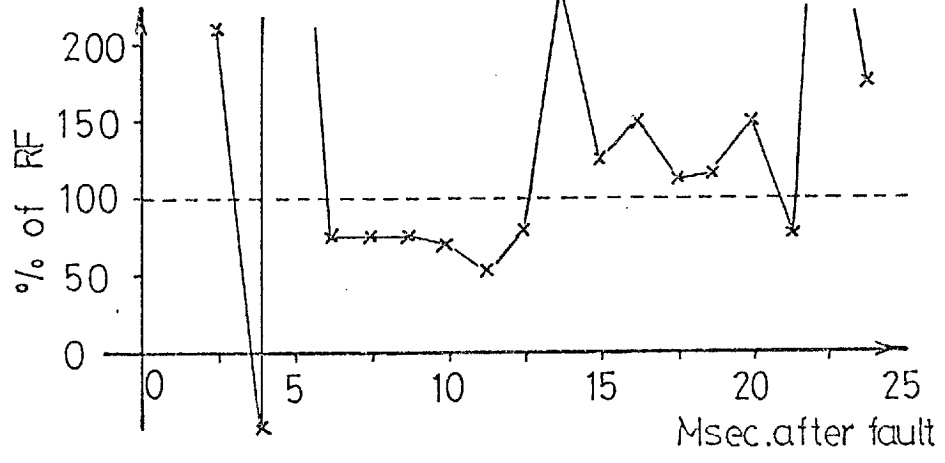

b

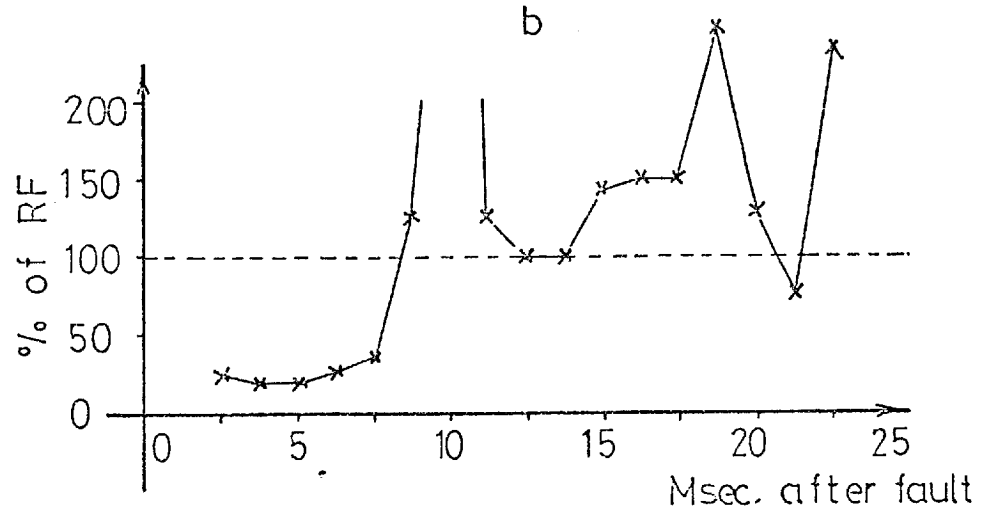

c

Fig.(7·8) On line calculated resistance with Shovlin method

a Three phase fault
b Double phase fault
c Single phase fault

RF = Actual fault resistance

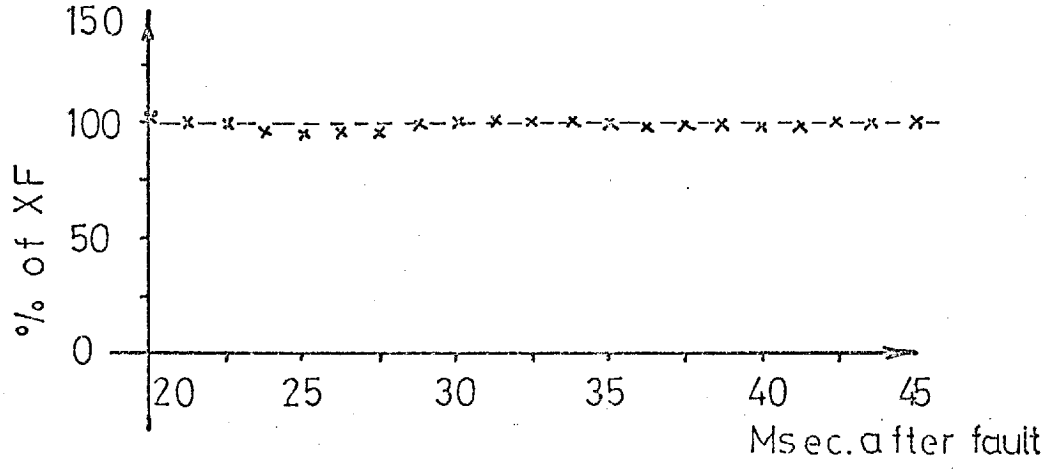

Three phase fault

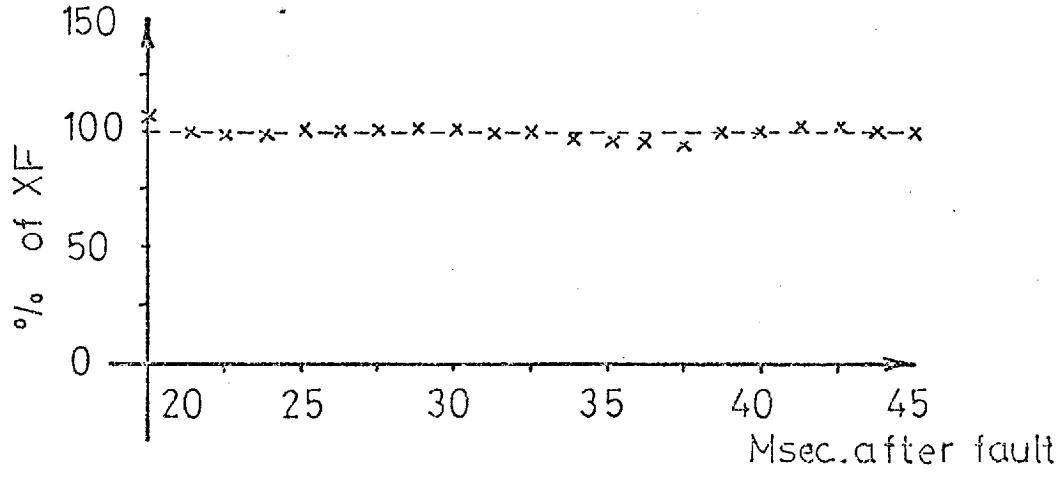

Double phase fault

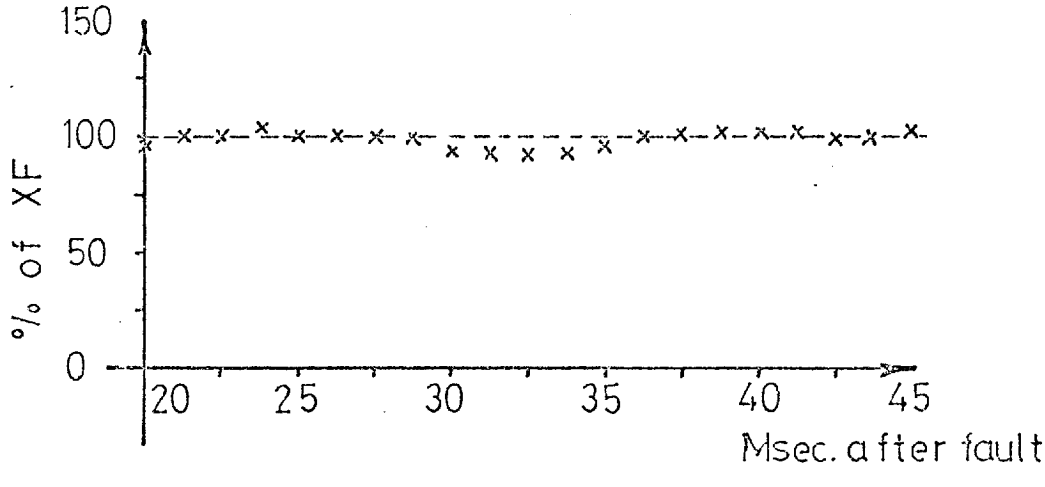

Single phase to earth fault

Fig.(7.9) On-line calculated reactance by Fourie method

XF=Actual fault resistance

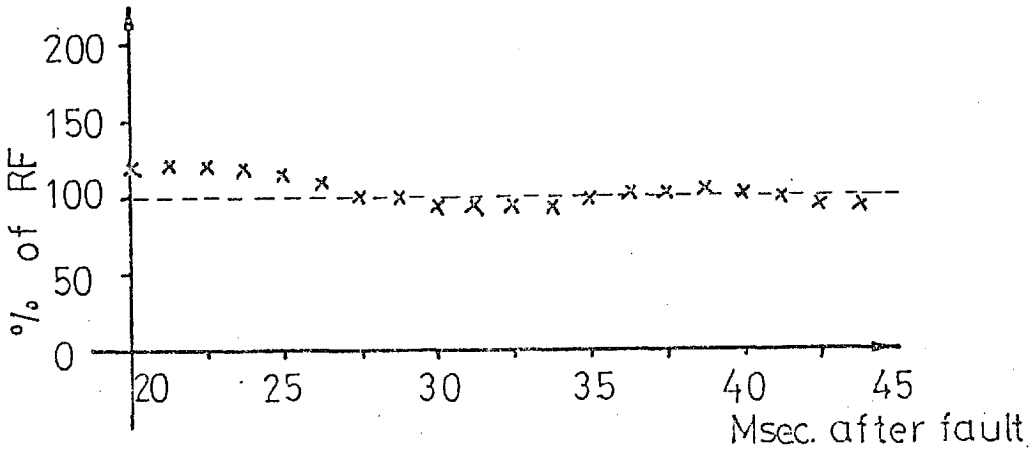

Three phase fault

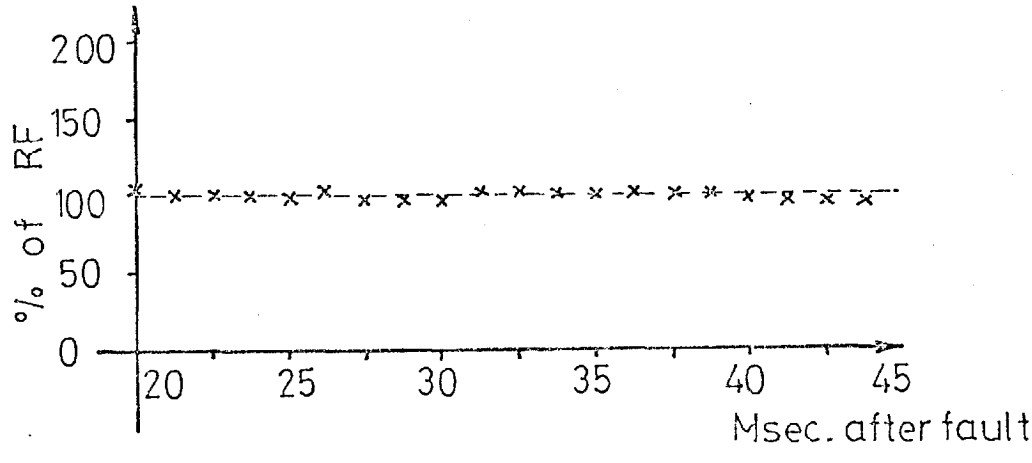

Double phase fault

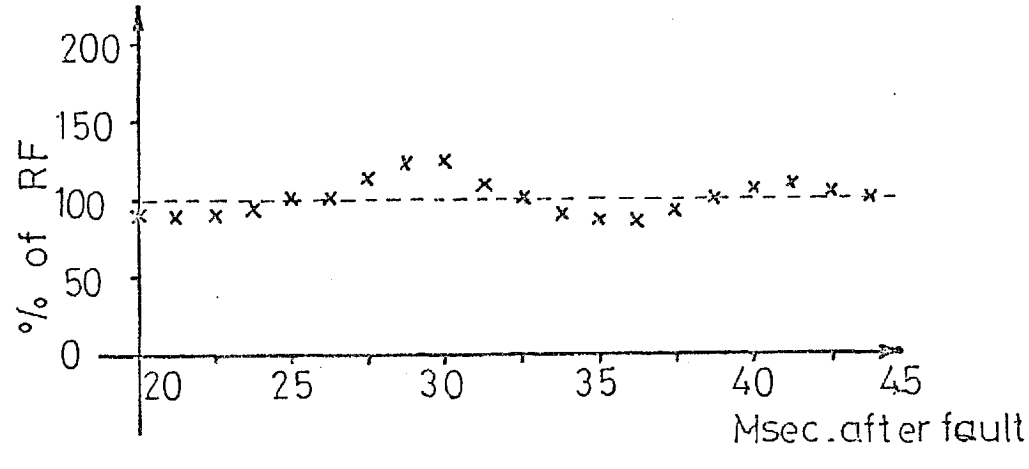

Single phase to earth fault

Fig.(7.10) On-line calculated resistance by Fourier metho

RF= Actual fault resistance

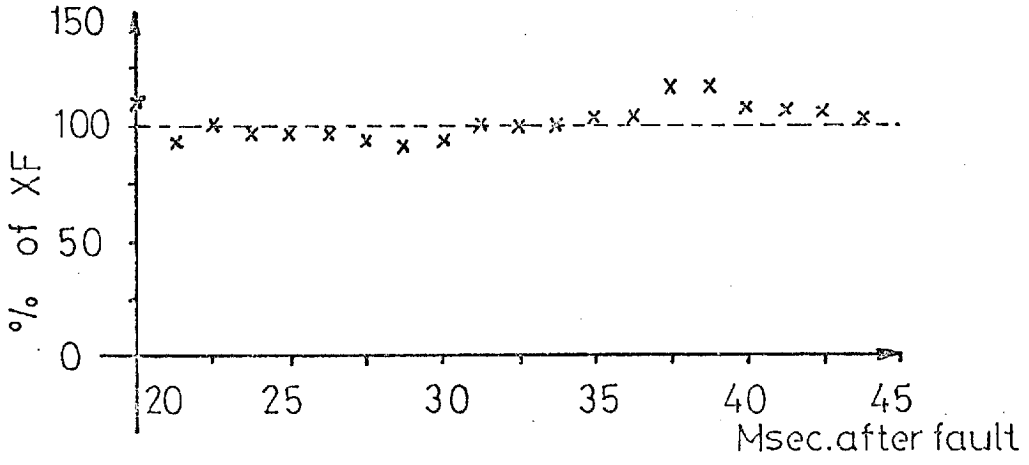

Three phase fault

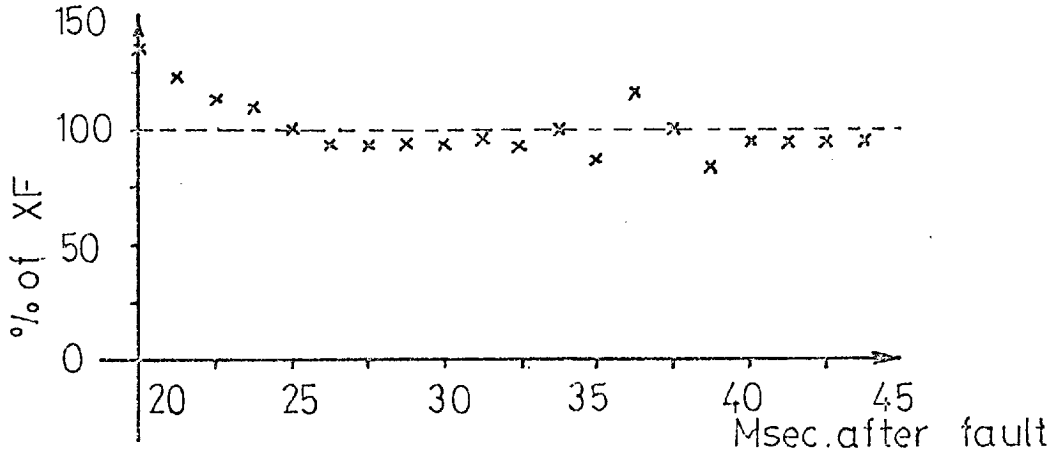

Double phase fault

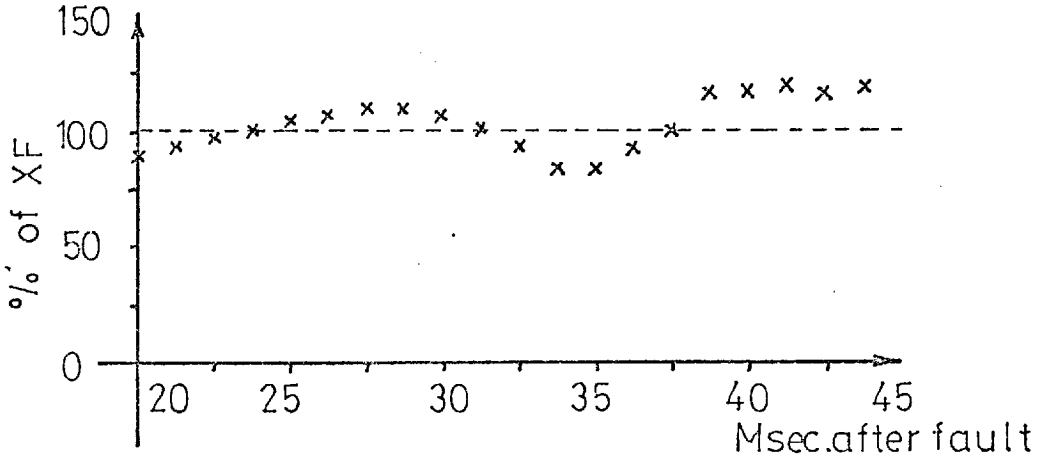

Single phase to earth fault

Fig.(7.11) On-line calculated reactance by square wave method
XF = Actual fault reactance

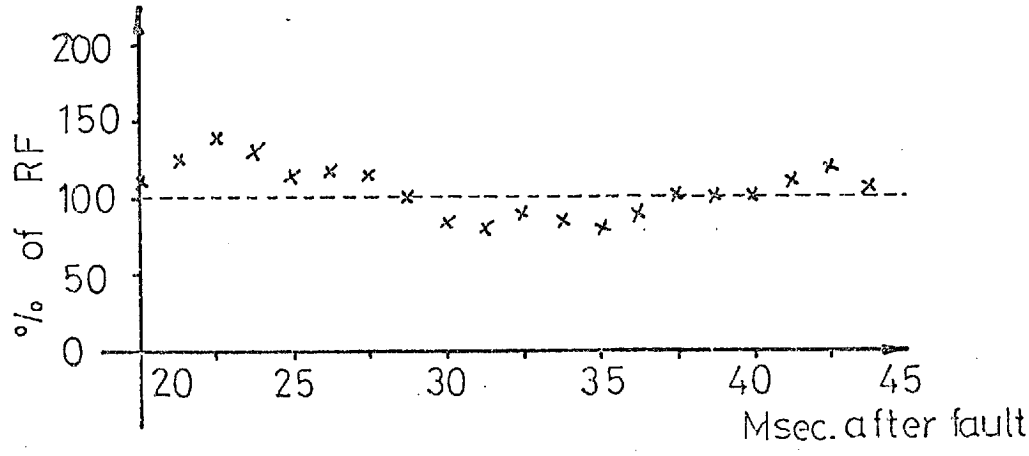

Three phase fault

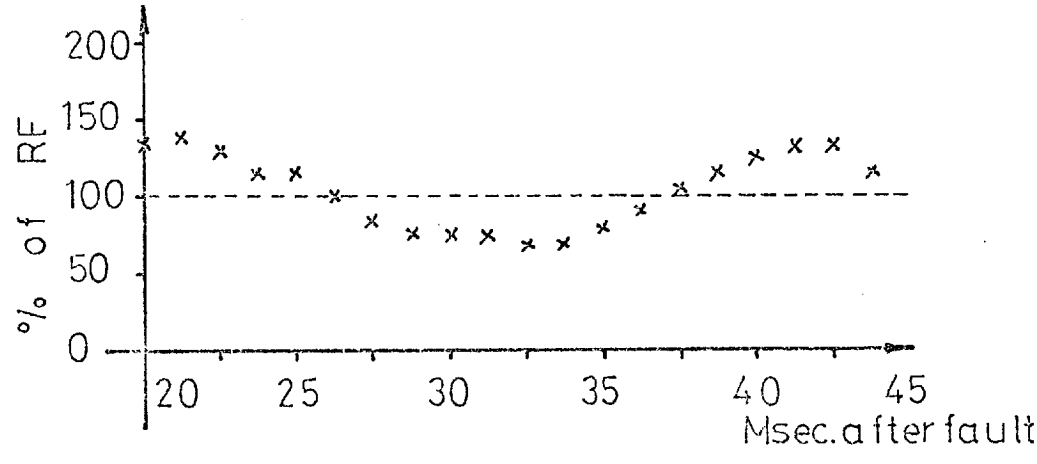

Double phase fault

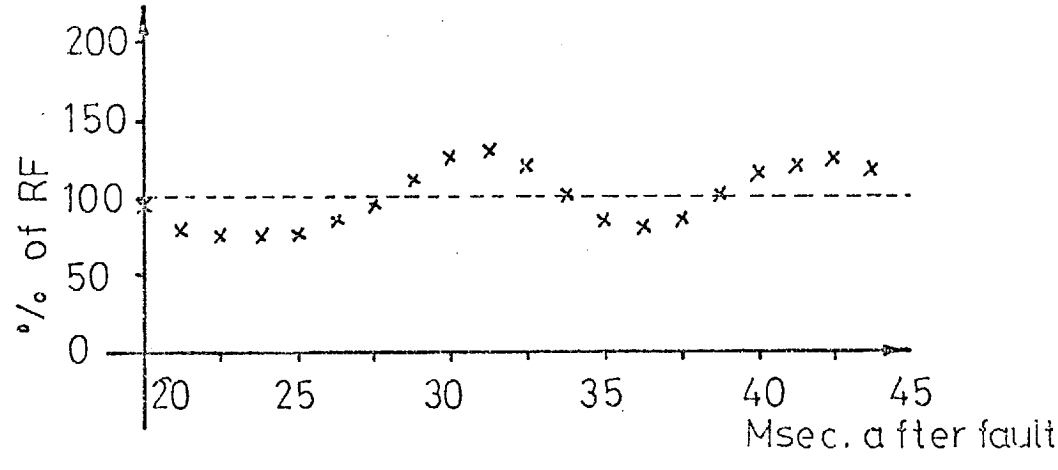

Single phase to earth fault

Fig.(7.12) On-line calculated resistance by square wave method

RF= Actual fault resistance

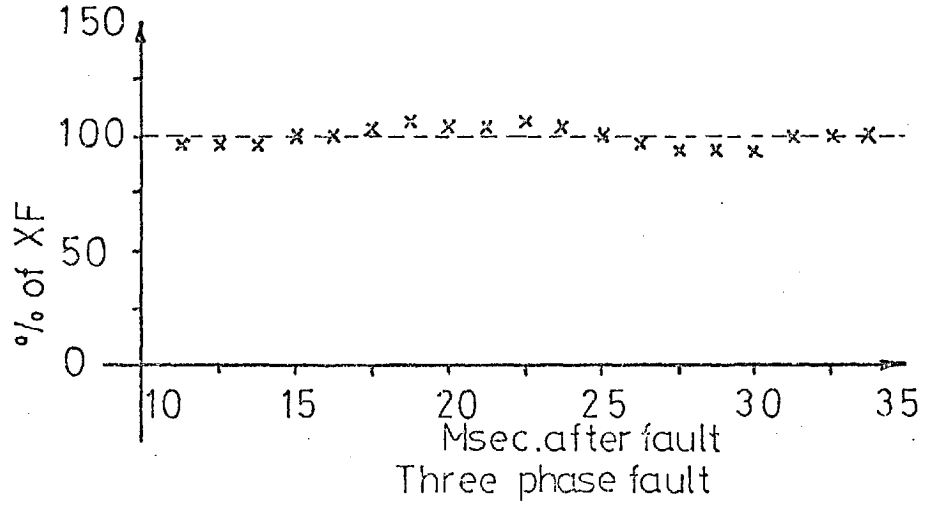

Three phase fault

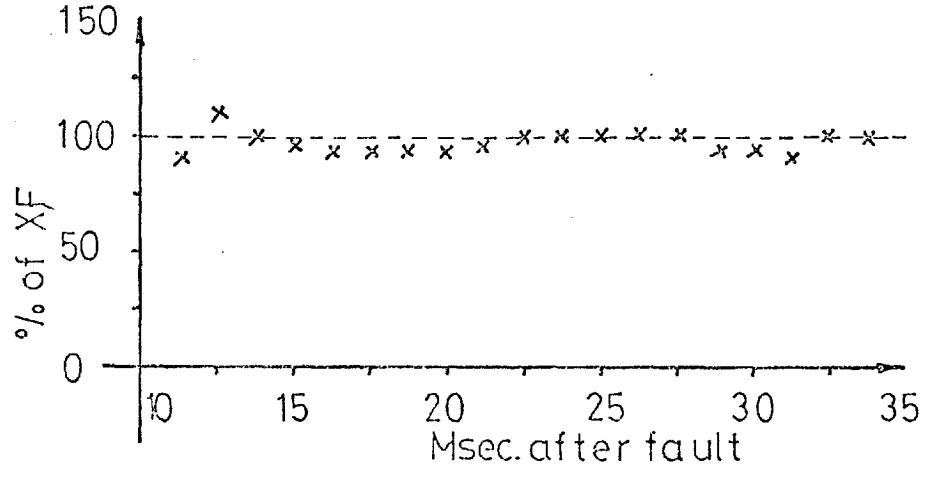

Double phase fault

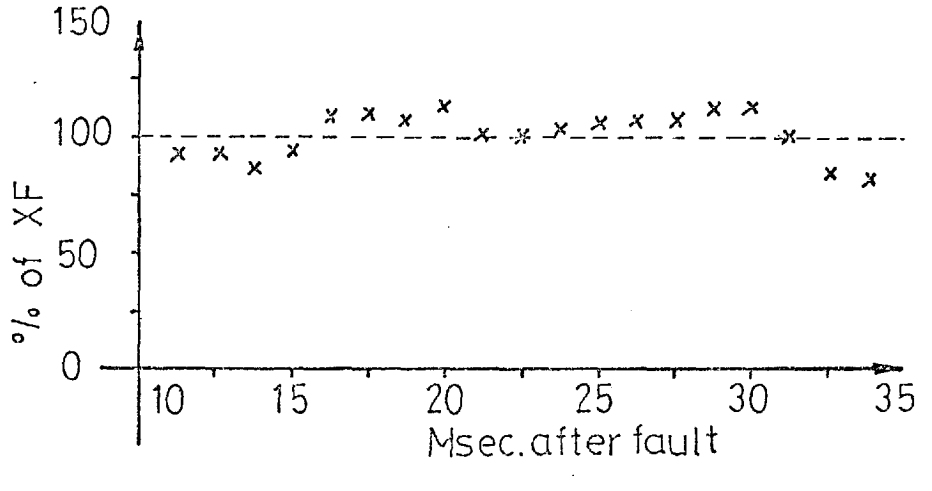

Single phase to earth fault

Fig.(7.13) On-line calculated reactance by McInnes method

XF = Actual fault reactance

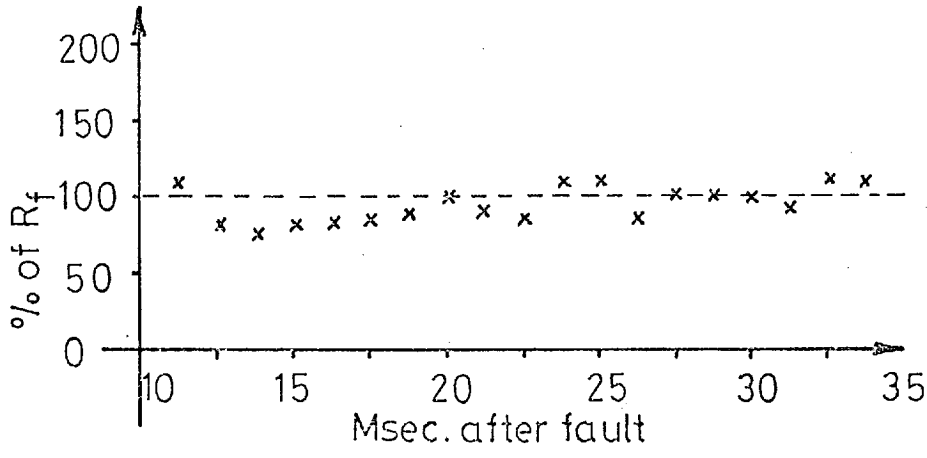

Three phase fault

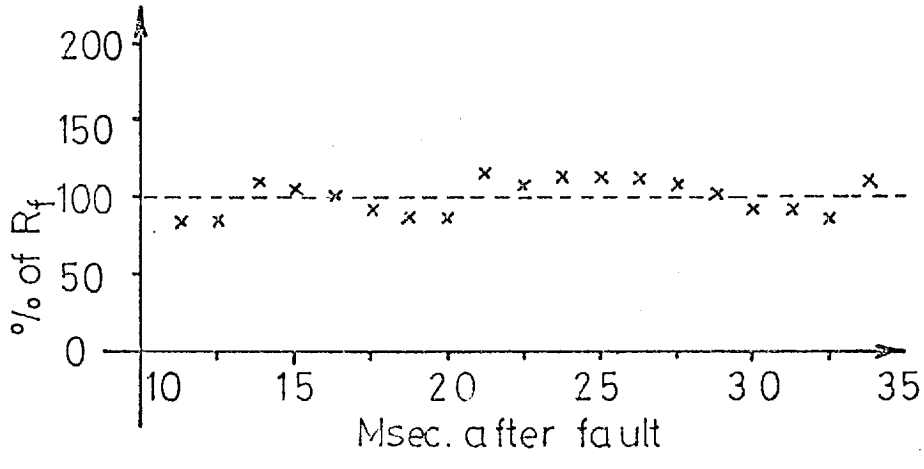

Double phase fault

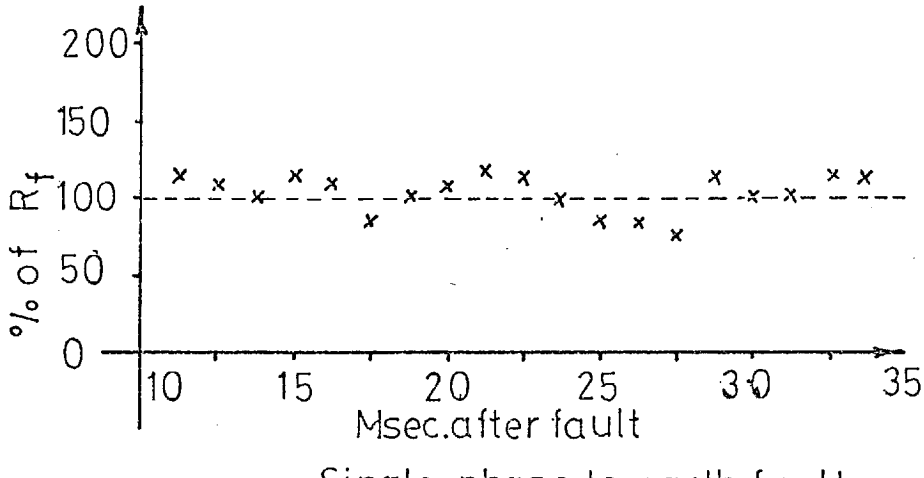

Single phase to earth fault

Fig. (7·14) On-line calculated resistance by McInnes method

R_f =Actual fault resistance

Figures (7.7) to (7.14) show some typical results for the different algorithms, and table (7.3) shows the mean deviation of these results from the true values.

Table (7.3) Mean deviation of resistance and reactance

Algorithms	M.D. of R %			M.D. of X %		
	S.P.F.	D.P.F.	T.P.F.	S.P.F.	D.P.F.	T.P.F.
Fourier method	9	2	6.5	2.4	1.3	1.1
Square wave method	17	22	14	9.6	9.3	5.6
McInnes method	11	11	10.8	8.2	4	3.1

M.D. = Mean deviation
S.P.F. = Single phase to earth fault
D.P.F. = Double phase fault
T.P.F. = Three phase fault

Figures (7.15) to (7.17) show the traces of R and X values during the fault. In most experiments McInnes' method was faster than the Fourier or square wave methods.

In off-line tests it was shown that by increasing the sampling rate, the accuracy of the McInnes method increases. In on-line tests the accuracy of this method for 8 and 16 S/C was almost the same because of the considerable attenuation of the exponential d.c. off-set by the linear coupler. For the Fourier and square wave methods, the results for different S/C were also the same. Also the Fourier method with exact and approximated coefficients, had almost the same results. From simplicity point of view McInnes' method was simpler than both the Fourier and square wave methods.

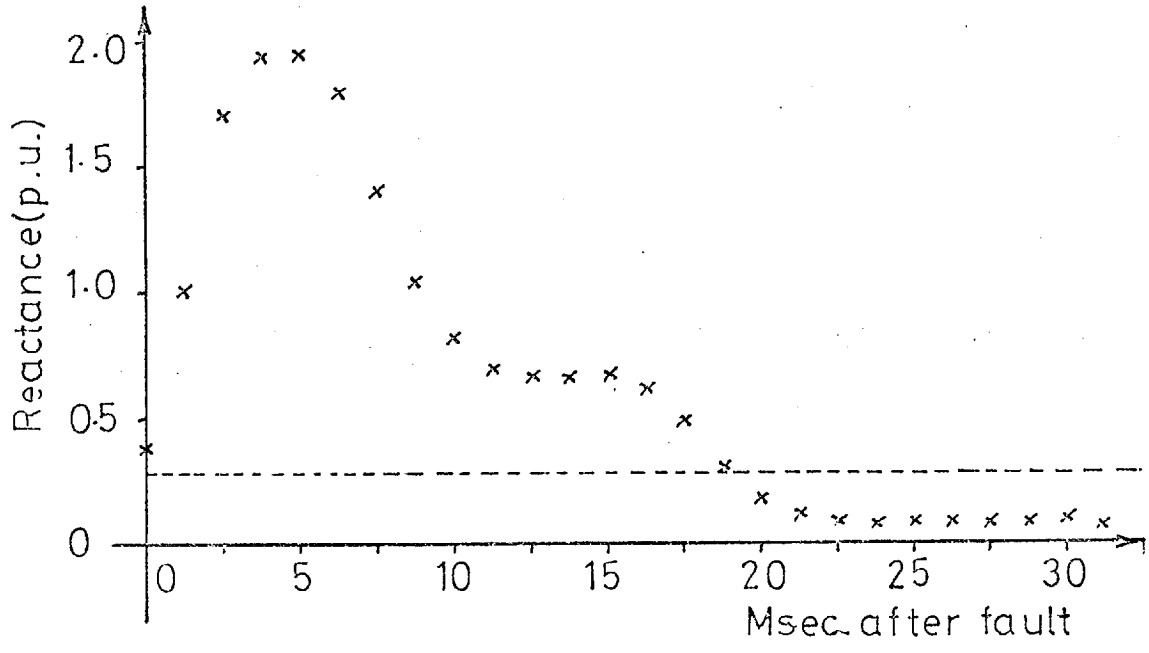

a
Three phase fault

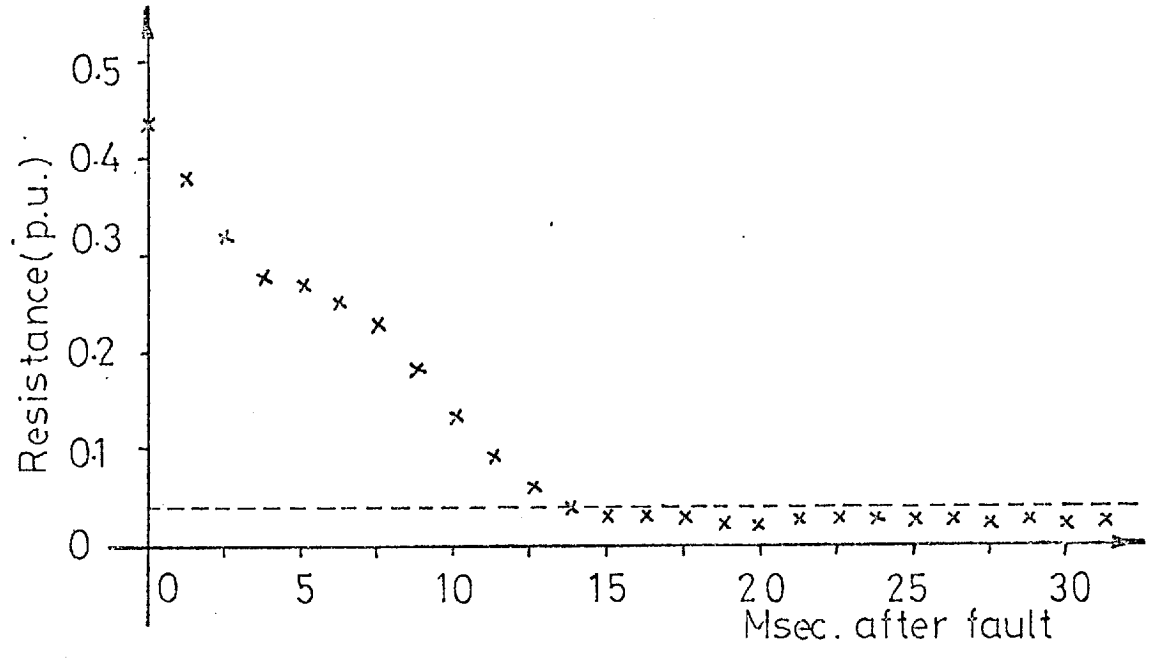

b

Fig.(7.15) On-line calculated X and R
by Fourie method
a Reactance
b Resistance

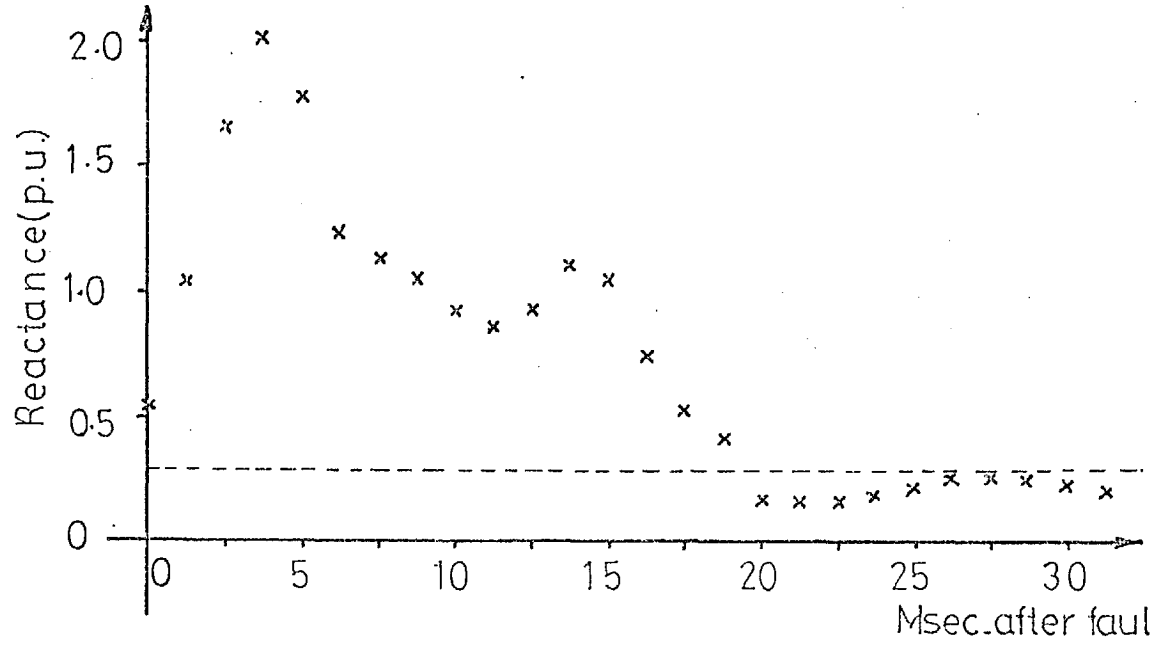

a

Three phase fault

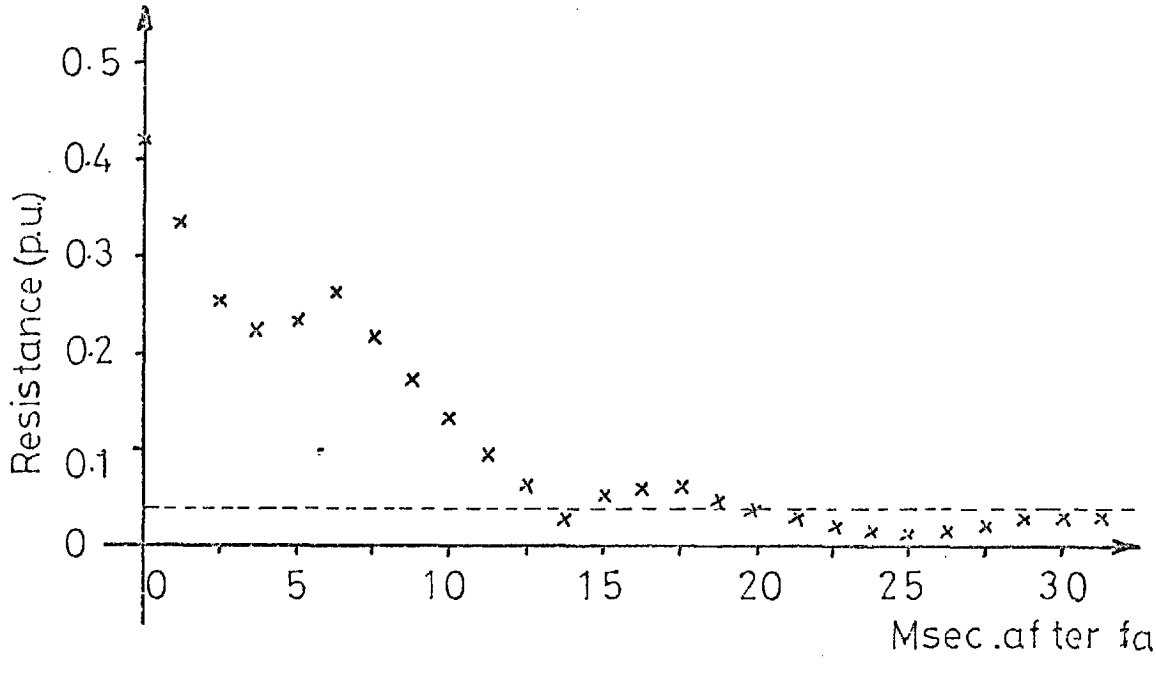

b

Fig.(7·16) On-line calculated X and R by square wave method

a Reactance

b Resistance

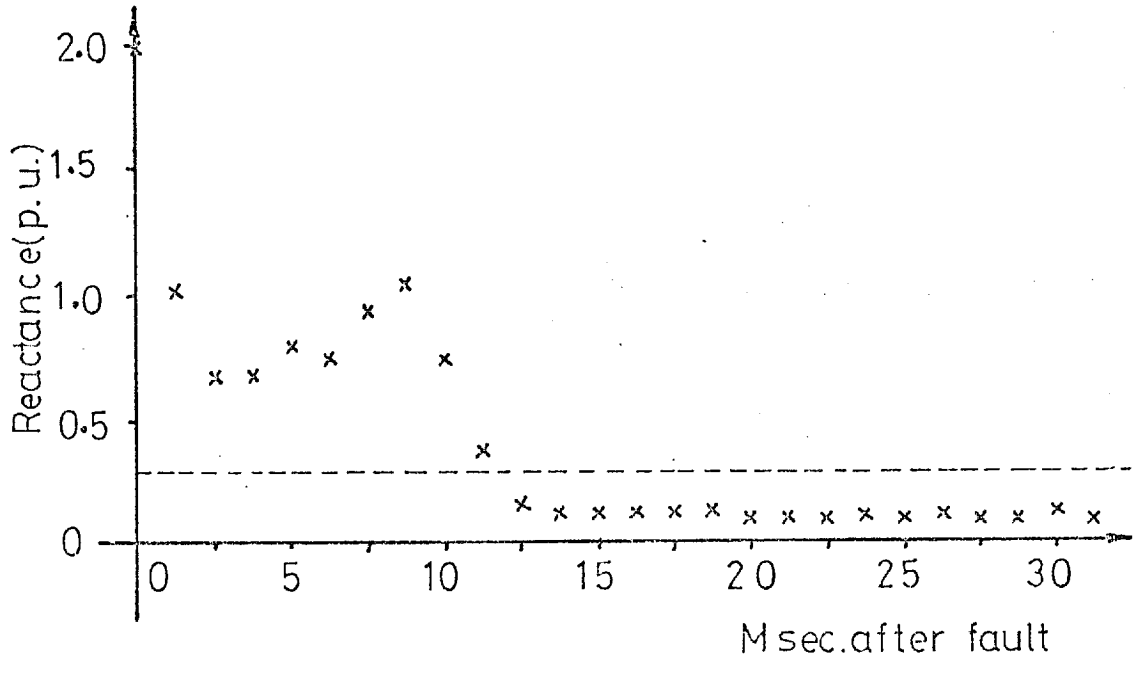

a

Three phase fault

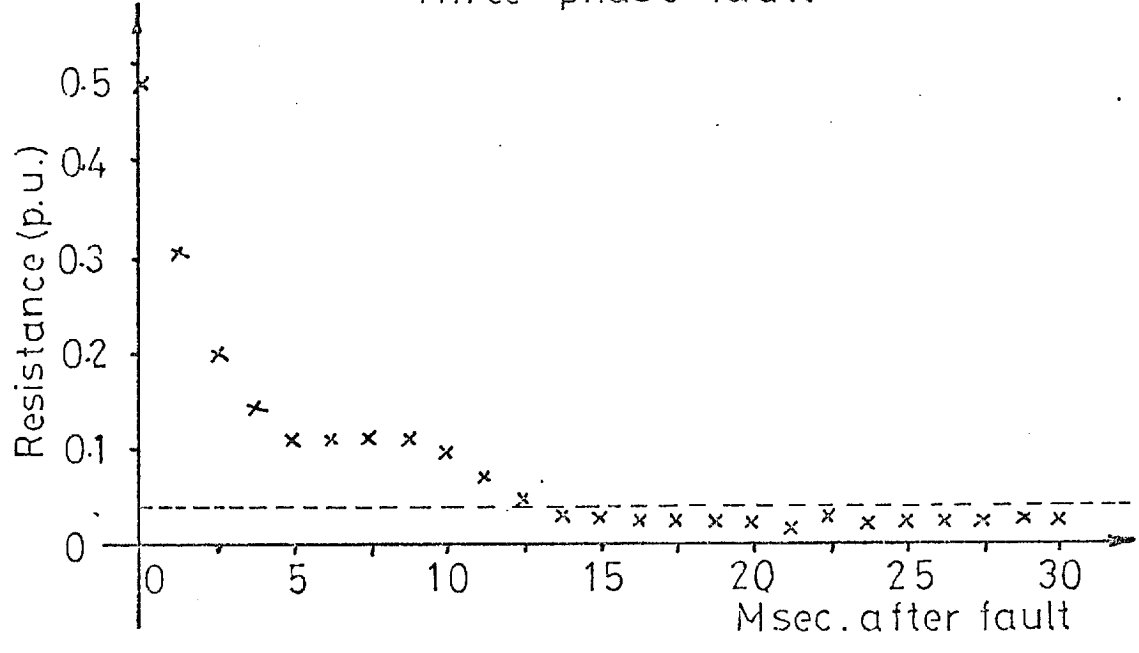

b

Fig.(7-17) On-line calculated X and R by McInnes method

a Reactance

b Resistance

Finally it is worth mentioning, that the linear coupler output is the derivative of the current and so if the current itself is necessary, it must be calculated. For example, assume that the fundamental components of i and $\frac{di}{dt}$ (which can be measured at linear coupler output) are as follows:

$$i = A_i \sin\omega t + B_i \cos\omega t \tag{7.1a}$$

$$\frac{di}{dt} = A_i' \sin\omega t + B_i' \cos\omega t \tag{7.1b}$$

calculating $\frac{di}{dt}$ from (7.1a) and putting it into (7.1b) gives:

$$\omega A_i \cos\omega t - \omega B_i \sin\omega t = A_i' \sin\omega t + B_i' \cos\omega t$$

Hence:

$$A_i = \frac{1}{\omega} B_i' \tag{7.2a}$$

$$B_i = -\frac{1}{\omega} A_i' \tag{7.2b}$$

By applying the Fourier method to the samples of the linear coupler output A_i' and B_i' will be obtained. Then from equations (7.2) the component of current itself can be calculated. Also we can write the R and X formulas in terms of A_i' and B_i' as:

$$R = \omega \frac{A_v B_i' - B_v A_i'}{A_i'^2 + B_i'^2} \tag{7.3a}$$

and

$$X = \omega \frac{A_v A_i' + B_v B_i'}{A_i'^2 + B_i'^2} \tag{7.3b}$$

7.4 CONCLUSION

4 different algorithms were implemented on-line and test results have been presented. The Fourier method gave the best results when judged on accuracy. Because of improper design of interface and particularly the sample and hold circuits, current and voltage waveforms were shifted causing

the McInnes method to show less accuracy than the Fourier method. In most of the experiments, the McInnes method was faster than the Fourier and square wave methods.

CHAPTER 8

CONCLUSION

8.1 GENERAL CONCLUSION

This thesis has attempted to obtain a simple and practical algorithm for high voltage transmission line protection using digital techniques. The algorithm must cope with the many fault generated high frequency components and also exponential d.c. offset. In dealing with these components, the role of the analogue filter, its cut-off frequency and the sampling rate is very important.

In chapter 3 it was shown that the cut-off frequency of the analogue filter is determined by its order and the type of the algorithm used. It was found that in the peak determination method, to have all frequency components attenuated with respect to 50 Hz, the sampling rate should be 4 S/C which from a numerical point of view is not acceptable. This method also is unable to cope with exponential dc component.

The Fourier method, with 8 S/C and a 150 Hz, two pole Butterworth filter from filtering point of view is quite acceptable, but its accuracy might be impaired by its inability to remove the exponential d.c. off-set effectively. In this method by approximating the coefficients multiplication in real and imaginary parts of a phasor can be avoided, without any practical changes in the spectrum or results.

The square wave method accentuates some components and as a whole it has a poorer characteristic than the Fourier method, chiefly because the exponential dc off-set behaviour is poor.

In the McInnes method, the interval of integrations must

be half a cycle, otherwise the fault generated high frequency components will be accentuated. It directly accounts for exponential d.c. off-set which is its great advantage over other methods. If it is used with 60 Hz, two pole Butterworth filter, it will filter out all noise and other unwanted components.

In chapter 4 the off-line tests showed that the McInnes method with Simpson's rule gives the most accurate results among all the algorithms. Two conditions apply:

i) The integration terms in the method must be performed over half a cycle of samples;

ii) The method must be used with a second order analogue filter at least, with a 60 Hz cut-off frequency.

It was shown that 8 S/C gives quite acceptable performance.

In chapter 5 the analogue and digital filters are compared for spectrums and transient time responses and it was concluded that for protection purposes analogue filters are preferred. No clear advantage can be seen in any type of analogue filter. A second order Butterworth filter with any algorithm gives satisfactory results. This filter can be realized by only one operational amplifier.

In chapter 6 it was shown that, in the case of a parallel line, if inter-circuit mutual coupling is incorporated, overreaching would occur. Neglecting the mutual coupling and reducing the protected zone length is therefore preferable. In addition, the sound phase voltage principle is recommended for close-up faults.

Different algorithms were implemented on-line and the test results presented in chapter 7. Because of linear coupler characteristics, the Fourier method was shown to give the best

result. The sample and hold circuits were imperfect and they shifted the waveforms, and this caused the McInnes method to be less accurate than the Fourier method.

In general, from off-line and on-line test results it can be said that if the current transducer is linear coupler, both Fourier's method with modified coefficients and also McInnes' method can be used succesfully for distance measurement. With a current transformer, the results of the Fourier method are not acceptable. In this case the McInnes method is recommended. In using the McInnes method care must be taken over the constant d.c. off-set produced by the interface.

The original contributions presented in this thesis are as follows:

1) Z-transform analysis of protection algorithms.
2) Mathematical presentation of the frequency responses for different algorithms, in the most general form.
3) Determination of the filter cut-off frequency.
4) Presentation of a new technique[32] for R and X calculation.
5) Determination of the optimum interval for the integration terms in the McInnes method.
6) Presentation of a new method[26] for harmonic filtering.

8.2 FURTHER RESEARCH

The model which has been constructed for digital protection research can be improved by reassembling the linear couplers symmetrically and reducing the mutual coupling effect. The connectors should be screened effectively and the terminations tightened. The sample and hold circuits should also be replaced by integrated circuits.

The idea of using a modest size computer for primary protection of the whole substation or even a corner, from the reliability point of view is now the subject to some controversy.[30,68,69] For primary protection, the use of one computer alone is not reliable. By using 2 or 3 computers the reliability can be increased, but economic considerations may not justify this number. Experience shows that, a computer such as the PDP 15 cannot manage all the jobs that are necessary for protection and switching of a mesh corner satisfactorily and there is a need for a multi-computer system which from the economic point of view needs further justification.

Because of the foregoing a fully segregated system for primary protection is preferred, and so the future research in the digital protection field should be concentrated in developing simple digital hardware (digital relay) for every transmission line or transformer etc. If these relays are used in a substation, a central processor can check and monitor these relays and provide information about their status. For transmission line protection, effort should be made to develop simple hardwares for implementation of the McInnes method. Cory, Dromy and Murrey have presented[72] a scheme for primary and back-up protection in which the role of a central processor for back-up protection and also monitoring every individual digital relay has been shown.

REFERENCES

1. Crichton, L.N., "The distance relay for automatically sectionalising electrical networks", Trans. AIEE, 1923, 42, p. 527.

2. Fitzgerald, A.S., "A carrier current pilot system of transmission line protection", Trans. AIEE, 1928, 47, p. 22.

3. Wideroe, R., "Thyratron tubes in relay practice", Trans. AIEE, 1934, 53, p. 1347.

4. Macpherson, R.H., Warrington, A.R., Vanc. and McConnell, A.J., "Electronic protective relays", Trans. AIEE, 1948, 67, part II, p. 1702.

5. Kennedy, L.F., "Electronic relaying provides faster fault clearing times", CIGRE, Paris, 1954, paper No. 332.

6. Adamson, C. and Wedepohl, L.M., "Power system protection with special reference to the application of junction transistor to distance relays", Proc. IEE, 1956, 103A, p. 379.

7. Adamson, C. and Wedepohl, L.M., "A dual comparator mho-type distance relay, utilizing junction transistors", ibid, 1956, 103A, pp. 509-517.

8. Jackson, L., Patrickson, J.B., Wedepohl, L.M., "Distance protection: Optimum design of static relay comparators", Proc. IEE., Vol. 115, No. 2, Feb. 1968, pp. 280-287.

9. Jackson, L., "Distance protection comparator with signal dependent phase-angle criterion", IEE, 1974, Vol. 121, No.8, p. 817.

10. Mathews, P., Nellist, B.D., "Generalized circle diagrams and their application to protective gear", IEEE, Trans., PAS, Feb. 1964, p. 165.

11. Narayan, V., "Some aspect of distance protection", IEE international conference on developments in power system protection", March 1975.

12. Warrington, A.R., Vanc., "Control of distance relay potential connections", AIEE, 1934, 53, p. 206.

13. Clarke, E., "Impedance seen by relays in three phase systems with and without faults", ibid, 1945, 64, p. 372.

14. Lewis, W.A. and Tippet, L.S., "Fundamental basis for distance relaying", ibid, 1931, 50, p. 420.

15. Crichton, L.N., "High speed protective relays", ibid, 1930, 49, p. 1232.

16. George, E.E., "Operating experience with reactance type distance relays", ibid, 1931, 50, p. 288.

17. Bancker, E.H., Hunter, E.M., "Distance relay action during oscillation", ibid, 1934, 53, p. 1073.

18. Crichton, L.N., "A system out of step and its relay requirements", ibid, 1937, 56, p. 1261.

19. Mason, C.R., "Relay operation during system oscillation", ibid, p. 823.

20. Warrington, A.R., Vanc."Protective Relays: their theory and practice", Vols. I and II, published by Chapman and Hall, London.

21. Mann, B.J., and Morrison, I.F., "Digital calculation of impedance for transmission line protection", IEEE, Trans., Vol. PAS-90, No.1, January/February, 1971.

22. Rockefeller, G.D., and Udren, E.A., "High speed distance relaying using a digital computer" parts I and II. IEEE T-PAS-91, No. 3, May/June 1972, pp. 1235-1258.

23. Slemon, G.R., Robertson, S.D.T. and Ramamoorty, M., "High speed protection of power systems based on improved models", CIGRE paper 31-09, 1968.

24. Hope, G.S. and Umamaheswaran, V.S., "Sampling for computer protection of transmission lines", IEEE paper TP74-0345 Winter power meeting, New York, January 1973.

25. McInnes, B.E. and Morrison, I.F., "Real time calculation of resistance and reactance for transmission line protection by digital computer", IEA (Australia) March 1971, p. 16.

26. Ranjbar, A.M. and Cory, B.J., "An improved method for the digital protection of high voltage transmission lines", IEEE T-PAS-94, No. 2., March/April 1975, p. 544.

27. Poncelct, R., "The use of digital computers for network protection", CIGRE paper No. 32-08, 1972.

28. Gilbert, J.G. and Shovlin, R.J., "High speed transmission line fault impedance calculation using a dedicated mini-computer", IEEE paper T74032-9 winter power meeting, New York, January 1974.

29. Carr, J. and Jackson, R.V., "Frequency domain analysis applied to digital transmission line protection", IEEE paper T75 055-9 winter power meeting, New York, January 1975.

30. Luckett, R.G., Munday, P.J. and Murray, B.E., "A substation based computer for control and protection", IEE conference on Developments in power system protection, 11-13 March 1975.

31. Sabberwall, S.P., "The application of phase comparator techniques to high speed distance protection and automatic synchronising", PhD thesis, the victoria University of Manchester.

32. Ranjbar, A.M., Cory, B.J., "Algorithms for distance protection", IEE Conference on modern developments in protection, No. 125, March 1975.

33. Horne, E. and Cory, B.J., "Digital processors for substation switching and control", IEE conference on modern developments in protection, March 1975.

34. Mann, B.J. and Morrison, IF., "Relaying a three-phase transmission line with a digital computer", IEEE Trans. Vol. PAS-90, No.2 March/April 1971, pp. 742-750.

35. Foster, E.J., "Active low-pass filter design", IEEE Transactions on audio, Vol. AU-13, No.5, p. 104.

36. Papoulis, A., "Optimum filters with monotonic response", Proc. IRE, Vol. 46, pp. 606-609; March, 1958.

37. Fukada, M., "Optimum filters of even orders with monotonic response", Proc. IRE, p. 277, September 1959.

38. Sallen, R.P. and Key, E.L., "A practical method of designing RC active filters", IRE Transactions, p. 74, March 1955.

39. Rader, C.M. and Gold, B., "Digital filtering design techniques in the frequency domain", Proceeding of IEEE, Vol. 55, No. 2, February 1967.

40. Steiglitz, K., "Computer-aided design of recursive digital filters", IEEE Transactions on Audio and Electroacustics, Vol. AU-18, No. 2, June 1970.

41. McClellan, J.H. and et al, "A computer program for designing optimum FIR linear phase digital filters", IEEE Transaction on Audio and Electroacoustics, Vol. AU-21, No.6, December, 1973.

42. Fletcher, R. and Powell, M.J.D., "A rapidly convergent descent method of optimization", Comput. J., Vol. 6, No.2, 1963, pp. 163-168.

43. Kaiser, J.F., "Digital filters" in System analysis by digital computers (Ed. F.F. Kuo, and J.F. Kaiser), Wiley, New York, 1966, Chapt. 7.

44. Rabiner, L.R., Gold, B., and McGonegal, C.A., "An approach to the approximation problem for nonrecursive digital filters", IEEE Trans. on audio and electroacoustics, AU-18 No. 2, 83-106 (1970).

45. McClellan, J.H. and Parks, T.W., "A unified approach to the design of optimum FIR linear-phase digital filters", IEEE Trnas. on circuit theory, Vol. CT-20, No. 6, November, 1973.

46. Parks, T.W. and McClellan, J.H., "Chebyshev approximation for nonrecursive digital filters with linear phase", IEEE Trans. on circuit theory, Vol. CT-19, No. 2, March 1972.

47. Herrmann, O., "Design of nonrecursive digital filters with linear phase", Electron. lett., pp. 328-329, 1970.

48. Cheney, E.W., "Introduction to approximation theory", New York, McGraw-Hill, 1966, pp. 72-100.

49. Temes, G.C. and Bingham, J.A.C., "Iterative Chebyshev approximation technique for network synthesis", IEEE Trans. Circuit theory, Vol. CT-14, pp. 31-37, March 1967.

50. Hans Hoel, Humpage, W.D., Chapman, C.P., "Composite polar charachteristic in multizone systems of phase-comparison distance protection", Proc. IEE, Vol. 113, No. 10, October 1966, p. 1631.

51. Johns, A.T. and El-Alaily, A.A., "Variable charcteristic generalised techniques for distance protection", proc. IEE, Vol. 120, No. 8, August 1973, p. 891.

52. Rushton, J. and Humpage, W.D., "Power-system studies for the determination of distance protection performance", proc. IEE, Vol. 119, No. 6, June 1972, p. 677.

53. Humpage, W.D. and Sabberwal, S.P., "Developments in phase-comparison techniques for distance protection", Proc. IEE, Vol. 112, No. 7, July 1965, p. 1383.

54. Wedepohl, L.M., "Polarised mho distance relay", proc. IEE, Vol. 112, No. 3, March 1965, p. 525.

55. Choudhuri, S., Basu, S.K. and Patra, S.P., "Polyphase distance relaying by phase coincidence principle", IEEE, paper, T72428-1 presented at the IEEE PES Summer meeting, San Francisco, Calif., July 9-14, 1972.

56. Wheeler, S.A., "Influence of mutual coupling between parallel circuits on the setting of distance protection", Proc. IEE , Vol. 2, February 1970, p. 439.

57. Adamson, C. and Türeli, A., "Errors of sound-phase compensation and residual compensation systems in earth-fault distance relaying", Proc. IEE, Vol. 112, No. 7, July 1965.

58. Butterworth, S., "On the theory of filter amplifiers, Wireless Engr." Vol. 7, pp. 536-541, October 1930.

59. Steiglitz, K., "An introduction to discrete systems", book published by John Wiley and Sons, 1974.

60. Hilburn, J.L. and Johnson, D.E., "Manual of active filter design", Book published by McGraw-Hill, 1973.

61. Ra biner, L.R., "The design of finite impulse response digital filters using linear programming techniques", the Bell System technical Journal, Vol. 51, No. 6, July/August 1972.

62. McVey, P.J., "Sensitivity in some simple RC active networks", Proc. IEE, Vol. 112, No. 7, July 1965.

63. Miniesy, S.M., "Power system report No. 94, Imperial College, University of London.

64. Distance relays with memory action, Reyrolle pamphlet No. 1314.

65. Holden, A.E.K., and Morrison, I.F., "Directional discrimination for close-up faults in transmission line protection by digital computer", IEE conference on modern developments in protection, March 1975.

66. Holden,A.E.K., M.E. Thesis, 1972, School of Electrical Engineering, University of N.S.W., Australia.

67. Davison, E.B. and Wright, A., "Some factors affecting the accuracy of distance-type protective equipment under earth fault condition", Proc. IEE 110, No. 9, September 1963, pp. 1678-1688.

68. Carter, R.P. and Cavero, L.P., "Considerations on future system philosophy, for power system protection, control and measurements", IEE conference publication No. 125, March 1975, pp. 22-26.

69. Cheetham, W.J., "Computerised protection or not ?primary and local back-up protection", ibid pp. 291-296.

70. Cheetham, W.J., Computerised protection or not ? remote back-up protection", ibid pp. 297-303.

71. Jaleeli, N., Ph.D. thesis, 1975, Imperial College of Science and Technology, University of London.

72. Cory, B.J., Dromey, G. and Murray, B., "Digital Techniques in protection" paper to be presented at CIGRE conference, 1976.

APPENDIX A1

A1.1 System parametres

The system used for off-line study was as follows:

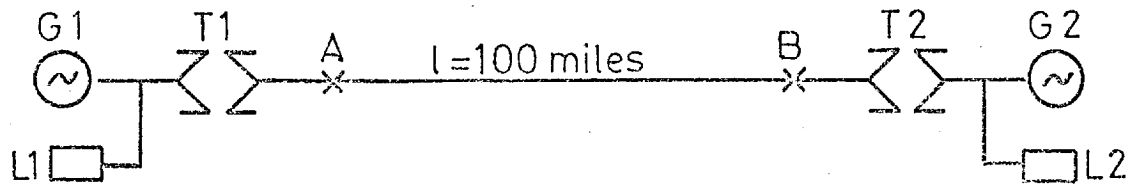

Fig.(A1.1) System for off-line study

The parametres of this system are given in table A1.1

Table A1.1 Parametres of Fig. A1.1

Equipment	Positive and negative reactance per unit ohm	zero sequence reactance per unit ohm
Generators 1, 11 KV	0.1	0.08
Transformers 1, 11/400 KV	0.1	0.08
Equivalent generator 2	0.04	0.06
Transformers 2	0.07	0.05
Transmission line 400 KV	$Z = 0.02+J0.276$	$Z_o = 0.104+J0.794$
400 KV	$B = 10.5\times10^{-6}$	$B_o = 5.9\times10^{-6}$ p.u.mho

A1.2 Transmission line model

The voltage drop per unit length for a small section of the transmission line can be written as:

$$\frac{dV_a}{dX} = Z_1 I_a + \frac{1}{3}(Z_o - Z_1)(I_a + I_b + I_c) \qquad \text{(A1.1a)}$$

$$\frac{dV_b}{dX} = Z_1 I_b + \frac{1}{3}(Z_o - Z_1)(I_a + I_b + I_c) \qquad \text{(A1.1b)}$$

$$\frac{dV_c}{dX} = Z_1 I_c + \frac{1}{3}(Z_o - Z_1)(I_a + I_b + I_c) \qquad \text{(A1.1c)}$$

Also the rate of current change per unit length along the line, due to the capacitive link between phases and also between phases and earth can be written as:

$$-\frac{dI_a}{dX} = V_a Y_s + (V_a - V_b) Y_m + (V_a - V_c)\, Y_m \qquad \text{(A1.2a)}$$

$$-\frac{dI_b}{dX} = V_b Y_s + (V_c - V_a)\, Y_m + (V_b - V_c)\, Y_m \qquad \text{(A1.2b)}$$

$$-\frac{dI_c}{dX} = V_c Y_s + (V_c - V_a)\, Y_m + (V_c - V_b)\, Y_m \qquad \text{(A1.2c)}$$

Putting

$$Y_s = Y_o$$

$$Y_m = \frac{1}{3}(Y_1 - Y_o)$$

equations (A1.2) become:

$$-V_a = \frac{1}{Y_1}\frac{dI_a}{dX} + \frac{Y_1 - Y_o}{3Y_o Y_1}\frac{d}{dX}(I_a + I_b + I_c) \qquad \text{(A1.3a)}$$

$$-V_b = \frac{1}{Y_1}\frac{dI_b}{dX} + \frac{Y_1 - Y_o}{3Y_o Y_1}\frac{d}{dX}(I_a + I_b + I_c) \qquad \text{(A1.3b)}$$

$$-V_c = \frac{1}{Y_1}\frac{dI_c}{dX} + \frac{Y_1 - Y_o}{3Y_o Y_1}\frac{d}{dX}(I_a + I_b + I_c) \qquad \text{(A1.3c)}$$

Equations (A1.1) and (A1.2) describe the behaviour of a small section of a three phase transmission line. These equations can be simulated by figures (A1.2) and (A1.3) respectively. Figure (A1.4) represents both equations and so it can be used as a model for a transposed transmission line with short length. Slemon and et al[23] have shown that if ten of these networks are cascaded, it can simulate the behaviour of a long transmission line. For off-line studies 10 of these networks were cascaded, but for on-line tests only three of them were available to be cascaded.

A1.3 Generator model

For the Generator model a constant voltage behind subtransient reactance was chosen. Jaleeli has shown that[71] the waveforms generated by using full representation of the

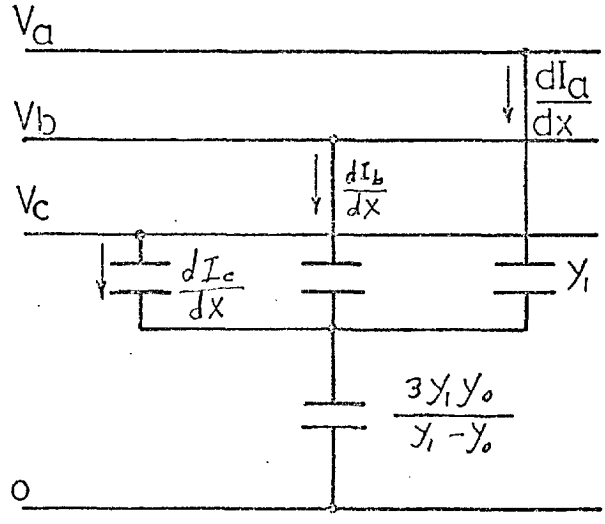

Fig.(A1·3) Model representing equation (A1·2)

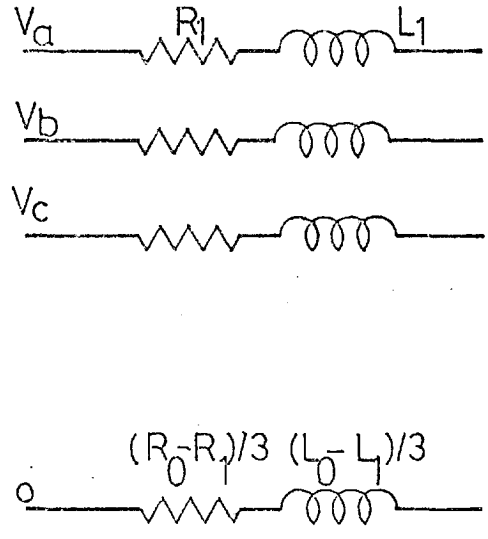

Fig.(A1·2) Model representing equation (A1·1)

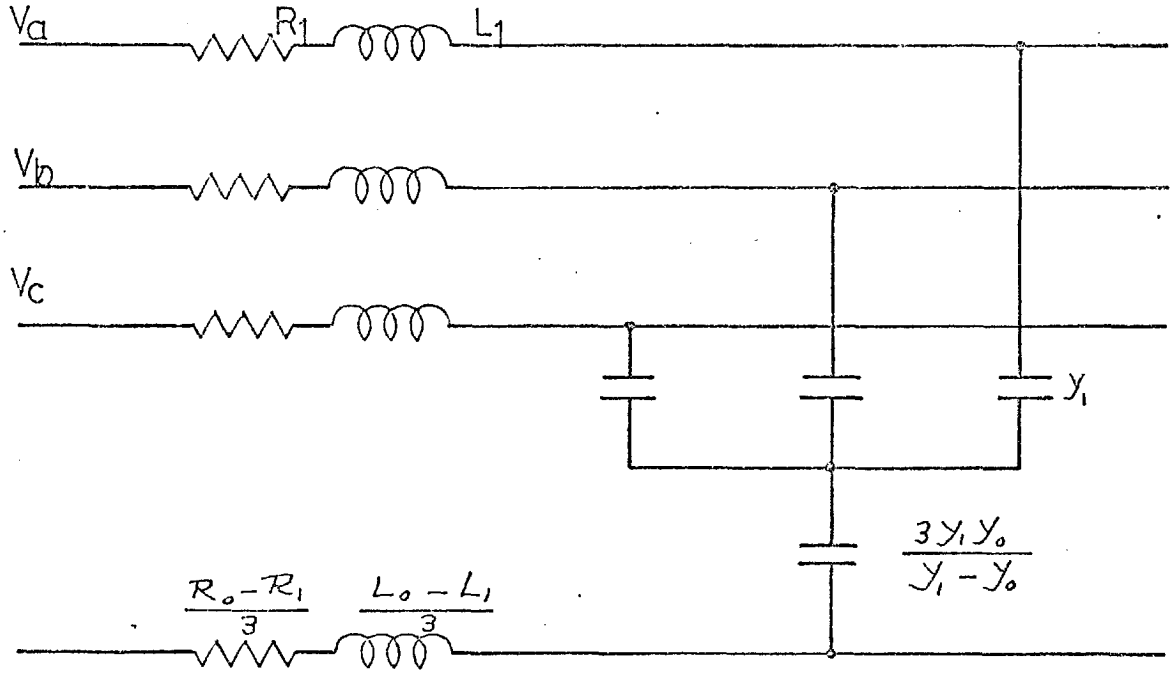

Fig.(A1·4) Model representing a short length of transmission line

generator in the first cycle, is almost the same as if the generator is simulated by a constant voltage behind a reactance.

APPENDIX A2

DIGITAL BUTTERWORTH AND CHEBYSHEV FILTERS, DESIGNED BY BILINEAR TRANSFORMATION METHOD

(I) Butterworth digital filters (cut-off frequency equal to $\frac{1}{8}$ th sampling frequency):

$$u_k = 0.542(v_k+v_{k-1}) - 0.085u_{k-1}$$

$$u_k = 0.133(v_k+2v_{k-1}+v_{k-2})+ 0.799u_{k-1}-0.361u_{k-2}$$

$$u_k = 0.028(v_k+3v_{k-1}+3v_{k-2}+v_{k-3})+1.693u_{k-1}-1.293u_{k-2} + 0.378u_{k-3}$$

$$u_k = 0.006(v_k+4v_{k-1}+6v_{k-2}+4v_{k-3}+v_{k-4})+2.56u_{k-1}-2.92u_{k-2} + 1.66u_{k-3}+ 0.4u_{k-4}$$

$$u_k = 0.001(v_k+5v_{k-1}+10v_{k-2}+10v_{k-3}+5v_{k-4}+v_{k-5})+ 3.42u_{k-1} - 5.26u_{k-2}+4.43u_{k-3}-2.02u_{k-4}+0.4u_{k-5}$$

(II) Butterworth digital filters (cut-off frequency equal to $\frac{1}{16}$ th sampling frequency:

$$u_k = 0.363(v_k+v_{k-1})+ 0.27u_{k-1}$$

$$u_k = 0.042(v_k+2v_{k-1}+v_{k-2})+1.399u_{k-1}-0.578u_{k-2}$$

$$u_k = 0.004(v_k+3v_{k-1}+3v_{k-2}+v_{k-3})+2.41u_{k-1}-2.058u_{k-2} + 0.61u_{k-3}$$

$$u_k = 0.0004(v_k+4v_{k-1}+6v_{k-2}+4v_{k-3}+v_{k-4})+0.34u_{k-1}-4.46u_{k-2} + 2.7\ u_{k-3} - 0.62u_{k-4}$$

$$u_k = 0.00004\ (v_k+5v_{k-1}+10v_{k-2}+10v_{k-3}+5v_{k-4}+v_{k-5}) +4.36u_{k-1}-7.8u_{k-2}+7.11u_{k-3}-3.31u_{k-4}+ 0.63u_{k-5}$$

(III) Chebyshev digital filters (1 db ripple, cut-off frequency equal to $\frac{1}{16}$ th sampling frequency):

$$u_k = 0.28(\upsilon_k+\upsilon_{k-1}) + 0.44u_{k-1}$$

$$u_k = 0.031(\upsilon_k+2\upsilon_{k-1}+\upsilon_{k-2})+1.51u_{k-1} -0.65u_{k-2}$$

$$u_k = 0.003(\upsilon_k+3\upsilon_{k-1}+3\upsilon_{k-2}+\upsilon_{k-3})+2.51u_{k-1}-2.21u_{k-2}+0.68u_{k-3}$$

$$u_k = 0.00031(\upsilon_k+4\upsilon_{k-1}+6\upsilon_{k-2}+4\upsilon_{k-3}+\upsilon_{k-4})+3.48u_{k-1}-4.7u_{k-2} + 2.9u_{k-3}-0.688u_{k-4}$$

$$u_k = 0.00003(\upsilon_k+5\upsilon_{k-1}+10\upsilon_{k-2}+10\upsilon_{k-3}+5\upsilon_{k-4}+\upsilon_{k-5})\upsilon+4.45u_{k-1} -8.1u_{k-2}+7.54u_{k-3}-3.57u_{k-4}+0.69u_{k-5}$$

(IV) Chebyshev digital filters (1 db ripple, cut-off frequency equal to $_8$ th sampling frequency):

$$u_k = 0.49(\upsilon_k+\upsilon_{k-1}) + 0.102\ u_{k-1}$$

$$u_k = 0.102(\upsilon_k+2\upsilon_{k-1}+\upsilon_{k-2})+0.98u_{k-1} -0.447u_{k-2}$$

$$u_k = 0.021(\upsilon_k+3\upsilon_{k-1}+3\upsilon_{k-2}+\upsilon_{k-3})+1.866u_{k-1}-1.5u_{k-2}+0.46u_{k-3}$$

$$u_k = 0.004(\upsilon_k+4\upsilon_{k-1}+6\upsilon_{k-2}+4\upsilon_{k-3}+\upsilon_{k-4})+2.7u_{k-1}-3.25u_{k-2} + 1.92u_{k-3}-0.47u_{k-4}$$

$$u_k = 0.00085(\upsilon_k+5\upsilon_{k-1}+10\upsilon_{k-2}+10\upsilon_{k-3}+5\upsilon_{k-4}+\upsilon_{k-5}) + 3.58u_{k-1}-5.72u_{k-2}+4.99u_{k-3}-2.35u_{k-4}+0.48u_{k-5}$$

Supporting Publication

IEEE TRANSACTIONS

ON POWER APPARATUS AND SYSTEMS

Vol. PAS-94, No. 2, March/April 1975

IEEE Transactions on Power Apparatus and Systems, vol. PAS-94, no. 2, March/April 1975

AN IMPROVED METHOD FOR THE DIGITAL PROTECTION OF HIGH VOLTAGE TRANSMISSION LINES

A. M. Ranjbar and B. J. Cory
Imperial College
London, S.W. 7.

Abstract--This paper explores the accuracy of the digital methods for protection of high voltage transmission lines under transient fault condition on a long line and describes an improved method for future digital protection schemes. With this method it is possible to calculate R and L of high voltage transmission lines so that any number of harmonics on the current and voltage waveforms can be eliminated and it is shown to be suitable for distance protection during the first cycle of fault occurrence.

INTRODUCTION

Increasing interest is being shown in the use of digital computers for the protection, switching and data acquisition required in modern high voltage sub-stations. One of the most difficult functions to fulfill by digital methods is that of transmission line protection employing samples of the voltage and current waveforms taken from high voltage transducer equipment at the usual relaying point. Given adequate speed of sampling and conversion to digital form for processing, problems remain of calculating the fault conditions within a defined protection zone of the transmission line, particularly when harmonics and noise are present. One method, proposed by Slemon, Robertson and Ramamoorty[3], is based on the calculation of the fundamental components of the voltage and current waveforms by a Fourier technique requiring evenly spaced samples taken over a complete cycle of the system frequency. From the fundamental components, the impedance magnitude and angle seen from the relaying point can be calculated. The use of a mini-processor for this purpose requires a time longer than that obtainable from modern static analog relays with the added difficulty of achieving an ideal relay characteristic in the X-R plane.

Another method, described by Rockefeller[4] for a practical installation based on the work of Mann and Morrison[6], uses samples to predict the peak values of fault voltage and current as well as the phase angle between the peaks. In these methods the desired differentiation techniques employed tend to amplify the harmonics present in the waveforms due to the line shunt capacitance characteristics and transducer effects. High frequency noise can readily be eliminated by analog filters with suitable cut-off characteristics but to reduce the harmonic effects, particularly those up to 11th and 13th, it is necessary to use digital integration techniques as proposed by Couch et al [10] and Poncelet[8]. These techniques involve a form of digital filtering, an application which has been highly developed in the telecommunication field, but to be useful for high speed power system line protection it is necessary to combine them with the minimum number of sequential samples consistent with desired accuracy and speed of detection. Consequently a measurement and calculation time equivalent to about half a cycle (10 ms in a 50Hz system) and a measurement error of no greater than 5% of line reactance to the fault point is sought.

This paper explores the accuracy of various digital methods under transient fault conditions on a long line and proposes an improved method which, by filtering out low order harmonics, enables greater accuracy to be obtained.

Paper T 74 380-2, recommended and approved by the IEEE Power System Relaying Committee of the IEEE Power Engineering Society for presentation at the IEEE PES Summer Meeting & Energy Resources Conf., Anaheim, Cal., July 14-19, 1974. Manuscript submitted January 28, 1974; made available for printing June 4, 1974.

THEORY OF DIGITAL FAULT MEASUREMENT

The voltage drop per unit length of an overhead line consisting of three phase conductors a, b and c with no shunt capacitance can be represented by:

$$\begin{vmatrix} \frac{dV_a}{dx} \\ \frac{dV_b}{dx} \\ \frac{dV_c}{dx} \end{vmatrix} = \begin{vmatrix} Z_{sa} & Z_{mab} & Z_{mac} \\ Z_{mba} & Z_{sb} & Z_{mbc} \\ Z_{mca} & Z_{mcb} & Z_{sc} \end{vmatrix} \begin{vmatrix} I_a \\ I_b \\ I_c \end{vmatrix} \quad (1)$$

where Z_{s-} are the self impedances and Z_{m-} are the mutual impedances per unit length. If the line is perfectly transposed all phases have the same self and mutual impedances of Z_s and Z_m per unit length respectively, so that equations (1) become:

$$\begin{aligned} \frac{dV_a}{dx} &= Z_s I_a + Z_m(I_b + I_c) \\ \frac{dV_b}{dx} &= Z_s I_b + Z_m(I_a + I_c) \\ \frac{dV_c}{dx} &= Z_s I_c + Z_m(I_a + I_b) \end{aligned} \quad (2)$$

In terms of the positive and zero sequence impedances of the line, Z_1 and Z_0, equations (2) become:

$$\begin{aligned} \frac{dV_a}{dx} &= Z_1 I_a + (Z_o - Z_1) I_o \\ \frac{dV_b}{dx} &= Z_1 I_b + (Z_o - Z_1) I_o \\ \frac{dV_c}{dx} &= Z_1 I_c + (Z_o - Z_1) I_o \end{aligned} \quad (3)$$

From equations (2) and (3) the voltage drops due to measured fault currents I_a, and I_b and I_c and/or the residual current I_o can be calculated for any given fault condition. Such conditions will now be considered in turn.

Single-phase to Earth Fault

When a solid single phase to earth fault occurs on phase a at a distance x along the line from the transducer, the instantaneous phase to earth voltage v_a can be calculated by use of eq. (1) for an untransposed line or by eq. (2) or (3) for a transposed line.

Using instantaneous (sampled) values of voltage, current and rate of change of current, eq. (1) can be written:

$$v_a = xR_{sa}\left(i_a + \frac{R_{mab}}{R_{sa}} i_b + \frac{R_{mac}}{R_{sa}} i_c\right) + xL_{sa} \frac{d}{dt}\left(i_a + \frac{L_{mab}}{L_{sa}} i_b + \frac{L_{mac}}{L_{sa}} i_c\right) \quad (4)$$

Putting $\left(i_a + \frac{R_{mab}}{R_{sa}} i_b + \frac{R_{mac}}{R_{sa}} i_c\right) = i_x$

and $\left(i_a + \frac{L_{mab}}{L_{sa}} i_b + \frac{L_{mac}}{L_{sa}} i_c\right) = i_y$

equation (4) becomes:

$$v_a = xR_{sa}\, i_x + xL_{sa} \frac{di_y}{dt} \quad (5)$$

Similarly equations (2) and (3), using instantaneous values, become:

$$v_a = xR_s \left[i_a + \frac{R_m}{R_s}(i_b + i_c)\right] + xL_s \frac{d}{dt}\left[i_a + \frac{L_m}{L_s}(i_b + i_c)\right]$$

and

$$v_a = xR_1\left(i_a + \frac{R_o - R_1}{R_1} i_o\right) + xL_1 \frac{d}{dt}\left(i_a + \frac{L_o - L_1}{L_1} i_o\right)$$

and these can also be written in the form of equation (5).

Double Phase and Three Phase Faults

For a double phase fault between conductors a and b and a three phase fault involving all three conductors, the voltage between the faulty phases can be written as:

$$V_a - V_b = xZ_1 (I_a - I_b) \quad (7)$$

when the line is perfectly transposed. In instantaneous form this equation becomes:

$$v_a - v_b = xR_1 (i_a - i_b) + xL_1 \frac{d}{dt} (i_a - i_b) \quad (8)$$

Corresponding equations can be written for the other phases and more complicated equations can be derived for untransposed lines. If necessary, the value of (xR_1) in equation (8) can be replaced by $(xR_1 + R_f)$, where R_f is the fault resistance.

CALCULATION OF RESISTANCE AND INDUCTANCE

In the previous section, an equation of the form:

$$v = Ri_x + L \frac{di_y}{dt} \quad (9)$$

is obtained for all fault conditions where the values of v, i_x and i_y can be found by appropriate choice and combination of sampled voltages and currents. It should be noted that the required samples must be taken simultaneously on all three phases as can be achieved by suitable sample-and-hold peripheral equipment.

From equation (9) the values for R and L can be calculated by several methods. To compare them for accuracy and speed of computation, a particularly difficult case was simulated using the parameters of a 300 mile long, 230kv overhead line. The representation was obtained by a multi-section lumped parameter model consisting of 10 cascaded T sections in which self and mutual impedances and shunt capacitance were included[3] (see Appendix). In each case the current and voltage waveforms at the relaying point for four fault inception angles were computed off-line for faults at a distance of 300 miles and 150 miles. Two such typical waveforms are shown in figures 1 and 2 where the distorted nature can be noted, particularly during the first fundamental cycle. The various calculation methods for R and L are reviewed in this section, where sampled values taken at 625 μs intervals (32 samples/cycle in a 50Hz system) were used as input data to a fault detection program.

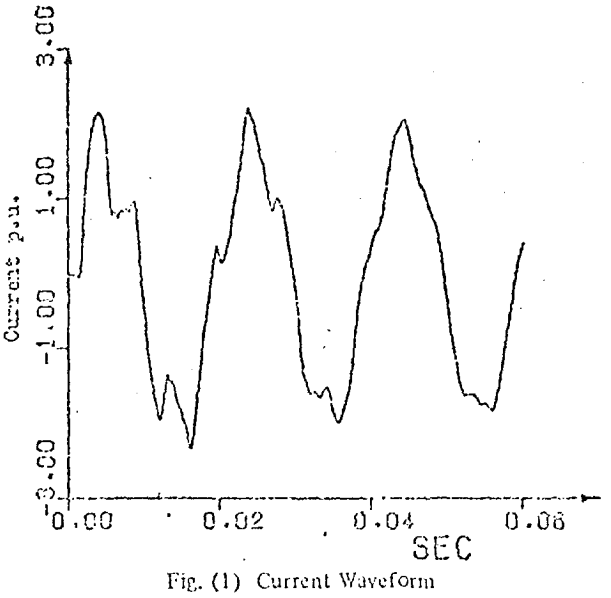

Fig. (1) Current Waveform

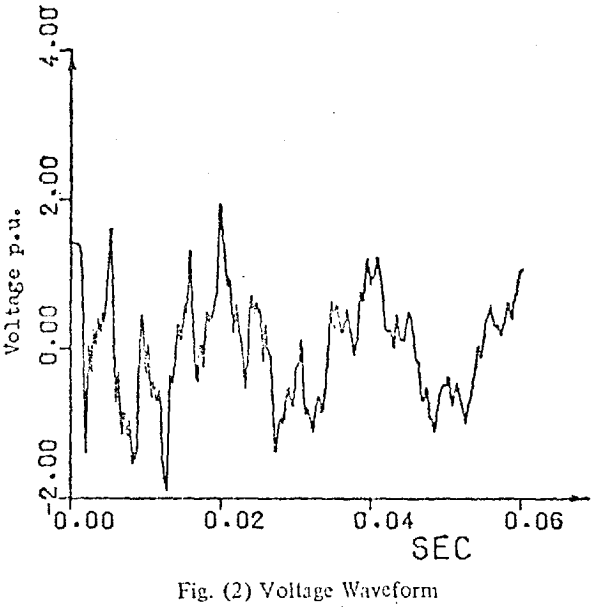

Fig. (2) Voltage Waveform

Simple Integration (Method 1)

By integrating equation (9) once over time instants t_1 and t_2 and again over t_3 and t_4, the following two equations are obtained:

$$\int_{t_1}^{t_2} v\,dt = R\int_{t_1}^{t_2} i_x\,dt + L\,(i_{y2} - i_{y1}) \quad (10a)$$

$$\int_{t_3}^{t_4} v\,dt = R\int_{t_3}^{t_4} i_x\,dt + L\,(i_{y4} - i_{y3}) \quad (10b)$$

From this pair of simultaneous equations, R and L can be calculated after 4 samples have been taken giving the results of Table I for double-phase and three-phase faults. Despite satisfactory computation times using a PDP 15 processor of 3.6 ms for double-phase and three-phase faults and 5 ms for single-phase-to-ground faults these times include data acquisition, fault detection, classification and impedance calculation) it can be seen that the errors in L are unacceptable. If the error is to be kept below 5% only 0.1% harmonic on current and voltage waveforms could be tolerated. With this method the errors in R are correspondingly high (see table IV).

TABLE I

Double-phase and three-phase faults: transposition assumed, simple integration (Method 1).

Fault distance (miles)	Actual value of L ($\times 10^3$ p.u)	Fault inception angle (degrees)	Calculated L ($\times 10^3$ p.u.)	Error in L %
300	1.18	0	0.51	56
		45	0.31	73
		90	0.35	70
		135	0.28	75
150	0.59	0	0.50	16
		45	0.84	44
		90	0.90	56
		135	0.90	56

Mean square error minimisation method (Method 2)

Equation (9) can be rewritten as:

$$L\frac{di_y}{dt} + Ri_x - v = \epsilon \qquad (11)$$

where ϵ is the error caused by shunt capacitance harmonics and low frequency noise effects. By integrating both sides over (o,t) we obtain:

$$L\int_o^t di_y + R\int_o^t i_x dt - \int_o^t v dt = \epsilon_t \qquad (12)$$

The average of the square of the errors over the interval T is given by:

$$\epsilon_m = \frac{1}{T}\int_o^T \left[L\int_o^t di_y + R\int_o^t i_x dt - \int_o^t v dt\right]^2 dt \qquad (13)$$

We can choose L and R so that ϵ_m is a minimum, for which the partial derivatives of ϵ_m with respect to R and L should be zero. The following equations are obtained:

$$R\int_o^T \left(\int_o^t di_y\right)\left(\int_o^t i_x dt\right)dt + L\int_o^T \left(\int_o^t di_y\right)^2 dt = \int_o^T \left(\int_o^t v dt\right)\left(\int_o^t di_y\right) dt \qquad (14a)$$

and

$$R\int_o^T \left(\int_o^t i_x dt\right)^2 dt + L\int_o^T \left(\int_o^t di_y\right)\left(\int_o^t i_x dt\right)dt = \int_o^T \left(\int_o^t i_x dt\right)\left(\int_o^t v dt\right) dt \qquad (14b)$$

From these two equations R and L can be calculated which, with 6 samples, takes 8 ms on the PDP 15 computer for double and three-phase faults. Typical results are shown in Table II where it can be seen that the accuracy is still unacceptable although overall a small improvement can be noted. For an error in L of 5% to be obtained, only 0.3% harmonic on the current and voltage waveforms can be tolerated.

TABLE II

Double-phase and three-phase faults: minimisation of error (Method 2).

Fault distance (miles)	Actual value of L ($\times 10^3$ p.u.)	Fault inception angle (degrees)	Calculated L ($\times 10^3$ p.u.)	Error in L %
300	1.18	0	0	100
		45	0.54	54
		90	0.57	51
		135	0.22	81
150	0.59	0	0.46	22
		45	0.78	33
		90	0.84	44
		135	0.81	38

Minimisation of errors over several intervals (Method 3)

In equation (12) the interval (o-t) can be divided into n parts by taking a sequence of samples[8]. This allows n equations of the type

$$R\int_{t_i}^{t_j} i_x dt + L(i_{yj} - i_{yi}) - \int_{t_i}^{t_j} v dt = \epsilon_j \qquad (15)$$

to be written for the interval t_i to t_j. Minimising $\sum_{j=i}^{n} \epsilon_n^2$ in relation to R and L gives two equations from which R and L can be calculated as before. The accuracy of this method was found to be less than for method 2 although the speed of computation was about the same.

An Improved Digital Harmonic Filtering Method (Method 4)

The methods shown so far are particularly sensitive to low order harmonics on the voltage and current waveforms. In long high voltage transmission lines there are considerable harmonics generated in the first cycle due mainly to the shunt capacitance effects which for the voltage waveform with high source impedance can amount to more than 100% of the fundamental. Consequently unless steps are taken to eliminate the harmonics, calculation of R and L will inevitably involve a large unacceptable error. Filtering the signal waveforms by analogue means to reduce low order harmonics is also unacceptable because of the slow response then achieved following fault initiation.

In general, it is possible to calculate R and L so that any number of harmonics can be eliminated. For example, to remove the third harmonic, equation (9) can be integrated once over the intervals o,α (α is an arbitrary constant) and again over the interval $\pi/3$, $(\alpha + \pi/3)$, the resulting equations, when added give:

$$L\left[\int_o^\alpha di_y + \int_{\pi/3}^{\alpha+\pi/3} di_y\right] + R\left[\int_o^\alpha i_x dt + \int_{\pi/3}^{\alpha+\pi/3} i_x dt\right] = \left[\int_o^\alpha v dt + \int_{\pi/3}^{\alpha+\pi/3} v dt\right] \qquad (16)$$

In this equation the third harmonic and all its multiples are completely filtered. The time to calculate R and L from two equations such as (16) is about 6 ms when nine sampled values are taken at 667μs intervals (30 samples/cycle in a 50 Hz system). Also to remove the third and fifth harmonics and all their multiples equation (9) can be integrated over $(o, \frac{2\pi}{5})$ and again over the interval $\pi/3$, $(\pi/3 + \frac{2\pi}{5})$. The resulting equations, when added, give:

$$L\left[\int_o^{\frac{2\pi}{5}} di_y + \int_{\frac{\pi}{3}}^{\frac{2\pi}{5}+\frac{\pi}{3}} di_y\right] + R\left[\int_o^{\frac{2\pi}{5}} i_x dt + \int_{\frac{\pi}{3}}^{\frac{2\pi}{5}+\frac{\pi}{3}} i_x dt\right] = \left[\int_o^{\frac{2\pi}{5}} vdt + \int_{\frac{\pi}{3}}^{\frac{2\pi}{5}+\frac{\pi}{3}} vdt\right] \quad (17)$$

The time needed to calculate R and L from two such equations and 13 samples is about 9 ms. In general to remove two harmonics of order m and n and multiples thereof the resulting equation will be:

$$L\left[\int_o^{\frac{2\pi}{m}} di_y + \int_{\frac{\pi}{n}}^{\frac{2\pi}{m}+\frac{\pi}{n}} di_y\right] + R\left[\int_o^{\frac{2\pi}{m}} i_c dt + \int_{\frac{\pi}{n}}^{\frac{2\pi}{m}+\frac{\pi}{n}} i_x dt\right] = \left[\int_o^{\frac{2\pi}{m}} vdt + \int_{\frac{\pi}{n}}^{\frac{2\pi}{m}+\frac{\pi}{n}} vdt\right] \quad (18)$$

This principle can be extended to any number of harmonics by making a sufficient number of integrations. For example, three harmonics of orders, m, n, and k can be eliminated by using:

$$L\left(\sum\int di_y\right) + R\left(\sum\int i_x dt\right) = \sum\int vdt \quad (19)$$

where:

$$\sum\int vdt = \int_o^{\frac{2\pi}{k}} vdt + \int_{\frac{\pi}{m}}^{\frac{2\pi}{k}+\frac{\pi}{m}} vdt + \int_{\frac{\pi}{n}}^{\frac{2\pi}{k}+\frac{\pi}{n}} vdt + \int_{\frac{\pi}{m}+\frac{\pi}{n}}^{\frac{2\pi}{k}+\frac{\pi}{m}+\frac{\pi}{n}} vdt$$

and $\Sigma\int di_y$ and $\Sigma\int i_x dt$ are calculated similarly. In this way with 2nd, 3rd and 5th harmonics removed (leaving only 7th, 11th and higher prime harmonics) the time for calculation including the acquisition of samples, fault classification and impedance calculation can be about 17 ms. It should be noted that for efficient and accurate calculation the rate of sampling is best chosen as a multiple of the order of the harmonics which it is intended to remove.

TABLE III

Double-phase and three-phase faults: improved filtering method (Method 4).

Fault distance (miles)	Actual value of L ($\times 10^3$ p.u.)	Fault inception angle (degrees)	Calculated L_3 (10^3 p.u.)	Error in L %
300	1.18	0	1.24	5
		45	1.18	0
		90	1.33	13
		135	1.43	21
150	0.59	0	0.59	0
		45	0.62	5.5
		90	0.52	11
		135	0.41	16

TABLE IV

The accuracy for the calculation of R

Fault inception angle (degrees)	% Error in R			
	Method 1	Method 2	Method 3	Method 4
0	650	950	96	12
45	400	35	85	50
90	260	240	220	52
135	600	1300	880	7

The accuracy for the calculation of L is shown in Table III for a double and three-phase fault where it can be seen that acceptable measurements are now being achieved when 2nd, 3rd and 5th harmonics are filtered out by this improved method.

The accuracy of the calculation for R with the different methods already described is shown in Table IV. Since allowance for the fault arc resistance needs to be made, the fourth method again gives acceptable accuracy.

USE OF A COMPUTER FOR DIGITAL RELAYING

By adopting suitable algorithms as have been described a mini-computer with modest storage but fast cycle time (1μs on the PDP 15) can be used to calculate fault impedances for protection purposes. Even if such a device is not acceptable for main protection purposes it would be very useful for locating the position of faults on long lines and perhaps to provide a back-up protection feature. In any case, if given access to the appropriate waveforms, it could prepare comprehensive fault reports which include fault types, location, event sequences etc., and such a tool would be invaluable to operating and maintenance engineers.

Using small process computers, improvements on conventional distance relaying techniques can be made because provision of a quadrilateral characteristic and 3 zone protection presents no problem. The sides of the quadrilateral can be adjusted by program, the discrimination between a power swing and genuine fault can be obtained by successive calculation of R and L and even high resistance faults can be located if communication channels to adjacent substation computers are installed. In addition, the problems involved with conventional analog relays in dealing with residual compensation for single-phase to ground faults no longer exist. It has been shown[9] that the assumption that the coefficient $\frac{Z0 - Z1}{Z1}$ is real causes a large error in conventional impedance measurement whereas this coefficient appears as $\frac{L0 - L1}{L1}$ and $\frac{R0 - R1}{R1}$ in the digital relay, both of course being real. The method proposed can also deal with untransposed lines if equation (4) is implemented in full. In practice this adds very little to the calculation time because much of the delay occurs in waiting for the samples to be taken.

One area that needs further investigation is that of determining the best combination of analog and digital filters to apply in each particular case.

Off-line Fourier analysis of voltage and current waveforms for the line simulated in section 3 has shown that there is no discernible pattern in the occurance of dominant harmonics for faults of varying types at

different distances from the relaying point. From Fig. (2) it is obvious that the voltage waveform is the worst affected and care with the selection of a filter on the output of the voltage transducer would be most beneficial.

The method requires further development for application to particular systems which may require consideration to be given to pre-fault loadings, remote end infeed and parallel lines with strong mutual couplings. Most of these conditions are well known in present relaying practice and the methods used in analog relaying to obtain the desired accuracy can be incorporated into the digital method.

CONCLUSION

The improved method of calculating resistance and inductance to the fault by a digital processor as proposed in this paper can in theory compete with conventional relaying techniques in speed and accuracy. It filters out the low order harmonics and to the authors knowledge it has not been used before but it does require special consideration of the likely positions of fault. This needs careful thought to be given to the combination of analog and digital filter to be applied.

Further development will be necessary under simulated conditions and in an actual substation environment before an assessment of such factors as reliability and cost can be made.

ACKNOWLEDGEMENT

The authors gratefully acknowledge the financial assistance provided by the Science Research Council in the pursuance of this work. A. M. Ranjbar is indebted to the British Council for his research scholarship.

REFERENCES

[1] E. B. Davison and A. Wright, "Some factors affecting the accuracy of distance-type protective equipment under earth fault conditions", Proc. IEE *110*, No. 9, September, 1963, pp. 1678-1685.

[2] W. A. Lewis and L. S. Tippet, "Fundamental basis for distance relaying on 3-phase systems", AIEE Transaction Vol. 66, 1947, pp. 694-709.

[3] G. R. Slemon and S. D. T. Robertson and M. Ramamoorty, "High speed protection of power system based on improved power system models" (CIGRE, paper No. 31-09, 1968).

[4] G. D. Rockefeller and E. A. Udren, G. Gilcrest, "High speed distance relaying using a digital computer" Parts I and II, IEEE T-PAS-91, No. 3, May/June 1972, pp. 1235-1258.

[5] B. J. Mann, and I. F. Morrison, "Relaying a three-phase transmission line with a digital computer", IEEE PAS-90, No. 2, March/April 1971, pp. 742-750.

[6] B. J. Mann and I. F. Morrison, "Digital Calculation of Impedance for transmission line protection," IEEE PAS-90, No. 1, Jan./Feb. 1971.

[7] B. E. McInnes and I. F. Morrison, "Real time calculation of resistance and reactance for transmission line protection by digital computer", IEA (Australia) March 1971, p. 16.

[8] R. Poncelet, "The use of digital computers for network protection", (CIGRE, paper No. 32-08 1972).

[9] W. D. Humpage and M. S. Kandil, "Measuring accuracy of distance protection with particular reference to earth fault conditions on 400 kv looped-circuit interconnection", IEE, 117, No. 2, Feb. 1970, pp. 431-438.

[10] Couch, Dewsnap, McInnes, Mann, Morrison and Sykes, "Application of Digital Computers to Protection, Switching and Metering", IEE Conference, Bournemouth, England, May, 1970.

APPENDIX

Symbol Definition

V_a, V_b, V_c	Phase voltages p.u., complex.
v_a, v_b, v_c	Phase voltages p.u., instantaneous.
I_a, I_b, I_c	Phase currents p.u., complex.
i_a, i_b, i_c	Phase currents p.u., instantaneous.
I_1, I_0	Positive and zero sequence currents p.u. complex.
i_1, i_0	Positive and zero sequence currents p.u. instantaneous.
Z_s-, Z_m-	Self and mutual impedances, p.u./mile.
Z_1, Z_0	Positive and zero sequence impedances p.u./mile.
R_1, L_1	Positive sequence resistance and inductance p.u./mile.
x	Distance between transducers and fault point in miles.
R, L	$R = xR_1$, $L = xL_1$
ϵ	Error
t_i, t_j	Time intervals

Transmission Line and Source Simulation Date

Base data	230KV, 100MVA	
Line parameters:		
Positive sequence resistance	0.223×10^{-3}	p.u./mile
Zero sequence resistance	1.226×10^{-3}	p.u./mile
Positive sequence inductive reactance	$j0.123 \times 10^{-2}$	p.u./mile
Zero sequence inductive reactance	$j0.320 \times 10^{-2}$	p.u./mile
Positive sequence capacitive reactance	-j420	p.u./mile
Zero sequence capacitive reactance	-j714	p.u./mile
Source impedance:		
Positive sequence reactance	j0.35	p.u.
Positive sequence resistance	0.033	p.u.

Discussion

A. G. Phadke, T. Hlibka, and M. Ibrahim (American Electric Power Service Corporation, N.Y.): We have read the authors' paper with a great deal of interest. Our own work in this area started with the algorithms described in the authors' references 4, 5, and 6. We will present our results in greater detail in a forthcoming paper; for the present we would like to confine ourselves to a few observations on the techniques used in this paper.

It would be interesting to know some details of the simulation program used by the authors to generate the waveforms of their Figures 1 and 2. In particular, we would be interested in knowing the modeling techniques of ground mode damping. We have found that unless care is exercised in setting up the model, the computer generated waveforms – especially after the first few reflections depart considerably from the waveforms obtained in practice. Evaluating fault impedance algorithms based on such waveforms leads to a performance which is far too erratic. We have redrawn in our Figure 1 a field oscillogram of a line-to-ground fault on our 765 KV line (125 miles) and it can be seen that qualitatively both the current and voltage waveforms are much smoother than the authors' Figures 1 and 2 would indicate. In our own work, we tend to test most of our algorithms on the waveforms generated by a model.

We would also like to know whether the waveforms of Figures 1 and 2 were filtered to band-limit the signals presented to the sampler below the Nyquist frequency. With the somewhat slower sampling rate we are using (12 times per cycle), we have found that the required analog filtering produces a delay of about 1.2 millisecond which we consider to be quite acceptable. Such a filter also renders harmonics beyond the 7th quite insignificant.

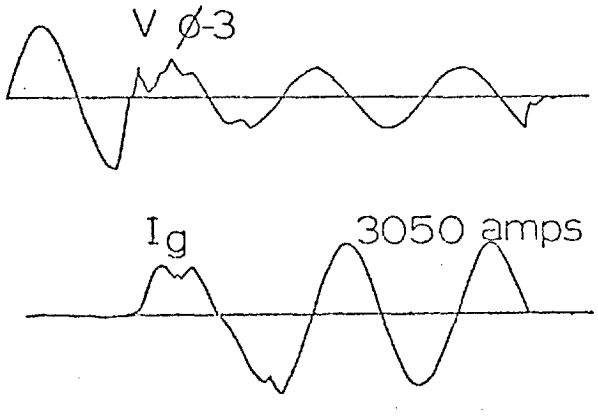

Fig. 1

Manuscript received August 2, 1974.

We note the authors comment that the algorithms using derivatives are prone to harmonic amplification. We would like to know the authors' views on the discussion of their reference 6, where it is shown that at the sampling rates being considered, the algorithms using derivatives perform almost identically to those using integrals.

Next, we would like to summarize our experience with algorithms which seems to parallel the authors'. The simplest algorithms using a quantity and its derivative (or the first and the second derivative, or the first derivative evaluated at two points) without any smoothing perform as poorly as the authors' method 1. The techniques which use an n'th order least-square-fit polynomial on m points ($n < m$) as a digital filter, perform almost as poorly when the previous algorithms are used on the filtered data. We think this procedure is quite similar to the authors' methods 2 and 3. Digital filtering (in the conventional sense) gives the most satisfactory results.

In applying the conventional digital filter equations (as in all others) the exponentially decaying dc offset must be compensated for. This is quite easily done by a preprocessor to the digital filter. In this sense, the authors method deserves attention as it directly accounts for the dc offset. We wonder whether the authors have tested their algorithm on data where the fault path included an arc whose resistance is variable.

Finally, the authors' point about the ratio $(Z_0-Z_1)/Z_0$ not being a real number is well taken. In many cases the ground relaying is not of the impedance type, and this poses no serious problem. Even when impedance relays are used for ground protection, currently available conventional relays permit an adjustment in this factor only within the nearest 10%. The complex factor must be taken into account if its effect is found to be significant.

G. H. Couch and J. A. Dembecki (Electricity Commission of New South Wales, Australia): The paper describes techniques for relaying transmission lines by impedance measurement, assuming a line model of the form

$$v = Ri + L\frac{di}{dt}$$

This model overcomes the disadvantages of earlier models which assumed sinusoidal voltages and currents. However, the model used ignores the fact that the transmission line is distributed and the effects of shunt capacitance.

The authors are to be congratulated for designing an elegant technique in which the effects of certain high frequency components can be eliminated in the measurement of impedance assuming a simple first order model. The results quoted are indicative of the power of the technique. Further comments on the following aspects would be of interest.

1. The noise which occurs in the voltage and current signals may cover a continuous frequency spectrum and not simply consist of discreet harmonics of the power system nominal frequency. It is essential that the elimination of some frequencies does not result in the accentuation of others. Have the authors analyzed this possibility?

2. The discussion of the mode of simulation of the system whether by digital computer or using an analog model would be of interest.

3. The accuracy of each of the methods described in the paper is a function of:

   (a) The fault data acquisition time interval.

   (b) The sampling frequency.

In this respect the results of the methods appear to be given for different values of these parameters. The longer times used for method 4 if available for methods 1, 2, and 3, could be expected to reduce the differences in accuracy quoted. An explanation of the reasons for treating the methods differently would assist evaluation of the technique proposed.

Manuscript received July 25, 1974.

A. M. Ranjbar and B. J. Cory: We wish to thank the discussers for their comments and kind remarks on our technique. As a general point our off-line simulation using a CDC 6600 digital computer was taken largely from ref. 3 of our paper supplemented by techniques described in Uram and Miller[A] and Subramaniam and Malik[B]. The waveforms obtained tend to be idealistic and neglect the effects of random and non-predictable parameters such as arc-resistance variations, sensitivity of zero-sequence impedance to earth resistivity and changes in mutual coupling between parallel circuits due to varying power flows. However, the simulation does allow the merits of different algorithms to be compared on the same basis and, for any particular application, studies should be made involving these parameters. We have not done any such studies to date.

In reply to Messrs. Couch and Dembecki our technique does not result in amplification of some frequencies during the elimination of others. In fact, all harmonics above the fundamental are attenuated as the following analysis will show.

Consider the equation

$$sv = \int_0^{\pi} v\,dt + \int_{\pi/3}^{\pi+\pi/3} v\,dt \qquad (a)$$

Using the trapezoidal rule and with 30 samples per cycle in a 50Hz system, sv can be calculated as

$$T.sv = \left(\frac{v_1}{2} + v_2 + \ldots\ldots\ldots v_{15} + \frac{v_{16}}{2}\right) + \left(\frac{v_6}{2} + v_7 + \ldots\ldots\ldots v_{20} + \frac{v_{21}}{2}\right) \qquad (b)$$

where T is the sample period and v_1, v_2 etc. are the samples of voltage taken at evenly spaced time periods. Equation (16) of our paper shows that using equation (a), the second and third harmonics as well as their multiples will be eliminated using this technique. The effect on harmonics which are *not* multiples of the second and third can be found by the z-transform technique using a general form of equation (b) as follows:-

$$T.sv_k = \left(\frac{v_{k-20}}{2} + v_{k-19} + \ldots\ldots\ldots v_{k-6} + \frac{v_{k-5}}{2}\right) + \left(\frac{v_{k-15}}{2} + v_{k-14} + \ldots\ldots\ldots v_{k-1} + \frac{v_k}{2}\right) \qquad (c)$$

where $T.sv_k$ is the kth value and requires the kth sample of v and 20 samples before it. If desired, $T.sv_k$ can be calculated for each new set of samples continuously by adding the newest sample and subtracting the oldest during each sample period. Equation (c) has the form of a non-recursive digital filter and its z-transform is:

$$H(Z) = \frac{T.SV(Z)}{V(Z)} = \left(\frac{Z^{-20}}{2} + Z^{-19} + \ldots\ldots\ldots Z^{-6} + \frac{Z^{-5}}{2}\right) + \left(\frac{Z^{-15}}{2} + Z^{-14} + \ldots\ldots Z^{-1} + \frac{1}{2}\right)$$

$$\text{giving } H(Z) = \frac{(1+Z^{-5})(1+Z^{-1})(1-Z^{-15})}{(1-Z^{-1})} \qquad (d)$$

The frequency response of equation (d) is then given by:

$$H(j\omega) = \left[\frac{4\cos\frac{\omega T}{2}\cos\frac{5\omega T}{2}\sin\frac{15\omega T}{2}}{\sin\frac{\omega T}{2}}\right]\exp(-j10\omega T) \qquad (e)$$

The amplitude of this function has been plotted in figure 1 and it can be seen that it effectively attenuates both integer and non-integer harmonics.

Surprisingly, the apparently simple addition required to evaluate equation (b) has a very sharp cut-off characteristic which is impossible to obtain with an analogue filter without considerable delay. It should be noted from fig. 1 that the d.c. component and all sub-harmonics have been amplified. In fact the d.c. component can be regarded as providing valuable information for fault identification and is accounted for in the

Manuscript received November 18, 1974.

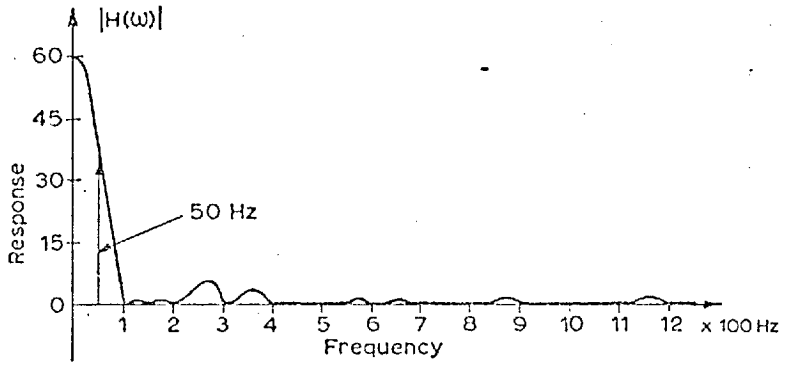

Fig. 1 Amplitude characteristic of filter.

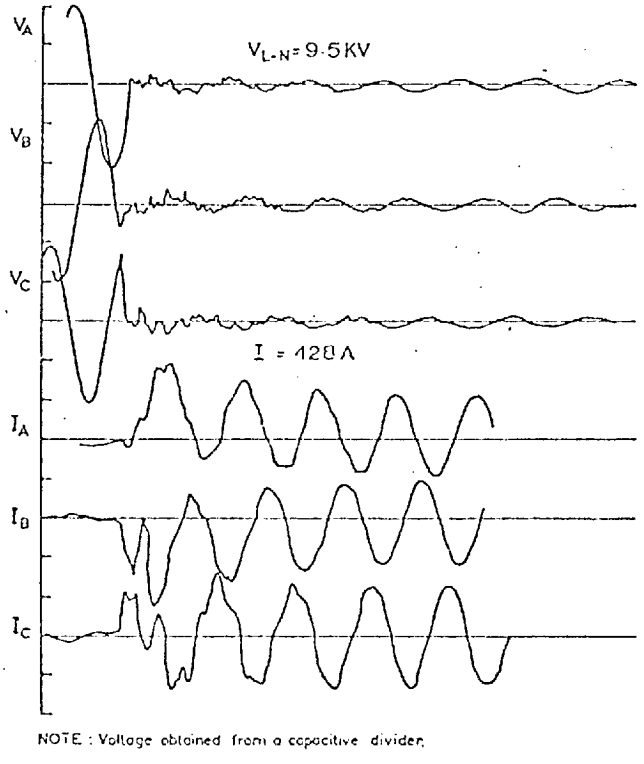

Fig. 2. Field oscillogram for 3 phase fault on long line.

choice of algorithm which uses $v = Ldi/dt + Ri$ as the basis for calculation.

Equation (b) should be compared with a full Fourier analysis technique which would involve taking samples generally over a full cycle and employing many multiplications unless the Fourier algorithm is based on a square wave orthogonal function. Our method can respond with less samples if the fault is severe. Reduction in the number of samples per cycle is possible with minor degradation of performance and the limits of this are now being investigated. Our experience shows that the accuracy of methods 1 to 3 cannot reach that of method 4 even with a greater number of samples. The second integration term adjusts the cut-off frequency and produces a sharp characteristic which depends on the lowest harmonic removed. The cut-off can also be varied by adjusting the interval of the second integral.

In reply to Messrs. Phadke, Hlibka and Ibrahim, the smoothness of the current and, particularly, the voltage waveform depend upon generator source reactances and transmission line length. For a high reactance source and long line considerable distortion occurs as is born out by a field oscillogram reproduced in figure 2 for a 3 phase fault.

It will be noted that the current waveforms are similar to our simulation during the first fault cycle and the voltages exhibit considerable noise although in this case such noise could be attributed to the use of a capacitor-divider voltage transducer.

We agree that in many cases a band limiting analogue filter can be used and that perhaps a 1.2 ms delay is acceptable. Our simulated waveforms were not band-limited but the nature of the lumped constant simulation (see ref. 3 of our paper) does tend to limit the frequency response of the line.

In connection with the discussion of ref. 6, it has been shown that for the simple case of $v = v_p \sin \omega t$ waveform both differentiation and integration give the same result which can be understood intuitively. However, the difference between these two methods is apparent when harmonics are present because differentiation must accentuate them but integration can be used to provide attenuation when the technique is correctly chosen. A method which uses a quantity and its derivative cannot be satisfactory because it is not able to account for d.c. off-set even if noise and harmonics are neglected. Even first and second derivative methods involve considerable numerical calculation error which make the result unacceptable for long lines. The use of a simple digital filter would considerably improve the accuracy and could be used for all the methods given in our paper but would also involve an extension to the fault detection time. By the continuous calculation of resistance and inductance after each new set of samples is obtained, a reduction in fault detection times is achieved, which is particularly marked for close-up faults.

Finally, the approximation involved in using the scalar value for $(Z_0 - Z_1)/Z_1$ in residual compensation schemes introduces error in both resistance and inductance calculations. This error depends upon the pre-fault load condition and the source impedances. For high source impedance the resistance error may reach 8% and the inductance error 4%.

REFERENCES

[A] R. Uram, R. W. Miller: "Mathematical analysis and solution of transmission line transients" AIEE Transactions Vol. *83*, 1964, p. 1116.

[B] P. Subramaniam, O. P. Malik: "Digital simulation of a synchronous generator in direct phase quantities", Proc. I.E.E., Vol. 118. No. 1. Jan. 1971.

International Conference on

Developments in Power System Protection

11 - 13 March 1975

Organised by the

Power and Control and Automation Divisions of the
Institution of Electrical Engineers

in association with the

Institute of Electrical and Electronics Engineers
(United Kingdom and Republic of Ireland Section)

Venue

Institution of Electrical Engineers, Savoy Place, London WC2

ALGORITHMS FOR DISTANCE PROTECTION

A.M. Ranjbar and B.J. Cory

1. Introduction

Several methods have been published[1,2,3,4] for the digital calculation of transmission line fault impedance using a mini-computer on-line. All methods rely on sampling and storing voltage and current waveforms at a single measurement or relaying point. For measurement purposes, the most onerous condition is when a fault occurs at a voltage maximum on one phase because the consequent discharge of capacitive energy through the line inductance causes harmonics to be generated in the current and voltage. In addition, noise and non-linearity of the transducers result in further harmonics against which any algorithm used to calculate fault impedance should be immune.

This paper examines and compares three algorithms suitable for fault impedance measurement, with particular reference to their accuracy and speed of calculation. These algorithms have been chosen because of their ability to deal with low order harmonics.

2. Fourier Technique

Using a hardware sample/hold technique it can be shown that with N samples per fundamental cycle, harmonics not of order K x N ± 1 can be filtered out by a suitable digital technique, where K is an integer taking values from 1 to ∞. However, an analogue filter on the input to each sample/hold circuit can attenuate high order harmonics, leaving the low orders 2,3,4 etc. to be eliminated by digital means. It is convenient for hardware design to use 8, 16 or 32 samples per fundamental 50 Hz cycle thus allowing the possibility of eliminating everything below the 7th, 15th or 31st harmonic. One method is as follows:

Assume the fundamental components of voltage and current waveforms are

$$\left.\begin{aligned} v &= V_p \sin(\omega t + \phi + \delta) = A_v \sin \omega t + B_v \cos \omega t \\ i &= I_p \sin(\omega t + \delta) = A_i \sin \omega t + B_i \cos \omega t \end{aligned}\right\} \quad \ldots\ldots\ldots\ldots (1)$$

In complex form

$$\left.\begin{aligned} V &= A_v + j B_v \\ I &= A_i + j B_i \end{aligned}\right\} \quad \ldots\ldots\ldots\ldots\ldots\ldots\ldots\ldots\ldots\ldots (2)$$

Hence

$$Z = \frac{V}{I} = R + jX = \frac{A_v A_i + B_v B_i}{A_i^2 + B_i^2} + \frac{B_v A_i - A_v B_i}{A_i^2 + B_i^2}$$

$$\text{or } R = \frac{A_v A_i + B_v B_i}{A_i^2 + B_i^2} \quad \text{and } X = \frac{B_v A_i - A_v B_i}{A_i^2 + B_i^2} \quad \ldots\ldots\ldots\ldots (3)$$

A.M.Ranjbar is at Imperial College, London, SW7 2BT.
B.J. Cory is at Imperial College, London, SW7 2BT.

If A_v, B_v, A_i and B_i are calculated for each phase, the impedance of a transmission line seen from a single relaying point can be determined.

Now using Fourier analysis, we have that

$$A_v = \frac{2}{T}\int_{t_o}^{t_o+T} \omega . v \sin \omega t \, d(\omega t), \quad B_v = \frac{2}{T}\int_{t_o}^{t_o+T} \omega . v \cos \omega t \, d(\omega t)$$

$$A_i = \frac{2}{T}\int_{t_o}^{t_o+T} \omega . i \sin \omega t \, d(\omega t), \quad B_i = \frac{2}{T}\int_{t_o}^{t_o+T} \omega . i \cos \omega t \, d(\omega t) \qquad .....(4)$$

where T is the period of the fundamental and t_o is an arbitrary time from which to start the calculation. By using the trapezoidal rule (which produces less manipulations than Simpsons rule with the same accuracy in this case) the values of A_v, A_i, B_v and B_i can be calculated from N samples per cycle as follows:

$$A_v = \frac{1}{N}\left[v(t_o) \sin \omega t_o + 2\, v(t_o + \frac{T}{N}) \sin \omega(t_o + \frac{T}{N}) + \ldots\right.$$

$$\left.\ldots + 2v(t_o + \frac{N-1}{N}.T) \sin \omega(t_o + \frac{N-1}{N}.T) + v(t_o+T) \sin \omega(t_o+T)\right]$$

and $$B_v = \frac{1}{N}\left[v(t_o) \cos \omega t_o + 2v(t_o + \frac{T}{N}) \cos \omega(t_o + \frac{T}{N}) + \ldots\ldots\right. \qquad (5)$$

$$\left.\ldots + 2v(t_o + \frac{N-1}{N}.T) \cos \omega\,(t_o + \frac{N-1}{N}.T) + v(t_o+T) \cos \omega\,(t_o+T)\right]$$

where $v(t_o)$, $v(t_o + \frac{T}{N})$.... are evenly spaced samples of voltage. Similar equations can be written for A_i and B_i.

The method shown has the property that the harmonics not filtered remain without change in magnitude. Its disadvantage is that samples taken over one cycle of fundamental are required before R and X can be determined. However, by adding the newest sample as it is measured into A_v, B_v etc. and discarding the oldest, an updated value can always be readily obtained so that the change in R and X can be tracked. If a close up fault occurs, the new samples will be radically different from the old and R and X will move rapidly into the fault zone. With a typical 400 kV, 100 mile long system fed from generators and transformers having the parameters given in Table I and fig. 1, figs. 2 and 3 show the tracking of X and R for various 3 phase fault conditions using 16 samples per cycle in an off-line study. It can be seen from the movement of the line reactance and resistance into the tripping zone that a close up fault at end A can be detected in less than ½ cycle (10ms) whereas a fault near the far end would take at least 3/4 cycle (15ms). Faults in transformer I and on the neighbouring line do not cause X and R to reach the tripping zone simultaneously.

The following sections consider some typical faults in more detail.

2.1 Close-up faults

The import and export of power can cause different values of R and X to be measured. Fig. 4 shows the tracking of X for a three phase solid fault close to end A on line L1. If the fault is inside the distance zone, the

reactance reaches near zero from the positive side for both import and export of power. When the fault is outside the protected zone, the reactance approaches from the negative side. It is obviously important to track the direction of X towards the tripping zone, otherwise incorrect tripping could occur.

2.2 Phase-to-phase and phase-to-earth faults

To avoid having to calculate six impedances (3 phase-phase and 3 phase-earth) after each set of samples, time can be saved by first calculating the zero sequence or residual current. If the residual is greater than a predefined value, only phase-to-earth impedances are calculated and if it is less, only phase-to-phase impedances are determined. Residual compensation, as used in analogue form on conventional distance relays, is applied for phase-to-earth faults in the calculation. With phase-to-phase faults, delta currents and voltages are computed from the measured values.

To ensure reliable tripping, three successive calculations using at least three new sample values are required to be within the trip zone to initiate a trip signal using the algorithm.

2.3 Double circuit lines

In the double circuit case, the mutual reactance between the lines should be included in the impedance calculation. However, with measurements at only one end, overreaching occurs in the digital method as with the conventional analogue relay[5]. The only solution, other than a fast data link between the ends of each line, is to reduce the reach and to use an intertripping signal. It may be advantageous to utilise an existing data link to coordinate fault measurements at the line ends, in special circumstances.

2.4 Quadrilateral characteristic

One of the advantages of the digital method is that the trip zone can be altered to account for the pre-fault flows on the protected line. A characteristic can be defined as in fig. 5 by the points A, B and C, so that R and X must satisfy the following inequalities:

$$X > 0\,, \quad R > 0\,, \quad X < X_b\,, \quad X + K_1 R > K_2 \qquad \ldots\ldots\ldots\ldots (6)$$

where $K_1 = \dfrac{-X_b}{R_b - R_c}$ and $K_2 = \dfrac{-X_b R_c}{R_b - R_c}$.

R_b, X_b and R_c can be varied depending upon a defined relationship with pre-fault P and Q flow measured on the line (by sampling or otherwise). This flexibility enables the largest tripping zone to be maintained for both directions of power flow. Zones 2 and 3 can be bounded in a similar manner.

2.5 Sampling rate

In the method described, the maximum useful sampling rate is dependent, among other things, on the speed of calculation of R and X and their comparison with pre-set values. At least 33 multiplications and 6 divisions are necessary taking at least 1050μs on the PDP 15 computer. With A/D conversion and housekeeping procedures at least another 500 μs are necessary so that 8 samples per cycle is about the fastest feasible rate. Consequently, an analogue filter cutting-off at around 350 Hz is necessary to ensure good performance.

3. Square wave correlation

To reduce the amount of arithmetic in the calculation of R and X, othogonal functions based on the square waves of fig. 6 can be used[1]. (Note that the technique of section 2 employs sine and cosine waveforms as orthogonal functions). With square waves, the values of A_v and B_v can be calculated as

$$A_v = \frac{1}{4}\int_0^{\pi} V\, d(\omega t) - \frac{1}{4}\int_{\pi}^{2\pi} V\, d(\omega t)$$

$$B_v = \frac{1}{4}\int_0^{\pi/2} V\, d(\omega t) - \frac{1}{4}\int_{\pi/2}^{3\pi/2} V\, d(\omega t) + \frac{1}{4}\int_{3\pi/2}^{2\pi} V\, d(\omega t) \qquad \text{.....(7)}$$

With harmonics up to order n present, the integrations of (7) theoretically should result in:

$$A_v = A_{v1} + \frac{1}{3} A_{v3} + \frac{1}{5} A_{v5} + \text{.....} \frac{1}{2n+1} A_{v2n+1}$$

$$B_v = B_{v1} - \frac{1}{3} B_{v3} + \frac{1}{5} B_{v5} - \text{.....} (-1)^n \frac{1}{2n+1} B_{v2n+1} \qquad \text{.....(8)}$$

where A_{v1}, A_{v3} and B_{v1}, B_{v3} are the associated parameters of the fundamental, third harmonic etc. Equations 8 show that this method filters out the d.c. component A_{vo} and B_{vo}, and all the even harmonics whilst attenuating the odd harmonics in inverse proportion to their orders. By using the trapezoidal rule on (7) with N samples per fundamental cycle, it can be shown that

$$A_v = \frac{\pi}{N} \cot \frac{\pi}{N} \left(A_{v1} + \frac{\tan \pi/N}{\tan 3\pi/N} A_{v3} + \text{.....} + \frac{\tan \pi/N}{\tan \frac{(2n+1)\pi}{N}} A_{v2n+1} \right)$$

$$\text{and } B_v = \frac{\pi}{N} \cot \frac{\pi}{N} \left(B_{v1} - \frac{\tan \pi/N}{\tan \frac{3\pi}{N}} B_{v3} + \text{.....} (-1)^n \frac{\tan \pi/N}{\tan \frac{(2n+1)\pi}{N}} B_{v2n+1} \right) \qquad (9)$$

With $N = \infty$, equations (9) reduce to equations (8). The coefficients of these equations are constants depending upon the sampling rate chosen.

As with the method of section 2, even harmonics are removed but in this case all odd harmonics are either attenuated somewhat or come through unaltered. The algorithm can be applied in the same way using a running total for the calculation of A_v and B_v etc. as each new set of samples is taken. Its main advantage is that it requires 12 less multiplications so saving on computer time, but its accuracy is impaired by the presence of odd harmonics.

4. Harmonic filtering method

This method has been discussed by the authors in some detail in reference 4. It consists of the simultaneous solution of two equations of the form $L\frac{di}{dt} + Ri = v$ taken at successive intervals of time so that the inductance to the fault, L and the resistance R can be calculated.

By using several successive samples, any desired harmonic can be removed although in this case the sampling rate must be a multiple of the unwanted harmonic. The simplest form of the equations are obtained by considering four samples taken at time intervals, t_1, t_2, t_3 and t_4 as follows:

$$L\int_{t_1}^{t_2}\left(\frac{di}{dt}\right)\,dt + R\int_{t_1}^{t_2} i\,dt = \int_{t_1}^{t_2} v\,dt$$

$$L\int_{t_3}^{t_4}\left(\frac{di}{dt}\right)\,dt + R\int_{t_3}^{t_4} i\,dt = \int_{t_3}^{t_4} v\,dt \qquad \text{.....(10)}$$

The integral terms can again be computed by the trapezoidal or Simpson's rule as before.

The accuracy of the method has been discussed in reference 4 and depends upon the harmonics eliminated and the magnitude of the remaining harmonics in the waveform. It has the advantage that samples need only be taken over a portion of the waveform before a trip signal can be determined. On the PDP 15 the algorithm takes about 500 μs for execution using four sets of samples previously obtained.

5. On-line tests and conclusions

Using part of the simulator described in a companion paper[6], on-line tests were performed to check the accuracy of the algorithms. A three-phase 400 kV, 100 mile long transmission line was modelled by four - L sections which were sufficient to generate a number of low order harmonics when faults were simulated towards the line end. A micro-machine was used to model a 1300 MW source. From many tests with different types of fault, the results of a double-phase to earth fault are shown in figs. 7a and b where the calculated values of reactance and resistance to the fault are tracked using the three methods discussed in this paper. The superior accuracy of the Fourier technique is evident, followed by square wave correlation. Although the harmonic filtering method shows some variations due to unfiltered harmonics, this method's speed of calculation may, however, be the deciding factor in its favour for practical implementation.

6. Acknowledgement

The authors are grateful to the Science Research Council for their financial support and to the British Council, and Arya-Mehr University of Technology, Tehran, Iran for a scholarship for A.M. Ranjbar to study at Imperial College.

7. References

1. Hope G.S. and Umamaheswaran V.S. : Sampling for computer protection of transmission lines. IEEE paper TP74-034-5 Winter Power Meeting, New York, January 1974.

2. Slemon G.R., Robertson S.D.T. and Ramamoorty M. : High speed protection of power systems based on improved models. CIGRE paper 31-09, 1968.

3. Mann B.J. and Morrison I.F. : Digital calculation of impedance for transmission line protection. IEEE PAS-90 No. 1, Jan/Feb.1971.

4. Ranjbar A.M. and Cory B.J. : An improved method for the digital protection of high voltage transmission lines. IEEE paper TP74 380-2. Summer Power Meeting, Anaheim, July 1974.

5. Davison, E.B. and Wright, A. : Some factors affecting the accuracy of distance-type protective equipment under earth-fault conditions. PROC. IEE, Vol. 110, No. 9, September 1963 pp.1678-1688.

6. Horne E.and Cory B.J. : Digital processors for substation switching and control. IEE Conference on "Modern Developments in Protection" March, 1975.

TABLE I : System data (on 1000 MVA base)

Equipment	Positive and negative sequence reactance per unit ohm	Zero sequence reactance per unit ohm
Generators 1, 11 kV	0.1	0.08
Transformers 1, 11/400 KV	0.1	0.08
Equivalent generators 2	0.04	0.06
Transformers 2	0.07	0.05
Transmission lines L1,L2 400 kV	Z =0.02 + j 0.276 (B =10.5x10^{-6}p.u.mho)	Z_o=0.104 +j0.794 (B_o=5.9x10^{-6} p.u mho)

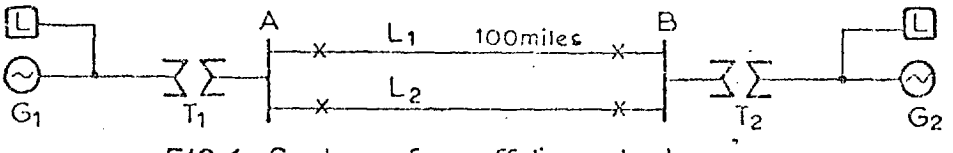

FIG.1: System for off-line study

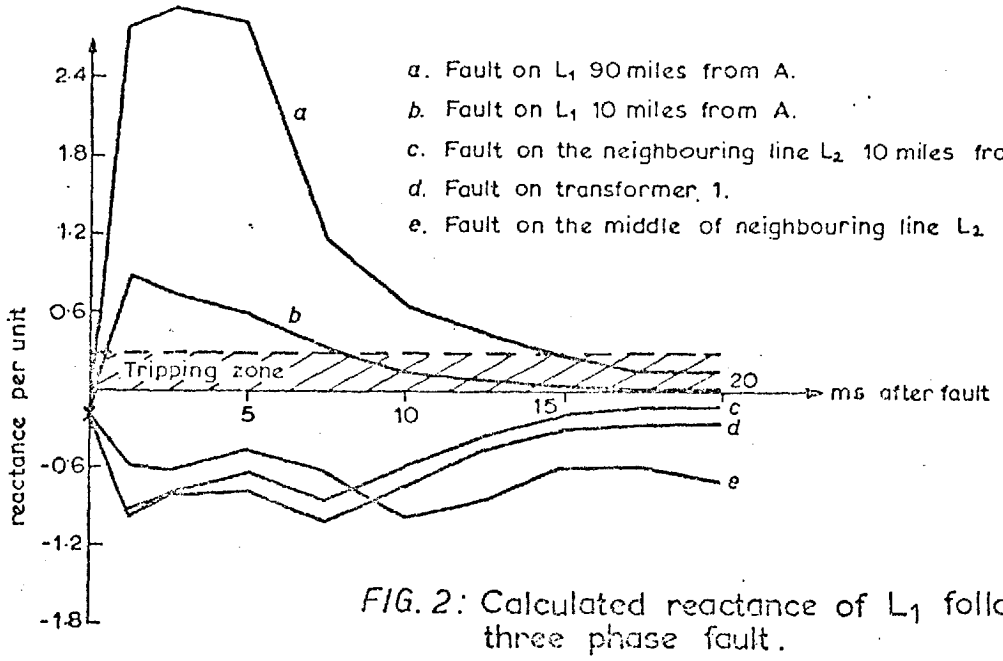

FIG. 2: Calculated reactance of L_1 following three phase fault.

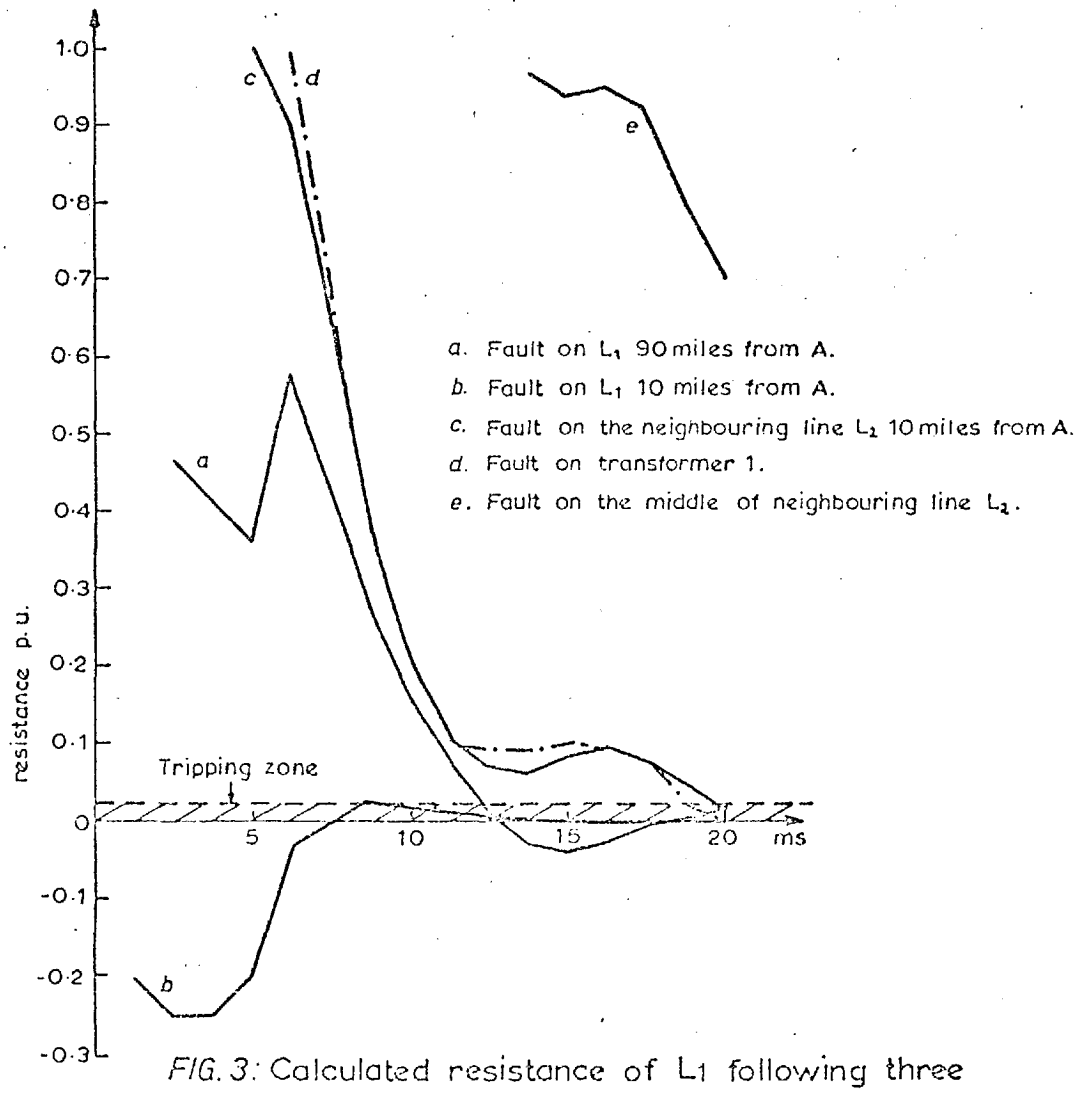

FIG. 3: Calculated resistance of L_1 following three phase fault.

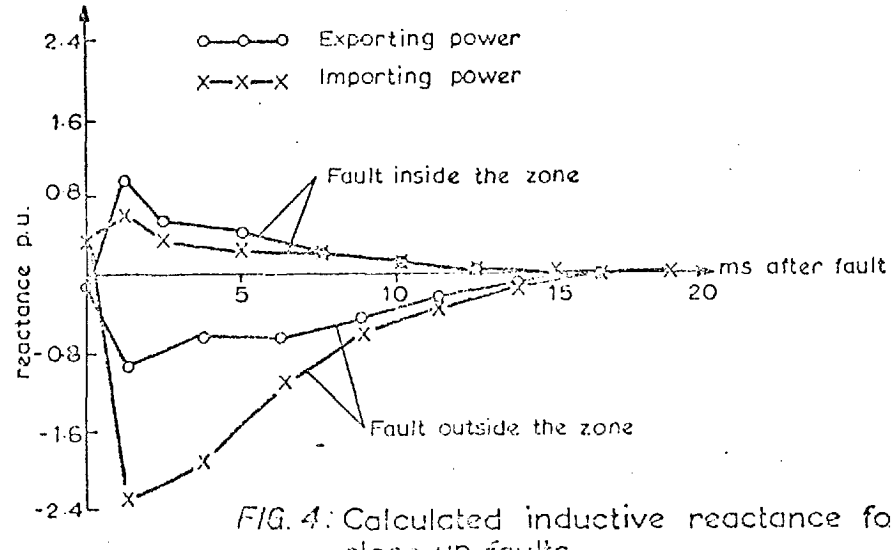

FIG. 4: Calculated inductive reactance for close up faults.

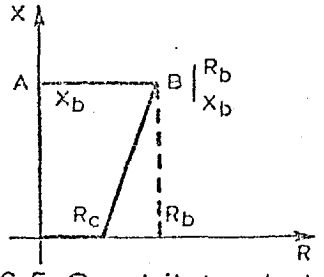

FIG.5: Quadrilateral characteristic

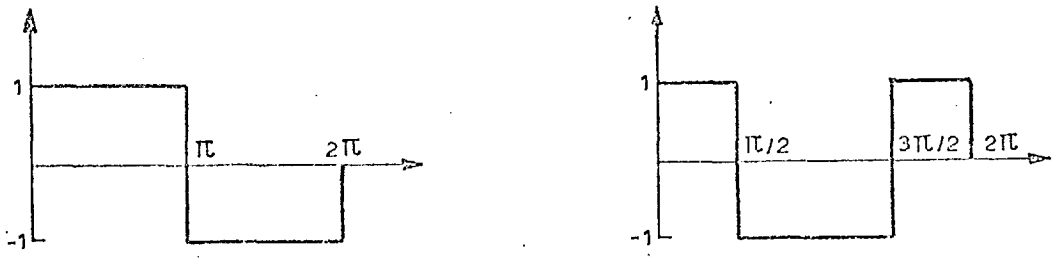

FIG.6: Orthogonal square waves.

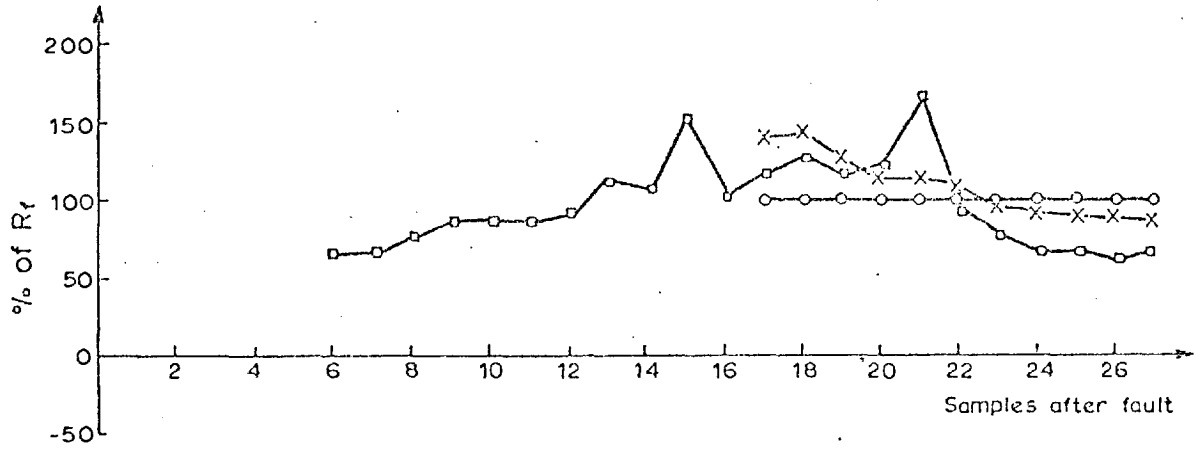

FIG.7a: Resistance for double phase fault.

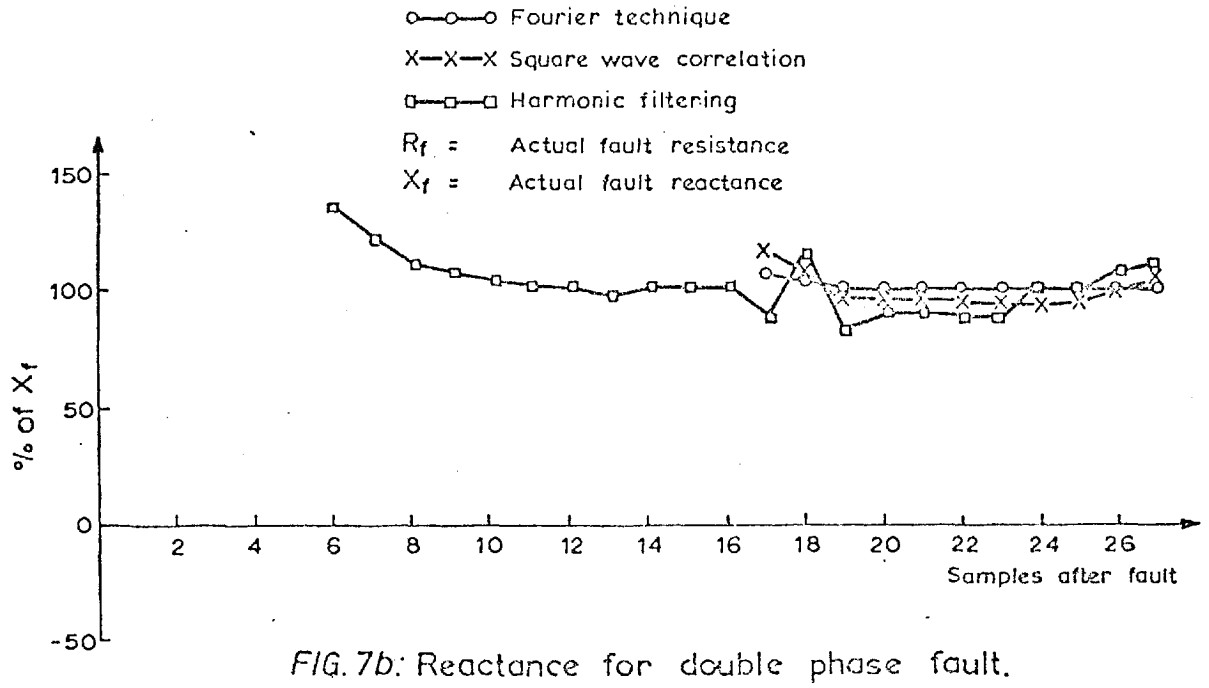

FIG.7b: Reactance for double phase fault.

IEEE WINTER POWER MEETING

NEW YORK 1974

Discussion on paper: Sampling for Computer Protection of Transmission Lines

by

G.S. Hope, V.S. Umamaheswaren

Discussion prepared by A.M. Ranjbar and B.J. Cory,

Imperial College, London S.W.7, England.

In large high voltage transmission lines considerable harmonics are generated in the first cycle following a fault due mainly to the shunt capacitance effects. In the case of the voltage waveform these harmonics can amount to more than 100% of the fundamental[3]. Consequently unless steps are taken to eliminate the harmonics, calculation of the line impedance by digital means will inevitably involve a large unacceptable error.

The authors have investigated in the frequency domain the sensitivity of previously published methods of digital protection (1968 and 1971)[1,2] to the current wave harmonics and have obtained results which are obvious by an intuitive understanding. The first method that the authors have analysed, is the one proposed by Slemon et al[2] based on the calculation of fundamental components of the voltage and current waveforms by the Fourier technique which requires evenly spaced samples taken over a complete cycle at the system frequency. From the fundamental components the impedance magnitude and angle, from the relaying point can be calculated. After analysing this method in the frequency domain the authors have reached the conclusion that it has a high rejection to d.c. and to the higher order harmonics. It is well known that by the Fourier technique we can obtain the fundamental and filter out all harmonics as well as the d.c. component, and hence investigation of this method in the frequency domain does not add to knowledge. The authors then propose that in place of the sine and cosine function, other orthogonal functions are used and as an example they have investigated the employment of even and odd square waves. They have obtained the not

unsurprising result that square functions do not reject the harmonics but only tend to limit them. There exists, however a large number of sets of mutually orthogonal functions[4] but it can be seen that to obtain the fundamental component the sine and cosine function only are applicable. The last method investigated is that proposed by MANN and MORRISON[1]. In this method the voltage and current peak are calculated as follows:

$$v = V_p \sin \omega t$$
$$v' = \omega V \cos \omega t \quad \ldots\ldots\ldots\ldots\ldots (1)$$
$$i = I_p \sin (\omega t + \phi)$$
$$i' = \omega Ip \cos (\omega t + \phi) \ldots\ldots\ldots\ldots (2)$$
$$V_p^2 = v^2 + \left(\frac{v'}{\omega}\right)^2$$
$$I_p^2 = i^2 + (i'/\omega)^2$$

from which the impedance can be calculated as:

$$z^2 = V_p^2/I_p^2$$

and also $\phi = \arctan (\omega i/i') - \arctan (\omega v/v')$.

The authors show that this method amplifies the harmonics. From the equations (1) and (2) it can be seen that differentiation amplifies the harmonics and this is why we believe that this method can not be used for protection in a real system because of inevitable existance of noise and harmonics. Orthogonal functions to be useful in digital protection schemes, must be chosen such that will eliminate or, at least severely attenuate the lower harmonics in the voltage and current waveforms. Such harmonics cannot be filtered by analogue means because the inherent delay in response of the filter slows the fault measuring

time unacceptably, and consequently a digital scheme using an integral method is thought to be most appropriate. If the authors could devise an orthogonal function which reduces the 3rd, 5th and 7th harmonics and still allow the fault to be measured with better than 10% error in less than half a cycle, they are in business.

REFERENCES

1. B.J. Mann and I.F. Morrison, "Digital calculation of impedance for transmission line protection" IEEE Trans. PAS, Vol.90, No: 1, pp. 270 - 78, January, 1971.

2. G.R. Slemon, S.D.T. Robertson and M. Ramamoorty, "High Speed protection of power systems based on improved power system models", Paper No: 31 p. 9, CIGRE, Paris, France, June, 1968.

3. B.J. Cory and A.M. Ranjbar, "The effect of fault generated harmonics on digital protection of HV transmission line.

4. B.P. Lathi, Communication Systems, John Wiley and Sons, Inc.

IEEE WINTER POWER MEETING

NEW YORK 1974

Discussion on Paper T74 - 032 - 9: High Speed Transmission Line Fault Impedance Calculation Using a Dedicated Mini-Computer

by

J.G. Gilbert and R.J. Shovlin

Discussion prepared by A.M. Ranjbar and B.J. Cory

Imperial College, London S.W.7, England.

In simulation sets # 2 and # 3 the authors have investigated the accuracy of their method in the presence of inrush current and third harmonic on the fundamental waveform. They admit that the calculated impedance was in error but they claim that the third harmonic content of fault currents within the response capability of the sensors would be sufficiently small to assure correct relay operation. For short transmission lines operating at low or medium voltages, neglecting the inherent non-linearity of transducers, the authors claim could be substantiated, but experience shows that for high voltage transmission lines especially of considerable length the shunt capacitance effect produces a large amount of harmonics on the voltage and current waveforms, particularly in the first cycle after fault occurrence. These harmonics in the case of a high source impedance can be more than 100% on the voltage waveform. Low order harmonics cannot be filtered out by analogue means because of the time delay in the response. By considering the existence of these harmonics we believe that all the methods which neglect the harmonic and the d.c. component of the waveform during fault occurrence cannot give acceptable results.

In simulation set # 5 the authors have calculated the output of a linear coupler using the equivalent circuit of Fig. (3). In computer relaying the output of the linear coupler is usually connected to sampling circuits through an operational amplifier and so the output impedance is very high and can be assumed open circuit. In Fig. (3) it seems that the output of the linear coupler is short circuited as for a C.T. and r2 is the resistance of the secondary

winding. If this is the case, then it is not clear what the voltage across r2 means. It is true that the linear coupler reduces the d.c. component relative to the fundamental but this reduction is not enough in order to neglect the d.c. component in digital calculation. Using linear couplers will cause an increase in noise and harmonics[1], due to inherent amplification of these quantities. Disregarding the harmonics in order to show the effect of the d.c. component of the fault current current and voltage waveforms on the accuracy of the authors' methods, we used it to calculate resistance and reactance of a three phase transmission line during a three phase fault. The results for several fault inception angles with respect to the voltage zero at phase a are given in Table A (the reactance of the line to the fault point was 1.5 ohm representing about 3 miles of 132kV line).

Table A

fault inception angle (Deg.)	calculated reactance (ohm)	Error %
0	5.91	294
20	1.93	28
40	1.67	11
60	1.57	5
80	1.51	1
100	1.46	2.2
120	1.41	5.6
140	1.35	9.7
160	1.37	8.4
170	4.36	191

It can be seen that large errors are involved under unfavourable conditions which would give a false indication unless other measures are taken to improve the accuracy of the computer relay.

We will be grateful if the authors would comment on the points we have raised and we look forward to further papers on their interesting and novel approaches to digital computer protection.

Reference

1. NELLIST, B.D., MATTHEWS, P. : The design of air cored toroids or linear couplers. Proc. IEE 1962 109 June pp 229-234.

IEEE WINTER POWER MEETING

NEW YORK 1975

Discussion on paper T75 0559: Frequency Domain Analysis Applied to Digital Transmission Line Protection

by

J. Carr and R.V. Jackson

Discussion prepared by A.M. Ranjbar and B.J. Cory,

Imperial College, London S.W.7, England.

The authors are to be complimented on establishing a method involving two orthogonal notch digital filters with sine characteristics from which the magnitude and phase angle of the fundamental component of a waveform can be calculated from samples taken at four equally spaced time intervals over a period. This method is the same as a Fourier technique with four samples per cycle. By using a Fourier series the real and imaginary parts of a phasor quantity can be calculated as follows:

$$\text{Real} = \frac{1}{\pi} \int_{\pi/2}^{2\pi+\pi/2} x. \quad \text{Sin}\ (\omega t)\ \ d(\omega t)$$

$$\text{Imag.} = \frac{1}{\pi} \int_{\pi/2}^{2\pi+\frac{\pi}{2}} x. \quad \text{Cos}\ \ (\omega t)\ \ d(\omega t) \qquad \ldots\ (a)$$

where x is the continuous function whose samples x_k, x_{k-1}, ... are the input of the digital filter. Using the trapezoidal rule with 4 intervals over a period, equations (a) can be rewritten as:

$$\text{Real} = \frac{1}{\pi} \cdot \frac{2\pi}{4} \cdot \frac{1}{2} \left(x_{k-4} \text{Sin}\ \frac{\pi}{2} + 2x_{k-3}\ \text{Sin}\pi + 2x_{k-2}\ \text{Sin}\ \frac{3\pi}{2} + 2x_{k-1}\right.$$

$$\left.\text{Sin}\ 2\pi + x_k\ \text{Sin}\ \frac{5\pi}{2}\right)$$

and

$$\text{Imag.} = \frac{1}{\pi} \cdot \frac{2\pi}{4} \cdot \frac{1}{2} \left(x_{k-4} \text{Cos}\ \frac{\pi}{2} + 2x_{k-3}\ \text{Cos}\pi + 2x_{k-2}\ \text{Cos}\ \frac{3\pi}{2} + 2x_{k-1}\right.$$

$$\left.\text{Cos}\ 2\pi + x_k\ \text{Cos}\ \frac{5\pi}{2}\right)$$

or:

$$\text{Real} = \frac{1}{4} \left(x_{k-4} - 2x_{k-2} + x_k\right)$$

$$\text{Imag.} = \frac{1}{4}(-2x_{k-3} + 2x_{k-1})$$

From here:

$$C_k \angle \phi_k = \frac{1}{4}(x_{k-4} - x_{k-2} + x_k) + \frac{j}{4}(-2x_{k-3} + 2x_{k-1})$$

or

$$4C_k \angle \phi_k = (x_{k-4} - 2x_{k-2} + x_k) - j(2x_{k-3} - 2x_{k-1})$$

By moving ahead with new samples the interval of the integrations changes to $(\pi,\ 2\pi + \pi)$, $(\frac{3\pi}{2}, 2\pi + \frac{3\pi}{2})$ and $(2\pi\ ,\ 4\pi)$ which give C_{k+1}, C_{k+2} and C_{k+3} as follows:-

$$4C_k \angle \phi_k = (x_{k-4} - 2x_{k-2} + x_k) - j(2x_{k-3} - 2x_{k-1})$$

$$4C_{k-1} \angle \phi_{k+1} = (-2x_{k-2} + 2x_k) - j(x_{k-3} - 2x_{k-1} + x_{k+1})$$

$$4C_{k+2} \angle \phi_{k+2} = (-x_{k-2} + 2x_k - x_{k+2}) - j(+2_{x-1} + 2x_{k+1})$$

$$4C_{k+3} \angle \phi_{k+3} = (-2x_{k+2} + 2x_k) - j(-x_{k-1} + 2x_{k+1} - x_{k+3})$$

These equations are similar to those of 17 in the paper.

The two-term brackets have a sine wave, and the three term brackets have a sine-squared wave characteristic. It should be noted that if we are interested in the magnitude of the phasor quantities, the left hand side of the equations (13) and also (17) of the paper should be multiplied by 2.

Our experience with digital algorithms for distance protection is that acceptable accuracy of measurement cannot be obtained with 4 samples per cycle, because the third harmonic cannot be effectively filtered or even attenuated. Cases have been noted in which the

third harmonic, particularly on the voltage waveform, has been as much as 100% of the fundamental in the first cycle of the fault. Increasing the sampling rate improves the filter characteristic and makes the filter more effective in removing the low order harmonics. Fig. (1) and Fig. (2) show the magnitude characteristic of Fourier technique with 4 samples (which is the same as authors' method) and 16 samples per cycle. In these figures the effect of sampling rate can be seen. If even sharper filter characteristics are desired then Bilinear transformation[A] or clasical optimisation methods[B,C] can be used. These filters will be much more complicated than the simple types discussed in the paper but with micro-processor techniques such an approach may be justified both economically and practically.

Continuous sampling before and after the fault, coupled to a continuous calculation of resistance and inductance has always, in our experience, resulted in faster fault detection times than any method proposed so far based on fundamental waveform filtering.

One great disadvantage of using only 4 samples per cycle is that, to prevent false detection, at least 3 successive calculations are necessary to produce impedance values within the protected zone before a trip initiation signal can be reliably sent to the circuit breaker. Thus the relaying time with the authors' method would be at least 2 cycles - not at all fast by present day solid state relaying standards.

Perhaps the authors would comment on the extension of their method to faster sampling rates and the application to long transmission lines with a significant source impedance.

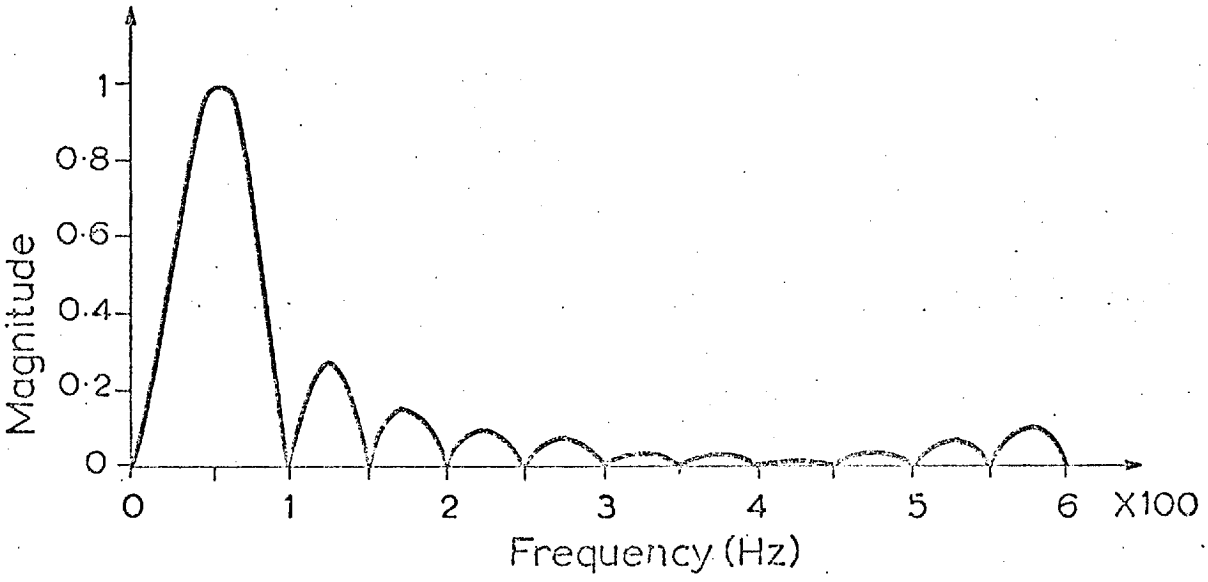

FIG. 2: Magnitude characteristic of Fourier technique with 16 samples per cycle (50 Hz).

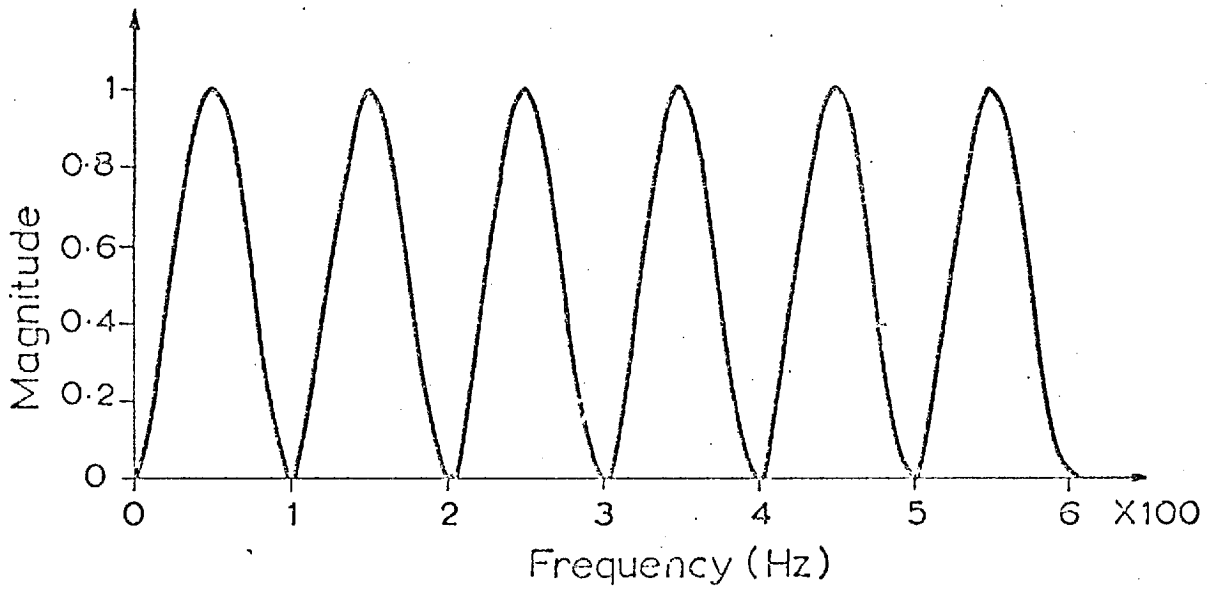

FIG. 1: Magnitude characteristic of authors' method with 4 samples per cycle.

References

A C.M. RADER and B. GOLD "Digital filter design techniques in the frequency domain" Proceedings of the IEEE, Vol. 55, No. 2, February, 1967.

B K. STEIGLITZ "Computer-Aided D sign of Recursive Digital Filters" IEEE Transactions on Audio and Electroacoustics, Vol. AU-18, No. 2, June 1970.

C J.H. McLELLAN, and et al "A Computer Program for Designing Optimum FIR Linear Phase Digital Filters" IEEE Transaction on Audio and Electroacoustics, Vol. AU-21, No. 6, December, 1973.

IEEE SUMMER POWER MEETING

SAN FRANCISCO 1975

Discussion on paper: Sampling Rates for Computer Transmission Line Protection

by

G.S. Hope and O.P. Malik

Discussion prepared by A.M. Ranjbar and B.J. Cory,

Imperial College, London S.W.7, England.

We would like to compliment the authors in their efforts to highlight one of the most decisive factors in the implementation of digital algorithms for on-line protection. Previously, many papers have suggested varying sampling rates from 4^A to 40^B samples per cycle without justifying the choice of an appropriate rate.

High rates of sampling require complicated and expensive hardware for digital implementation whilst too low a sampling rate impairs the accuracy from a numerical computation and filtering point of view. Somewhere between we believe there is an acceptable accuracy given by an optimum sampling rate.

Our investigations into this problem shows that a combination of digital and analogue filtering is required to give the best accuracy, speed of response and lowest cost. We agree with the authors that an optimum sampling rate is around 8 samples per cycle but that further work is required on the type and order of the analogue filter. For this purpose first, second or higher order Butterworth, Chebyshev or Bessel filters can be employed and the best choice is a matter for investigation when the exact protection requirements for a particular line are known.

We hope that this paper will stimulate further work in these areas.

References

A. Carr, J. and Jackson, R.V., 'Frequency Domain Analysis Applied to Digital Transmission Line Protection', IEEE Paper T75-055-9, Winter Power Meeting, January 1975.

B. Mann, B.J. and Morrison, I.F., 'Digital Calculation of Impedance for Transmission Line Protection', IEEE PAS 90, NO. 1, Jan/Feb. 1971.

IEEE SUMMER POWER MEETING

SAN FRANCISCO 1975

Discussion on paper F75 543-9: A Digital Computer System for EHV Substations, Analysis and Field Tests

by

A.G. Phadke, T. Hlibka and M. Ibrahim

Discussion prepared by A.M. Ranjbar and B.J. Cory,

Imperial College, London S.W.7, England.

We wish to compliment the authors for the useful work which they have done on digital protection and we would like to give a few comments on their paper.

1. From figures (3) to (5) it seems that the authors have used the modulus of impedance and (probably) its angle as a criterion for measurement thus providing the modulus of impedance with direction. It is well known that such a characteristic does not provide immunity against balanced system conditions such as heavy loads and power swings. By calculating the real and imaginary parts of the voltage and current it is possible to build an ideal quadrilateral characteristic[A] which has the necessary immunity against extreme loads and power swings. The authors have mentioned this (equation 1) but they have not used it throughout the paper.

2. In table I of the paper the authors have given the minimum data windows for different sampling rates. In determining these windows, one important factor which has been neglected is the spectrum of equations (5). By reducing the data window, the spectrum becomes worse and less unwanted components are filtered out. For example the spectrum of equations (6) for one cycle data window and equation (7) for half a cycle data window have been plotted in figures 1 and 2 and it can be seen that with half a cycle data window, even a constant dc offset cannot be filtered out.

3. In equations (10) and (11), R_{21} and R_{41} are not dependent only

upon harmonics of order 21 and 41. They are also functions of non-harmonic components and so we cannot agree with the authors that R_{41} is a negligible quantity. We can neglect R_{41} if the current and voltage waveforms consist only of odd harmonics, but in general this is not true. Our computations on transmission lines have shown that there is no discernable pattern for voltage and current spectrums and they might contain almost any harmonic or non-harmonic components.

4. The computation of $\tilde{Y}_k$ from equations (12) to (15) involves several multiplications. $\tilde{Y}_k$ is then used in equation (5) which in turn needs further computation, producing the real and imaginary parts of only one current. The whole process must now be repeated for at least two other currents (assuming that the dc offset of voltage is negligible), and then the computed real and imaginary parts are used in equation (1) for the resistance and reactance calculation. This is a tedious procedure which takes some time on a mini-computer. Can the authors say if they have given any consideration to reducing the computations necessary for fault determination ?

Reference:

A. RANJBAR, A.M., and CORY, B.J.: "Algorithms for Distance Protection" IEEE Conference on Modern Developments in Protection, March, 1975, Publication No. 125.

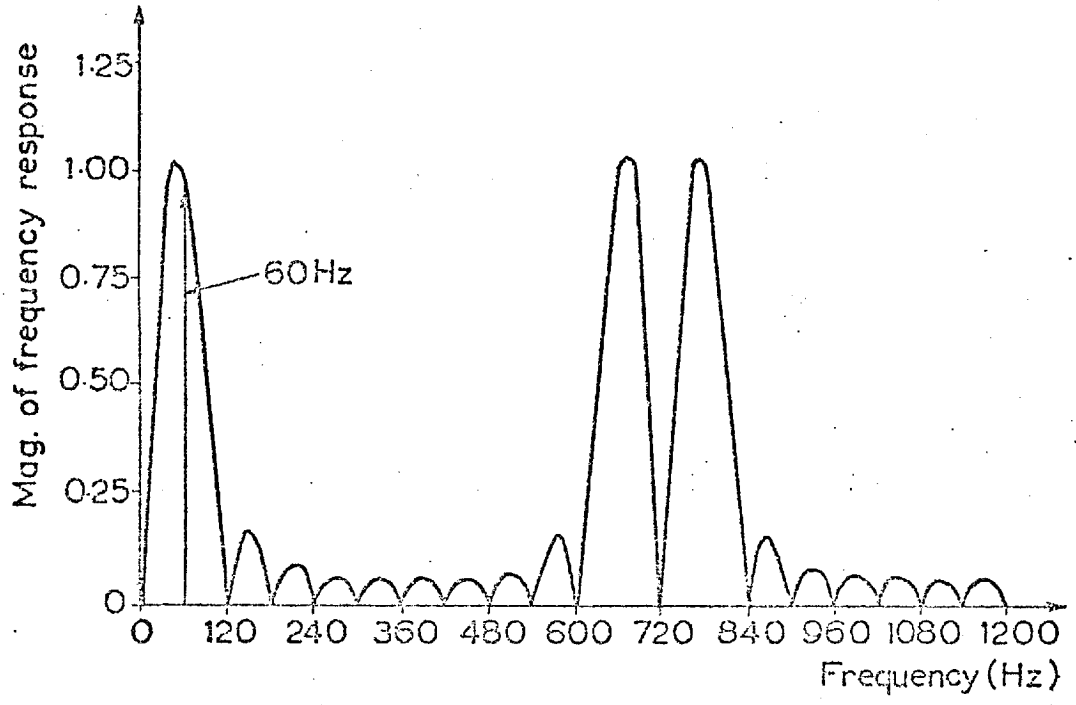

FIG.1: Spectrum of equation (6) (one cycle data window)

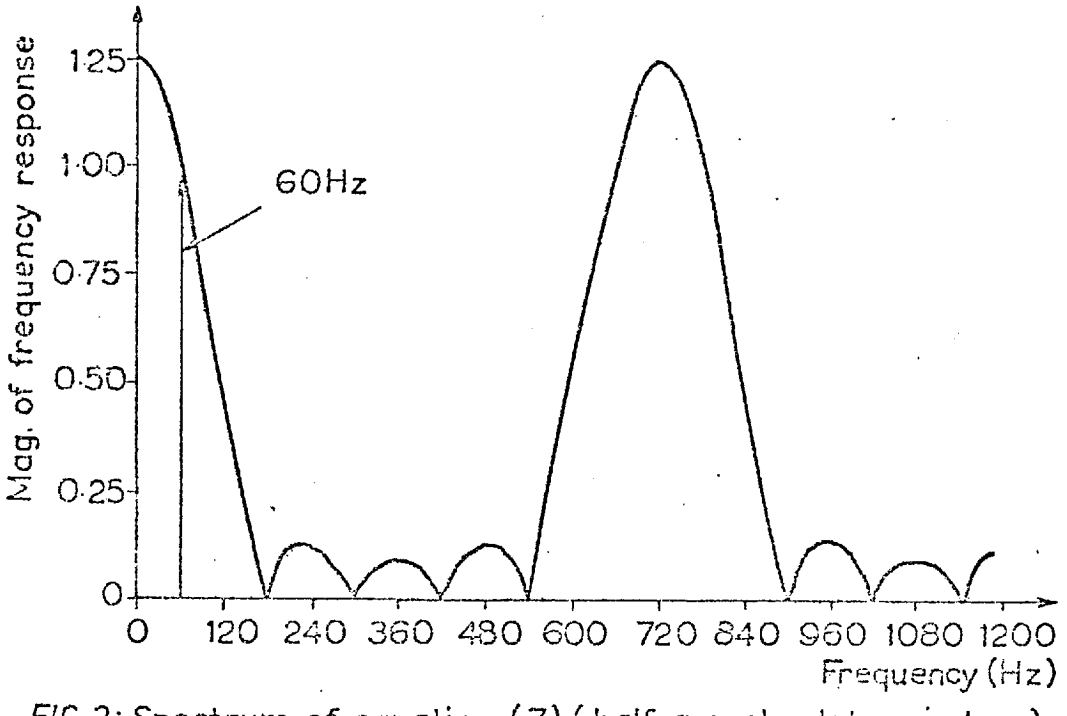

FIG.2: Spectrum of equation (7) (half a cycle data window)

IEE CONFERENCE

MODERN DEVELOPMENTS IN PROTECTION MARCH 1975

Discussion contribution on paper: Algorithms for Distance Protection

by

A.M. Ranjbar and B.J. Cory

Discussion prepared by A.M. Ranjbar

The ability of the Fourier and square wave correlation methods in removing the unwanted harmonic and non-harmonic components from the current and voltage waveforms depends on the sampling frequency. For a 200 Hz sampling rate (4 samples per cycle) the magnitude characteristic of the Fourier method is shown in Fig. (1). From this figure it can be seen that all the even harmonics have been completely filtered out; the odd harmonics have not been changed and many of the non-harmonic components have been only slightly attenuated. By increasing the sampling rate to 800 Hz (16 samples per cycle) the spectrum becomes as in Fig. (2) where it can be seen that all the harmonics and non-harmonics up to 700 Hz have been effectively attenuated. Higher frequencies can be removed by a suitable analogue filter.

In the third method mentioned in our paper the filtering depends on both the interval of integration and the frequency of sampling. If the integration interval is less or more than half a cycle, many components with high or low frequencies will be amplified. The optimum interval is half a cycle in which case all the unwanted components appear either attenuated or with no change. In this method also by increasing the sampling rate the spectrum will be improved. The first and second methods cannot remove the exponential d.c. offset completely, but they reduce it enough so that the error resulting from it is within an acceptable limit. The third method directly accounts for the exponential d.c. component.

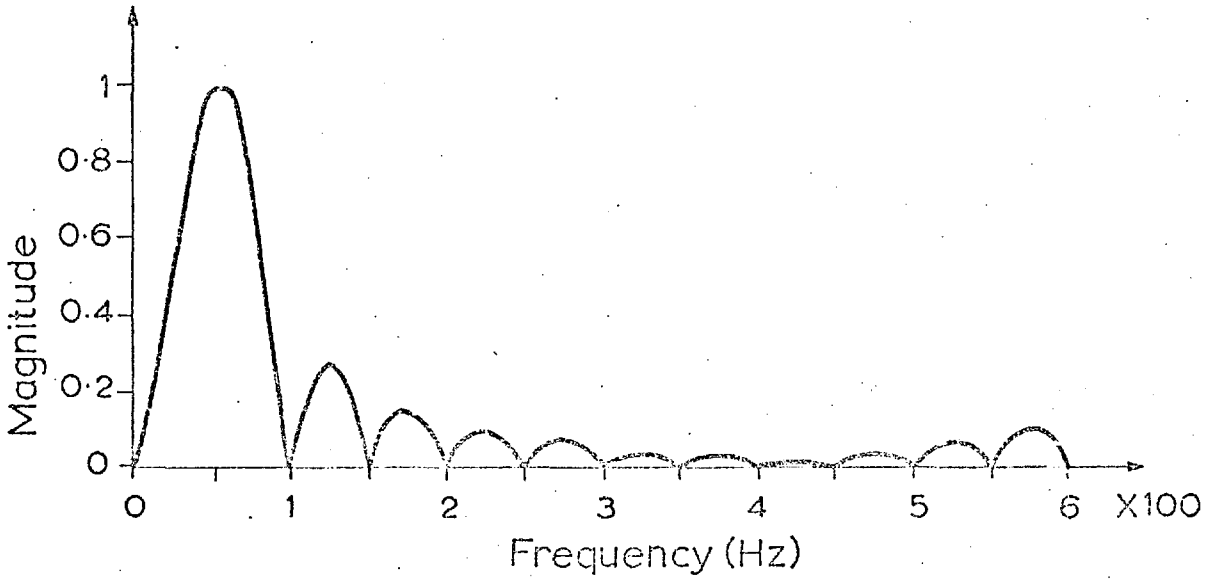

FIG. 2: Magnitude characteristic of Fourier technique with 16 samples per cycle (50 Hz).

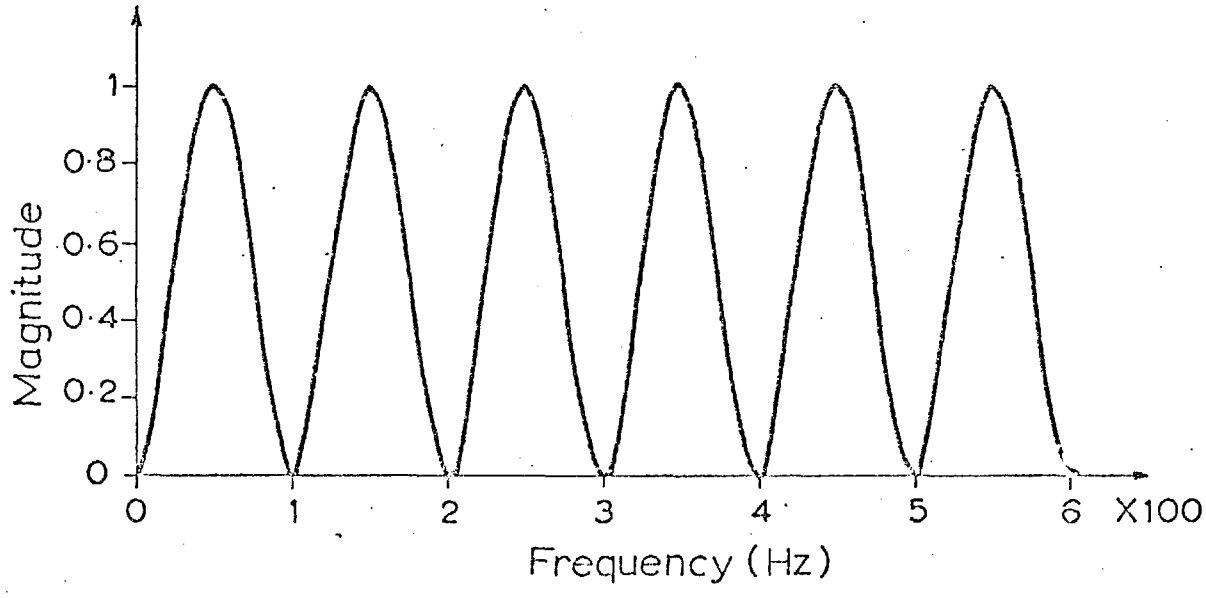

FIG. 1: Magnitude characteristic of Fourier technique with 4 samples per cycle.